

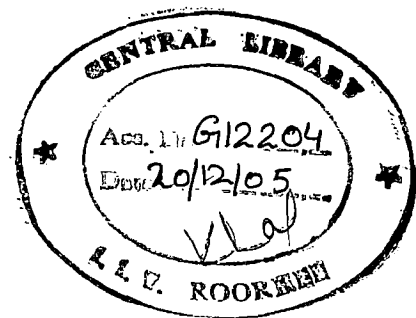
# FLOOD-PLAIN MODELING OF RIVER BRAHMAPUTRA, ASSAM, INDIA

## A DISSERTATION

*Submitted in partial fulfillment of the  
requirements for the award of the degree*  
of  
**MASTER OF TECHNOLOGY**  
in  
**WATER RESOURCES DEVELOPMENT  
(CIVIL)**

By

**AMBUJ DWIVEDI**



**DEPARTMENT OF WATER RESOURCES DEVELOPMENT & MANAGEMENT  
INDIAN INSTITUTE OF TECHNOLOGY ROORKEE  
ROORKEE - 247 667 (INDIA)  
JUNE, 2005**

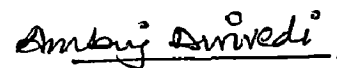
## CANDIDATE'S DECLARATION

I hereby declare that the work which is being presented in the dissertation entitled : "FLOODPLAIN MODELLING OF RIVER BRAHMAPUTRA, ASSAM, INDIA", is in partial fulfillment of the requirement for the award of the degree of the Master of Technology in Water Resources Development and Management (WRD&M) Department, Indian Institute of Technology Roorkee, is an authentic record of my own work carried out during period from July 2004 – June 2005 under the supervision and guidance of Dr Nayan Sharma and Dr. Prabhat K. Swamee.

The matter embodied in this dissertation has not been submitted by me for the award of any other degree.

Date : June 22, 2005

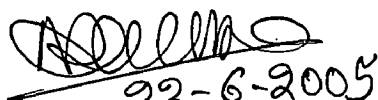
Place : Roorkee




Ambuj Dwivedi

---

Certified that the above declaration given by the candidate is correct to the best of my/our knowledge,

  
22-6-2005  
(Dr. Nayan Sharma)

Professor WRD&M,  
Indian Institute of Technology  
Roorkee, 247667  
India

  
(Dr. Prabhat. K. Swamee)

Professor Dept.of Civil Engineering  
Indian Institute of Technology  
Roorkee , 247667  
India

## ACKNOWLEDGEMENT

The writer is extremely indebted to his professors, Dr.P.K.Swamee, professor, Dept. of Civil Engineering, Indian Institute of Technology Roorkee and Dr.Nayan Sharma, Professor, Dept. of WRD & M, Indian Institute of Technology Roorkee, for their Invaluable guidance, supervision and encouragement during the course of this research.


Thanks are due to staff of computer lab, library and office for extending support directly or indirectly in completion of this dissertation

Sincere thanks are extended to Rabindra Nath Sankhua, PhD scholar, for his help in writer's M.Tech program.

The writer appreciates the encouragement lend by his father.

The writer's M.Tech studies were sponsored by Uttar Pradesh Water Sector Restructuring Project. The sponsorship is gratefully acknowledged.

Dated: June 22 , 2005

  
Ambuj Dwivedi

# CONTENTS

CANDIDATE 'S DECLARATION.....	i
AKCNOWLEDGMENT .....	ii
CONTENT .....	iii
LIST OF SYMBOLS .....	vi
LIST OF FIGURE .....	vii
LIST OF TABLES.....	vii
ABSTRACT .....	viii
CHAPTER - 1	
<b>INTRODUCTION</b> .....	1
1.1. GENERAL.....	1
1.2. OBJECTIVES OF THE STUDY.....	2
1.3. STUDY AREA AND DATA USED .....	3
1.4. METHODOLOGY.....	3
1.5. ORGANISATION OF THE THESIS.....	3
CHAPTER – 2	
<b>LITERATURE REVIEW</b>	
2.1. GENERAL.....	5
2.2. EARLIER WORK DONE .....	8
2.3. LISFLOOD-FP MODEL DEVELOPMENT .....	12
2.4. CONCLUDING REMARK.....	15
CHAPTER - 3	
<b>DISRIPTION OF STUDY AREA AND DATA USED</b>	
3.1 GENERAL .....	16
3.2 LONGITUDINAL SECTION OF THE BRAHMAPUTRA RIVER .....	18
3.3 THE BRAHMAPUTRA BASIN.....	19
3.4 THE BRAHMĀPUTRA RIVER SYSTEM .....	23
3.5 THE TRIBUTARIES OF THE BRAHMAPUTRA RIVER .....	25

3.5.1 THE NORTH BANK TRIBUTARIES .....	26
3.5.2 THE SOUTH BANK TRIBUTARIES .....	27
3.6 HYDROLOGICAL CHARACTERISTICS OF MAJOR TRIBUTARIES.....	28
3.7 HYDRAULIC CHARACTERISTICS.....	31
3.8 HYDROLOGIC AND PHYSIOGRAPHIC OFS BRAHMAPUTRA.....	31
3.9 GEOLOGY AND GEOMORPHOLOGY .....	32
3.10 CHANNEL PROCESSES.....	36
3.11 DATA USED .....	39
3.11.1 SATELLITE DATA.....	39
3.11.2 TOPOGRAPHIC DATA.....	40
3.11.3 HYDROLOGIC DATA .....	40
3.12 VALUES OF MEDIAN SIZE, KINEMATIC VISCOSITY AND ACCELERATION DUE TO GRAVITY.....	41
3.12.1 MEDIAN SIZE:.....	41
3.12.2 KINEMATIC VISCOSITY OF WATER:.....	41
3.12.3 ACCELERATION DUE TO GRAVITY: .....	42
3.13 COLLATERAL DATA .....	42

CHAPTER 4

**FLOODPLAIN MODELLING OF RIVER BRAHMAPUTRA**

4.1. GENERAL.....	43
4.2. FLOOD PLAIN DELIENATION.....	43
4.3. DATA USED .....	46
4.4. METHODOLOGY.....	47
4.4.1. GIS ANALYSIS .....	47
4.4.2. GEO-REFERENCING.....	47
4.4.3. TRANSFORMATION OF PIXEL CO-ORDINATES.....	48
4.4.4. DETERMINATION OF THE GRAY LEVEL VALUES OF THE PIXEL.....	48
4.4.5. REGISTRATION.....	48
4.4.6. PROCESSING OF SATELLITE DATA .....	49
4.4.7. FLOOD INUNDATED AREA .....	49
4.4.8. EXTRACTION OF CHANNEL FORMS .....	52
4.4.9. DIGITAL ELEVATION MODEL (DEM) .....	53
PROCESSING OF REMOTE SENSING DATA.....	57

4.6. DATA BASE GEO-REFERENCING .....	57
4.7. DIGITAL ELEVATION MODEL (DEM) .....	58
4.8. GIS ANALYSIS .....	59
4.9. DEVELOPMENT OF EQUATION FOR FLOOD PLAIN CROSS SECTIONAL AREA AND PERIMETER.....	60
4.9.1. GENERATION OF COMPUTER CODE FOR SECTION GEOMETRY .....	61
4.9.2. EQUATION FOR PERIMETER .....	61
4.9.3. ESTIMATION OF K OF EQUATION (1) .....	62
4.9.4. EQUATION FOR AREA .....	63
4.10. REGIME EQUATIONS FOR RIVER BRAHMAPUTRA.....	65
4.11. LACEY'S EMPIRICAL EQUATIONS .....	66
4.12. BACKGROUND .....	66
4.13. DATA COLLECTION.....	68
4.14. ANALYTICAL CONSIDERATIONS .....	69
4.15. VALIDATION OF RESULTS .....	70
4.16. SALIENT POINTS.....	70
4.17. EQUATION FOR GAUGE DISCHARGE CURVE FOR RIVER BRAHMAPUTRA .....	72
4.17.1. EQUATION FOR AREA AND PERIMETER .....	73
4.17.2. EQUATION OF GAUGE-DISCHARGE CURVE .....	73
4.18. INTRODUCTION.....	73

CHAPTER 5

<b>RESULT AND DISCUSSION.....</b>	<b>107</b>
-----------------------------------	------------

CHAPTER 6

<b>CONCLUSIONS.....</b>	<b>109</b>
-------------------------	------------

REFERENCES

APPENDIX

## LIST OF SYMBOLS USED IN DISSERTATION

- $y$  = water depth (m);
- $y^*$  = water depth at point of intersection of two lines (m);
- $m_1$  = slope of lower line (no dimension);
- $m_2$  = slope of upper line. (no dimension);
- $n = \log_2\left(\frac{P^*}{P_i}\right) = \log_2\left(\frac{A^*}{A_i}\right)$  (no dimension);
- $P^*$  = Perimeter corresponding to intersection point of two lines (m);
- $P_i$  = Actual perimeter at intersection line. (m);
- $A^*$  = Area corresponding to intersection point of two lines (m<sup>2</sup>) ;
- $A_i$  = Actual area at intersection line. (m<sup>2</sup>) ;
- $Q$  = discharge (m<sup>3</sup>/s);
- $d$  = median bed material size (m);
- $E^*$  = minimum power per unit length (W/m);
- $g$  = gravitational acceleration (m/s<sup>2</sup>);
- $P$  = flow perimeter (m);
- $Q$  = discharge (m<sup>3</sup>/s);
- $R$  = hydraulic radius (m);
- $S_0$  = stream bed slope (nondimensional);
- $s$  = specific gravity (nondimensional);
- $V$  = average flow velocity (m/s);
- $\nu$  = kinematic viscosity of water (m<sup>2</sup>/s);
- $\rho$  = mass density of water (kg/m<sup>3</sup>); and

### Superscript

\* = nondimensional

## LIST OF FIGURES

FIGURE 3.1 LONGITUDINAL SECTION OF THE BRAHMAPUTRA RIVER.....	19
FIGURE 3.2 RADARSAT IMAGE (FCC) AT D/S OF GUWAHATI.....	42A
FIGURE 3.3 RADARSAT IMAGE NEAR TEZPUR, 2002.....	42B
FIGURE 3.4 RADARSAT IMAGE OF KAZIRANGA RESERVE FOREST, 2002 ....	42C
FIGURE 3.5 RADARSAT IMAGE OF THE BRAHMAPUTRA, 2002.....	42D
FIGURE 4.1 INDEX TO IRS 1A COVERAGE .....	54
FIGURE 4.2 INDEX TO IRS 1D COVERAGE .....	55
FIGURE 4.3 FLOW CHART THE METHODOLOGY OF IMAGE PROCESSING AND GIS ANALYSIS.....	86
FIGURE 4.4 FALSE COLOUR COMPOSITE (FCC) OF THE MOSAIC IMAGE FRAME OF LISS III, 2000.....	87
FIGURE 4.5 FCC OF NOAA, AUGUST 2002.....	88
FIGURE 4.6 CLASSIFIED DEM MAP OF RIVER BRAHMAPUTRA .....	89
FIGURE 4.7 NOAA IMAGE SHOWING DEEP AND SHALLOW FLOOD PLAIN AREA .....	90
FIGURE 4.8 CROSS-SECTION NUMBER (2 TO 65) OF RIVER BRAHMAPUTRA .....	91
FIGURE 4.9 TYPICAL CROSS SECTION OF RIVER BRAHMAPUTRA .....	92
FIGURE 4.10 PLOT OF PERIMETER VS WATER DEPTH .....	93
FIGURE 4.11 SLOPE M1 AND M2 VS RIVER DISTANCE, FOR PERIMETER ...	94
FIGURE 4.12 PLOT OF $Y^*$ VS RIVER DISTANCE (KM).....	95
FIGURE 4.13 PLOT OF $K$ VS RIVER DISTANCE (KM).....	96
FIGURE 4.14 PLOT OF $N$ VS RIVER DISTANCE (KM).....	97
FIGURE 4.15 SLOPE M1 AND M2 VS RIVER DISTANCE.....	98
FIGURE 4.16 PLOT OF $Y^*$ VS RIVER DISTANCE .....	99
FIGURE 4.17 PLOT OF $K$ VS RIVER DISTANCE .....	100
FIGURE 4.18 COEFFICIENT FOR SLOPE, AREA AND PERIMETER .....	101
FIGURE 4.19 AREA A ( $M^2$ ) AND PERIMETER P (M) VS DISCHARGE.....	102
FIGURE 4.20 PLOT OF OBSERVED AND CALCULATED SLOPE .....	103
FIGURE 4.21 VALIDATION FOR FLOW PERIMETER .....	104
FIGURE 4.22 VALIDATION FOR FLOW AREA.....	105
FIGURE 4.23 GAUGE DISCHARGE .....	106



## **LIST OF TABLES**

TABLE 2.1 STATEMENT SHOWING FLOOD DAMAGES DURING 1953 TO 1998, ASSAM .....	6
TABLE 3.1 THE BRAHMAPUTRA RIVER: COUNTRY AND INDIAN STATE-WISE BREAK-UP OF BASIN AREA AND CHANNEL LENGTH.....	18
TABLE 3.2 HYDROLOGICAL CHARACTERISTICS OF SOME MAJOR TRIBUTARIES .....	29
TABLE 3.3 TRIBUTARY DISTANCE MEASURED FROM INDO BANGLADESH BORDER (FROM DHUBRI ALONG THE UPSTREAM) .....	30
TABLE 4.1 SATELLITE DATA .....	56
TABLE 4.2 THE AREA OF WATER BODIES ON EACH IMAGE .....	59
TABLE 4.3 FLOOD AFFECTED AREAS (%) FOR DISTRICTS .....	60
TABLE 4.4 DATA GENERATED FOR EQUATION OF PERIMETER.....	76
TABLE 4.5 DATA GENERATED FOR EQUATION OF AREA.....	81

## ABSTRACT OF DISSERTATION

### FLOOD PLAIN MODELLING OF RIVER BRAHMAPUTRA

---

The art of modeling an alluvial river of multi-channel configuration is still in a developing stage and a lot of ground yet remains to be covered. A number of contributions have been made for simulating flood routing, overland flow and related time-dependent transient flow problems by solving the gradually varied unsteady flow equations numerically however, invariably in all the existing models the solutions are obtained based on certain simplifications of geometric properties such as

**The geometric properties of all the irregular sections of a natural stream over the entire reach are averaged with respect to the flow depth to form a single representative cross-section. The cross-sectional areas and the top widths of the representative cross-section are then fitted by a polynomial.**

The above simplifications can work satisfactorily only when natural stream consists of single channel at all the stages of flow. However, in an alluvial stream of multi-channel configurations these simplifications can introduce serious error and the simulation results based on this cannot be relied upon.

The objectives of this study were to develop a methodology to delineate flood plain, to develop the simple mathematical equations for cross-sectional area and perimeter of river, to develop the hydraulic and

morphological characteristics of the river during floods, to develop the stage discharge relation for the river Brahmaputra.

A first effort is made to extract the floodplain section of the River during floods. For this purposes satellite images and field data were combined to extract the flooding extent which is further used in developing the mathematical equation for area and perimeter which can be used in flood routing problems.

The hydraulic characteristics of the river during floods were developed. For this, Lacey's equations were modified to develop the new equations, applicable to river Brahmaputra.

Subsequently, the development of stage-discharge equation for the river is carried out, which is applicable at any section of the river Brahmaputra.

The comparison of calculated results and the observed data are in reasonably good agreement .This proves the feasibility of applying the mathematical models for prediction of flooding extent, regime flow conditions and gauge-discharge relationship for river Brahmaputra at any section.

## CHAPTER - 1

# INTRODUCTION

---

### 1.1. GENERAL

The Brahmaputra basin in India, particularly its valley in Assam, represents an acutely flood-prone region characterized by awesome hazards of flood and erosion that create an annual mayhem of devastations bringing untold miseries to the people and causing colossal loss and damage to public property and infrastructure. Although occurrence of flood has been an age-old phenomenon in the riverine areas of this region, yet the extent of damage caused by the hazard has increased significantly in recent years particularly after the great Assam earthquake of 1950 which recorded 8.7 on the Richter scale. The Brahmaputra valley had experienced major floods in 1954, 1962, 1966, 1972, 1974, 1978, 1983, 1986, 1988, 1996, 1998 and 2000. With more than 40 percent of its land surface susceptible to flood damage, the total flood-prone area in the Brahmaputra valley is 32 lakh hectares which account for 9.6 percent of the country's total. The floods in Assam are caused by a combination of several natural and anthropogenic factors.

The unique environmental setting of the basin vis-à-vis the eastern Himalayas, highly potent monsoon regime, weak geological formations, active seismicity, accelerated rates of erosion, rapid channel aggradation, massive deforestation, intense landuse pressure and high population growth especially in the floodplain belt, and adhoc type temporary measures of flood control are some of the dominant factors that caused and/or intensify floods in Assam (Goswami, 1992). However, the single most important cause for frequent

occurrence of flood in this region is the extremely dynamic monsoon rainfall regime in the backdrop of the unique physiographic setting. The water yield of the Brahmaputra basin is among the highest in the world (Goswami, 1985). This, together with the limited width of the valley and the abruptly flattened gradient, leads to tremendous drainage congestion and resultant flooding. The scenario is further exacerbated by a myriad of social, economic and environmental factors causing increased vulnerability of people to the flood hazard. The flood problem has three main facets so far as the Brahmaputra is concerned. First, the problem of inundation of riverine areas due to overtopping of banks by the main river and tributaries. Second, the problem of drainage congestion especially near the outfalls of the tributaries during high flood stages of the river. Third, the problem of bank erosion and channel instability. The greatest single casualty due to recurrent floods, accounting for as much as 75 percent of the total flood loss, is the agricultural sector, which happens to be the mainstay of the economy.

## **1.2. OBJECTIVES OF THE STUDY**

The aim of flood plain modeling in this work is to establish simple mathematical relations for area and perimeter of flood plain, the knowledge of which is important for flood routing. It was also envisaged to develop the hydraulic and morphological characteristics of river Brahmaputra during floods. Further, with the combination of mathematical relations for area and perimeter of flood plain, and hydraulic and morphological characteristics of river Brahmaputra during floods, an equation for gage discharge is proposed to be established which is applicable for complete length of the river.

### **1.3 STUDY AREA AND DATA USED**

The entire river covering 623 km in India is covered in the present study. Satellite data of the study area, together with topographical, Hydrological and ancillary data is used in the study.

### **1.4 METHODOLOGY**

Flood plain modeling strategy is carried out to solve some of the problems related to floods in river Brahmaputra. Recent years have witnessed tremendous developments in the areas of space-based remote sensing applications with increasingly improved spatial, spectral and temporal resolutions, database technology, viz. Geographic Information System (GIS), modelling (simulations, digital elevation modelling, etc.). The current study, carried out for Brahmaputra flood plain, is aimed at establishing the synergistic coupling between space and the relevant mathematical modeling of flood plain for flood forecasting, and extent of flooding.

### **1.5 ORGANISATION OF THE THESIS**

This dissertation work has been arranged in six chapters as detailed below

#### **Chapter 1 INTRODUCTION**

Brief outline of Brahmaputra river basin and its unique environmental setting is discussed. The objectives of the study, data used and methodology has been discussed.

#### **Chapter 2 LITERATURE REVIEW**

Flood scenario of river Brahmaputra and latest research in flood plain modeling and existing models has been briefly discussed.

### **Chapter 3 DESCRIPTION OF STUDY AREA AND DATA USED**

Detailed discussion on Brahmaputra river system and its tributaries is carried out. The longitudinal slope of the river, discharge ranges of the river including hydrographic, physiographic, geology and geomorphology characteristics has been discussed in detail. The nature and type of data used is discussed in this chapter.

### **Chapter 4 FLOOD PLAIN MODELLING OF RIVER BRAHMAPUTRA**

In this chapter, methodology for flood plain delineation has been discussed. Methodology adopted for development of equation for cross sectional area and perimeter has been detailed out. Regime equation and stage discharge equation for river Brahmaputra has been developed.

### **Chapter 5 CONCLUSIONS**

This chapter contains conclusions emerged from the present study.

### **Chapter 6 DISCUSSIONS AND SCOPE FOR FUTURE WORK**

## CHAPTER - 2

### LITERATURE REVIEW

---

#### 2.1. GENERAL

The extent of flood damage in the Brahmaputra valley during the period 1953 to 1998 is shown in the Table 2.1. It indicates that flood damage rose up to as high as 664 crores in the year 1988 and 700 crores in 1998 (Goswami, 1998). The 1998 flood is considered to be the most severe one since 1950. During this flood season, the Brahmaputra remained above the danger level for 42 to 99 days at 6 major gauge sites on the river. The floods came in four major waves from June to September, the fourth one occurring in September being the most severe. The synchronization of flood peaks of several major tributaries with the main stream led to further intensification of the hazard. All the 21 districts in the valley were flooded affecting a population of 47 lakhs in 5300 villages and damaging 9.7 lakh hectares of cropland. Besides, 30900 houses were washed away or damaged and 156 numbers of human life and 7814 cattlehead were lost. Breaching of embankment had been a major cause of intensification of the 1998 flood hazard, which recorded as many as 139 breaches.



**Table 2.1 : Statement showing Flood Damages During 1953 to 1998, Assam**

Sl No.	Year	Area Affected (million ha)	Population Affected (million)	Total Damage (Rs. Crore)
1	1953	0.080	0.410	2.66
2	1954	3.150	1.680	15.97
3	1955	1.410	0.800	3.71
4	1956	0.600	0.560	3.26
5	1957	0.400	0.310	4.52
6	1958	1.250	0.470	2.70
7	1959	1.040	1.760	8.39
8	1960	0.470	1.320	7.76
9	1961	0.190	0.250	0.57
10	1962	1.620	4.050	20.23
11	1963	0.580	0.830	2.06
12	1964	0.760	0.770	2.76
13	1965	0.600	0.240	0.69
14	1966	1.780	4.650	22.53
15	1967	0.260	0.680	2.44
16	1968	0.410	0.920	8.36
17	1969	0.810	1.470	8.46
18	1970	0.720	1.710	10.43
19	1971	0.360	0.670	5.63
20	1972	1.100	3.200	24.15
21	1973	2.750	2.290	16.41
22	1974	1.120	2.850	20.14
23	1975	0.010	0.030	0.34
24	1976	0.570	1.460	11.98
25	1977	1.100	4.550	31.09
26	1978	0.310	0.920	4.08
27	1979	0.670	2.350	28.14
28	1980	1.160	3.360	39.80
29	1981	0.460	1.360	7.40
30	1982	0.610	1.420	21.89
31	1983	0.730	2.260	56.18
32	1984	1.520	5.680	50.83
33	1985	0.650	2.380	54.84

34	1986	0.430	2.350	204.60
35	1987	1.530	10.490	346.60
36	1988	3.820	8.410	663.84
37	1989	0.690	2.403	0.00
38	1990	0.488	1.692	74.56
39	1991	0.997	5.307	191.15
40	1992	0.213	0.974	26.56
41	1993	1.348	5.261	0.215
42	1994	0.053	0.177	0.20
43	1998	0.972	4.698	700.00

With about 40 million hectares flood-prone areas coupled with the average annual damage to the extent of Rs 500crores and affecting 10 per cent of total population, floods have been the most severe natural disaster in India. Ironically, the flood-affected areas have increased 3 times since 1960. The average total damage incurred presently is about six times that incurred in 1950s. Generally, 60%of the total damage due to floods is in the states of Assam, Bihar, Uttar Pradesh and West Bengal. Ever-increasing catastrophic flood profiles in the country call for utmost attention at all levels. Brahmaputra, the biggest river in the Indian subcontinent, is uniquely characterized by its narrow sized valley coupled with the steep slopes and transverse gradient along with catchments experiencing the highest rainfall and loading heaviest sediments, which are driven mainly due to deforestation and unsustainable agricultural practices. The recurring floods leave a trail of deaths, destruction and damages to existing infrastructure, including roads, bridges, embankments, irrigation canals, buildings and crops. Due to information gap during critical times and absence of precise damage assessment, the State and Central

mechanisms are unable to address the flood management-related issues more judiciously and efficiently.

## **2.2. EARLIER WORK DONE**

P.D. Bates, A.P.J. De Roo developed a model for flood plain analysis. The model is designed to operate with high-resolution raster Digital Elevation Models, which are becoming increasingly available for many lowland floodplain rivers and is based on what is hypothesized to be the simplest possible process representation capable of simulating dynamic flood inundation. This consists of a one-dimensional kinematic wave approximation for channel flow solved using an explicit finite difference scheme and a two-dimensional diffusion wave representation of floodplain flow. The model is applied to a 35 km reach of the River Meuse in The Netherlands using only published data sources and used to simulate a large flood event that occurred in January 1995. This event was chosen as air photo and Synthetic Aperture Radar (SAR) data for flood inundation extent are available to enable rigorous validation of the developed model. 100, 50 and 25 m resolution models were constructed and compared to two other inundation prediction techniques: a planar approximation to the free surface and a relatively coarse resolution two-dimensional finite element scheme.

Estimation of reach scale flood inundation is increasingly a major task for river engineers and managers (see Penning-Rowsell and Tunstall, 1996). For most rivers sufficient observations of flood inundation extent are not available to determine such areas and recourse must be made to some sort of predictive 'model'. These can range in complexity from simply intersecting a plane

representing the water surface with a Digital Elevation Model (DEM) of sufficient resolution to give the flooded area (Priestnall et al., 2000) to full three-dimensional solutions of the Navier–Stokes equations with sophisticated turbulence closure (Thomas and Williams, 1995; Younis, 1996). However, prediction of flood inundation is not straightforward. Out-of-bank flow in meandering compound channels is now known to be highly three-dimensional and involves the development of a strong shear layer between main channel and floodplain (Knight and Shiono, 1996) as well as spillage of water from the main channel across meander loops (Ervin et al., 1993; Ervin et al., 1994; Sellin and Willets, 1996). Moreover, flood inundation extent is highly dependent on topography, and shallow floodplain gradients mean that small errors in modelled water surface elevations may lead to large errors in the predicted inundation front position.

At present, it is still not yet known about the necessary still do not know what process representation to include in a floodplain inundation model to achieve given levels of predictive ability. Ultimately, the best model will be the simplest one that provides the information required by the user whilst reasonably fitting the available data. However, modellers tend to employ the most sophisticated scheme that can be practically applied in the belief that the more processes a model includes the better it will be. Whilst this may be a reasonable assumption, it has never been tested for the specific task of predicting flood inundation. For example, until relatively recently the most popular approaches to modelling fluvial hydraulics, and thus implicitly flood inundation, at the reach scale (5–50 km) have been one-dimensional finite difference solutions of the full St. Venant equations (Fread, 1984; Samuels,

1990; Fread, 1993; Ervine and MacLeod, 1999) such as MIKE11, ISIS, ONDA, FLUCOMP and HEC-RAS. Such schemes describe the river channel and floodplain as a series of cross sections perpendicular to the flow direction and are thus well suited to parametrisation using traditional field surveying methods. Numerical solution of the controlling equations for prescribed inflow and outflow boundary conditions then enables the cross section-averaged velocity and water depth at each location to be calculated. However, considerable skill is required to determine appropriate cross section locations for such models (Samuels, 1990) and, in addition, areas between cross sections are not explicitly represented. To simulate flood inundation extent the values of water depth at each cross-section are taken and either overlain onto a DEM or the inundation extents at each cross section are linearly interpolated. To overcome these limitations, two-dimensional finite difference and finite element models have been developed (Feldhaus et al., 1992; Bates et al., 1992; Bates et al., 1995). These provide a higher order representation of river hydraulics more consistent with known processes, include a continuous representation of topography and require no secondary processing step to determine the flood inundation. Recently, such schemes have been compared successfully to low resolution satellite imagery of flood inundation extent (Bates et al., 1997) and measured water levels internal to the model domain during dynamic simulations (Bates et al., 1998). However, they have the drawback of increased computational cost and are less well suited to parametrisation with traditional cross sectional surveys.

Two-dimensional models are best employed in conjunction with a DEM of the channel and floodplain surface that, in conjunction with suitable inflow

and outflow boundary conditions, allows the water depth and depth-averaged velocity to be computed at each computational node at each time step. Thus the sophistication of flood inundation modelling has increased in line with model developments and increased computational resources, but the possibility that simpler models may provide similar levels of predictive ability has not actually been considered. A further impetus for such a development is the increasing availability of high resolution, high accuracy Digital Elevation Models for floodplain areas. National topographic mapping agencies have tended to treat low-lying floodplain areas as relatively featureless. This lack of data has been addressed in a number of countries (UK, The Netherlands) using techniques such as aerial photogrammetry and airborne laser altimetry (Li, 1997), both of which are capable of rapidly generating high resolution DEMs. Two-dimensional numerical models are a possibility here as they can be readily integrated with such data sources (see Marks and Bates, 2000); however, for the reasons given above and the quantity of data and the number of reaches involved, the availability of simpler modelling tools would also be beneficial. These should ideally be capable of being used by environmental managers with relatively little hydraulic modelling experience.

Flood inundation model, LISFLOOD-FP, is capable of being integrated with newly available high resolution raster-based Digital Elevation Models. This new scheme is an extension of the LISFLOOD catchment model (De Roo et al., 1999a) and is specifically designed for channel and floodplain hydraulic routing problems. It aims to reduce the representation of floodplain hydraulics to the minimum necessary to achieve acceptable predictions when compared to typically available flood hydraulic data. At best this consists of gauged

discharge and stage records and satellite and air photo derived flood extent data, with simulation of the latter being the primary focus of the scheme. Flow velocity is not generally collected by environmental authorities and is not specifically required by most statutory flood risk regulations. It can, for the purposes of flood inundation prediction, be considered as a 'redundant' variable and for this reason is not explicitly considered by the model. Finally, the new scheme is simple to set up and run, computationally efficient, can be used by non-expert users and can be readily integrated with commercial Geographic Information Systems.

### **2.3. LISFLOOD-FP MODEL DEVELOPMENT**

The basic component of the LISFLOOD-FP model is a raster Digital Elevation Model of resolution and accuracy sufficient to identify both the channel (location and slope) and those elements of the floodplain topography (dykes, embankments, depressions and former channels) considered necessary to flood inundation prediction. In reality this resolution and accuracy cannot be known a priori and may vary between applications, so an informed guess is needed as a starting point for model development.. Having defined our basic data source the next step is to consider the process representation we need to include. A flood consists of a large, low amplitude wave propagating down valley. When the bankful flow depth is reached, water ceases to be contained solely in the main river channel and water spills onto adjacent shallow gradient floodplains. These floodplains act either as temporary stores for this water or additional routes for flow conveyance. For channel flow below bankful depth there is increasingly a consensus (Knight and Shiono, 1996) that flow

processes can be represented by a simple one-dimensional representation. For the out-bank case this situation is more complex. Floodplain flow is clearly two-dimensional, whilst at the channel-floodplain interface development of intense shear layers leads to a strongly turbulent and three-dimensional flow field (Tominaga and Nezu, 1991; Sellin and Willetts, 1996). Again, it is therefore difficult to make a priori decisions about which processes it is necessary to include in a flood inundation model. At its most basic level this is because floods are not planar surfaces but, rather, are waves where the shape of the wave (or hydrograph as it would appear to a stationary observer) will control the rate of floodplain wetting and drying.

Perhaps more importantly, the planar surface assumption can result in areas being flooded that are never connected to the flood. This consists of a one-dimensional hydraulic routing procedure for channel flow to capture the downstream propagation of the flood wave and some distributed means of routing water two-dimensionally over the floodplain to enable simulation of floodplain water depths and hence inundation extent. Ideally, some account of the interaction between main channel and floodplain could also be made; however, this is not an essential part of the minimum specification but rather a possible later refinement. The most basic dynamic wave routing scheme available consists of the kinematic wave approximation. This is a simplification of the full one-dimensional St. Venant equation obtained by eliminating local acceleration, convective acceleration and pressure terms in the momentum equation

The simplest numerical solution of the above equation system is an explicit finite difference procedure. A number of such schemes are available



and this model implements the one given by Chow et al. (1988). This simple linear scheme uses the backward-difference method to derive the finite difference equations. To implement the kinematic routing model LISFLOOD define a local drainage direction map that represents the line of the channel. Commencing at the inflow point each channel cell contains a marker indicating the direction of the next downstream channel cell. For each cell containing a channel, we define the channel width, slope, friction coefficient and bankful depth. Hence, the cross-sectional geometry is assumed rectangular. Whilst the channel width may be greater or smaller than the resolution of the raster DEM to give flexibility in the channel representation, these dimensions should not vary too greatly to avoid undue approximation errors. For each channel cell we therefore have all the necessary information to compute the kinematic wave approximation. Once the bankful depth is exceeded in a given channel, cell water may be routed into adjacent floodplain areas of the DEM. The simplest way to achieve distributed routing of water over the floodplain is to treat each cell as a storage volume for which we solve a continuity equation. LISFLOOD use the Manning equation, although it should be noted that a number of alternative uniform flow formulae could also be used such as the Chezy equation or the formulae for flow over free or drowned weirs.

1D models (MIKE11, ISIS, ONDA, HEC-RAS, FLUCOMP among others) Fread (1984) and Ervine and MacCleod (1999) Full solution of the 1D St. Venant equations treats domain as a series of cross sections perpendicular to the flow direction. Areas between cross sections are not explicitly represented typical application described by Penning-RowSELL and Tunstall (1996).

## **2.4. CONCLUDING REMARK**

All the existing models approximate the cross section of the channel either to be prismatic or rectangular. In real situation, the cross section is far away from the above assumption and therefore the results deviate away from true value when the models are used in the field. In the present study an attempt has been made to form the equation for cross section area and perimeter.

## CHAPTER - 3

### DISCRIPTION OF STUDY AREA AND DATA USED

---

#### 3.1 GENERAL

The Brahmaputra is a major international river covering a drainage basin of 580,000 km<sup>2</sup>, extending from 82°E to 97° 50' E longitudes and 25° 10' to 31° 30' N latitudes. The basin spans over an area of 293,000 km<sup>2</sup> (50.51%) in Tibet (China), 45,000 km<sup>2</sup> (7.75%) in Bhutan, 194,413 km<sup>2</sup> (33.52%) in India and 47,000 km<sup>2</sup> (8.1%) in Bangladesh. Arunachal Pradesh (41.88%), Assam (36.33%), Nagaland (5.57%), Meghalaya (6.10%), Sikkim (3.75%) and West Bengal (6.47%) share its basin in India (Goswami, 2000). Originating in a great glacier mass at an altitude of 5,300 m just south of the lake Konggyu Tso in the Kailas range, about 63 km southeast of Mansarovar lake in southern Tibet at an elevation of 5300m, the Brahmaputra flows through China (Tibet), India and Bangladesh for a total distance of 2880 km, before emptying itself into the Bay of Bengal through a joint channel with the Ganga. It is known as the Tsangpo in Tibet (China), the Siang or Dihang in Arunachal Pradesh (India), the Brahmaputra in Assam (India) and the Jamuna, Padma, and Meghana in Bangladesh.

Before entering India, the river flows in a series of big cascades as it rounds the Namcha-Barma peak. The river forms almost trough receiving the flows of its tributaries from both North and South. The river, with its Tibetan name Tsangpo in the uppermost reach, flows through southern Tibet for about 1,625 km eastward and parallel to tributaries, viz., the Nau Chhu, the Tsa Chhu, the Men Chhu, the Charta Tsangpo, the Raga Tsangpo, the Tong Chhu, the

Shang Chhu, the Gya Chhu, the Giamda Chhu, the Po Tsangpo and the Chindru Chhu and the right bank tributaries, viz. the Kubi, the Kyang, the Sakya Trom Chhu, the Rhe Chhu, the Rang Chhu, the Nyang Chhu, the Yarlang Chhu, and the Trulung Chhu join the river along its uppermost reach. At the extreme eastern end of its course in Tibet the Tsangpo suddenly enters a deep narrow gorge at Pe, where in the gorge section the river has a gradient ranging from about 4.3 to 16.8 m/km (Figure 3.1).

The river enters in India near Tuning in Arunachal Pradesh. After travelling for a distance of 278 km up to Kobo, it meets with two rivers Dibang and Lohit in Assam near Kobo. Below this confluence point, the river is known by the name of Brahmaputra. It passes through Assam into Bangladesh and at last it meets with Ganga near Goalundo in Bangladesh before joining the Bay of Bengal. Its total length is 2880 km comprising of 1625 km in Tibet, 918 km in India and 337 km in Bangladesh. It is also one of the most braided rivers in the world with width variation from 1.2 km at Pandu near Guwahati to about 18.13 km few km distances downstream to this point (Figure 3.2). This reduction in river width is only within length of 21km (Figure 3.3 and 3.4). Traversing through deep narrow gorges of the Himalayan terrain the Tsangpo takes a southward turn and enters Indian territory at an elevation of 660 m. The river then enters the State of Assam (India) taking two important tributaries the Dibang and the Lohit. At the exit of the gorge the slope of the river is only 0.27 m/km. At the head of the valley near Dibrugarh the river has a gradient of 0.09-0.17 m/km, which is further, reduced to about 0.1 m/km near Pandu (Figure 3.1). The mighty Brahmaputra rolls down the Assam valley from east to west for a distance of 640 km up to Bangladesh border (Table 3.1) (Figure 3.5).

**Table 3.1 The Brahmaputra River: Country and Indian state-wise break-up of basin area and channel length**

<b>Country</b>	<b>Basin area (Km<sup>2</sup>)</b>	<b>Channel Length (Km)</b>
1. Tibet (China)	293,000	1,625
2. Bhutan	45,000	-
3. India	194,413	918
(a) Arunachal Pradesh	81,424	278
(b) Assam	70,634	640
(c) Nagaland	10,803	-
(d) Meghalaya	11,667	-
(e) Sikkim	7,300	-
(f) West Bengal	12,585	-
4. Bangladesh	47,000	337

### **3.2 LONGITUDINAL SECTION OF THE BRAHMAPUTRA RIVER**

The longitudinal section of the Brahmaputra river from its origin to the outfall point is depicted in Figure-3.1.

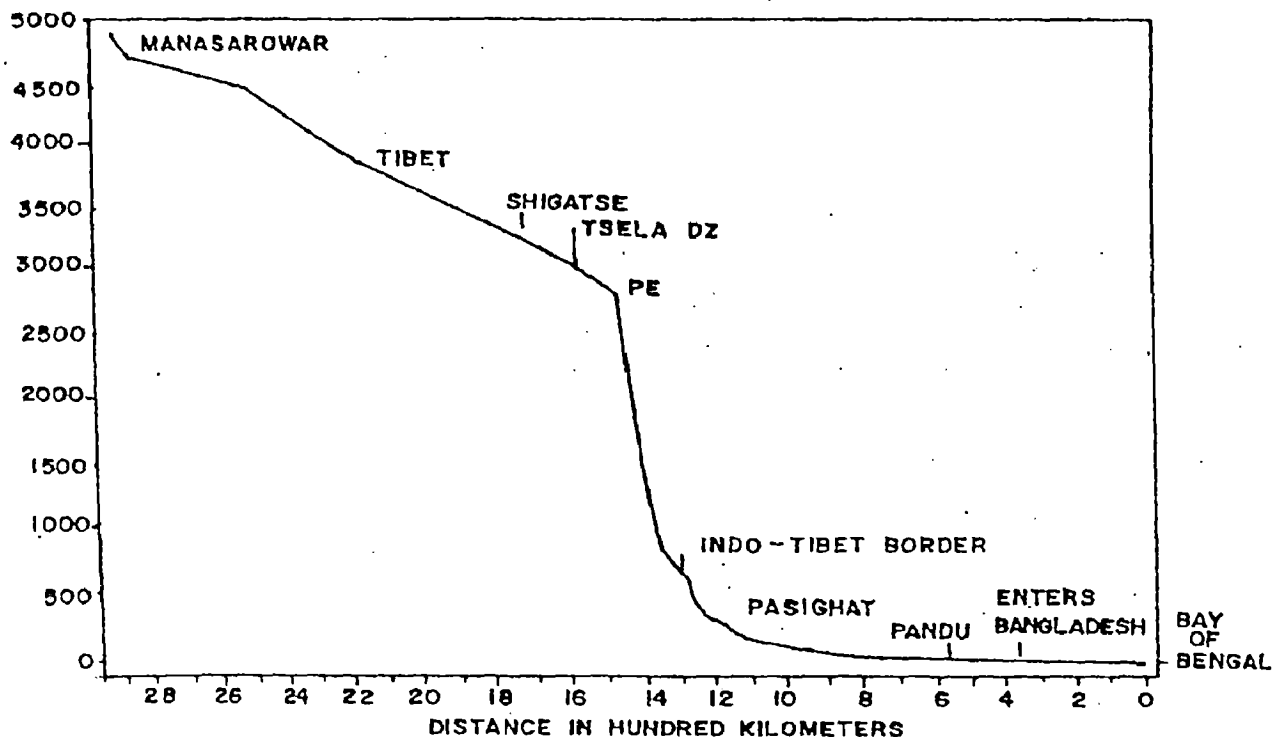


Figure 3.1 Longitudinal section of the Brahmaputra river

### 3.3 THE BRAHMAPUTRA BASIN

The Brahmaputra basin is confined by the great Himalayan ranges in the North and Northeast, Naga-Patkai hills in the East and Mikir hills and Shillong plateau in the South. The Assam valley is the eastern continuation of the Indo-Gangetic plains of the Indian subcontinent valley. It is very narrow in the east and gradually expands to the west to nearly 80 km width, covering an area of about 5,62,704 km<sup>2</sup>. In this valley, the river itself occupies a width of 6 to 12 km in most places. The basin of the river extends from parts of Tibet, Nepal, Bangladesh, Northeast India and Bhutan. The state wise distribution within India and the country wise distribution of the basin are presented in Table 3.1

The Indian part of the basin has a maximum east-west length of about 1,540 km and a maximum north-south width of about 682 km along 93° east longitude (Figure-3.5). The basin is characterized by large variations in relief

slope, landforms, climate, vegetation and land use. The upper basin lying in Tibet (China) and in the eastern Himalayas of Arunachal Pradesh, Sikkim and Nagaland comprise mostly mountain ranges and narrow valleys and the channels are restricted within steep and narrow valleys in the mountains. In Assam and Meghalaya, the basin consists of hills, plateaus and plains covered by forests, tea gardens, agricultural lands and built-up areas. In West Bengal also, the basin covers hills and valleys dominated by forests, tea gardens, agricultural lands and built-up areas. The lower portion of the basin in Bangladesh consists largely of fertile plains and delta regions.

The Brahmaputra basin in India is most generously gifted with a fabulous water wealth that accounts for nearly 30% of the total water resources and about 40% of the total hydropower potential of the country. However, so far the utilisation of this enormous water resources potential of the region is limited. For example, less than 5% of the existing hydropower potential, 10% of the irrigation potential and about 4% of the ground water potential have so far been harnessed.

The Brahmaputra river is characterized by high intensity flood which flows during the monsoon season, June through September, with an average annual flood discharge of 48,160 m<sup>3</sup>/sec. The highest flood discharge recorded in the Brahmaputra at Pandu (Assam) was of the order of 72,148 m<sup>3</sup>/sec (in year 1962), which had a recurrence interval of 100 years (WAPCOS, 1993). The daily hydrograph of the river at Pandu exhibits drastic fluctuations in discharge during the monsoon season, whereas the time series of annual maximum flood events for the period 1955-2000 do not indicate any perceptible trend (Goswami et al, 2000).

Analysis of 100-year rainfall records at Guwahati also does not show any distinct long term trend (Goswami et al, 2000). However, there is a considerable variation in the spatio-temporal distribution of rainfall with marked seasonality. For example, precipitation varies from as low as 120 cm in parts of Nagaland to above 600 cm in the southern slopes of the Himalayas. A gradual increase in rainfall from the valley bottom towards the lower ranges of the Himalayas, followed by a decrease towards the higher ranges is evident from the observed records at Dibrugarh (285 cm) in the eastern part of the valley through Pasighat (507 cm) in the foothills to Tuting (274 cm) further up in the Himalayas. Monsoon rains from June to September accounts for 60-70% of the annual rainfall. These rains that contribute a large portion of the runoff in the Brahmaputra and its tributaries are primarily controlled by the position of a belt of depressions, called the monsoon trough, extending from northwest India to the head of the Bay of Bengal. In the course of the north-south oscillations in summer, when this axis moves closer to the foothills of the Himalayas, heavy precipitation occurs in Assam and adjoining highlands. The severity of rainstorms occasionally reaches as high as 40 cm per day. The years 1998 and 2004 which saw extremely high floods in the region also recorded excessively high rainfall, especially in the upper basin areas. Rainfall recorded at Guwahati during the monsoon months in 1998, June through September, is 922 mm, while at Dibrugarh it is 2002 mm and Pasighat in Arunachal Pradesh 4573 mm accounting for 60%, 67% and 75% of the annual rainfall respectively (Goswami et al, 2000). During the flood season, all the districts in Arunachal Pradesh receive rainfall much above the normal rainfall. The intensity of rainfall recorded at Dibrugarh on June 28, 1998 is of the order of 17mm/hr.



The Brahmaputra basin, especially its monsoon dominated wetter parts, is enormously rich in biotic resources with a great diversity of flora and fauna types marked by significant variations, both in vertical and horizontal distributions. The forest cover of the basin in India, as indicated by recent satellite surveys, is 144,922 km<sup>2</sup>, which accounts for 59% of the total geographical area (Myint and Hofer, 1997). In contrast to this, the total basin forest cover including the portion outside India accounts for only 14.07% of the total geographical area of the basin. The distribution of forest cover in different states lying within the basin in India is estimated as: Arunachal Pradesh (82.8%), Nagaland (68.9%), Meghalaya (63.53%), Sikkim (39.52%), West Bengal (21.4%) and Assam (20.56%) (Myint and Hofer, 1997). In fact, Arunachal Pradesh accounts for about 60% of the forest cover in the Indian part of the basin.

The vegetation changes from tropical evergreen and mixed deciduous forest in the Assam valley and the foothills, through temperate coniferous belts in the middle Himalayas to alpine meadows and steppes in the still higher ranges. There has been considerable decline in the forest cover due to deforestation, land use conversion and land degradation in the basin. Shifting cultivation, involving traditional slash and burn technique of agriculture which is widely being practiced in the hills of northeast India, is a major cause of environmental degradation leading to deterioration of forest cover, loss of biodiversity, soil erosion, loss of soil fertility and crop yield, reduction in ground water recharge, increase in surface runoff, lowering of water table and acceleration in the rates of sedimentation in rivers and reservoirs downstream.

The Brahmaputra basin in northeast India provides a unique habitat for an exquisite variety of fauna, some of which belong to the most rare and endangered species. The floodplain of the Brahmaputra river in Assam is dotted with a large number of wetlands, numbering more than 3500, which have great significance as unique habitats for exquisite varieties of flora and fauna and also as natural flood water retention basins. Degradation and destruction of these wetlands have considerable impact on the deteriorating flood hazard scenario in the state.

### **3.4 THE BRAHMAPUTRA RIVER SYSTEM**

The Brahmaputra river, termed as a moving ocean, is an antecedent snow-fed large Trans-Himalayan river which flows across the rising young Himalayan range. Considerable variations in width, gradient, discharge and channel pattern occur throughout its course. Geologically, the Brahmaputra is the youngest of the major rivers of the world and unique in many respects. It happens to be a major river for three countries, viz., China, India and Bangladesh. The river basin of the Brahmaputra is bounded on the north by the Kailas and Nyen- Chen-Tanghla ranges of mountains; on the east by the Salween river basin and the Patkai range running along the Indo-Myanmar border; on the south by the Nepal Himalayas, the Naga and Barail ranges and the Meghalaya Plateau; and on the west by the Ganga river basin.

The maximum meridional extent of the basin is 1,540 km along 29°30' N latitude and maximum latitudinal extent is 780 km along 90° E longitude. The total length of the river is 2,880 km (Table-3.1). Several tributaries join the river all along its length. The average annual runoff of the Brahmaputra at Pasighat,

Pandu and Bahadurabad in Bangladesh is 186,290, 494,357 and 589,000 million cubic metre respectively. The monsoon flow of the Brahmaputra at Tesla Dzong in Tibet is 36.27% of the flow at Pasighat (WAPCOS, 1993).

Throughout its course within India, the Brahmaputra is braided with some well defined nodal points where the river width is narrow and restricted within stable banks. All along its course in the valley, abandoned wetlands and back swamps are common. The river carries about 735 million metric tons of suspended sediment loads annually.

The Indian section of the Brahmaputra river receives innumerable tributaries flowing down the northern, north-eastern and southern hill ranges. The mighty Brahmaputra along with the well-knit network of its tributaries controls the geomorphic regime of the entire region, especially the Brahmaputra valley. In the north, the principal tributaries are the Subansiri, the Jia Bhareli, the Dhansiri, the Puthimari, the Pagladiya, the Manas and the Champamati. Amongst these, the Subansiri, the Jia Bhareli and the Manas are the Trans-Himalayan rivers. The principal south bank tributaries are the Burhi-Dehing, the Disang, the Dikhow, the Dhansiri (south), the Kopili and the Krishnai. Hydrological characteristics of 18 important north bank tributaries and 10 important south bank tributaries are presented in Table 3.2.

It is observed that three Trans-Himalayan tributaries, the Subansiri, the Jia Bhareli and the Manas on the north have a basin more than 10,000 km<sup>2</sup>, i.e., only two south bank tributaries the Dhansiri and the Kopili form a basin area more than 10,000 km<sup>2</sup>. The Manas river combined with the Aie and the Beki rivers drains biggest area of 41,350 km<sup>2</sup>. The 442 km long Subansiri river and

the 360 km long Burhi Dehing river are considered longest, respectively, among the north-bank and south bank tributaries (Water Year book, CWC, 2002). In terms of the average annual discharge, the Subansiri carries a discharge of 755, 771 m<sup>3</sup>/sec, which ranks first among all the important tributaries. The Jia Bhareli and the Manas in the north carrying an average annual suspended sediment load of 2,013 ha.m and 2,166 ha.m, respectively, are the leading rivers in the case of sediment discharge (Goswami et al, 2000). Of all the north and south bank tributaries, as many as fourteen have sediment yields in excess of 500 tons/ km<sup>2</sup> /year, the highest being 4,721 tons/km<sup>2</sup> /year.

### **3.5 THE TRIBUTARIES OF THE BRAHMAPUTRA RIVER**

In the past, the Dibang and the Lohit, two major rivers joined the Dihang a short distance upstream of Kobo to form the Brahmaputra. Now, the situation has quite changed. Dibang and Lohit join Dihang through another channel Dibru, developed due to phenomenon called river avulsion. Dibru is receiving major part of the discharge of Lohit for the last few years. The river receives numerous tributaries from both sides all along its course, thereby progressively growing in its size. Some of the tributaries are trans-Himalayan rivers with considerable discharges. In the north, the principal tributaries are the Subansiri, the Jia Bhareli, the Dhansiri (north), the Puthimari, the Pagladiya, the Manas, the Champamati. On the south bank the main tributaries are the Burhi Dehing, the Disang, the Dikhow, the Dhansiri (south) and the Kopili. The Brahmaputra also has some important tributaries, like the Tista, the Jaldhaka, the Torsa, the Kaljani and the Raidak flowing through North Bengal.

The important tributaries on both the north and the south bank of Brahmaputra are listed in Table 3.3 along with chainage in km of their present outfalls from Indo Bangladesh border. The position of the outfall changes whenever bank erosion takes place there. Besides these tributaries, there are many other small streams which drain directly into the river.

Certain fluvio-geomorphic features which are found in the Brahmaputra basin have a significant bearing on the characteristics of the north and south bank tributaries. The variations in environmental settings, including geology, geomorphology, physiography, relief, precipitation and soils of the two regions belonging to the north bank and south bank river basins bring about notable differences between these two groups of rivers. On the north, the rainfall is heavier and the hills are less stable and more liable to soil erosion and landslides. In consequence, the north bank tributaries carry larger silt charge. The Brahmaputra river is closer to the hills on the south as if the river has been pushed southwards over geological period by the more numerous and heavier silt carrying north bank tributaries. The characteristics of north bank and south bank tributaries reveal the following points of differences.

### **3.5.1 THE NORTH BANK TRIBUTARIES**

1. The north bank tributaries have higher rainfall and pass through the Himalayan reaches with steep channel gradient.
2. In case of northern tributaries, the long section of river course is in the hilly terrain while the small section is in the plains.
3. The northern tributaries carry an enormous sediment load as compared to the southern tributaries. On an average, the sediment yield of the north-

bank tributaries is three times higher than that of the south bank tributaries coming out of the Naga, Mikir hills and the Meghalaya plateau (WAPCOS, 1993).

4. Due to steep slope and heavy sediment load, these streams are braided over major portion of their travel. These have shallow braided channels for a considerable distance from the foot of the hill and in some cases right up to the outfall.
5. The northern tributaries have generally coarse sandy beds with occasional gravel beds up to some distance from the foothills.
6. These tributaries generally have flashy floods.
7. The basins of all the north bank tributaries have hypsometric curves with a plateau indicating a relatively youthful stage in their development.
8. The north bank tributaries show a general parallel drainage pattern.
9. The northern tributaries have shallow braided channels.
10. The northern tributaries are characterized by frequent shifting of their channels during floods. As revealed by the study, the northern tributaries have peculiar channel shifting patterns. The Subansiri and all other eastern rivers shift their channels westward, while the rivers between the Pagladiya and Subansiri shift eastwards. Again from the Manas up to the river Sonkosh in the west, all the rivers migrate westward.

### **3.5.2 THE SOUTH BANK TRIBUTARIES**

1. These tributaries have comparatively flatter gradient and deep meandering channels almost from the foot hills.

2. The southern tributaries have beds and banks composed of fine alluvial soils.
3. The southern tributaries have their long courses over the plains.
4. These tributaries have comparatively less silt charge with finer fractions.
5. In contrary to the north bank basins, the basins of the tributaries from the south bank indicate much mature stage with hypsometric curves showing a continuously decreasing profile.
6. The south bank tributaries while keeping the parallel drainage pattern, show signs of dendritic configuration.
7. The southern tributaries change their courses less frequently.
8. The southern ones have their meandering channels over the plains.

### **3.6 HYDROLOGICAL CHARACTERISTICS OF SOME MAJOR TRIBUTARIES**

The hydrological characteristics such as basin area, length, average annual discharge, average annual suspended load and the sediment yield of some major tributaries are outlined in Table-3.2.

**Table-3.2 Hydrological characteristics of some major tributaries**

<b>Tributaries</b>	<b>Basin Area (Km<sup>2</sup>)</b>	<b>Length (Km)</b>	<b>Average annual discharges (m<sup>3</sup>/sec)</b>	<b>Average annual suspended load (ha. m)</b>	<b>Sediment yield (ton/ Km<sup>2</sup> /year)</b>
<b>Northern Tributaries</b>					
1. Subansiri	28,000	442	755,771	992	959
2. Ranganadi	2,941	150	74,309	186	1,598
3. Burai	791	64	20,800	16	529
4. Bargang	550	42	16,000	27	1,749
5. Jia Bhareli	11,716	247	349,487	2013	4721
6. Gabharu	577	61	8450	11	520
7. Belsiri	751	110	9300	9	477
8. Dhansiri (North)	1,657	123	26,577	29	463
9. Noa Nadi	907	75	4450	6	166
10. Nanoi	860	105	10,281	5	228
11. Bamadi	739	112	5756	9	323
12. Puthimari	1,787	190	26,324	195	2,887
13. Pagladiya	1674	197	15201	27	1,883
14. Manas-Aie-Beki	41,350	215	307,947	2,166	1,581
15. Champamati	1,038	135	32,548	13	386
16. Gaurang	1379	98	22,263	26	506
17. Tipkai	1,364	108	61,786	31	598
18. Gadadhar	610	50	7,000	0.21	272
<b>Southern Tributaries</b>					
1. Burhi Dehing	8,730	360	1411,539	210	1,129
2. Disang	3,950	230	55,101	93	622
3. Dikhow	3,610	200	41,892	34	252
4. Jhanzi	1,130	108	8,797	16	366
5. Bhogdoi	920	160	6072	15	639
6. Dhansiri (South)	10,242	352	68,746	147	379
7. Kopili	13,556	297	90,046	118	230
8. Kulsi	400	93	11,643	0.6	135
9. Krishnai	1,615	81	22,452	10	131
10. Jinari	594	60	7,783	3	96



**TABLE 3.3 Tributary distance measured from Indo Bangladesh Border  
(from Dhubri along the upstream)**

SI No	North Bank Tributaries	Chainage in km.
1.	Simen	580
2.	Jiyadhoh	540
3.	Subansiri	430
4.	Burai	392
5.	Bargang	382
6.	Jia Bhareli	338
7.	Gabhru	300
8.	Belsiri	280
9.	Dhansiri	270
10.	Noa Nadi	230
11.	Nanai Nadi	215
12.	Bar Nadi	205
13.	Puthimari	172
14.	Pagladiya	170
15.	Beki	115
16.	Manas	85
17.	Champamati	63
18.	Gurang	43
19.	Tipkai	40
20.	Sankosh	0

SI No	South Bank Tributaries	Change in km
1.	Dibru	592
2.	Burhi Dihing	540
3.	Disang	515
4.	Dikhow	505
5.	Jhanzi	495
6.	Dhansiri (south)	420
7.	Kopili	220
8.	Kulsi	140
9.	Deosila	130
10.	Dudhnai	108
11.	Krishani	107
12.	Jinari	100
13.	Jinjiram	0

### 3.7 HYDRAULIC CHARACTERISTICS

The hydraulic characteristics describing the average annual runoff of the Brahmaputra and its major tributaries are represented in Figure 3.4 a schematic diagram.

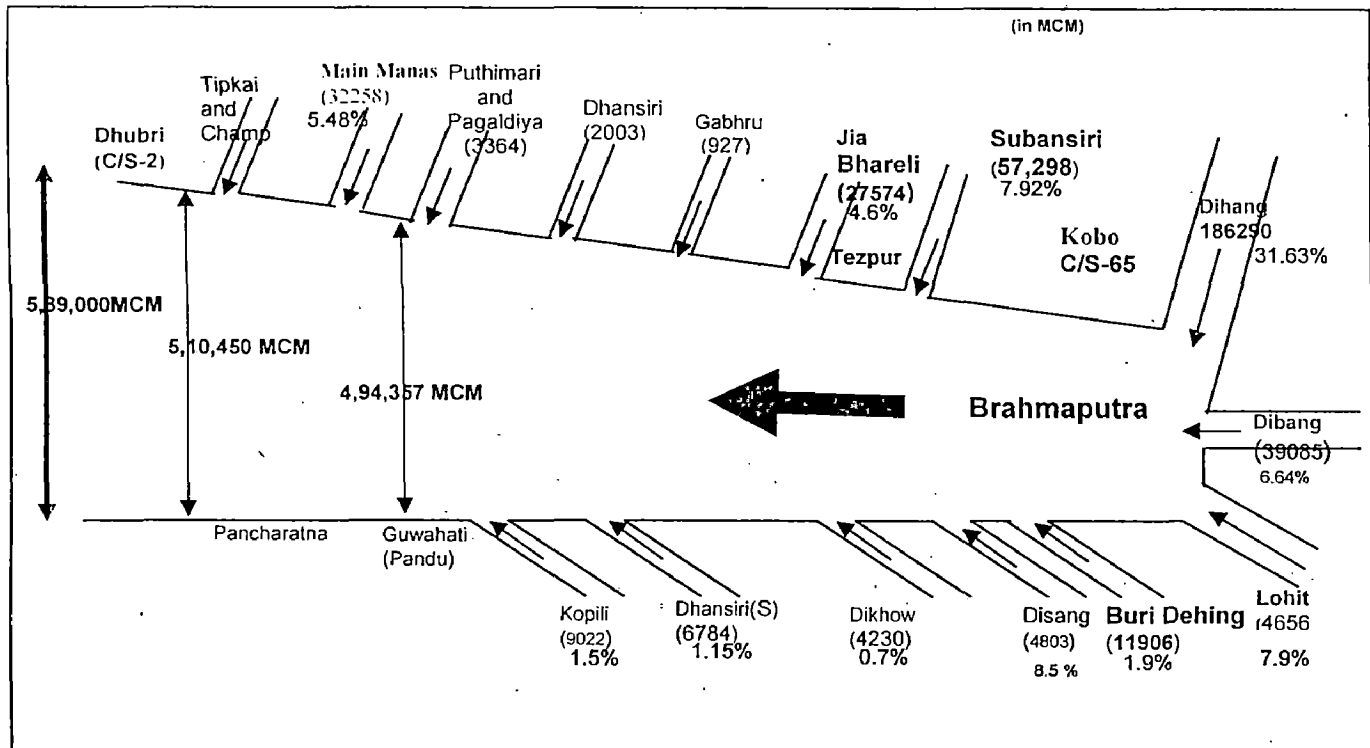


Figure-3.3 Average Annual Runoff of the Brahmaputra

### 3.8 HYDROLOGIC AND PHYSIOGRAPHIC CHARACTERISTICS OF THE BRAHMAPUTRA

The statistical details of the Brahmaputra river are described below:

(a) Total basin area from its source to its confluence with Ganga at Goalundo

- |                                  |                         |
|----------------------------------|-------------------------|
| in Bangladesh                    | 580,000 km <sup>2</sup> |
| • Basin area within Tibet        | 293,000 km <sup>2</sup> |
| • Basin area in Bhutan and India | 240,000 km <sup>2</sup> |
| • Basin area in Bangladesh       | 47,000 km <sup>2</sup>  |

- |     |   |                            |
|-----|---|----------------------------|
| (b) | Length from its source to outfall in Bay of Bengal  | 2,880 km                   |
|     | • Length within Tibet   | 1,625 km                   |
|     | • Length within India   | 918 km                     |
|     | • Length within Bangladesh  | 337 km                     |
| (c) | Gradient  |                            |
|     | • Reach within Tibet  | 1 in 385                   |
|     | • Reach between Indo-China border and Kobo in India   | 1 in 515                   |
|     | • Reach between Kobo and Dhubri   | 1 in 6,990                 |
|     | • Reach within Bangladesh   |                            |
|     | First 60 km from Indian Border  | 1 in 11,340                |
|     | Next 100 km stretch   | 1 in 12,360                |
|     | Next 90 km stretch  | 1 in 37,700                |
| (d) | Observed discharge  |                            |
|     | • Maximum observed discharge at Pandu (on 23.8.1962)  | 72,727 m <sup>3</sup> /sec |
|     | • Minimum observed discharge at Pandu (on 20.2.1968)  | 1,757 m <sup>3</sup> /sec  |
|     | • Average dry season discharge at Pandu   | 4,420 m <sup>3</sup> /sec  |
| (e) | Normal annual rainfall within basin ranges between 2125 mm in Kamrup district of Assam and 4,142 mm in Tirap district of Arunachal Pradesh. |                            |

### 3.9 GEOLOGY AND GEOMORPHOLOGY

The Brahmaputra basin in India, comprising of varying geologic and geomorphic characteristics, represents its peculiar physiographic make-up. The basin is bounded by the eastern Himalayas on the north and east, the Naga-Patkai ranges on the northeast and Meghalaya Plateau and Mikir hills on the south. The region can be geologically and tectonically divided into four major

zones, viz. the Himalayan folded and Tertiary hills and mountains, the Naga-Patkai ranges, the Meghalaya Plateau and Mikir hills and the Brahmaputra valley in Assam.

The Himalayan zone comprises of three topographic units that rise progressively to the north. The lowermost ranges, called sub-Himalayas with an average elevation of 1,000 m, consist mainly of Tertiary sand stones, and are conspicuous by the presence of many raised, relatively young terraces (Gansser, 1964). The middle Himalayas, having an average elevation of 4,000 m are underlain by lower Gondwana (Palaeozoic) deposits comprising shales, slates, and phyllites overlain by a thick horizon of basaltic rocks. The greater Himalayas with an average elevation of 6,000 m consist primarily of granites and gneisses (Goswami, 1985). The Himalayan Mountains with their syntaxial N-E bends originated out of the Tethyan Geo-syncline (Wadia, 1968) and are essentially composed of loose sedimentary rocks. The sub Himalayas and the lower Himalayas are characterized by piedmont zones, low discontinuous ridges, low linear ridges, high rugged hills and upland valley depressions.

The Patkai-Naga ranges stand on the eastern and south-eastern border of the Brahmaputra valley in Assam. These ranges, with an average elevation of 1,000 m, are composed of Tertiary sediments and characterized by the presence of a large number of active faults. This zone consists of piedmont plains, anticlinal ridges and synclinal valleys with terraced alluvial fills, undifferentiated sharp ridges and narrow valleys, upland valley depressions and plateau remnants. The Meghalaya plateau and the Mikir hills attaining an elevation ranging from 600 m to 1800 m are made up primarily of gneisses and schist. This part, being a rigid mass, belongs to the Deccan plateau of the

stable Indian peninsular block of Pre-Cambrian age. It is characterized by plateau remnants, inselbergs, deeply dissected uplands with faulted monoclines of Tertiary cover, denuded hills, basement controlled structural ridges covered with Tertiary rocks and upland valley depressions.

The Brahmaputra valley in Assam, on the other hand, is underlain by recent alluvium approximately 200-300 m thick, consisting of clay, silt, sand, and pebbles (Geological Survey of India, 1974). The valley is developed over the fore deep in between the peninsular mass and the Tethyan geosynclines. The fore deep is characterized by some complicated tectonic features represents a series of faults and thrust extending in the NE-SW direction from the eastern margin of the Meghalaya plateau across the North Cachar Hills to Tirap District of Arunachal Pradesh. These thrusts are originated at the time of the late Himalayan-Patkai-Naga Hills orogeny and pushed the tertiary deposits into folds and faults. The fore deep is believed to be under the sea till the sub-recent period received deposits during all the periods of the tertiary and quaternary ages. The tertiary deposits consist mainly of sand stones, shale, grit, conglomerate and lime stones.

Towards the close of the Pleistocene period, alluvium began to be deposited in the form of sand, pebbles and gravels especially along the northern foothills of the Brahmaputra valley. These valley deposits of reddish brown sandy clay with some pockets of unasserted pebble, cobble, sand and silt have been identified as older alluvium. The tertiary beds of the valley are overlain by a thick layer of newer alluvium composed of sand, silt and clay, which are being brought down from the rising Himalayas in the north, the Patkai Naga ranges in the east and south-east and the Meghalaya plateau in the south

by numerous tributaries of the Brahmaputra. The characteristic geological and tectonic framework coupled with structural complexities has rendered the Brahmaputra basin geo-morphologically a most complicated one. A variety of landform under varied climatic conditions has formed over the geologic and tectonic base of the region. The peri-glacial, glacio-fluvial, and fluvial processes are dominantly operative in the basin at varying altitudes.

The higher elevations of the Himalayas experience peri-glacial and glacio-fluvial erosion and deposition. The bare relief of the sub-Himalayas and greater Himalayas suffer from immense sheet erosion owing to peri-glacial solifluction. The low hill ranges with hot and humid climate and heavy rainfall concentrated to a few months of the year experience solifluction, sheet erosion and landslides.

The incidence of landslides is high in the Himalayan foothills, where heavy rainfall, high seismicity and toe cutting of hill slopes by the streams are most frequent. Heavy rains often loosen soil and the soft rocks of the young Himalayan ranges. Rainwater percolates through joints, fractures, foliations, and pores of rocks and soils and finally makes them loose and heavy, which cause heavy slope failure. Fluvial processes are, on the other hand, significantly dominant on the valley bottoms and plains where alluvial deposition takes place due to erosion of the higher surface by rivers and flooding in the valleys. The erosional and depositional processes conspicuously intensified by copious rainfall and frequent seismic movements, however, play a dominant role in creating various fluvio-geomorphic environments in the basin.

### 3.10 CHANNEL PROCESSES

The Brahmaputra river in India forms a complex river system characterized by the most dynamic and unique water and sediment transport pattern. The Brahmaputra is the fourth largest river in the world in terms of the average discharge at the mouth with a flow of 19,830 m<sup>3</sup>/sec (Goswami, 1982). The water yield from per unit basin area is among the highest of the major rivers of the world. The Jia Bhareli river, a major tributary for example carries a mean annual water discharge in the order of 0.0891 m<sup>3</sup>/sec/km<sup>2</sup> (Bora, 1990). As estimated by Goswami (1982), the Brahmaputra yields 0.0306 m<sup>3</sup>/sec/km<sup>2</sup> at Pandu. As regards sediment transport, the river has also set records in carrying large volumes of sediment. The high intensity of monsoonal rains, easily erodible rocks, steep slopes, and high seismicity contribute a lot by rendering the river a heavily sediment-laden one. Thus, the Brahmaputra becomes one of the leading sediment carrying rivers of the world. Amongst the large rivers of the world, it is second only to the Yellow river in China in the amount of sediment transport per unit of basin area (Goswami, 1985).

At Pandu, the river carries an average suspended load of 402 million metric tons. A river with such gigantic water and sediment discharge magnitudes represents its most dynamic fluvial regime. Its large alluvial channel having a width of 6 to 10 km is, therefore, marked by intense braiding, rapid aggradation and drastic bank line changes. The Brahmaputra is a uniquely braided river of the world. Although braiding seems to be best developed in rivers flowing over glacier outwash plains or alluvial fans, perfect braiding is also found to occur in large alluvial rivers having low slope, such as the Brahmaputra in Assam (India) and Bangladesh or the Yellow River in China. The Assam

section of the Brahmaputra River is in fact, highly braided and characterized by the presence of numerous lateral as well as mid channel bars and islands.

The high degree of braiding of the Brahmaputra channel near Dibrugarh and downstream of Guwahati is indicated by the calculated braiding indices of 5.3 and 6.7 respectively for the two reaches, following the method suggested by Brice (1964). A braiding Index of 4.8 for the entire Assam section of the river calculated on the basis of satellite data of 1993 also suggests a high degree of braiding of the Brahmaputra river.

The basin with varied terrain characteristics and being an integral part of the monsoonal regime of south-east Asia shows a marked spatial variation in the distribution of precipitation. The rainfall in the Tista valley varies from 164 cm in the south to 395 cm in the north. The average annual rainfall in the lower Brahmaputra valley is 213 cm while the same in the north-eastern foothill belt is 414 cm. The basin as a whole has the average annual rainfall of 230 cm with a variability of 15-20%. The Himalayan sector receives 500 cm of rainfall per year, the lower ranges receiving more than the higher areas (Goswami, 1985). During the monsoon, months of May to October receive about 12% of the annual total.

In the sub-Himalayan belt soils with little depth developed over the Tertiary sand stones generally belong to red loam, laterite, and brown hill soil type with admixtures of cobbles and boulders. The greater part of the Brahmaputra valley is made up of new alluvium of recent deposition overlying Tertiary, Mesozoic and Archaean bedrocks. Along the piedmont zone, there occurs some patches of older alluvium extending along the interfluves of the tributaries flowing from the Himalayan foothills. The soils of the Meghalaya



plateau and the Mikir Hills in the south are of laterite and loamy silt and fine silt types.

In general, braiding in the Brahmaputra follows the mechanism of central bar type of braid formation. During high flow, a central bar is deposited in the channel and gradually the bar accretes vertically to the level of the floodplain. It also builds on the downstream end through deposition of bed load material due to the slack water occurring behind the bar. The bar growth causes a decrease in total cross-sectional area leading, thereby, to the instability of the channel. Lateral erosion then follows on one or both the banks. Through repetition of this process in the divided reach, a well developed braided reach with multiple sandbars and islands is produced.

In the Assam section of the river, the presence of such nodes of stable banks is found to effect the formation and location of the bars. There are nine nodal reaches of narrow constriction at various locations along the Brahmaputra which are at Murkongselek (4.8 km), Disangmukh (5.10 km), downstream of Jhanjimukh (3.75), upstream of Dhansiri north (4.0 km), downstream of Dhansirimukh (4.4 km), upstream of Tezpur (3.6 km), Pandu, Guwahati (1.2 km), Soalkuchi (2.4 km) and Pancharatna (2.4 km). Since banks are relatively stable in these reaches, the river scours deeper to accommodate the flood discharge. The scoured debris is then deposited in the channel immediately downstream from the narrow section. As a result, the channel becomes wider and bars and islands are produced. Formation of bars causes reduction in cross sectional area and the river, therefore, cuts its banks laterally to accommodate the discharge. Thus the downstream of the nodes intense braiding develops

resulting in channel widening through continuous migration of both banks of the Brahmaputra.

As reported from the studies carried out on braided rivers of the world, the major factors thought to be responsible for braiding and bar formation are steep channel gradient, high erodibility of bank materials, great variability in discharge, overabundance of load, and aggradation of the channel bed. In case of the Brahmaputra river in Assam bar formation and channel division are owing to a combination of factors like high variability in discharge, excessive sediment transport, easily erodible bank materials and aggradation of the channel. Being the fourth largest river in the world with an average discharge of 19,830 m<sup>3</sup>/sec at its mouth (Goswami, 1982), the Brahmaputra carries 82% of its annual flow at Pandu (Assam) only during the rainy season from May to October. The mean annual maximum and minimum flows in the river during 1955-97 are 48,160m<sup>3</sup>/sec and 3,072 m<sup>3</sup>/sec, respectively. On an average, therefore, the maximum flow is more than fifteen times the minimum.

High variability in discharge of the river is mainly caused by seasonal rhythm of the monsoon and the freeze-thaw cycle of the Himalayan snow. As regards the pattern of sediment transport, the river has the record of carrying excessive sediment load which is believed to be one of the important factors responsible for braiding.

### **3.11 DATA USED**

#### **3.11.1 SATELLITE DATA**

The satellite index maps of the river Brahmaputra as covered by the Indian Remote Sensing Satellite (IRS) 1A and 1D are presented in Figure 3.4 and Figure 3.5 respectively. The satellite data used is listed below in Table 3.4.

Satellite scenes covering the study area are identified from the satellite pass index map of IRS. Dates of satellite passes over the area are selected from the orbital calendars available for the years under consideration. However, it was not possible to procure the data of monsoon period as the area acquired by the satellites indicated presence of cloud cover for the period under study. In all, the digital satellite data comprising of 8 scenes of Indian Remote Sensing Satellite (IRS) Linear Imaging Self Scanner (LISS) I and LISS III for the year 2002 is analyzed. Radarsat satellite data of February, 2002 have been made use of. In addition to the above, Advanced Very High Resolution Radiometer (AVHRR) sensor data of National Oceanographic and Atmospheric Administration (NOAA) satellite having resolution of 1.1 km of July and August 2002 have been used to study the flood scenario. Digital Elevation Model (DEM) data of the year 2002 for the sub basin also has been used to derive the drainage details of the area.

### **3.11.2 TOPOGRAPHIC DATA**

The study area comprised of 64 pre-defined cross sections stretched over 622.73 km length of the river Brahmaputra. It is also one of the most braided rivers in the world with width variation from 1.2 km at Pandu near Guwahati to about 18 km few km distances downstream to this point. In an individual cross section, the number of survey points varies from 50 to 150.

### **3.11.3 HYDROLOGIC DATA**

The maximum water levels of the river at discretized cross sections have been used. In the present study, average monthly discharge data for the monsoon period, i.e. 15<sup>th</sup> May to 15<sup>th</sup> October have been used. These data were

collected from Central Water Commission, New Delhi, India. Overall 36 set of data spanned over 12 years from 1991 to 2002 were collected.

### **3.12 VALUES OF MEDIAN SIZE, KINEMATIC VISCOSITY AND ACCELERATION DUE TO GRAVITY**

#### **3.12.1 MEDIAN SIZE:**

section 09: 0.148mm,

section 22: 0.150mm,

section 50: 0.152mm

The median size of bed material is important parameter in the analysis of almost all the aspects of alluvial rivers such as regime, resistance to flow, and the sediment transport. In this connection it can be seen that bed material at Panchratna is relatively fine. It contains about 10% of the material which is finer than 0.06mm and the material coarser than 0.40mm is only 2%. It is possible that some of the coarse material could not be sampled; yet the bed material seems to be very fine. As a result, the river is likely to carry relatively large amount sediment in suspension and relatively less amount as bed load. Because of the sediment being mostly in suspension, abrasion and attrition has not contributed to the variation of sediment size as one proceeds downstream along the river. This may probably be the reason why there is not much change in the sediment size along the length of the river.

#### **3.12.2 KINEMATIC VISCOSITY OF WATER:**

Viscosity of water varies with temperature, and at 20° Celsius the value is  $1.00 \times 10^{-6} \text{ m}^2/\text{sec}$ . Due to climatic condition of Brahmaputra basin it is wise to adopt the above value of kinematic viscosity.

### **3.12.3 ACCELERATION DUE TO GRAVITY:**

The value of acceleration due to gravity is  $9.8 \text{ m/sec}^2$  at poles and  $9.78 \text{ m/sec}^2$  at equator. Therefore a value of  $9.78 \text{ m/sec}^2$  is adopted for calculations.

### **3.13 COLLATERAL DATA**

Thematic maps and reports of Ministry of Water Resources, Government of India providing static information on land use, flood inundation, embankment systems etc. over the Brahmaputra basin are referred to while carrying out the satellite data interpretation work.

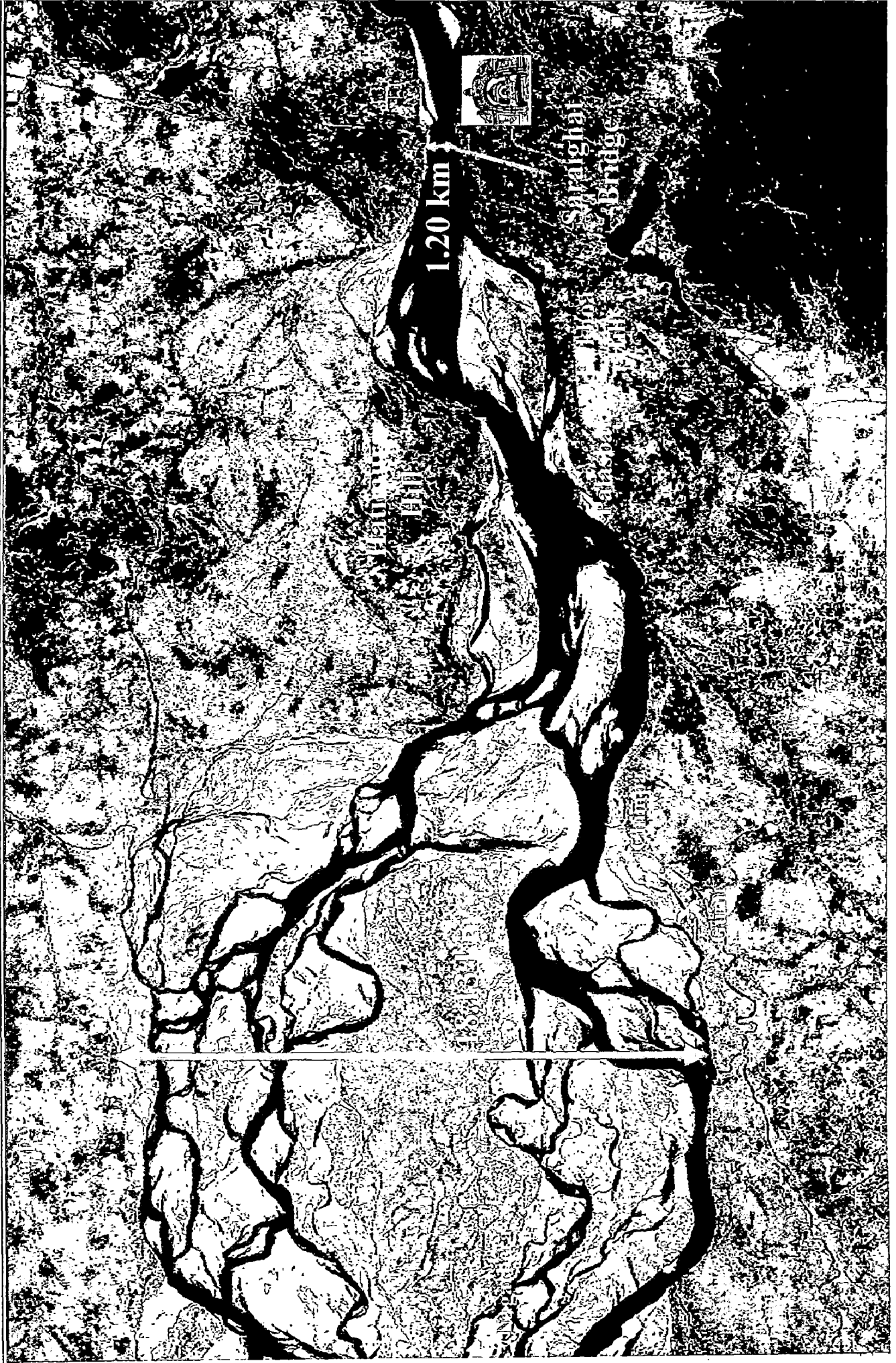


Figure 3.2 Radersat image (FCC) at d/s of Guwahati

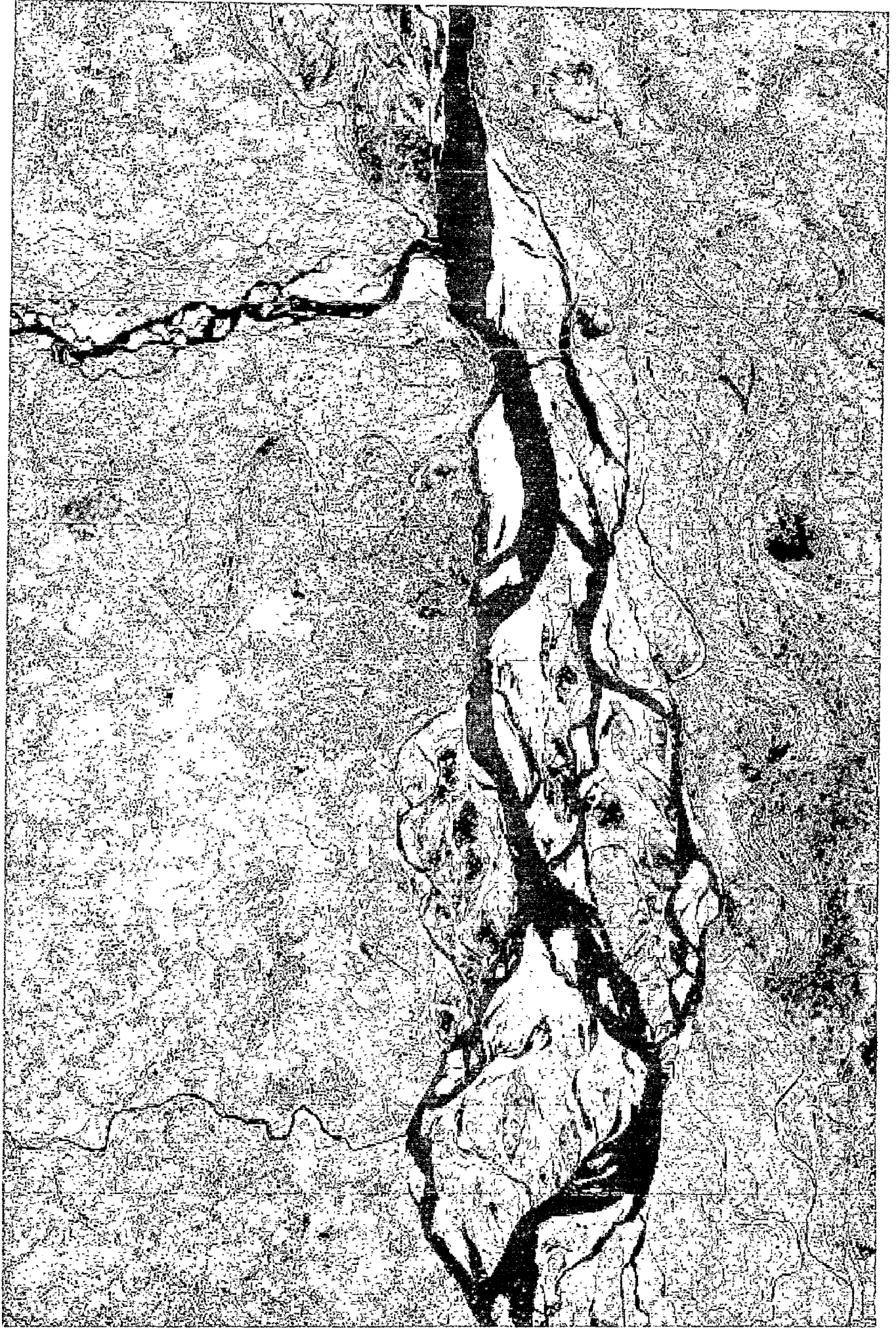


Figure 3.3 Radarsat image near Tezpur, 2002

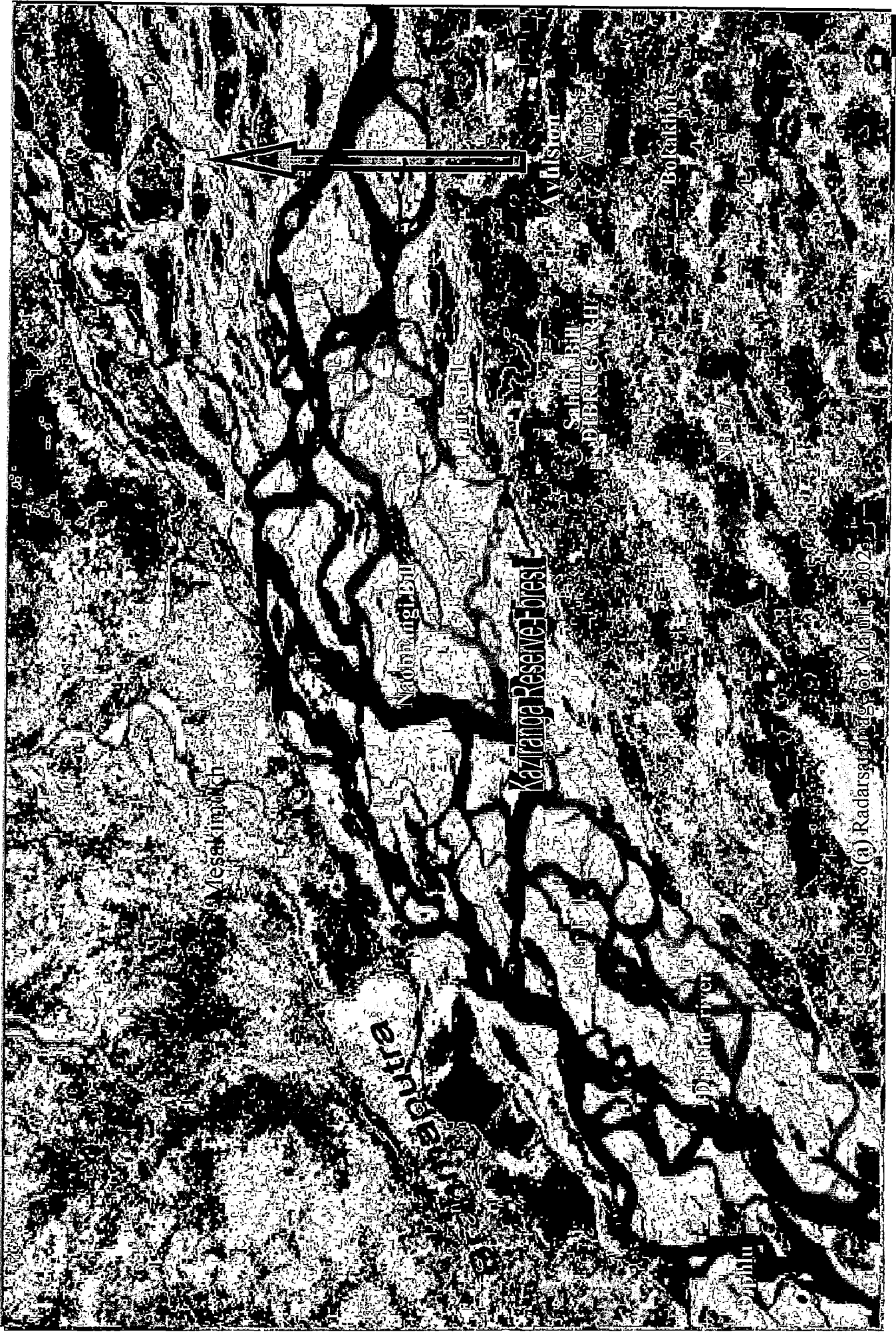


Figure 3.4 (a) Radarsat image of Kaziranga Reserve Forest, 2002

Figure 3.4 Radarsat image of Kaziranga Reserve Forest, 2002





Figure 3.5 Radersat image of the Brahmaputra, 2002

## CHAPTER 4

### FLOOD PLAIN MODELLING OF RIVER BRAHMAPUTRA

---

#### 4.1. GENERAL

Flood plain modelling of river Brahmaputra is carried out under the subheadings: Flood plain delineation, Formation of mathematical relationships for wetted area and perimeter, development of regime equations for river Brahmaputra, development of mathematical relationships for gauge discharge curve of river Brahmaputra

#### 4.2. FLOOD PLAIN DELIENATION

The river Brahmaputra flowing through the state of Assam (India) floods every year. The analysis of spatial extent and temporal pattern of flood-inundated areas is of prime importance for mitigation of floods. With the development of remote sensing techniques, flood mapping for large areas can be done easily. In case of flood inundation, mapping of large area it will not be feasible to use high-resolution data, because the whole area will be covered in number of scenes. Therefore, use of NOAA (National Oceanographic Atmospheric Administration) data is quite useful in flood of studies. NOAA-AVHRR (Advanced Very High Resolution Radiometer) data have the potential for flood monitoring due to high frequency of global coverage, wide swath, high repetitive and low cost. In this study, NOAA-AVHRR data have been used for flood monitoring during the year

2002. Based on spectral characteristics of land and water, a methodology for water identification has been presented.

The maximum spatial extent of floods, generated by compiling the available cloud free maps, is informative about flood damages. Analysis of results reveals that in the months of July and August almost 25-30% of the area was flood affected. In addition, the result indicates that in some districts, the flood inundation is very high.

Floods are the major disaster, affecting many regions around the world year after year. It is an inevitable natural phenomena occurring from time to time in all rivers and natural drainage system, which not only damages natural resources and environment, but also causes the loss of lives, economy and health. The impact of floods has been increased due to a number of factors, with rising sea levels and increase in development on flood plain areas (Sanders and Tabuchi, 2000). Among all natural disasters, floods are the most frequent to be faced by India. Floods in the eastern part of India (Orissa, Bengal, Assam, Bihar) in the recent times are the striking examples. The annual precipitation in India, including snowfall is estimated at 4000 Billion Cubic Meter (BCM). Out of this, the seasonal rainfall in monsoon is of the order of 3,000 BCM.

The rainfall in India shows great temporal and spatial variations, unequal seasonal distribution and geographical distribution and frequent departures from the normal (Mohapatra and Singh, 2003). Damage from flooding has been increasing each year resulting in loss of lives, property and production as well as affecting activities in the flooded areas. The large and long duration of flooding can be considered as the economic loss to the country. The non-structural methods of

mitigation of flood hazards are very cost effective as compared with structural ones (dams, dikes etc.). Among non-structural methods, modern flood forecasting and the association with real time data can tell us about the areas likely to be flooded.

Accurate information on the extent of water bodies is important for flood prediction, monitoring, and relief (Smith, 1997; Baumann, 1999). In addition, spatial extent and temporal variation of flood-affected areas are very much required for flood mitigation. Often this information is difficult to produce using traditional survey techniques because water bodies can be fast moving as in floods tides and storm surges or may be inaccessible. The synoptic, repetitive nature of satellite remotely sensed data have allowed monitoring of water bodies over large regions of land. Remote sensing techniques are used to measure and monitor the aerial extent of the flooded areas, to efficiently target rescue efforts and to provide quantifiable estimates of the amount of land and infrastructure affected.

In many studies Landsat data (TM and MSS), IRS or SPOT have been used to determine the extent of water bodies using simple classification procedures, usually with an infrared band. These studies have relied on the water bodies having a unique spectral response in this range of EMR when compared to the surrounding landscape (Wang, et al. 2002, Frazier and Page, 2000). Due to high resolution of these satellites, it requires a number of scenes to cover large area, which is neither economical nor feasible because of two different dates' scenes covering study area. NOAA AVHRR sensor provides data of an appropriate spatial and temporal resolution to support studies at regional to global scale. Because its temporal resolution is high, therefore possibility of cloud free data is more.

By combining data from two NOAA satellites (e.g. NOAA-16 and 17) the temporal resolution becomes almost double and hence chances for getting a cloud free scene are very high. In the early 1970, Wiesnet et al. (1974) recognized the use of AVHRR data in flood monitoring, since then a number of investigators have contributed in this area. Although the relatively coarse spatial resolution of 1.1 km at nadir confirms AVHRR data to monitoring major floods in plain areas, the high temporal frequency, the large area coverage, the low cost and easy processing of AVHRR data makes it a better option for use. Islam et al. (2000) assessed flood hazard in Bangladesh using NOAA AVHRR data. In order to estimate flooded area accurately, the images taken during the flood and dry season, which were classified into water and non-water categories, were superimposed. They also used elevation data to see the relation between elevation and remote sensing interpretation.

#### **4.3. DATA USED**

In this study NOAA AVHRR 16&17 data of March to October 2002 have been used. The data used have been browsed for the year 2002 starting from March 2002. In spite of the daily coverage of NOAA, only five cloud free scenes could be obtained and they are given as follows: March 24, May, July 23, August 05, and November 05.

Also, other collateral information from the journals is consulted during the present study. In addition, ground truth data have been collected during the field visits in the area, which confirmed the interpretation. The Brahmaputra river Atlas volume - I and volume-II, published by Brahmaputra Board, Government of India

have been consulted for deriving certain information. Bearing of cross-sections, latitude and longitudes of tributaries and important bridges have been collected from the Central Water Commission, Government of India.

#### **4.4. METHODOLOGY**

##### **4.4.1. GIS ANALYSIS**

The term digital image processing generally refers to processing of two – dimensional picture by a digital computer. A digital image is an array of real or complex numbers represented by finite number of bits. The processes are described in brief below.

##### **4.4.2. GEO-REFERENCING**

The image is assumed to be available as a matrix of M rows and N columns, with each element of the matrix being a vector of K components, each component representing the measurement in a particular wavelength band of electromagnetic spectrum. Each element of the image matrix is referred to as pixel (picture element). There are several processing operations, where each band of the data is processed separately. In such a case a single band image can be viewed as a black and white image and the value at each pixel may be viewed as shade of gray ranging from black to white. Thus, the pixel values are also referred to as gray levels (Lillesand and Kiefer, 1992). Geo-referencing the image to standard cartographic reference involves two major steps.

#### 4.4.3. TRANSFORMATION OF PIXEL CO-ORDINATES

The procedure requires that polynomial equation be fitted to the Ground Control Points (GCP) using least squares criteria to model the corrections in the domain without identifying the source of distortion. The image points are mapped from the distorted frame to the reference frame. An example of such a map can be represented by a polynomial in two dimensions as

$$x' = a_1x^2 + b_1y^2 + c_1xy + d_1x + e_1y + f_1 \quad (a)$$

$$y' = a_2x^2 + b_2y^2 + c_2xy + d_2x + e_2y + f_2 \quad (b)$$

x, y positions represent the coordinate positions in the distorted frame and x', y' the points in the reference frame.

#### 4.4.4. DETERMINATION OF THE GRAY LEVEL VALUES OF THE PIXEL MAPPED TO THE REFERENCE FRAME.

This step is necessary because integer co-ordinate locations in the distorted frame do not map to integer location in the reference frame. This process is more commonly known as re-sampling or registration.

#### 4.4.5. REGISTRATION

This involves extraction and interpolation of gray level from pixel location in the original distorted image and their re-location to the appropriate matrix coordinate locations in the rectified image. Methods of interpolating gray level include nearest neighbourhood, bilinear interpolation and cubic-spline interpolation. These methods produce increasingly better interpolated images, while consuming more computer time.

#### **4.4.6. PROCESSING OF SATELLITE DATA**

To study the extent of flood inundation, the analysis of time series NOAA data have been performed. Before processing of satellite data, base map of the study area has been prepared at a scale of 1:1 million. This base map shows rivers, canals and water bodies etc. Original NOAA data were rectified using radiometric calibration. For geometric registration, fifteen number of ground control points have been taken. For this purpose, second order transformation has been performed to account for conversion of lat/long data to a planar projection, earth's curvature, and distortion of data. In this study, data of the month of March were geo-referenced with the map of the state. The remaining AVHRR scenes were geo-corrected by image-to-image transformation techniques using the corrected image of the month of March.

#### **4.4.7. FLOOD INUNDATED AREA**

There are many possible methods for identifying water versus non-water areas using satellite data. Deep-water bodies have quite distinct and clear representation in the imagery. However, very shallow water/turbid water can be mistaken for soil while saturated soil can be mistaken for water pixels. Secondly, it is also possible that a pixel, only at the soil/water interface, may represent mixed conditions (some part as water and other part as soil).

Some of the methods of water identifications are as follows:

1. Single band slicing model



Many investigators (Lin, 1989, Sheng et al. 1998) have given that AVHRR channel 2 is more effective in distinguishing water from land than other channels following a simple model:

Water, if  $CH_2 \leq T_0$

Land, if  $CH_2 > T_0$

Where,  $CH_2$  is the reflectance of channel 2 and  $T_0$  is a threshold.

## 2. Temperature model

Barton and Bathols (1989) found that the night image of brightness temperature derived from AVHRR channel 4 was effective in monitoring the 1988 Darling flood in Australia. Vermin (1996) used a daytime image of brightness temperature from channel 5 for water and land discrimination in western Niger.

Water, if  $CH_{4/5} \leq T_0$

Land, if  $CH_{4/5} > T_0$

Where,  $CH_{4/5}$  is the brightness temperature of channel 4 and 5 and  $T_0$  is a threshold.

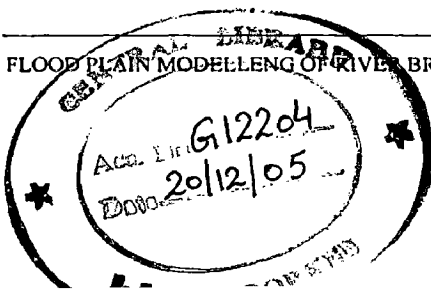
## 3. Differential model between channel 2 and 1

Xizo and Chen (1987) succeeded in identifying water bodies using the difference between channel 2 and the channel 1.

Water, if  $CH_2 - CH_1 \leq T_0$

Land, if  $CH_2 - CH_1 > T_0$

Where,  $CH_1$  and  $CH_2$  are the reflectance of channel 1 and 2 and  $T_0$  is a threshold.



#### 4. Ratio model between channel 2 and 1

Based on the spectral characteristics of ground features during floods, Sheng and Xiao (1994) designed a ratio scheme of Ch2.

Water, if  $CH2/CH1 \leq T_0$

Land, if  $CH2/CH1 > T_0$

Where, CH1 and CH2 are the reflectance of channel 2 and  $T_0$  is a threshold.

In case of individual AVHRR channel histogram with a bi-modal distribution is not possible therefore; it is difficult to determine the threshold value that separates water from land. However in some cases when there is sufficient moisture/water on the surface then single band thresholding methods can give good results. The temperature model usually works well in areas with a significant temperature difference between day and night, especially for floods resulting from melted snow water, because there is usually a temperature discrepancy between water and land. However, it may not work during rainy seasons in the summer when there is relatively low or no temperature difference between land and water, and when there are clouds.

The ratio image and the difference image between CH2 and CH1 can be used to enhance the difference between water and land in a better way.  $CH2/CH1$  has a better enhancing capability than  $CH2 - CH1$ . In the ratio image, water has extremely low value, while land has relatively high value. The histogram of the ratio image usually presents a distinct bi-modal distribution.

In areas covered by clouds and shadows, it is more difficult to identify water bodies. As an optical sensor, AVHRR cannot penetrate thick clouds. No method can eliminate cloud contamination under such circumstances. In case of this

clouds, the sensor does receive some signal from the underlying surface, even though mixed with cloud signal. Moreover, the spectral characteristics of water and land are so different that it is possible to distinguish water from land under thin cloud covers. The ratio image is immune to thin cloud contamination but the original channels are vulnerable. When cloud contamination is not very severe (thin clouds), some of the cloud influences (including clouds and their shadows) can be removed by the ratio image (model 4). Sheng et al. (1998) demonstrated the effectiveness of the ratio image in reducing cloud effect on water body recognition during floods. Figure 4.3 shows deep and shallow flood plain area.

#### **4.4.8. EXTRACTION OF CHANNEL FORMS**

The incident energy striking on the water surface is absorbed; hence it appears blackish blue on the satellite imagery. The highest absorption is in Near Infra-Red (NIR) band. In contrast to water the land features absorb much less incident energy depending on cover type, roughness, composition etc. This sharp contrast between land and water boundaries in NIR band makes delineation of the river boundary from the land mass easier.

As the study reach is covered by seven image frames, these are made into a single mosaic for 2002. The geo-referenced mosaic image frames is used to delineate the active river segments, tributaries, islands and bars in each period. The river braid belt is used to delineate the margins of the primary braided channel from each set of imageries and the channel patterns are digitized using Arc Info software to assess lateral movement between images for a spatial analysis of channel morphology over the period. On screen digitization on geo-referenced

satellite data is carried out for delineation of river boundaries and flood plain boundaries.

#### **4.4.9. DIGITAL ELEVATION MODEL (DEM)**

In this study, digital elevation model of the study area was extracted from global DEM. The input data used was the GTOPO30 global DEM developed in the late 1990's by a number of contributing organizations, which were coordinated by the U.S. Geological Survey's EROS data center in Sioux Falls, South Dakota. GTOPO30 was developed to meet the needs of the geospatial data user community for regional and continental scale topographic data. GTOPO30 is a global data set covering the full extent of latitude from 90 degrees south to 90 degrees north, and the full extent of longitude from 180 degrees west to 180 degrees east. Elevation in GTOPO30 is regularly spaced at 30-arc seconds (approx. 1 km). This release represents the completion of global coverage of 30-arc second elevation data that have been available from the EROS data center beginning in 1993. The horizontal grid spacing is 30-arc seconds, resulting in a DEM having dimensions of 21,600 rows and 43,200 columns. The horizontal coordinate system is decimal degrees of latitude and longitude referenced to WGS84. The vertical units represent elevation in meters above mean sea level. The elevation values ranges from -407 to 8,752 meters. The GTOPO30 DEM for India was downloaded by FTP from the USGS Eros Data Centre web site: (<http://edcdaac.usgs.gov/gtopo30/gtopo30.html>) and imported in ERDAS. The portion covering study area was extracted from the data set and used in this study. A classified DEM map is shown in Figure 4.2.

#### **4.5. PROCESSING OF REMOTE SENSING DATA**

Multi-date IRS-1A, 1C and 1D LISS III digital satellite data of the Brahmaputra river corridor are identified and selected for the study. Although, each satellite image is collected during the post monsoon (February), when cloud-free imagery is available and when water levels, vegetation cover and other ground conditions are relatively consistent, so that the morphological interpretations are not substantially affected. The study area covered the river Brahmaputra from Kobo at the upstream side to Dhubri at the downstream side 17.34 km from the Indian border with Bangladesh, for a distance of 622.73 km. This area under study is covered by seven image frames made into a single mosaic for each period. The images are performed using the ERDAS Imagine 8.6 software for image processing and raster GIS analysis and ARC/INFO for vector analysis. The analysis comprised of,

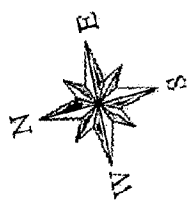
- a. Data base geo-referencing
- b. Extraction of channel forms
- c. Preparation of theme layers
- d. DEM preparation
- e. GIS analysis

The methodology adopted in remote sensing and GIS analysis is shown in the flow chart (Figure 4.3).

#### **4.6. DATA BASE GEO-REFERENCING**

In order to bring all the images under one geometric co-ordinate system, 39 numbers of survey of india (soi) toposheets are scanned and converted into

FIGURE NO-A.1



**INDEX TO IRS 1A COVERAGE**

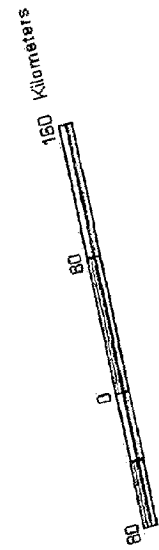
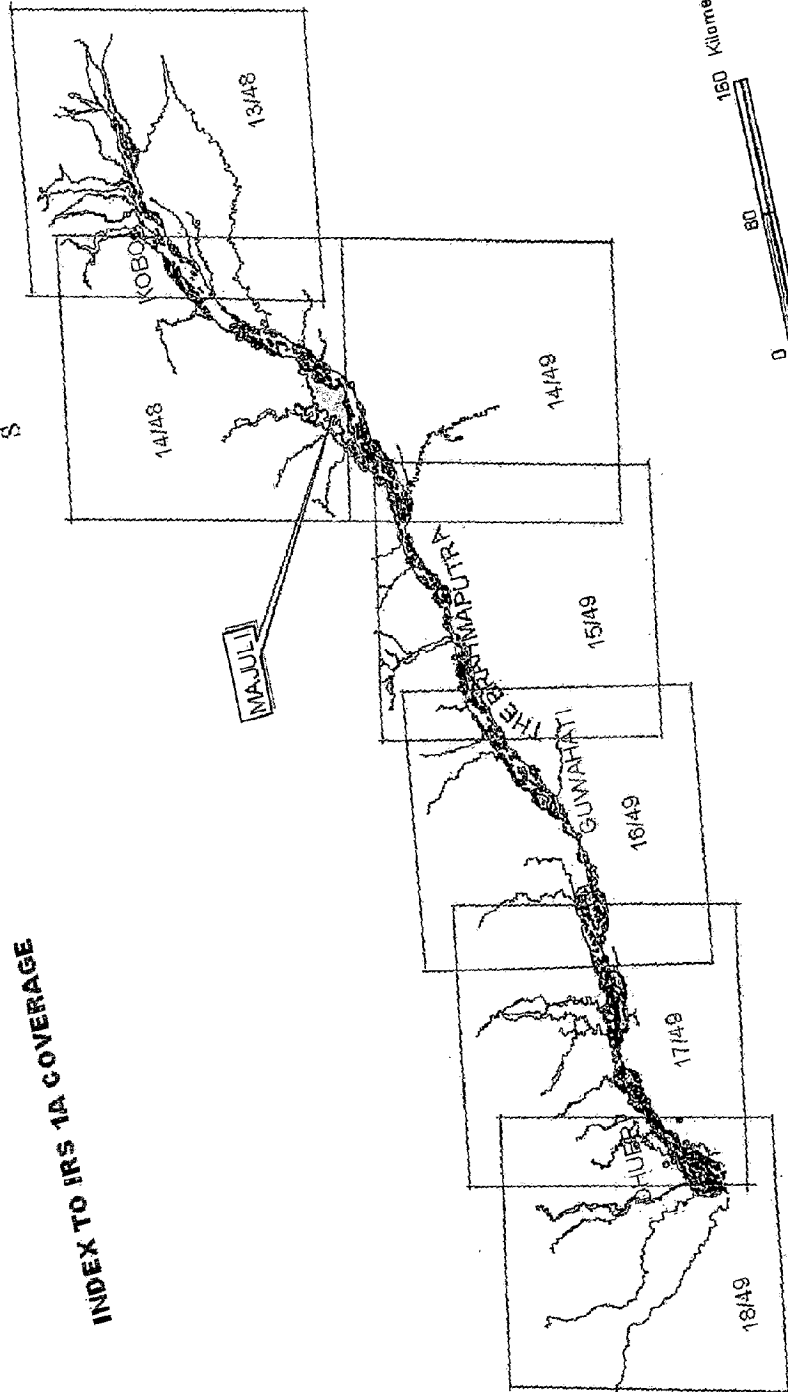
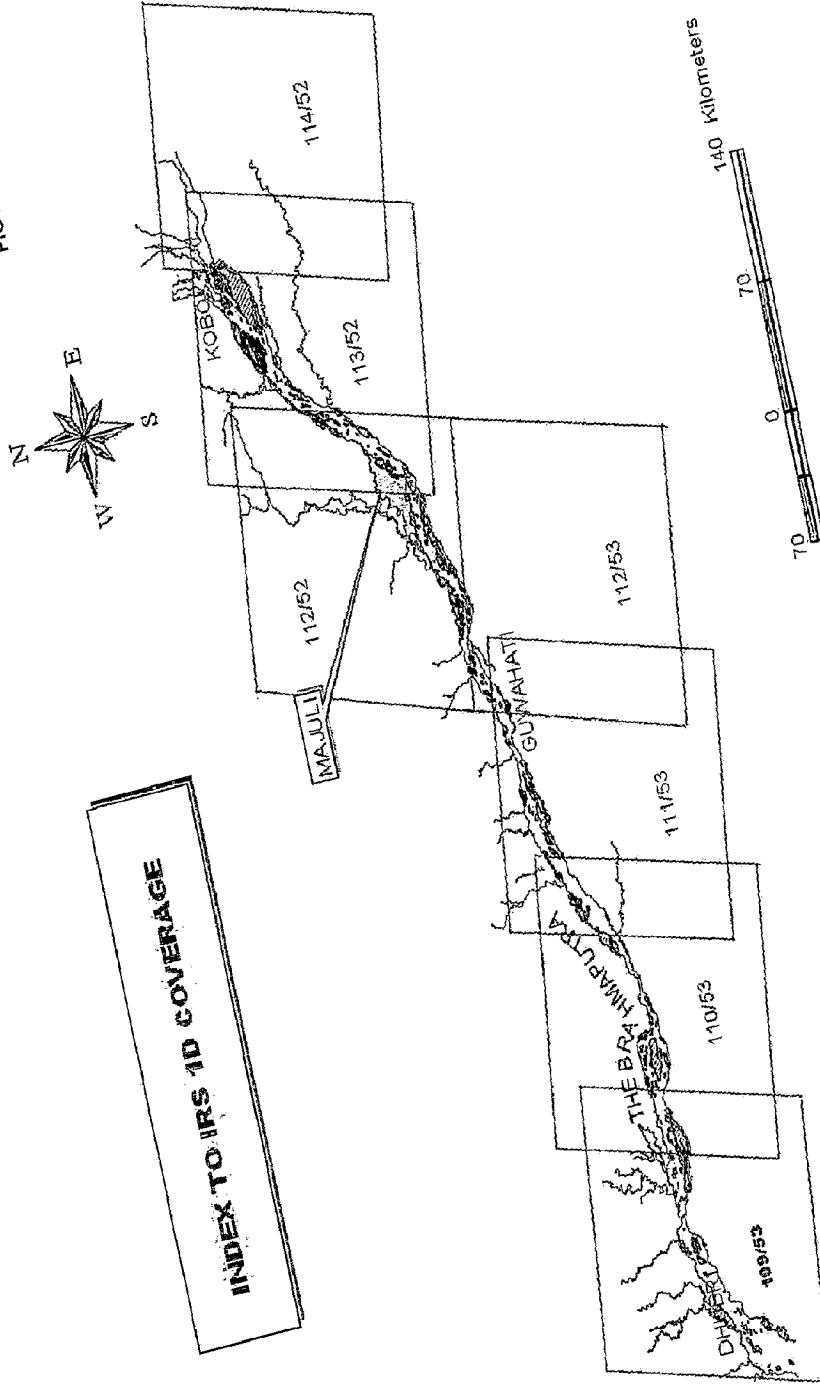


FIGURE NO-4.2



digital format and then geo-referenced with twenty five or more ground control points (gcps) to form the master map base for registration of the images subsequently. The IRS images are geo-referenced by first projecting the data onto a plane, and then rotating and scaling to polyconic map projection system with respect to the geo-referenced topomap base. The geo-referencing is done using second order polynomial to create a geo-referenced image of pixel size 23.5m x 23.5m and 72.5m x 72.5m in case of LISS III and LISS I images respectively. A root mean square error less than 0.5 pixel is obtained using the nearest neighbourhood re-sampling technique. Subsequently, other images are also registered with the geo-referenced images using image-to-image registration technique. Figure 4.4 shows the False Colour Composite (FCC) of the mosaiced image frame of LISS III for the year 2000.

#### **4.7. DIGITAL ELEVATION MODEL (DEM)**

Digital satellite data provided by National Oceanographic & Atmospheric Administration (NOAA), AVHRR sensor having spatial resolution of 1.1 km for the year August, 2002 has been used for deriving the Digital Elevation Model (DEM) and shallow and deep flooding phenomena in the Brahmaputra valley. Figure 4.5 shows the FCC of NOAA data. The elevation range is divided into eight classes from 30m to greater than 600m and DEM map is prepared with drainages overlaid as shown in Figure 4.6. Figure 4.7 depicts the shallow and deep flooding map based on subjective classification of the Assam area into three classes.



#### 4.8. GIS ANALYSIS

Some of the advantages of using a GIS are the convenience of data storage; the ease of statistical analysis and data manipulation, including quantification of error; and the flexibility of graphical display. The conceptual GIS for flood plain of river Brahmaputra includes map base creation, overlay preparation and analysis. In addition, dynamic information extracted from the analysis of satellite data for the lean season as well as active channel in February, 2002 are registered as GIS layers. A more quantitative flood extent assessment, carried out here with the aid of the GIS, and with the practical incentive for such an analysis; the models could be addressed in studying the flood extent of the river Brahmaputra.

**Table 4.2: The area of water bodies on each image**

Date	Area of water bodies		Flood affected area		Note
	km <sup>2</sup>	%	km <sup>2</sup>	%	
March, 24,2002	6028	8.2	2304	3.2	Before monsoon
May, 13, 2002	6124	8.3	3129	4.2	Just before floods
July, 23,2002	6357	8.6	22543	30.6	Flood period
August, 05,2002	6431	8.7	25201	34.2	Flood period
November, 02,2002	6028	8.2	3744	5.1	After flood retreated

**Table 4.3: Flood affected areas (%) for districts**

District	July 2002		August 2002	
	River/deep water	Flood affected area	River/deep water	Flood affected area
Dhubri	17.27	32.1	24.7	35.1
Goalpara	21.3	32.0	25.45	27.7
Kamrup	18.8	23.1	18.9	37.5
Sonitpur	5.25	43.8	7.4	42.23
Golaghat	15.8	27.1	13.1	39.4
Jorhat	20.6	54.1	22.3	54.1
Dibrugarh	14.4	56.6	7.9	55.1
Sibsagar	1	67.1	5.3	51.56
Lakhimpur	16.7	56.21	16.7	65.3
Dhemaji	11.46	66.9	4.9	47.8
Barpeta	5.5	39.3	10.6	45.2
Nagaon	10.1	12.6	9.7	58.2
Darrang	12.6	33.8	9.7	62.5
Margaon	10.3	61.3	34.1	55.8
Nalbari	.6	26.6	4.8	46.4

#### **4.9. DEVELOPMENT OF EQUATION FOR FLOOD PLAIN CROSS SECTIONAL AREA AND PERIMETER**

After flood plain delineation, at each of the 64 predefined cross sections of the river (Figure 4.8), new cross section coordinate for the river extending beyond the riverbank up to flood plain is calculated. These coordinates were further used for development of equation.

#### 4.9.1. GENERATION OF COMPUTER CODE FOR SECTION GEOMETRY

A computer code was written in FORTRAN 90 for the multi-braided cross sections of the river Brahmaputra. The generated computer code is able to calculate perimeter and cross sectional areas at incremental water depth of 0.5meter. Figure (4.9) depicts typical cross sections of the river Brahmaputra.

#### 4.9.2. EQUATION FOR PERIMETER

Wetted perimeters of extended cross-sections (from river bank to flood plain) are computed for all the 64 cross sections at incremental water depth of 0.5m and are plotted on the log-log scale with perimeter as y-axis and flow depth as x axis. On plotting, it is observed that there are two distinct lines with slope  $m_1$  and  $m_2$  Fig (4.10)

Similar to Fig 4.10 , 64 figures were drawn for each cross section and data extracted were tabulated and shown in **Table 4.4**

The combined equation of the two lines is of the following form

$$P = ky^{m_1} \left[ 1 + \left( \frac{y}{y_*} \right)^{\frac{m_2 - m_1}{n}} \right]^n \quad (1)$$

Where  $k$  = perimeter of cross section at depth of 1 meter,

$y$  = flow depth in meters,

$y_*$  = flow depth at point of intersection of two lines,

$m_1$  = slope of lower line and

$m_2$  = slope of upper line.

$$n = \log_2 \left( \frac{P_*}{P_i} \right) \quad (2)$$

$P_*$  = Perimeter corresponding to intersection point of two lines and

$P_i$  = Actual perimeter at intersection line.

- (i) The values of  $m_1$  and  $m_2$  were calculated for all the 64 cross section located at various distance and the values of  $m_1$  and  $m_2$  obtained were plotted against river distance .The average values of  $m_1$  and  $m_2$  is averaged out for the total river reach as 0.8 and 3.5 respectively as shown in figure (4.11).
- (ii) The value of  $y_*$  is obtained for all the sections. Plotting  $y_*$  as y axis and river distance as x-axis, it is observed that

$$y_* = 5.0 \text{ m} \quad \text{fig(4.12)}$$

#### 4.9.3. ESTIMATION OF K OF EQUATION (1)

- (i) The perimeter of the river at depth of 1m was obtained at all the sections. Upon plotting perimeter at  $y = 1.0$  m on normal scale with perimeter as y axis and river distance as x-axis a scattered plot resulted which is difficult to be approximated by an algebraic equation.

Therefore data were fitted with simple sinusoidal form .Data seems to be having hidden frequency. From figure (4.13), it seems that the fitted curve is in good agreement with the data.

$$k = \left[ 439 + 400 \sin \left( \frac{3.72\pi x}{l} + 1.34 \right) \right] \quad (3)$$

- (ii) Similarly index  $n$  was obtained for all the sections. On plotting  $n$  versus river distance on normal scale with  $n$  as  $y$  axis and river distance as  $x$  – axis the approximated  $n$  value is 0.20 fig (4.14)
- (iii) After calculating all the variables and coefficients, equation (1) is written in the form.

$$P = \left[ 439 + 400 \sin \left( \frac{3.72\pi x}{l} + 1.34 \right) \right] \left[ y^3 + \left( \frac{y}{3.624} \right)^{15.0} \right]^{0.2} \quad (4)$$

#### 4.9.4. EQUATION FOR AREA

Analysis similar to, as for arriving at equation for perimeter, was adopted for area. Area generated from computer code for all the 64 cross sections are plotted on the log-log axis with area as  $y$ -axis and water depth as  $x$ -axis. The data extracted is shown in Table 4.5 On plotting the data, it was observed that there were two distinct lines one representing to area at water depths greater than 10 m and other representing to area at water depth less than 10 m. Thus, the equation is of the form

$$A = ky^{m_1} \left[ 1 + \left( \frac{d}{d_*} \right)^{\frac{m_2 - m_1}{n}} \right]^n \quad (5)$$

Where  $k$  = Area of cross section at depth of 1 meter,

$y$  = water depth in meters,

$y_*$  = water depth at point of intersection of two lines,

$m_1$  = slope of lower line

$m_2$  = slope of upper line

$$n = \log_2 \left( \frac{A_*}{A_i} \right) \quad (6)$$

$A_*$  = Area corresponding to intersection point of two lines and

$A_i$  = Actual area at intersection line.

- (i) The plot of  $m_1$  and  $m_2$  against river distance gives  $m_1$  and  $m_2$  as 2.0 and 3.5 respectively as shown in Fig (4.15).
- (ii) Plotting  $y_*$  as y axis and river distance as x-axis, it is observed that  $y_* = 7.0$  m Fig(4.16)
- (iii) Upon plotting perimeter at  $y = 1.0$  m on normal scale with perimeter as y- axis and river distance as x-axis a scattered plot resulted which is difficult to be approximated by an algebraic equation. Therefore data are fitted with simple sinusoidal form .Data seems to be having hidden frequency. From fig (4.17) it seems that the fitted curve is in good agreement with the data.

$$k = \left[ 178 + 143 \sin \left( \frac{4.3\pi x}{l} + 0.36 \right) \right] \quad (7)$$

- (iv) On plotting  $n$  versus river distance on normal scale with  $n$  as y- axis and river distance as x -axis, the approximated  $n$  value is 0.20.

After calculating all the variables and coefficients equation (5) is written as

$$A = \left[ 178 + 143 \sin \left( \frac{4.3\pi x}{l} + 0.36 \right) \right] \left[ y^{10} + \left( \frac{y}{3.624} \right)^{17.5} \right]^{0.2} \quad (8)$$

#### 4.10. REGIME EQUATIONS FOR RIVER BRAHMAPUTRA

In 1930, Lacey formulated Lindley's ideas on the regime canals employing three sets of data, none of which were complete. In the next 55 years, the formulas have undergone scrutiny but are used today in a form quite similar to the original. The regime approach, although it does not incorporate physical explanations for the phenomenon, is an empirical approach that has been developed by observing the characteristics of stable channels. Initial investigations have been carried out in India, Pakistan and Egypt. Extended investigations on this approach have been performed in the USA and Canada. The method was initiated by Kennedy (1895). Based on extensive field investigations, additional contributions to the regime concept were made by other researchers. Some of the works, which are of practical importance, are attributed to Lindley (1919), Blench (1957), Lacey (1966) and Simons and Albertson (1963).

The regime equations have been verified using additional field data beyond those used in the development of a particular equation. This approach sizes an erodible channel such that its sections and slope are in equilibrium with discharges. Therefore, increments or decrements in  $Q$  modify  $W$  and  $y$ . That is why, after the annual periods, sections and slopes remain practically constant. With these characteristics, a regime equation, which is developed using extensive field data, is assumed to be adequate for the preliminary design. However, care must be taken in applying a particular regime equation to a specific site. The designer must verify that the local conditions are similar to those used in the derivation of that particular equation. The applicability of

Lacey's equations is tested for the river Brahmaputra. It is found that the river follows the structure of Lacey's equations. The perimeter and area coefficients found in the modified regime equations are much larger than the corresponding coefficients in the Lacey's equations. Similarly, the velocity coefficient for the river Brahmaputra is considerably smaller than the coefficient occurring in the Lacey's velocity equation. However the coefficients of equations for hydraulic radius are of the same order

#### 4.11. LACEY'S EMPIRICAL EQUATIONS

Lacey (1930) gave a set of empirical equations for flow area  $A$ , flow perimeter  $P$ , and bed slope  $S_0$ . These equations can be written in SI system of units as:

$$A = 2.23 f^{1/3} Q^{5/6} \quad (9)$$

$$P = 4.75 Q^{1/2} \quad (10)$$

$$S_0 = 0.0003 f^{5/3} Q^{-1/6} \quad (11)$$

$$f = 55.66 d^{1/2} \quad (12)$$

$$A = 0.584 d^{1/6} Q^{5/6} \quad (13)$$

$$S_0 = 0.243 d^{5/6} Q^{-1/6} \quad (14)$$

$$R = 0.123 d^{1/6} Q^{1/3} \quad (15)$$

#### 4.12. BACKGROUND

The regime approach is an empirical approach that has been developed by data collected from stable artificial channels and natural rivers. The method was initiated by Kennedy in 1895. Some of the works, which is of practical



importance, is attributed to Lindley (Singh 2003). Lacey (1929-1930, 1933-34 and 1957-1958) formulated Lindley's ideas on the regime canals by giving a set of empirical equations for flow perimeter  $P$ , flow area  $A$ , and bed slope  $S_0$ . These equations as expressed in SI system of units are

$$P = 4.75Q^{1/2} \quad (16)$$

$$A = 2.23f^{-1/3}Q^{5/6} \quad (17)$$

$$S_0 = 0.0003f^{5/3}Q^{-1/6} \quad (18)$$

where  $Q$  = discharge; and  $f$  = silt factor given by the following equation in SI units:

$$f = 55.66d^{1/2} \quad (19)$$

where  $d$  = average bed material size. Using Eq. (19), Eqs. (17) and (18) are written as

$$A = 0.584d^{-1/6}Q^{5/6} \quad (20)$$

$$S_0 = 0.243d^{5/6}Q^{-1/6} \quad (21)$$

Using Eqs. (16) and (20) the hydraulic radius  $R$  is

$$R = 0.123d^{-1/6}Q^{1/3} \quad (22)$$

Using Eq. (20) and the continuity equation, the average velocity of flow  $V$  is

$$V = 1.712d^{1/6}Q^{1/6} \quad (23)$$

Eliminating  $Q$  between Eqs. (21) and (22)

$$d^{1/6} = 1.728S_0^{2/9}R^{1/9} \quad (24)$$

Similarly Eliminating  $d$  between Eqs. (21) and (22)

$$Q^{1/6} = 3.749S_0^{1/9}R^{5/9} \quad (25)$$

Using Eqs. (23), (24) and (25) gives the following resistance equation used in estimating the flood discharge in streams:

$$V = 10.98R^{2/3}S_0^{1/3} \quad (26)$$

The exponent of the bed slope in Manning's equation, which is applicable for flow of pure water, is 1/2. On the other hand, in Eq. (20) the corresponding exponent is 1/3. This difference can be attributed to the additional energy consumed in the transport of the equilibrium sediment load by the stream.

The present investigation is undertaken to obtain regime equations for the river Brahmaputra. For this purpose, twelve year data of discharge observations taken at three measurement sites, namely Pancharatna, Bessamara and Pandu, on the river have been used. The observed perimeter and cross-sectional area were also taken in the analysis

#### 4.13. DATA COLLECTION

As Lacey (1929-1930) found the regime equations for canals carrying full supply discharge, for the application of these equations to rivers, near bankful stage discharge forming the channel geometry needs to be considered. Thus, measurement of discharge and corresponding sectional attributes should confine to monsoon seasons only. Hence in the present study, average monthly discharge data for the monsoon period, i.e. 15<sup>th</sup> May to 15<sup>th</sup> October have been used. These data were collected from Central Water Commission, New Delhi, India. Overall 36 set of data spanned over 12 years from 1991 to 2002 were collected. The summary of the data collected is given in **Table 4.6**.

$$S_0 = k_s d^{5/6} Q^{-1/6} \quad (29)$$

where  $k_p$ ,  $k_a$  and  $k_s$  = unknown coefficients for perimeter, area and bed slope respectively. Using the data collected, the coefficients  $k_p$ ,  $k_a$  and  $k_s$  are obtained for each set of data  $i$  for  $i = 1, 2, 3, \dots, N$ ; where  $N$  = the number of the data sets. These data are shown plotted in Fig. 4.18. A perusal of Fig 4.18 shows that the coefficients  $k_p$ ,  $k_a$  and  $k_s$  fairly remain constant. Thus their following average value can be adopted:  $k_p = 11.8$ ;  $k_a = 1.069$ ; and  $k_s = 0.771$ . Thus the perimeter, area and slope equations for the river Brahmaputra are

$$P = 11.8Q^{1/2} \quad (27)$$

$$A = 1.069d^{-1/6} Q^{5/6} \quad (28)$$

$$S_0 = 0.771d^{5/6} Q^{-1/6} \quad (29)$$

Using Eqs. (27) and (28), the hydraulic radius is obtained as

$$R = 0.0906d^{-1/6} Q^{1/3} \quad (30)$$

Combining Eqs. (27), (28) and (29) and following the similar procedure as used for obtaining Eq. (24), one gets

$$V = 5.82R^{2/3} S_0^{1/3} \quad (31)$$

#### 4.15. VALIDATION OF RESULTS

A validation plot for equation of Area ,Perimeter and river slope is shown in figure (4.19 and 4.20)

#### 4.16. SALIENT POINTS

Comparing Lacey's Eqs. (16), (20), (21), (22) and (26) and the corresponding Eqs. (27), (28), (29), (30) and (31) for the river Brahmaputra, it

can be seen that though their structure is similar, however, there is considerable difference in the coefficients. Under similar condition the perimeter of the river Brahmaputra is two and a half times larger than the Lacey's canal. This may be on account of braided nature of the river where there are multiple flow canals. Further the river velocity is less than half that of the Lacey canal. This can be explained by the increased resistance on account of braiding, meandering and large suspended sediment in river Brahmaputra compared to Lacey's straight, single and relatively silt free canal. In the amount of sediment transport per unit of basin area river Brahmaputra is second only to the Yellow river in China (Goswami, 1985). Due to reduced velocity the river area is increased to twice of the corresponding Lacey canal. On the other hand compared to the Lacey canal, three and a quarter times increase in the river slope can be attributed to the increase in resistance.

Swamee (2000) synthesized an energy function whose minimization gives the optimal dimensions in the form of Lacey equations; where the corresponding minimum power per unit canal length  $E^*$  associated with the Lacey canals is

$$E^* = 0.009023\rho g \left\{ \frac{[(s-1)g]^4}{\nu^5} \right\}^{\frac{1}{18}} d^{5/6} Q^{5/6} \quad (32)$$

where  $\rho$  = mass density of water;  $g$  = gravitational acceleration;  $s$  = specific gravity of bed material; and  $\nu$  = kinematic viscosity of water. Using the similar process as described by Swamee (2000), the minimum power per unit length of the river Brahmaputra is

$$E^* = 0.01011 \rho g \left\{ \frac{[(s-1)g]^4}{v^5} \right\}^{\frac{1}{18}} d^{5/6} Q^{5/6} \quad (33)$$

Though, as compared to the Lacey canals, there is considerable difference in the equations of the dimensions and slope, the minimum power per unit length of the river Brahmaputra is only about 12% more than that of the Lacey canals.

#### 4.17. EQUATION FOR GAUGE DISCHARGE CURVE FOR RIVER

##### BRAHMAPUTRA

This study is undertaken to develop the gauge discharge relationship for the river Brahmaputra. The developed equation uses the potentially observable variables to estimate river discharge at any section of the river.. For early warning of the floods or prediction of discharge corresponding to a specific gauge, there are only three gauging sites in the total length of 623km. of the river The existing stage-discharge equations can predict the given variable at a particular station with assumption that cross sectional area is equal to depth  $d$  multiplied by width  $w$ . For river like Brahmaputra which has high frequency of floods and high variation in cross sectional area along length of river, it is imperative to have a stage discharge relation, which can predict the variables at any point of the river with reasonable accuracy in cross sectional area measurement.

#### 4.17.1. EQUATION FOR AREA AND PERIMETER

The equation for area and perimeter developed earlier in this chapter are

$$P = \left[ 439 + 400 \sin \left( \frac{3.72\pi x}{L} + 1.34 \right) \right] \left[ y^3 + \left( \frac{y}{3.624} \right)^{15} \right]^{0.2} \quad (4)$$

Where  $P$  = flow perimeter (m);  $x$  = longitudinal distance (km);  $L$  = 623 km (The total distance between sections 2 and 65); and  $y$  = flow depth (m). Similarly, using the data for all the 64 cross sections, the following equation is fitted for area

$$A = \left[ 178 + 143 \sin \left( \frac{4.3\pi x}{L} + 0.36 \right) \right] \left[ y^{10} + \left( \frac{y}{3.624} \right)^{17.5} \right]^{0.2} \quad (8)$$

where  $A$  = flow area ( $m^2$ ). A perusal Figs. 4.21 and 4.22 depict the agreement of the data with the Eqs. (8) and (4) respectively.

#### 4.17.2. EQUATION OF GAUGE-DISCHARGE CURVE

#### 4.18. INTRODUCTION

Direct measurement of discharge in open channels is time consuming and costly (and sometimes impractical during large floods). Therefore, most discharge records are developed from converting measured water stages to discharges by using a calibrated stage-discharge rating, which permits a fast and relatively inexpensive means to determine the discharge (Corbett et al., 1943; Kennedy, 1984; Rantz et al., 1982). Discharge-rating curves showing the relationship between water-surface stage and the flow discharge have been a widely used tool in hydrology for over a century. Rating curves are established by concurrent measurements of stage,  $h$ , and discharge,  $Q$ , (through velocity

measurements, dilution methods, or other techniques) and the results are fitted to yield the rating curves. Discharge measurements need to cover the range of flows at the site and need to be continued over time to account for temporal changes in the rating. Stage-discharge ratings are generally treated as following a power curve of the form given by the following equation (Kennedy, 1984):

$$Q = c(a+h)^\alpha \quad (34)$$

in which  $\alpha$  is an index exponent, and  $a$  and  $c$  are constants. The constant  $a$  is often referred to as the "offset" or as the "gage-height of zero flow." For most stations the rating will be a compound curve consisting of different segments, each of which may follow the form of equation 34, but have unique values of  $c$ ,  $a$ , and  $\alpha$ . For most gauging stations the "offset" is a mathematical constant determined by successive approximations to obtain the best fit between measured discharges and stages.

Lacey (1929-1930, 1933-34 and 1957-1958) gave empirical equations for regime perimeter for canals as

$$P = 4.75Q^{1/2} \quad (16)$$

To obtain regime Perimeter for the river Brahmaputra, twelve year (1991 to 2002) data of discharge observations taken at three measurement sites, namely Pancharatna, Pandu, and Besamara, on the river have been used. The observed perimeter and cross-sectional area were also taken in the analysis.

For river Brahmaputra the regime equation for perimeter is fitted as

$$P = 11.8Q^{1/2} \quad (27)$$

Where  $Q$  = river discharge ( $\text{m}^3/\text{s}$ ); and  $P$  = wetted perimeter. Eliminating  $P$  between Eqs. (27) and (4) one gets the equation for gauge discharge as

$$Q = \left[ 37.2 + 33.9 \sin \left( \frac{3.72\pi x}{L} + 1.34 \right) \right]^2 \left[ y^3 + \left( \frac{y}{3.624} \right)^{15} \right]^{0.4} \quad (35)$$

A perusal of Eqn (35) reveals that for a particular river section along river length the first term of Eqn (35) is a constant quantity. Thus the Eqn (35) can be written in simplified form as

$$Q = K \left[ y^3 + \left( \frac{y}{3.624} \right)^{15} \right]^{0.4} \quad (36)$$

Knowing  $K$  and  $y$ , which are potentially observable variables at a particular cross section, the discharge can easily be known. Fig (4.23) shows, the data has fairly good agreement with the gauge discharge Eqn (35)



Table 4.4 DATA GENERATED FOR EQUATION OF PERIMETER

CROSS SECTION	X (km)	X (m)	m <sub>1</sub>	m <sub>2</sub>	P*	d*	P at d=1m	P <sub>i</sub>	P*/P <sub>i</sub>	n
2	17.34	17340	0.75	1.65	2850	5	690	2200	1.295	0.373
3	28.05	28050	2.74	8.85	40000	20	11	39000	1.026	0.037
4	38.25	38250	1.25	3.69	200	4.8	30	190	1.053	0.074
5	46.92	46920	0.77	1.96	820	4.5	290	740	1.108	0.148
6	56.61	56610	0.68	1.73	3600	4	900	2300	1.565	0.646
7	66.3	66300	1.08	4.92	6000	9	550	5800	1.034	0.049
8	73.44	73440	0.93	4.64	500	6.9	80	400	1.250	0.322
9	82.62	82620	0.73	3.65	720	5.4	190	500	1.440	0.526
10	92.82	92820	0.52	1.98	410	4	150	400	1.025	0.036
11	100.98	100980	0.92	2.51	1400	5.4	195	950	1.474	0.559
12	109.65	109650	0.66	2.30	600	3.6	280	260	2.308	1.206
13	119.85	119850	1.85	4.29	2100	9.5	38	2000	1.050	0.070

CROSS SECTION	X (km)	X (m)	m <sub>1</sub>	m <sub>2</sub>	P*	d*	P at d=1m	P <sub>i</sub>	P*/P <sub>i</sub>	n
14	128.01	128010	1.72	4.35	1800	10	32	1750	1.029	0.041
15	137.7	137700	1.11	4.04	800	4.8	50	240	3.333	1.737
16	146.37	146370	0.97	2.53	180	2	90	170	1.059	0.082
17	156.06	156060	1.83	3.94	800	3.9	40	750	1.067	0.093
18	167.28	167280	0.76	3.15	3200	4.9	700	2200	1.455	0.541
19	175.95	175950	0.72	1.68	1600	4.6	300	900	1.778	0.830
20	182.5	182500	0.20	6.24	1600	7.2	390	480	3.333	1.737
21	189.21	189210	1.13	2.13	3000	7.8	360	2900	1.034	0.049
22	197.37	197370	0.91	4.79	1900	15	170	1850	1.027	0.038
23	206.55	206550	0.44	5.07	2100	8	850	2000	1.050	0.070
24	213.18	213180	0.91	2.95	340	4	74	260	1.308	0.387

CROSS SECTION	X (km)	X (m)	m <sub>1</sub>	m <sub>2</sub>	P*	d*	P at d=1m	P <sub>i</sub>	P*/P <sub>i</sub>	n
25	218.79	218790	0.66	3.15	1700	7.4	530	1500	1.133	0.181
26	224.91	224910	0.27	12.51	1900	10.5	170	310	6.129	2.616
27	234.6	234600	0.78	2.99	1500	7.5	290	670	2.239	1.163
28	241.23	241230	1.22	4.74	6700	9.5	450	700	9.571	3.259
29	251.95	251950	1.57	1.85	2400	6	280	2350	1.021	0.030
30	262.15	262150	1.16	3.51	5900	9.9	400	5850	1.009	0.012
31	272.35	272350	0.65	2.51	2600	7.5	720	2550	1.020	0.028
32	284.08	284080	0.55	3.88	4300	12	1000	3800	1.132	0.178
33	296.83	296830	1.45	3.01	3400	9.5	800	2000	1.700	0.766
34	310.1	310100	1.01	2.77	9000	12	700	8000	1.125	0.170
35	325.9	325900	0.39	2.86	200	6	100	190	1.053	0.074
36	341.1	341100	0.33	5.70	1200	19	230	600	2.000	1.000
37	352.94	352940	0.50	2.10	1300	4.5	240	1250	1.040	0.057

CROSS SECTION	X (km)	X (m)	m <sub>1</sub>	m <sub>2</sub>	P*	d*	P at d=1m	P <sub>i</sub>	P*/P <sub>i</sub>	n
38	365.18	365180	0.02	5.51	1100	9.8	90	1050	1.048	0.067
39	371.81	371810	1.18	0.15	2850	5	450	2800	1.018	0.026
40	383.03	383030	0.95	2.66	3500	7.4	550	3450	1.014	0.021
41	389.66	389660	0.96	3.26	1500	5.8	130	700	2.143	1.100
42	398.33	398330	0.55	1.50	3900	7.5	1300	3850	1.013	0.019
43	412.09	412090	3.05	4.91	29000	19	3.5	28000	1.036	0.051
44	423.31	423310	0.55	3.32	3400	7	1000	2900	1.172	0.229
45	439.63	439630	0.74	3.10	4500	8.2	950	4450	1.011	0.016
46	453.91	453910	0.21	21.85	6500	9.1	3200	5000	1.300	0.379
47	465.13	465130	1.01	6.64	1800	10.5	110	1200	1.500	0.585
48	474.82	474820	1.15	3.40	3600	7.2	340	3550	1.014	0.020
49	483.49	483490	0.13	2.73	250	3.8	210	240	1.042	0.059

CROSS SECTION	X (km)	X (m)	m <sub>1</sub>	m <sub>2</sub>	P*	d*	P at d=1m	P <sub>i</sub>	P*/P <sub>i</sub>	n
50	490.63	490630	1.08	19.23	2000	16	100	1900	1.053	0.074
51	498.8	498800	0.35	6.88	1300	7.1	400	780	1.667	0.737
52	505.94	505940	0.63	7.65	1100	6.4	210	680	1.618	0.694
53	513.08	513080	2.57	0.24	3100	3.9	75	3000	1.033	0.047
54	522.77	522770	0.54	10.69	740	7	230	620	1.194	0.255
55	531.95	531950	0.75	4.15	1300	4.2	350	1000	1.300	0.379
56	541.13	541130	0.60	4.11	2100	5.1	750	2000	1.050	0.070
57	558.98	558980	1.01	4.32	2900	4.9	700	2600	1.115	0.158
58	570.2	570200	1.05	9.45	1600	10.5	18	200	8.000	3.000
59	579.38	579380	1.54	2.53	3700	3.8	460	3700	1.000	0.000
60	589.07	589070	0.87	0.40	2700	2	1500	2650	1.019	0.027
61	601.82	601820	1.21	1.91	110	1.5	75	100	1.100	0.138
62	613.04	613040	0.50	2.21	2900	6.7	900	2400	1.208	0.273
63	626.3	626300	0.86	0.72	750	1.6	530	740	1.014	0.019
64	634.46	634460	0.58	1.18	780	3.3	395	770	1.013	0.019
65	640.07	640070	0.76	1.37	3400	5.2	670	2400	1.417	0.503

Table 4.5 DATA GENERATED FOR EQUATION OF AREA

CROSS SECTION	X	X (m)	m <sub>1</sub>	m <sub>2</sub>	A.	d.	A at d=1m	A <sub>1</sub>	A./A <sub>1</sub>	n
2	17.34	17340	1.90	2.66	26000	8	200	20000	1.300	0.020
3	28.05	28050	2.04	3.79	2800	6.5	15	1000	2.800	0.400
4	38.25	38250	4.06	3.43	6000	7.6	17	5950	1.008	0.012
5	46.92	46920	1.90	2.42	2000	5.5	80	1950	1.026	0.037
6	56.61	56610	1.99	2.84	15000	5.9	300	12000	1.250	0.322
7	66.3	66300	1.95	2.48	19000	7.2	200	17000	1.118	0.160
8	73.44	73440	2.02	4.85	2200	8.5	37	1800	1.222	0.290
9	82.62	82620	2.51	2.70	12000	6	150	11900	1.008	0.012
10	92.82	92820	1.30	3.51	2800	6.9	150	1800	1.556	0.300
11	100.98	100980	1.96	4.18	11000	8	110	8800	1.250	0.322
12	109.65	109650	2.04	3.50	9000	8	93	7000	1.286	0.363
13	119.85	119850	2.99	4.25	9000	12	9	8000	1.125	0.170

CROSS SECTION	X	X (m)	m <sub>1</sub>	m <sub>2</sub>	A	d	A at d=1m	A <sub>1</sub>	A/A <sub>1</sub>	n
14	128.01	128010	2.57	4.30	11000	7	9	10000	1.100	0.138
15	137.7	137700	2.23	2.78	490	5	20	400	1.225	0.293
16	146.37	146370	1.97	4.15	1000	3.8	45	600	1.667	0.300
17	156.06	156060	1.97	4.59	620	5	36	400	1.550	0.030
18	167.28	167280	1.89	3.48	15000	6.9	380	14900	1.007	0.010
19	175.95	175950	1.82	2.19	4500	5.2	160	3200	1.406	0.492
20	182.5	182500	2.12	1.46	8000	9.2	90	7950	1.006	0.100
21	189.21	189210	1.84	2.52	6000	5.5	200	5000	1.200	0.263
22	197.37	197370	1.44	1.78	3200	6.6	28	3100	1.032	0.046
23	206.55	206550	2.59	1.54	1800	2.9	90	1750	1.029	0.041
24	213.18	213180	2.88	3.99	2600	6.5	39	1700	1.529	0.613
25	218.79	218790	1.59	3.41	12000	9.5	280	11500	1.043	0.061

CROSS SECTION	X	X (m)	m <sub>1</sub>	m <sub>2</sub>	A <sub>•</sub>	d <sub>•</sub>	A at d=1m	A <sub>i</sub>	A <sub>•</sub> /A <sub>i</sub>	n
26	224.91	224910	1.58	2.66	800	6	150	600	1.333	0.415
27	234.6	234600	1.77	3.87	10500	8	110	7800	1.346	0.429
28	241.23	241230	1.86	4.00	21000	8	295	17000	1.235	0.305
29	251.95	251950	1.69	3.76	8000	7	180	3900	2.051	0.400
30	262.15	262150	1.92	3.20	21000	9.2	195	19000	1.105	0.144
31	272.35	272350	1.63	2.88	18000	9.1	300	16500	1.091	0.126
32	284.08	284080	1.48	2.30	12000	7.1	450	9000	1.333	0.415
33	296.83	296830	2.84	3.64	10000	7	29	8500	1.176	0.234
34	310.1	310100	1.79	2.50	17000	7.4	230	10000	1.700	0.200
35	325.9	325900	1.42	4.92	4000	12	51	2000	2.000	0.200
36	341.1	341100	2.00	6.13	17000	7.5	20	15000	1.133	0.181
37	352.94	352940	1.82	2.60	14000	9	200	10000	1.400	0.485



CROSS SECTION	X	X (m)	m <sub>1</sub>	m <sub>2</sub>	A*	d*	A at d=1m	A <sub>i</sub>	A/A <sub>i</sub>	n
37	352.94	352940	1.82	2.60	14000	9	200	10000	1.400	0.485
38	365.18	365180	2.10	4.91	10000	5	45	6900	1.449	0.535
39	371.81	371810	2.76	1.96	16000	8	295	14000	1.143	0.193
40	383.03	383030	1.95	3.32	12000	7.3	30	9500	1.263	0.337
41	389.66	389660	1.75	4.13	4500	6.7	80	2100	2.143	0.400
42	398.33	398330	2.16	1.82	7500	4.5	280	7490	1.001	0.002
43	412.09	412090	2.43	3.85	7000	9	12	1200	5.833	0.200
44	423.31	423310	1.75	2.77	20000	8.9	300	18000	1.111	0.152
45	439.63	439630	1.65	3.15	12000	6.8	300	8000	1.500	0.585
46	453.91	453910	1.24	6.39	38000	7	600	30000	1.267	0.341
47	465.13	465130	1.94	5.30	7500	8	52	6000	1.250	0.322
48	474.82	474820	2.32	2.99	20000	9	120	19900	1.005	0.007
49	483.49	483490	2.22	3.27	3900	7	150	2100	1.857	0.300
50	490.63	490630	1.91	5.97	13000	7	80	12900	1.008	0.011

CROSS SECTION	X	X (m)	m <sub>1</sub>	m <sub>2</sub>	A <sup>*</sup>	d <sup>*</sup>	A at d=1m	A <sub>i</sub>	A <sup>*</sup> /A <sub>i</sub>	n
51	498.8	498800	1.54	4.19	5200	7.9	220	4800	1.083	0.115
52	505.94	505940	1.46	4.52	3100	6.8	160	2800	1.107	0.100
53	513.08	513080	1.21	2.14	7000	4.9	230	6900	1.014	0.021
54	522.77	522770	1.93	3.17	3100	7.2	50	2900	1.069	0.096
55	531.95	531950	1.75	4.98	4300	5.5	190	3800	1.132	0.178
56	541.13	541130	1.75	3.20	9500	6.1	390	9000	1.056	0.078
57	558.98	558980	2.92	3.66	9500	5.7	300	8000	1.188	0.248
58	570.2	570200	2.03	9.80	600	7.8	9	520	1.154	0.206
59	579.38	579380	1.28	2.19	2500	6.5	650	2400	1.042	0.059
60	589.07	589070	1.85	1.56	3100	5	790	3000	1.033	0.047
61	601.82	601820	2.20	3.41	700	6	31	600	1.167	0.222
62	613.04	613040	4.52	2.10	7000	5.4	280	6900	1.014	0.021
63	626.3	626300	1.62	1.61	1800	6	280	1790	1.006	0.008
64	634.46	634460	3.03	2.33	4990	6	100	4800	1.040	0.056
65	640.07	640070	1.70	2.20	10000	6.5	420	9900	1.010	0.014

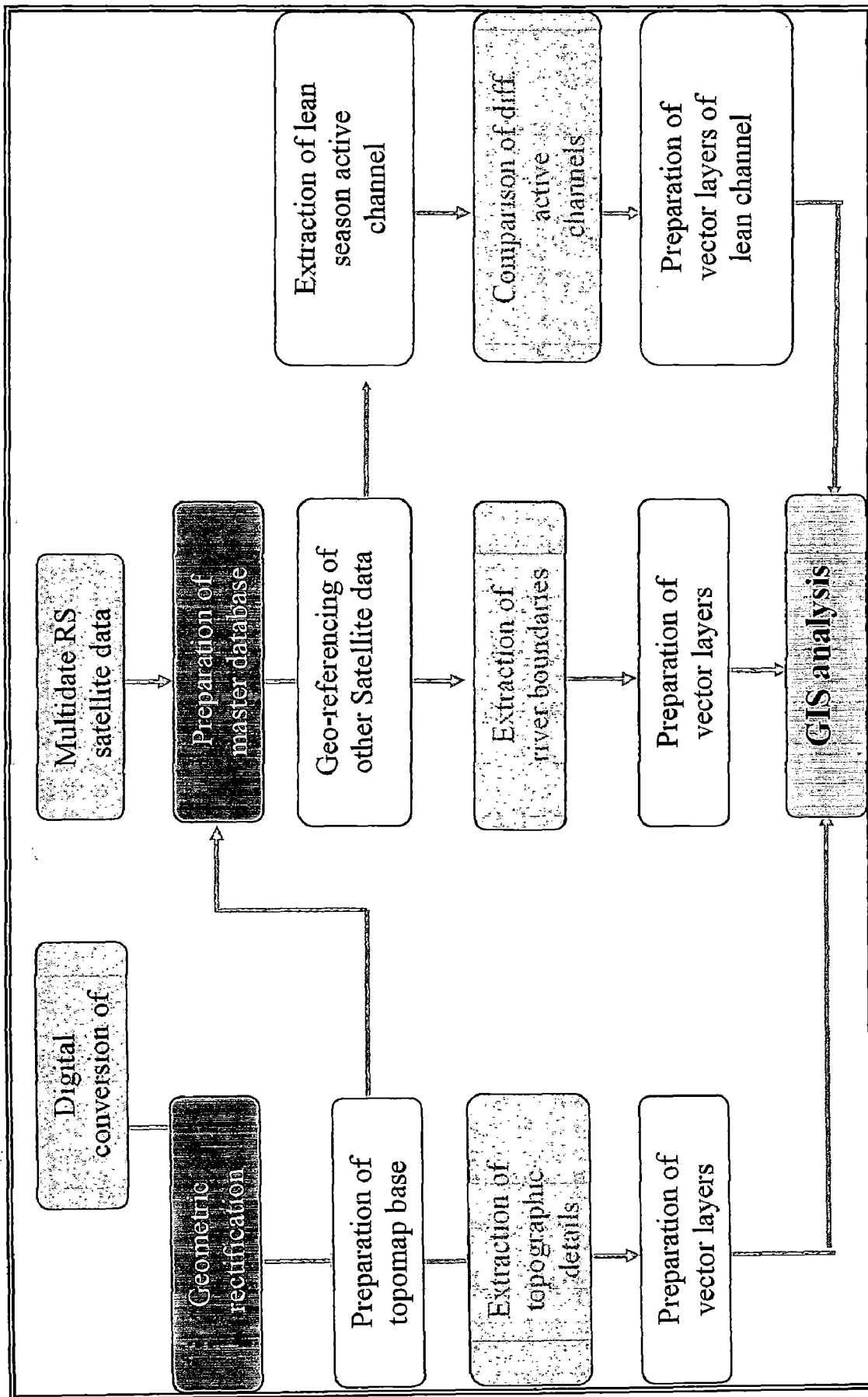


FIGURE 4.3 FLOW CHART SHOWING THE METHODOLOGY OF IMAGE PROCESSING AND GIS ANALYSIS



FIGURE 4.4 FALSE COLOUR COMPOSITE (FCC) OF THE MOSAIC IMAGE FRAME OF LISS III, 2000

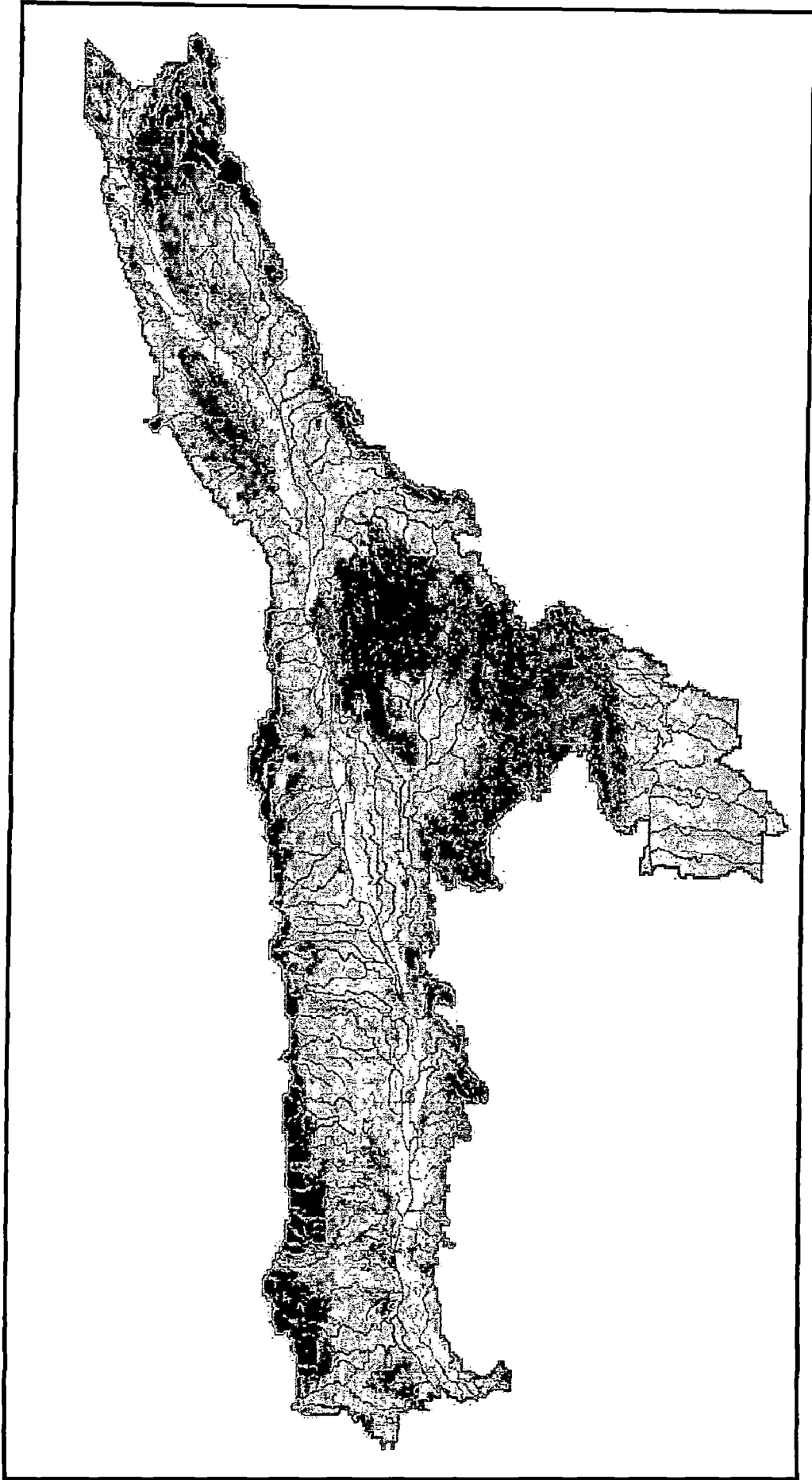


FIG 4.5 FCC OF NOAA, AUGUST 2002

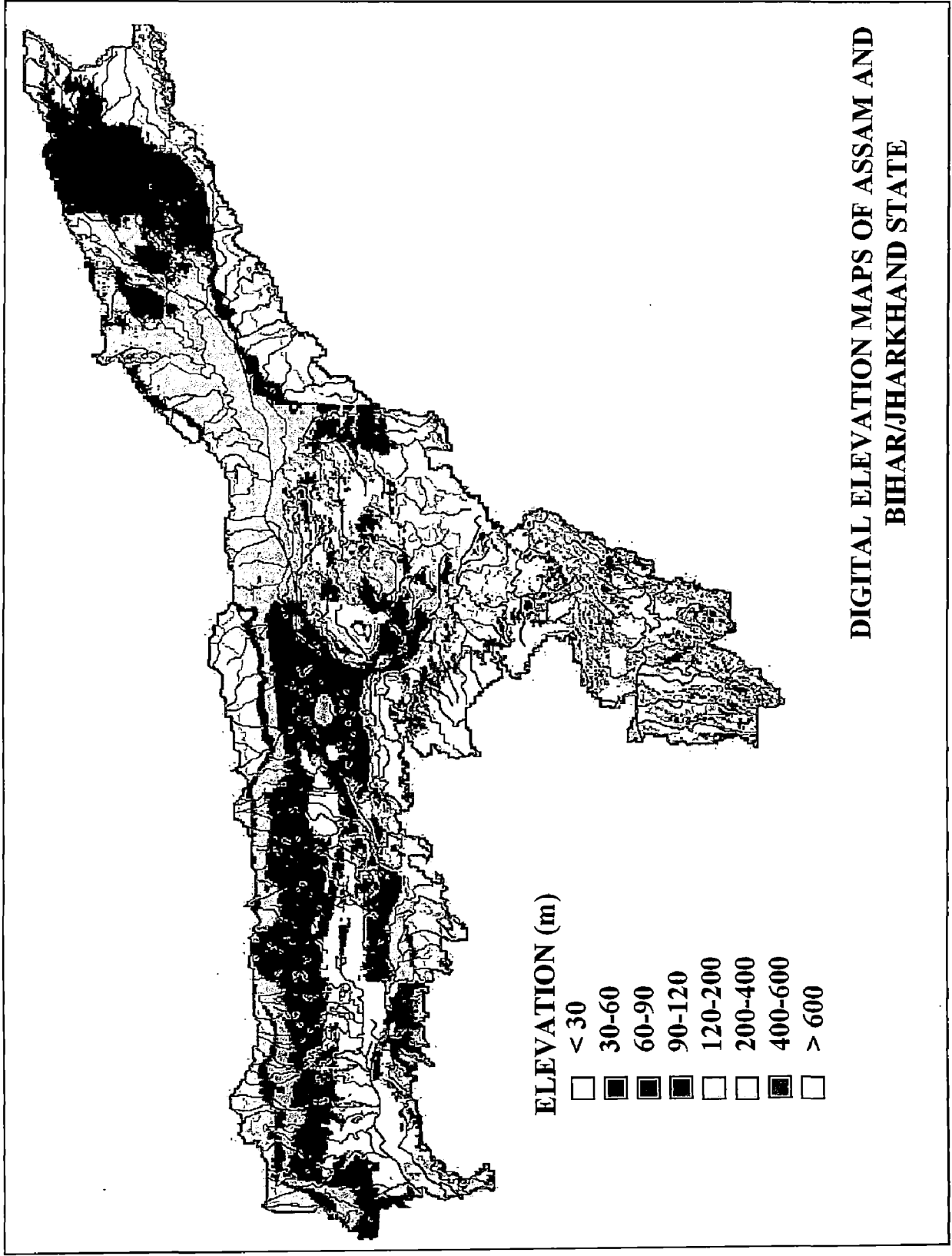
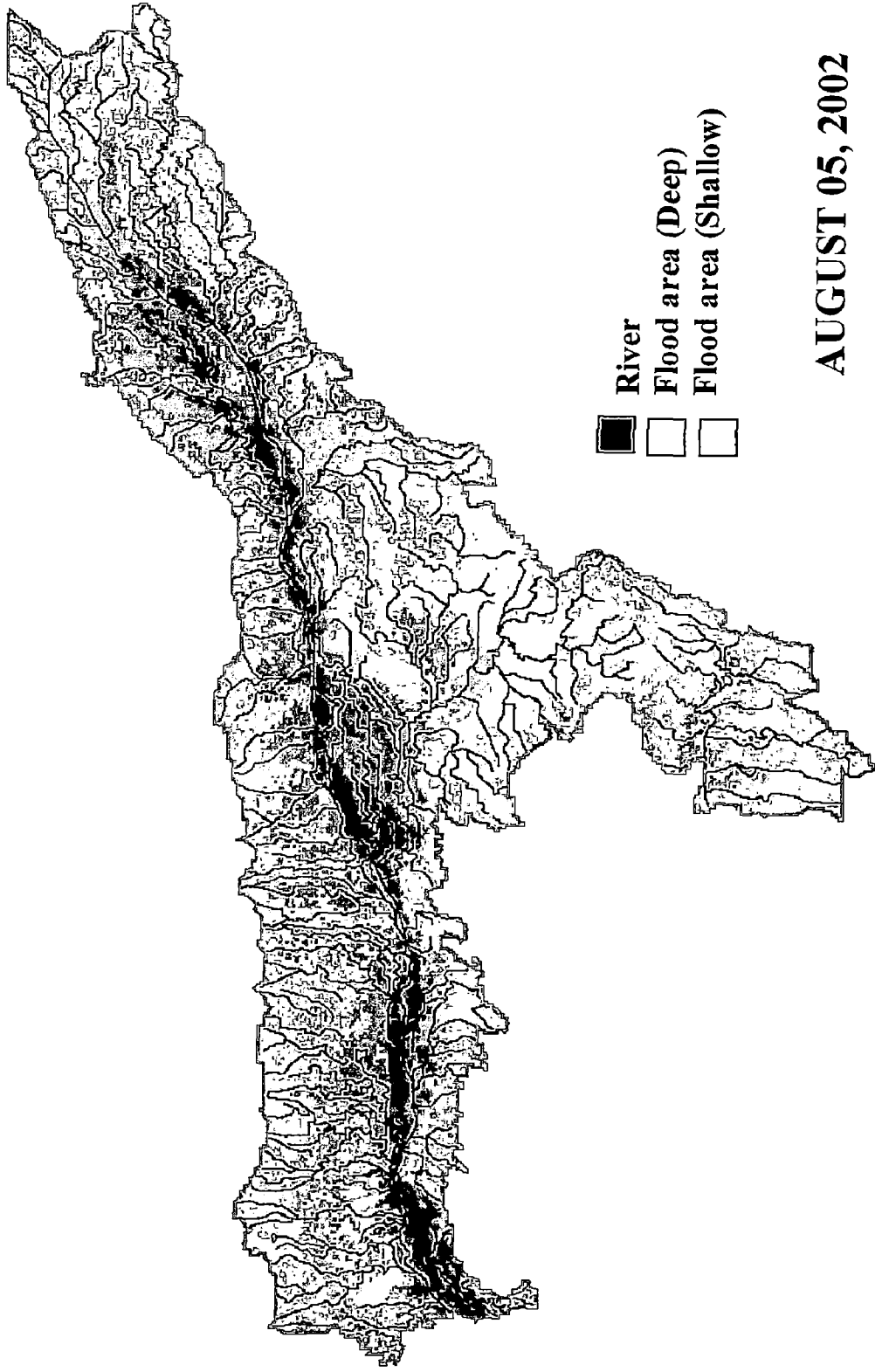


FIG 4.6 CLASSIFIED DEM MAP OF RIVER BRAHMAPUTRA



**FLOOD INUNDATED AREA OF ASSAM AND BIHAR/JHARKHAND STATE**

FIG 4.7 NOAA IMAGE SHOWING DEEP AND SHALLOW FLOOD PLAIN AREA

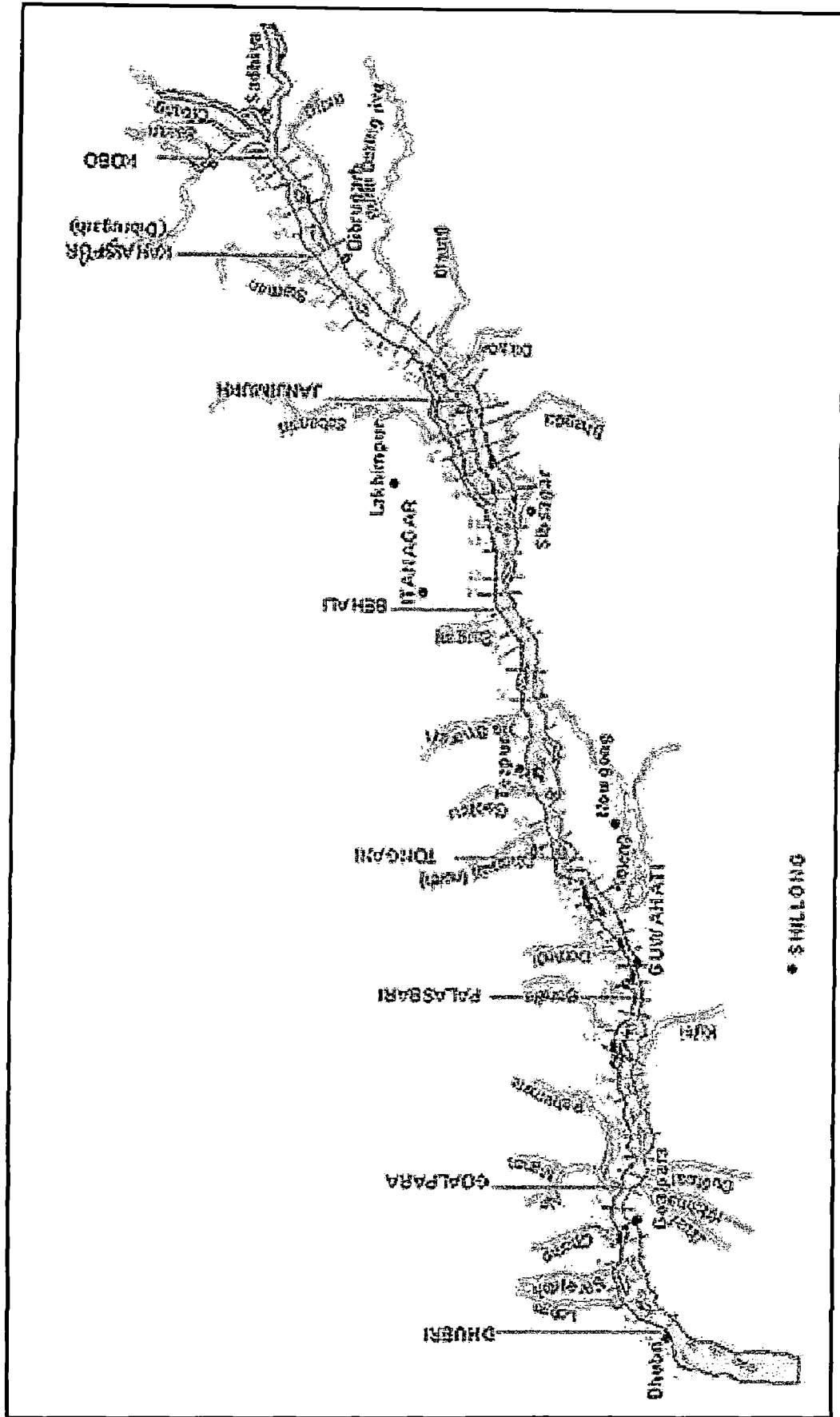


FIG 4.8 CROSS-SECTION NUMBER (2 to 65) OF RIVER BRAHMAPUTRA



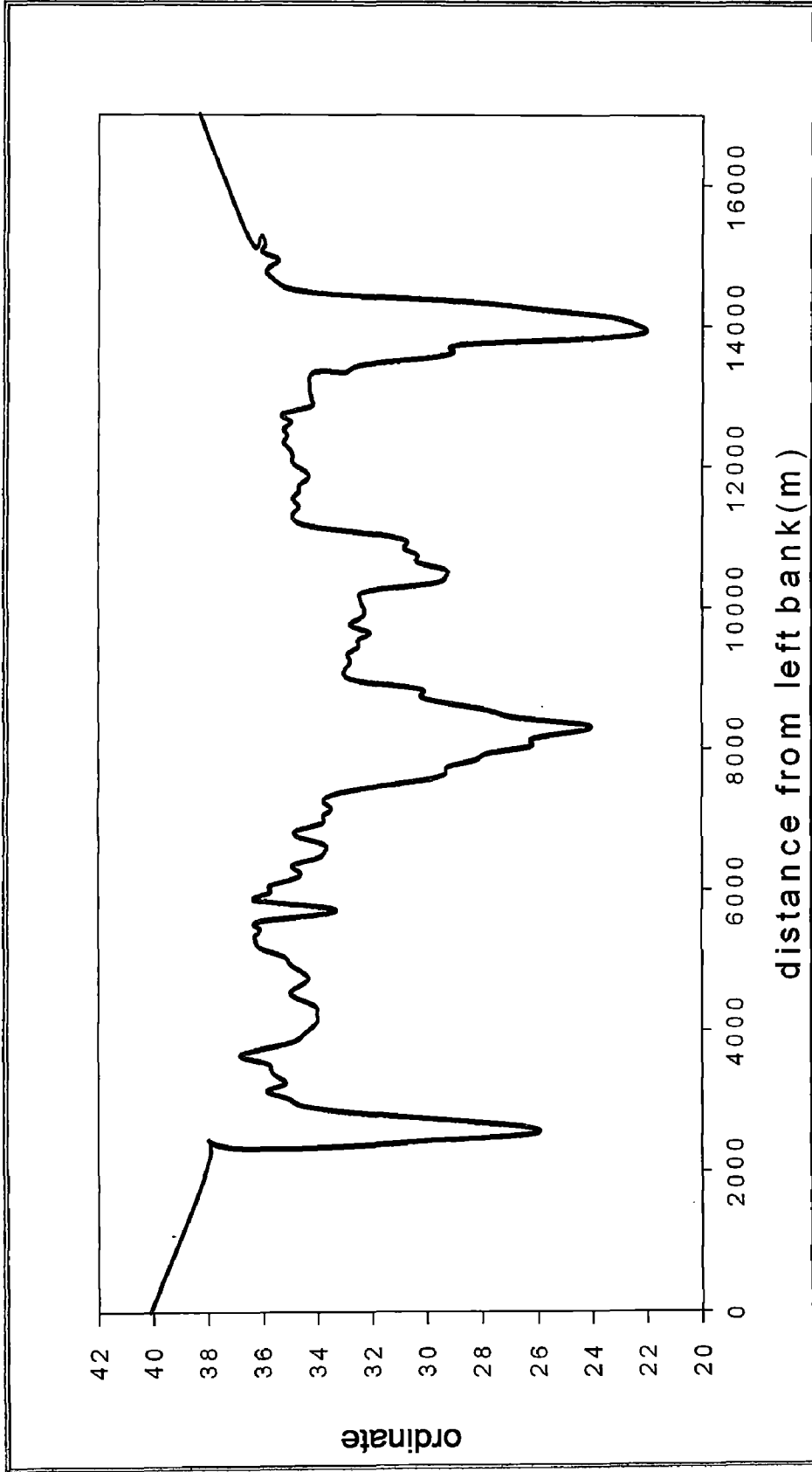


FIG 4.9 TYPICAL CROSS SECTION OF RIVER BRAHMAPUTRA

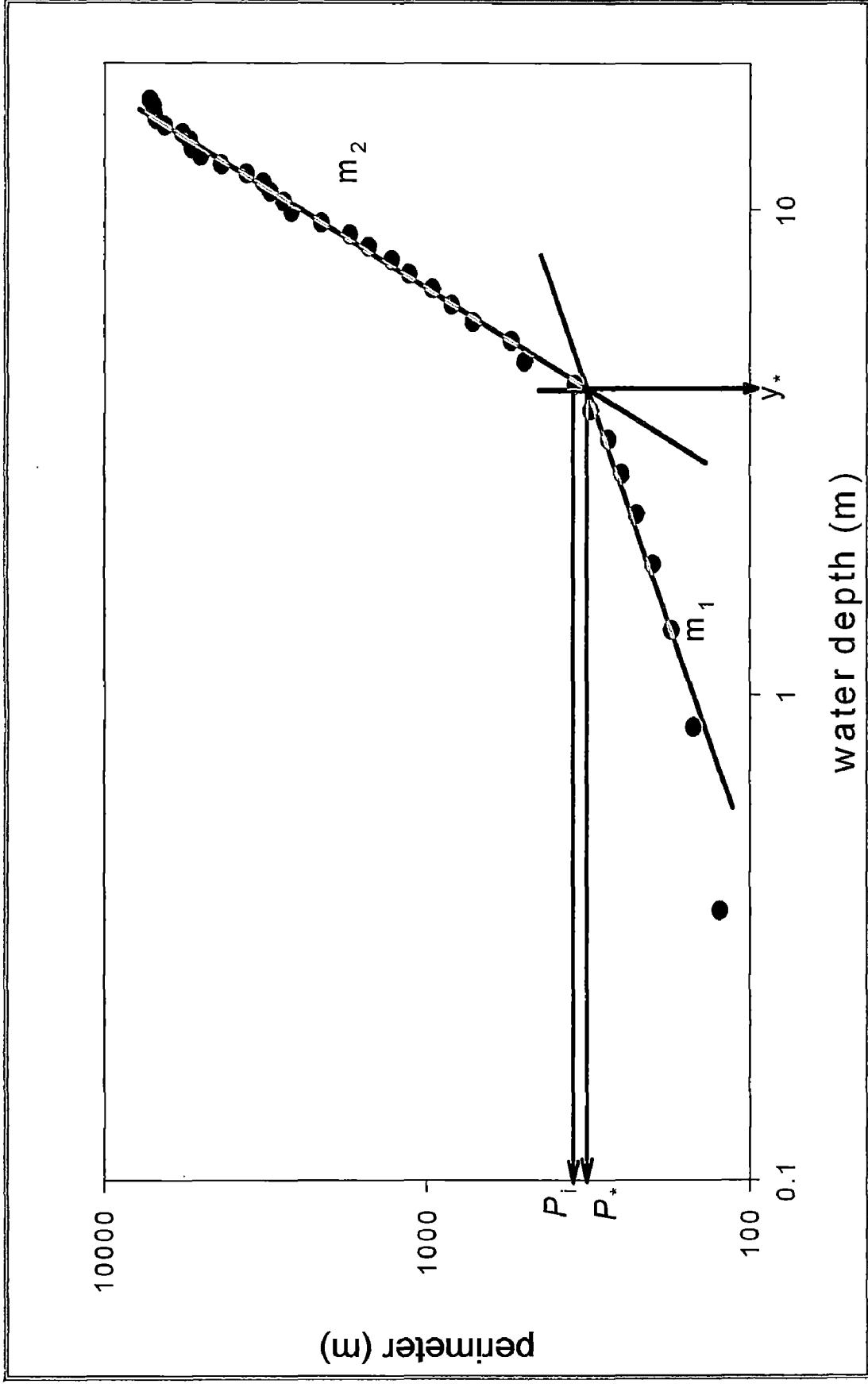


FIG 4.10 PLOT OF PERIMETER VS WATER DEPTH

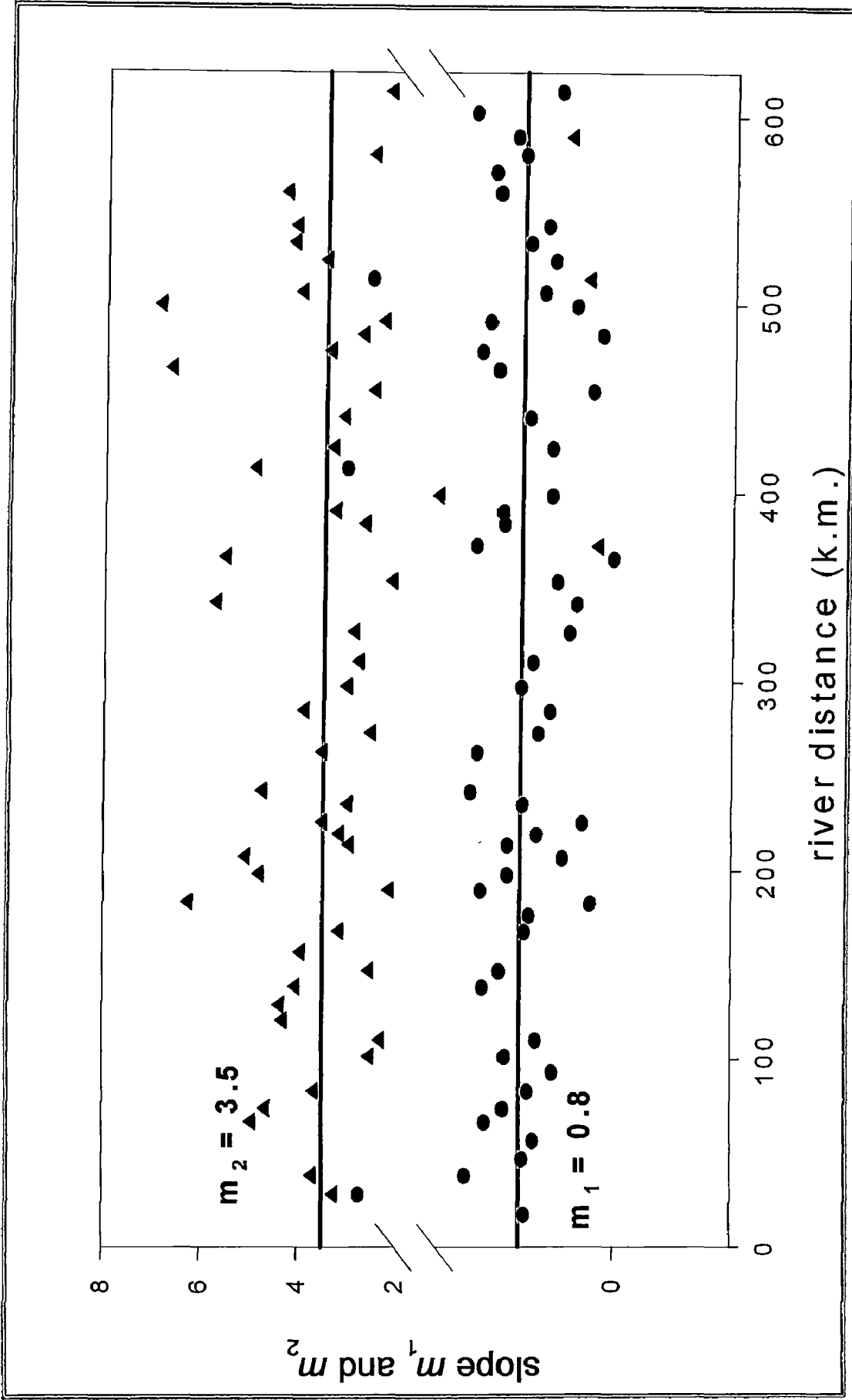


FIG 4.11 SLOPE  $m_1$  AND  $m_2$  VS RIVER DISTANCE, FOR PERIMETER

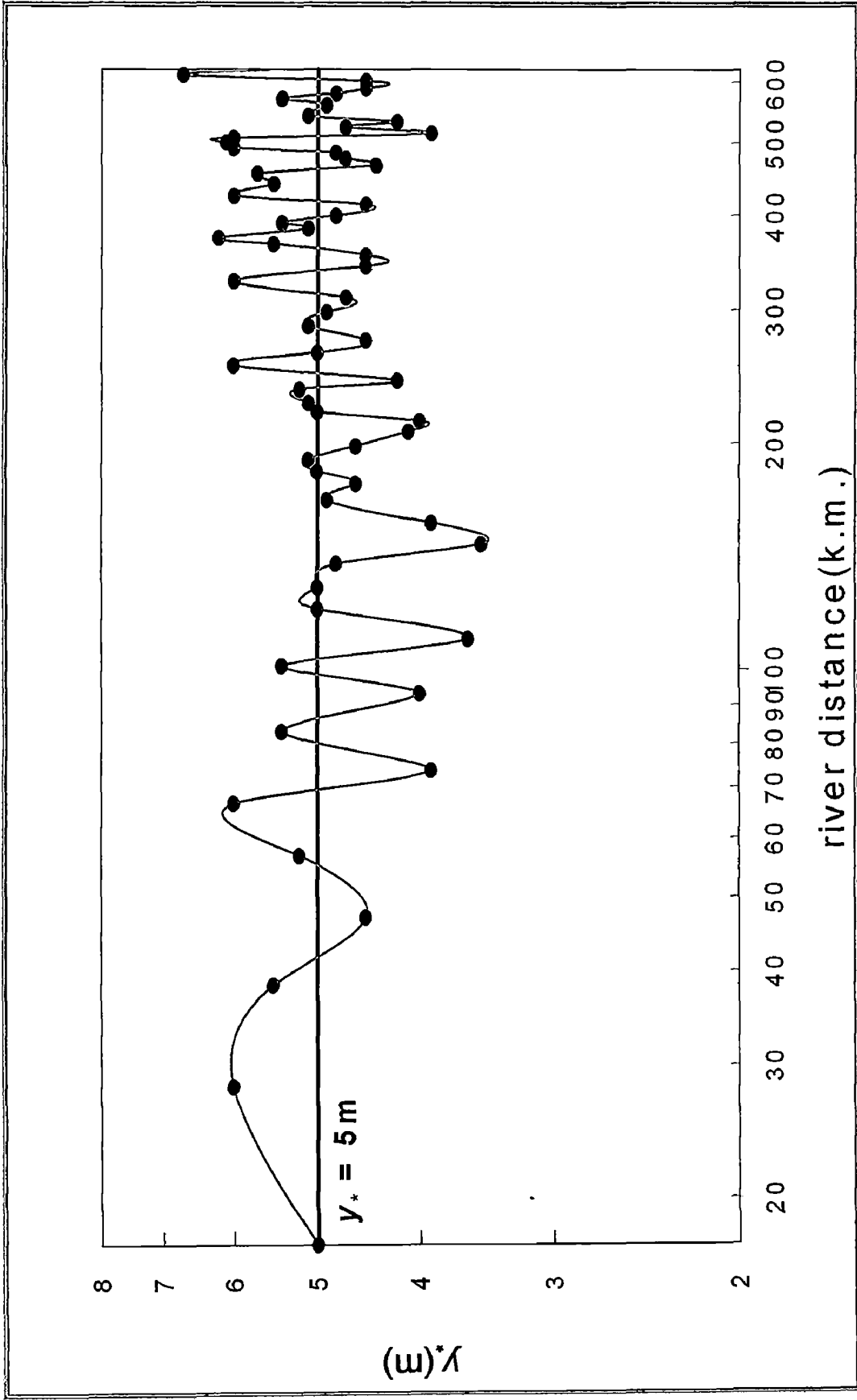


FIG 4.12 PLOT OF  $y^*$  VS RIVER DISTANCE (km)

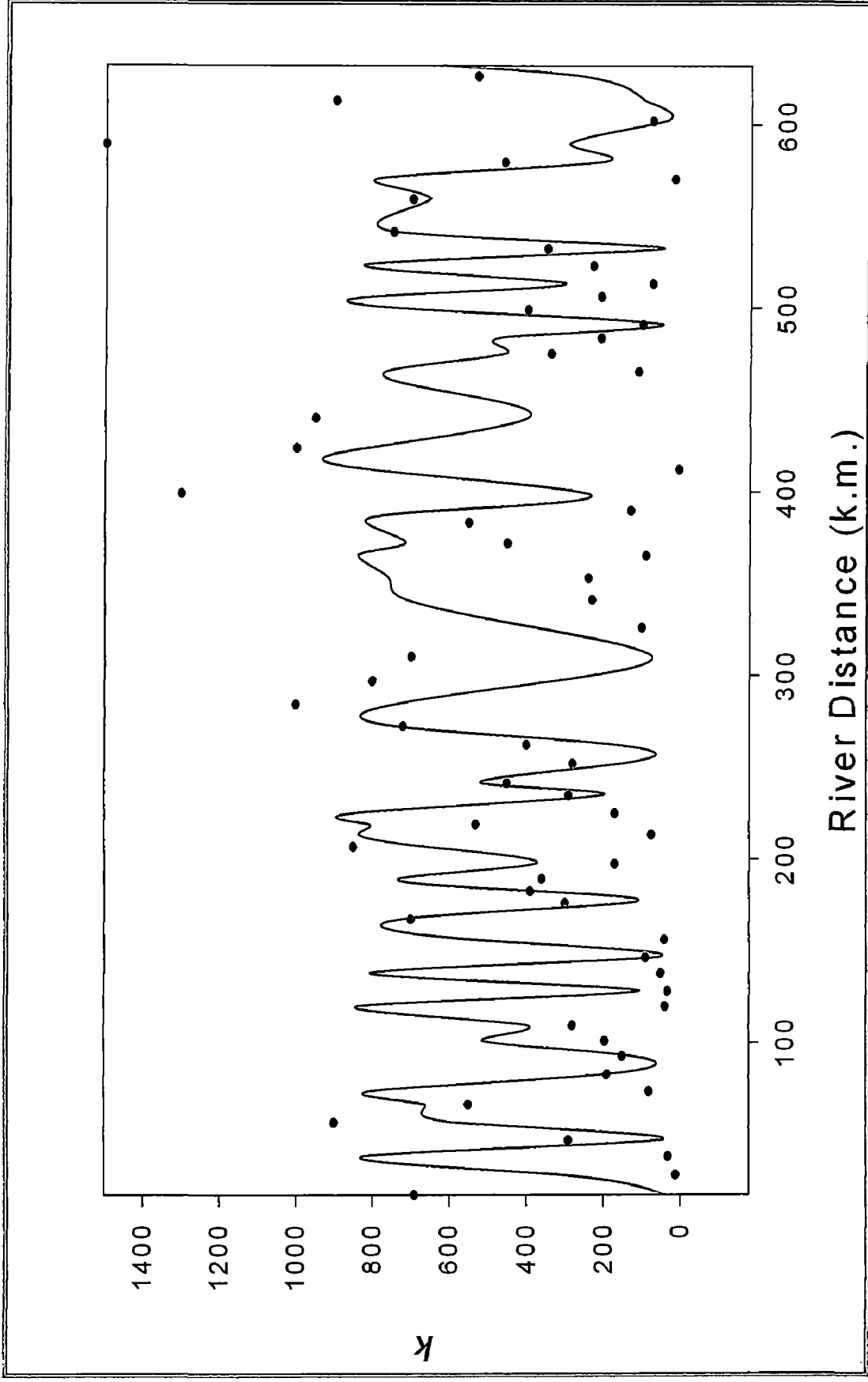


FIG 4.13 PLOT OF K VS RIVER DISTANCE (km)

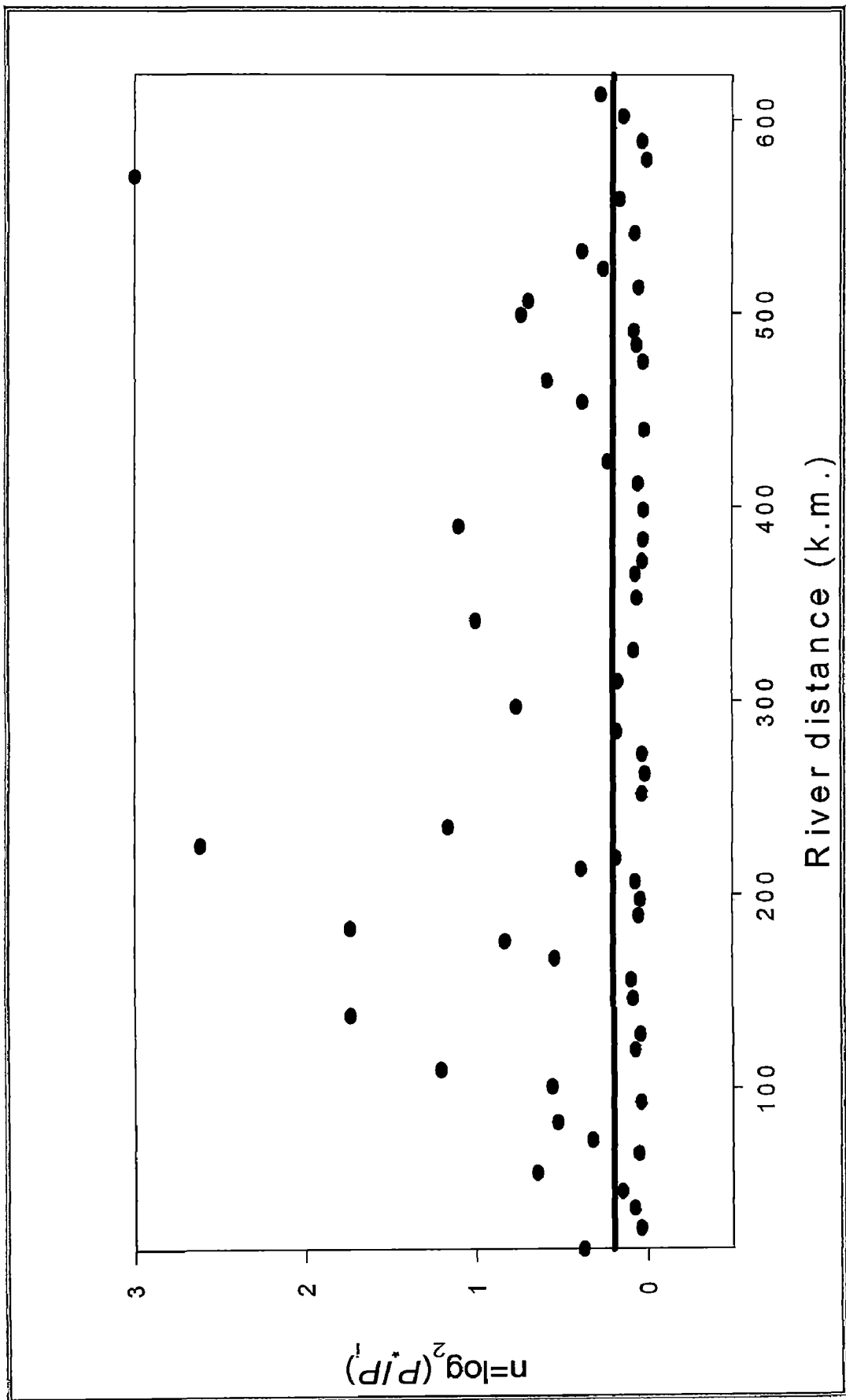


FIG 4.14 PLOT OF  $n$  VS RIVER DISTANCE (km)

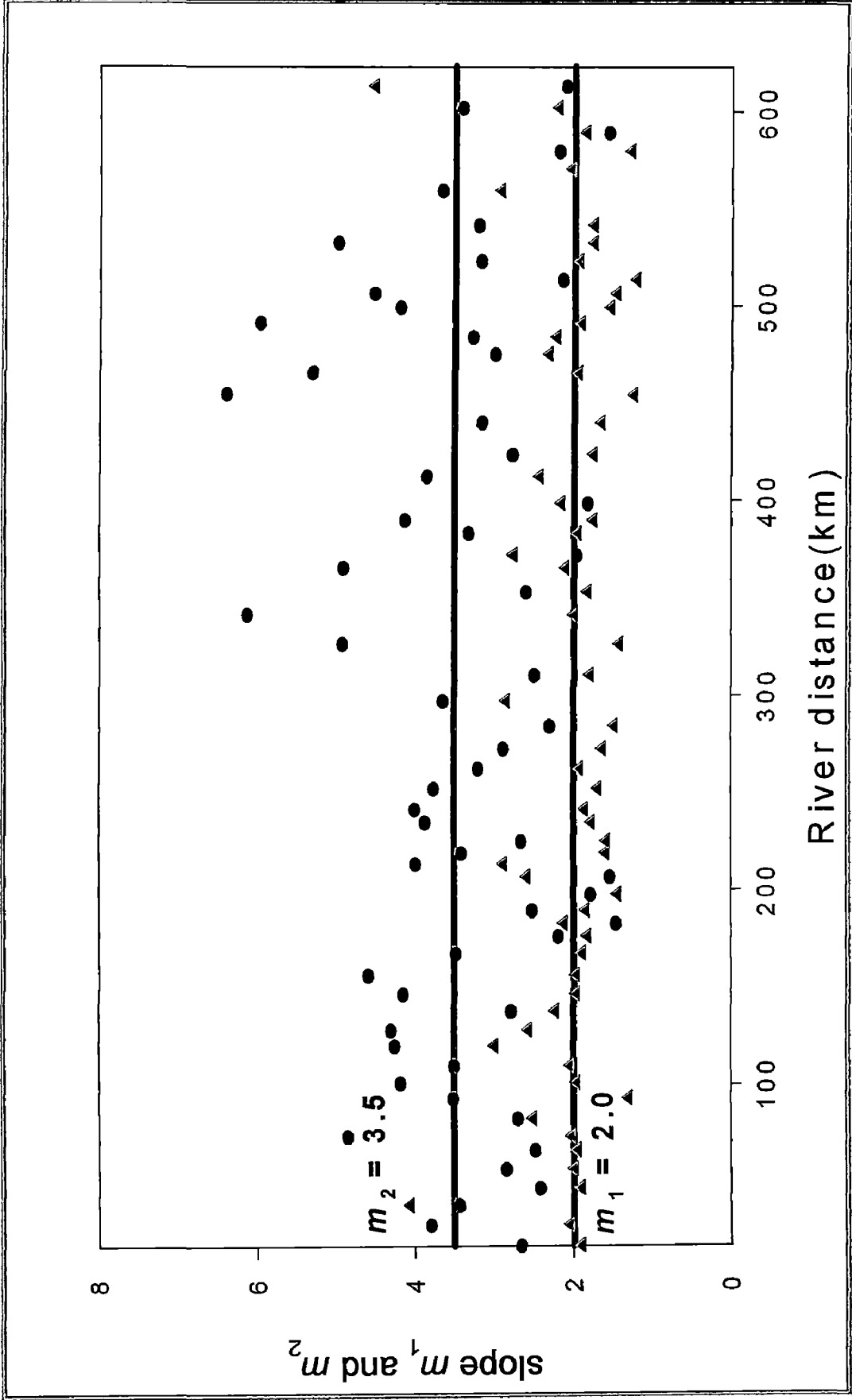


FIG 4.15 SLOPE  $m_1$  AND  $m_2$  VS RIVER DISTANCE

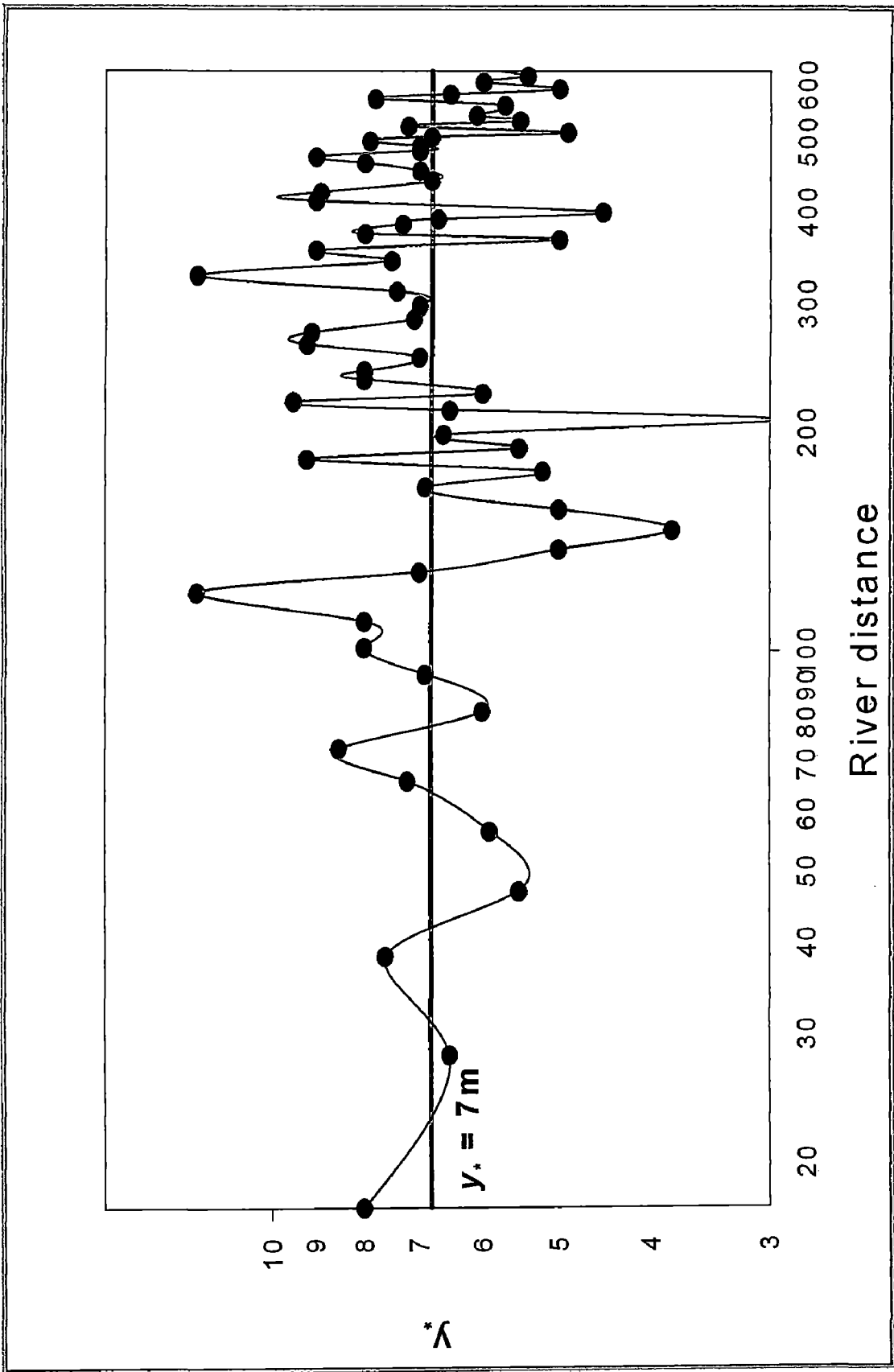


FIG 4.16 PLOT OF  $y^*$  VS RIVER DISTANCE



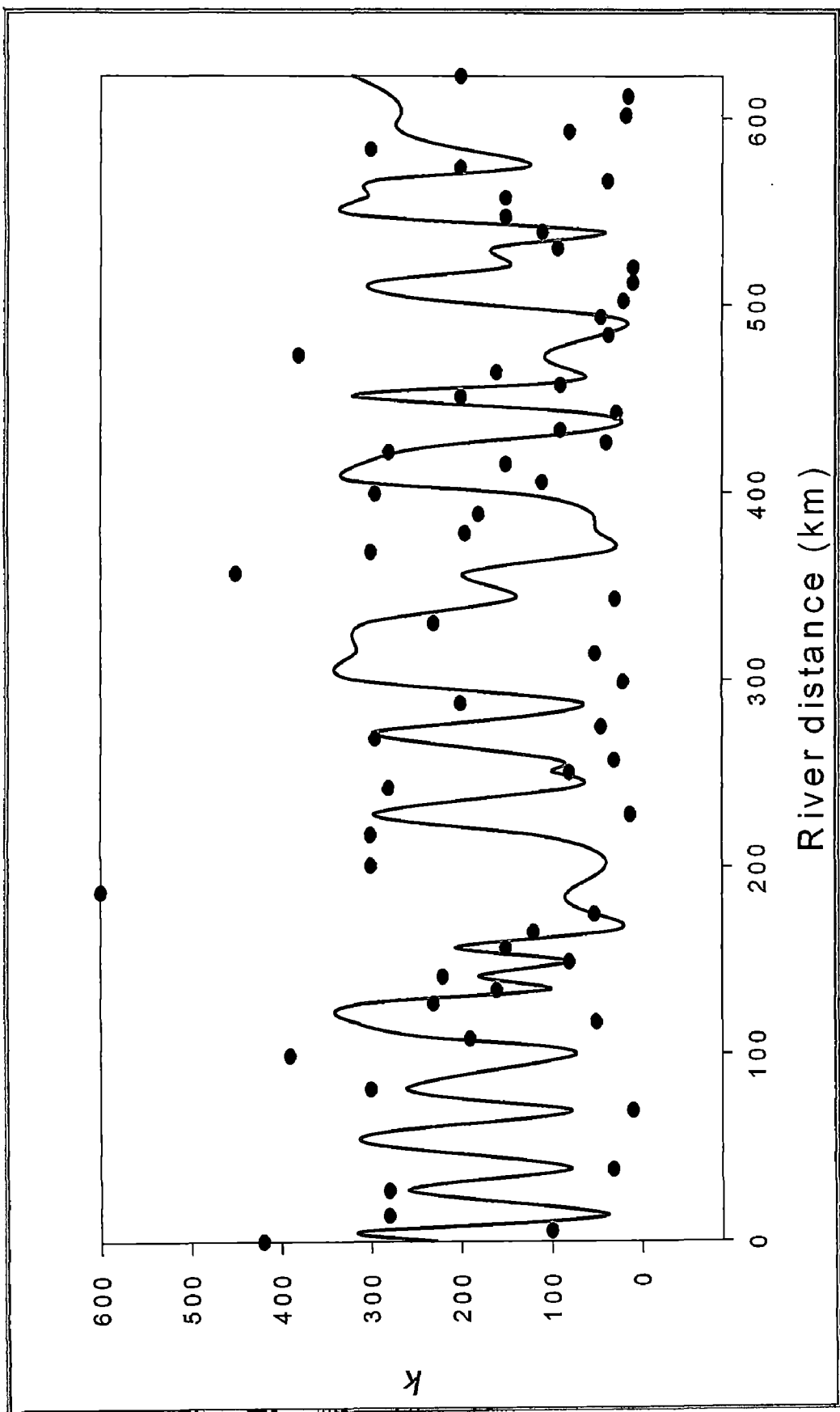


FIG 4.17 PLOT OF K VS RIVER DISTANCE

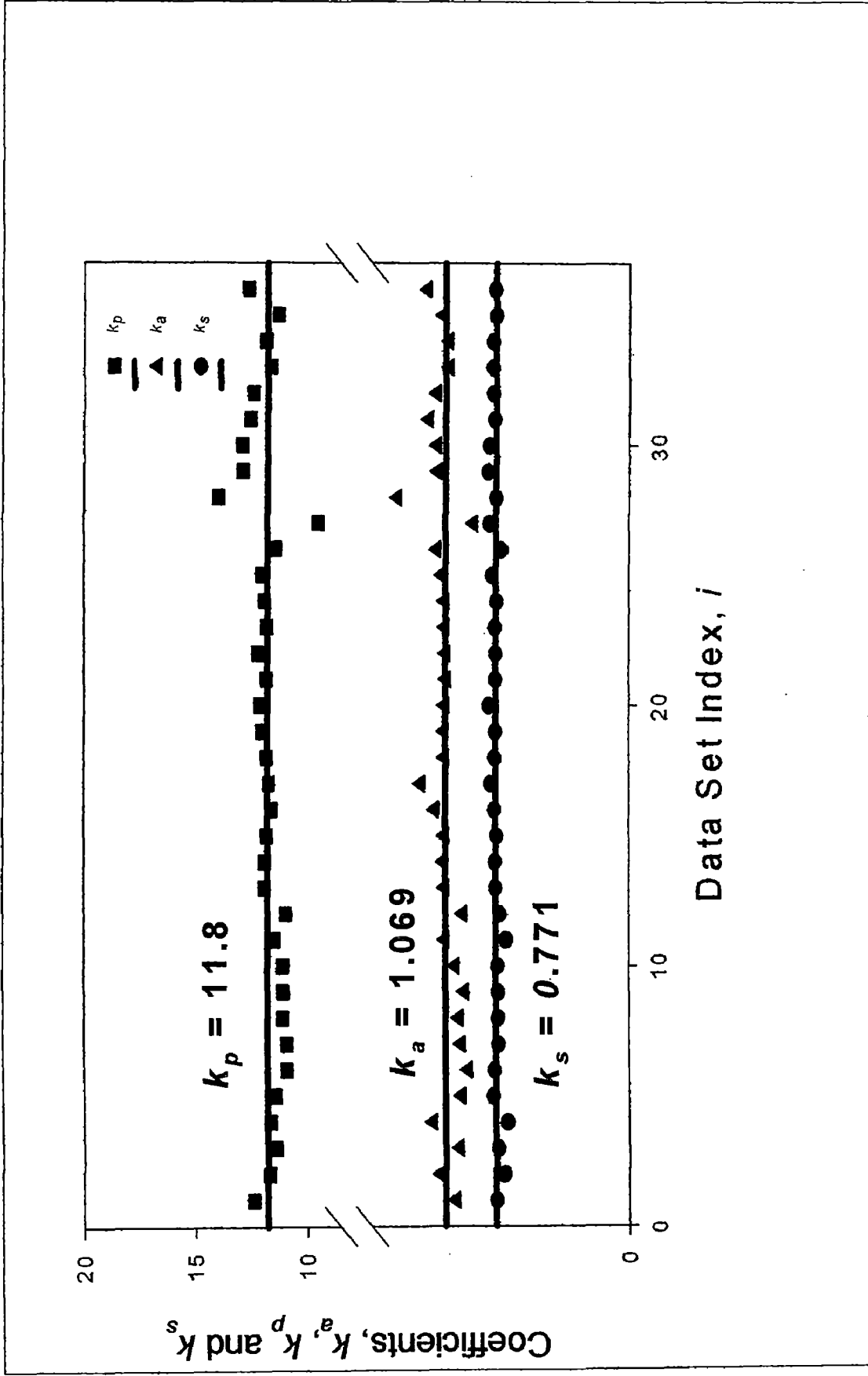


FIG 4.18 COEFFICIENT FOR SLOPE, AREA AND PERIMETER

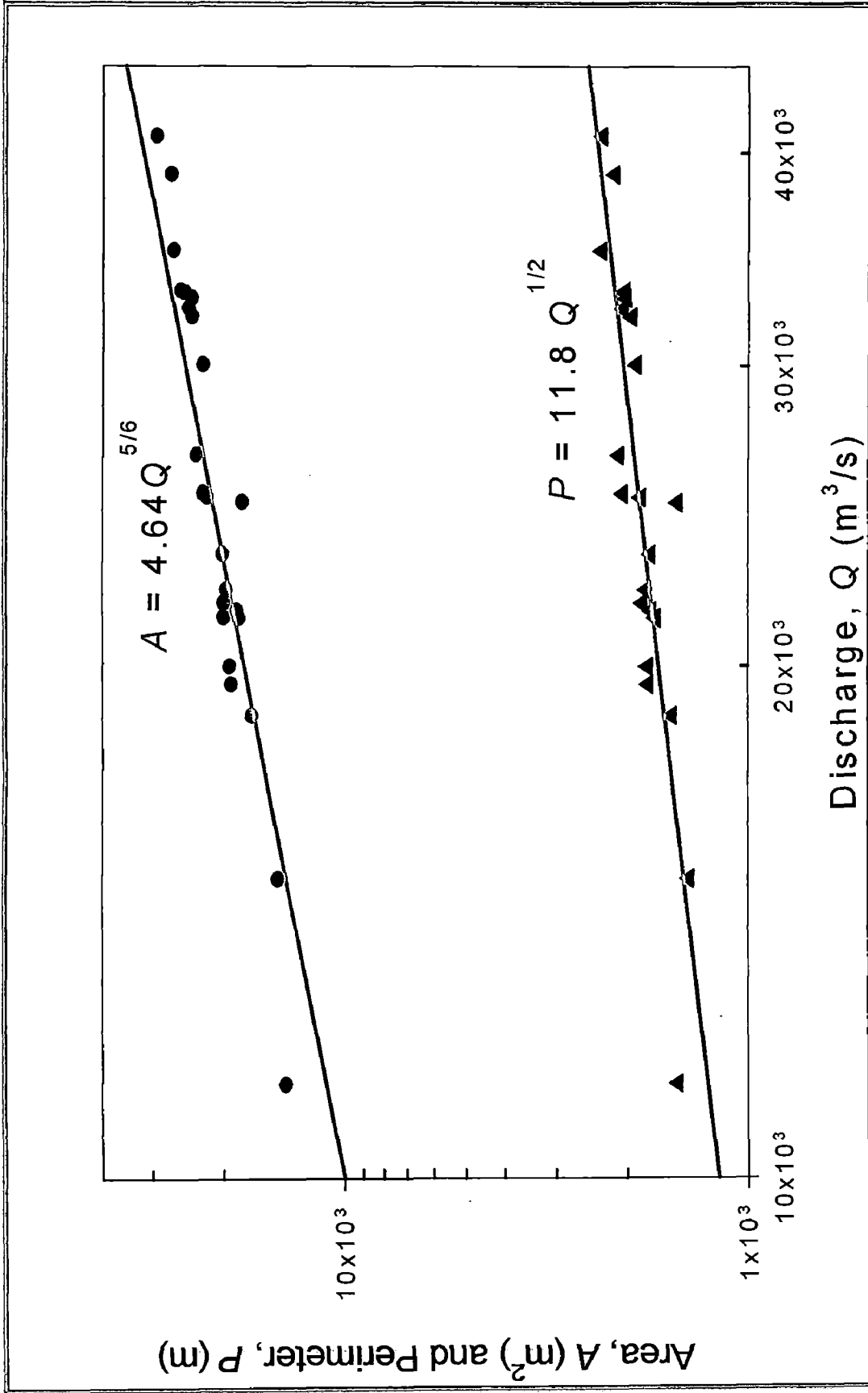


FIG 4.19 AREA A ( $m^2$ ) AND PERIMETER P (m) VS DISCHARGE

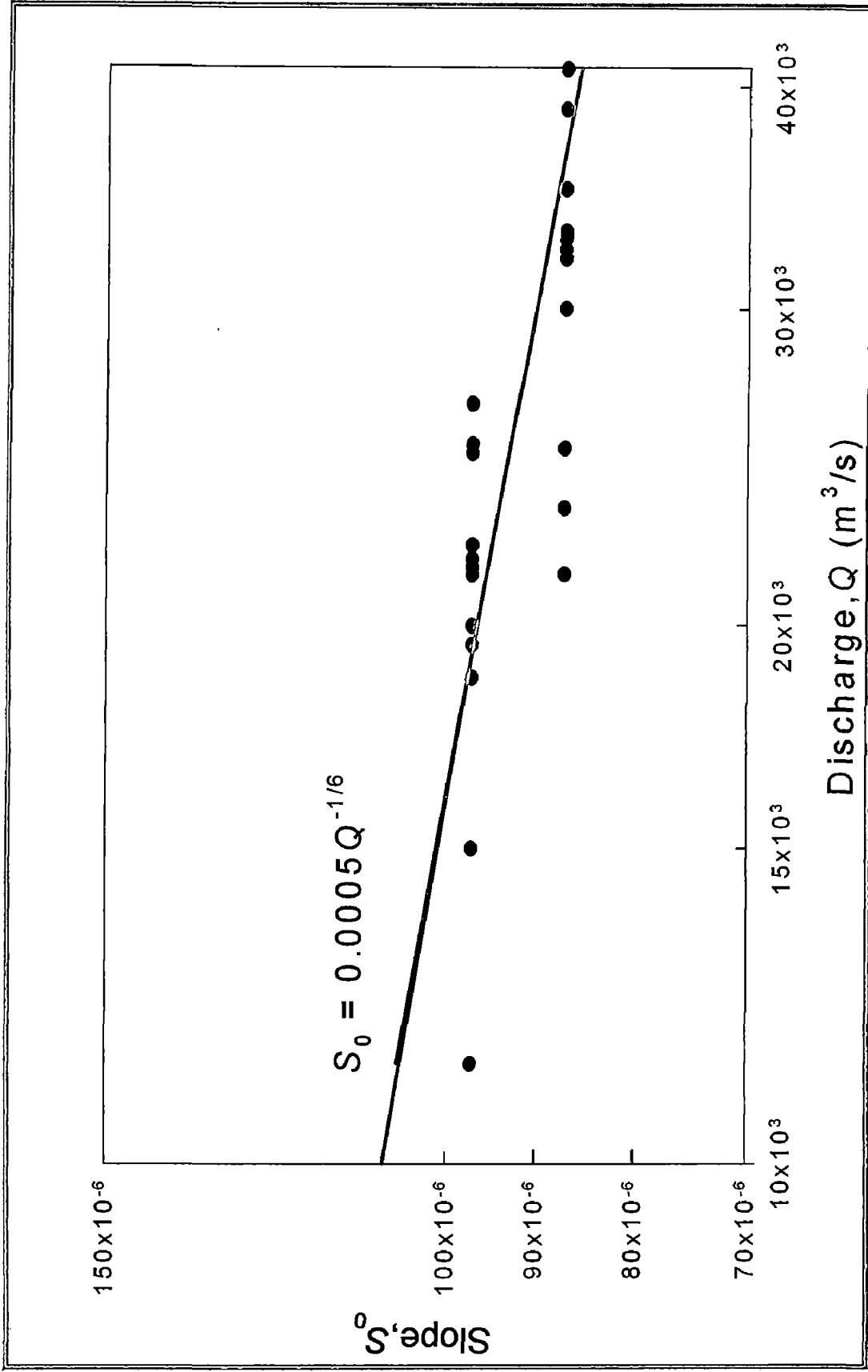


FIG 4.20 PLOT OF OBSERVED AND CALCULATED SLOPE

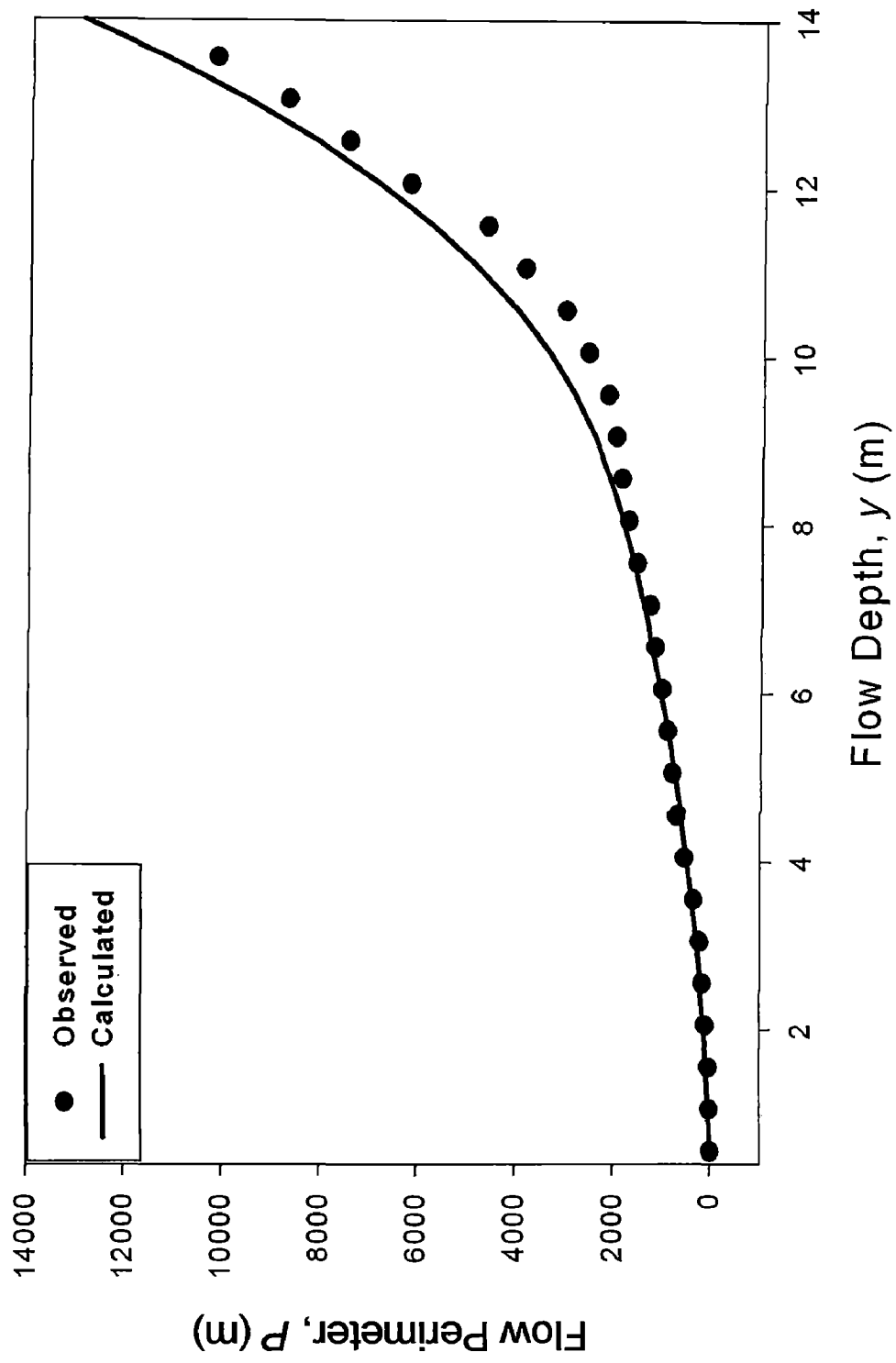


FIG 4.21 VALIDATION FOR FLOW PERIMETER

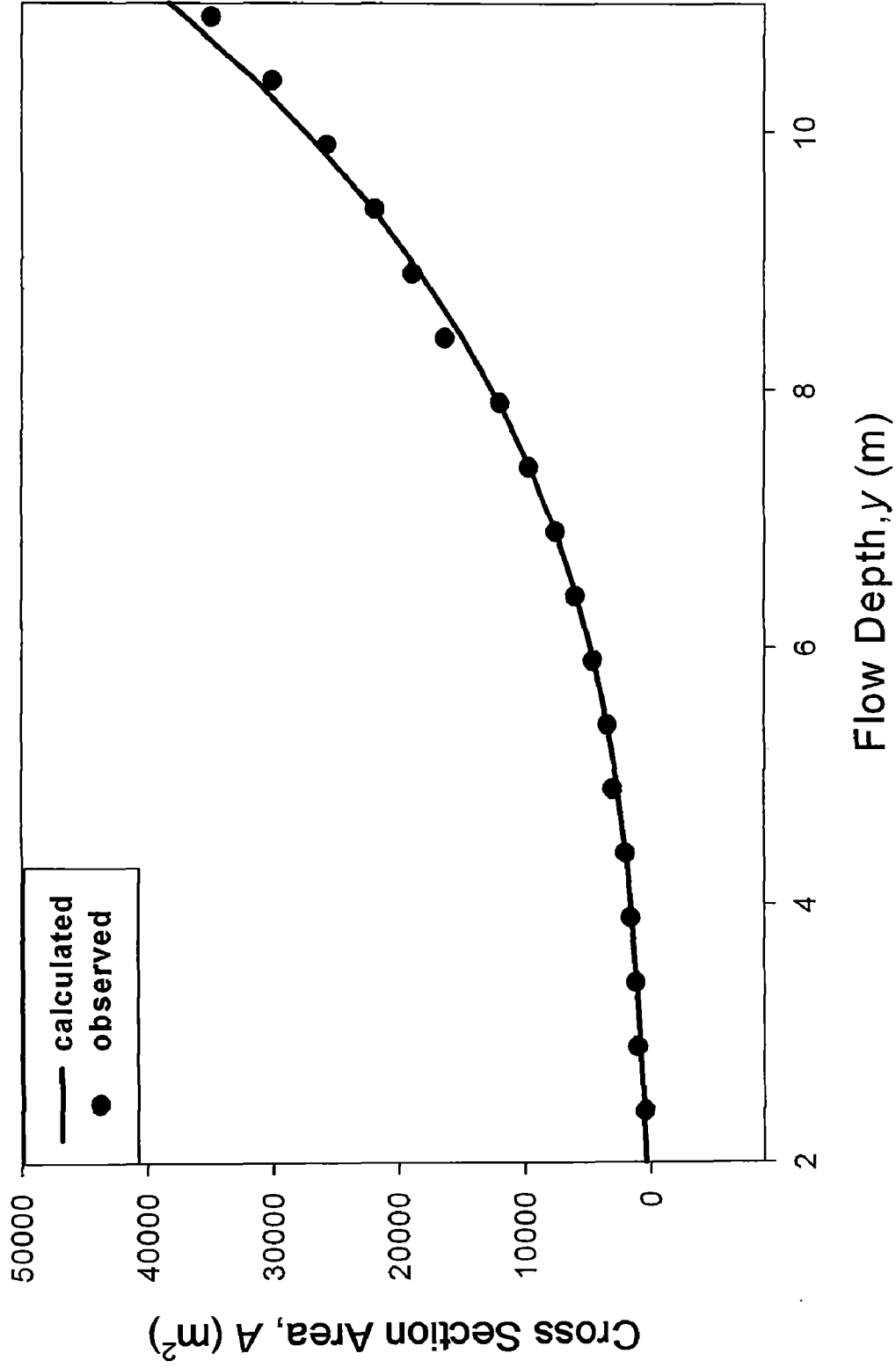


FIG 4.22 VALIDATION FOR FLOW AREA

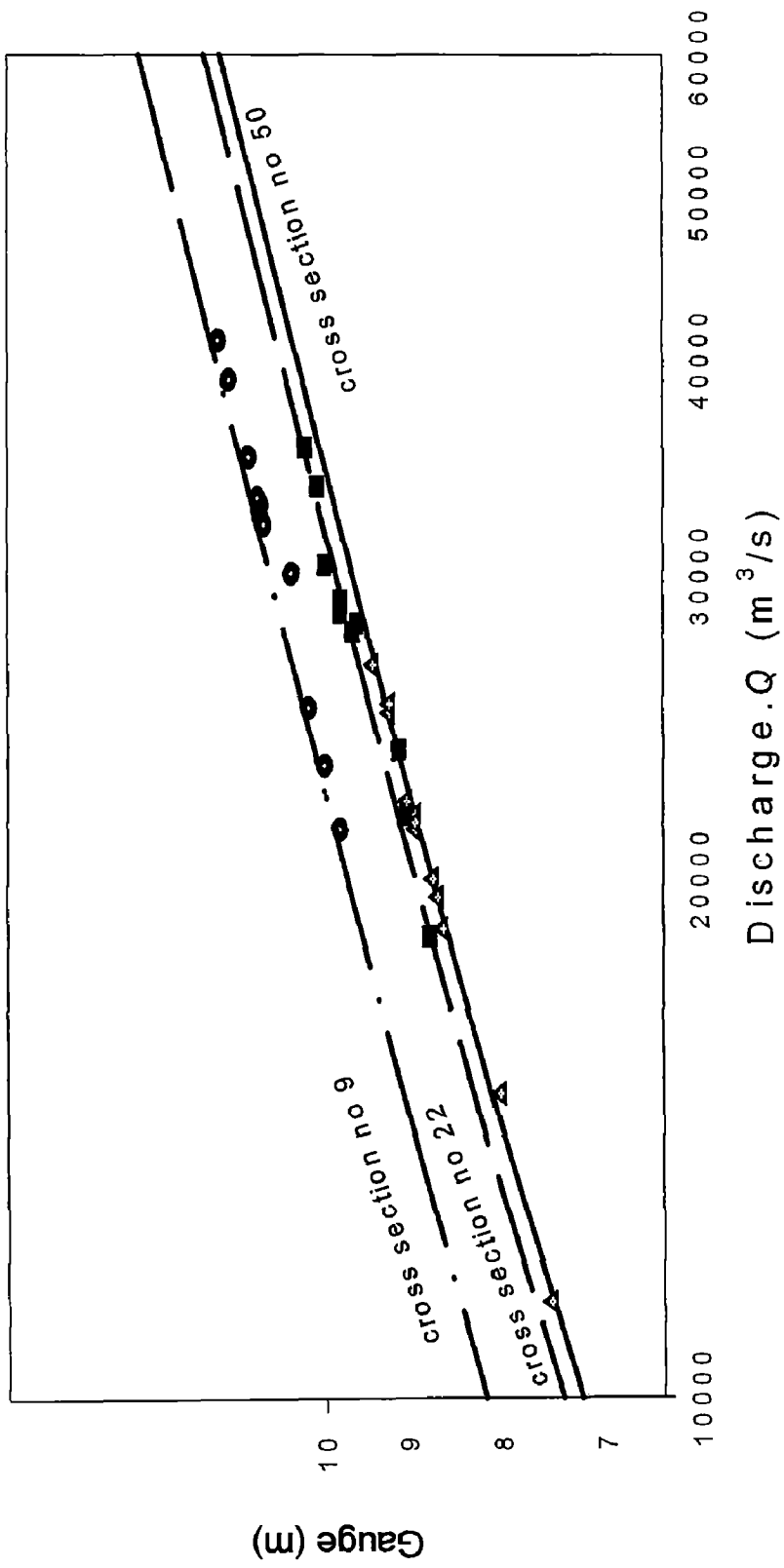


FIG 4.23 GAUGE DISCHARGE

**CHAPTER 5**  
**RESULTS AND DISCUSSION**

---

- 1) Generally, the cross-sections are not available beyond the river boundary to the extent of flood plain because of economic reasons. The cross-sectional area and perimeter of flooded river could reasonably be obtained from the modeled simplified equations (1) and (2). The simplified equations for area and perimeter can be used for flood routing of river Brahmaputra without assuming the river to be prismatic or rectangular. The accuracy of calculation can be increased by using satellite images of high resolution. The factor K in both the equation has foremost bearing on the results. Increasing the number of terms in Fourier series can increase the accuracy but simplicity of equation should not be compromised.
  
- 2) Perimeter for river Brahmaputra is two and a half times greater than that of the Lacey's perimeter. This conclusion is vital for finding out the preliminary waterway of hydraulic structures especially for braided rivers like Brahmaputra. It has been observed in many hydraulic structures on braided rivers, the operation and maintenance cost increases manifolds due to reduced waterway calculated by Lacey's perimeter. Moreover, the width of the river should not be approximated with wetter perimeter of braided rivers. It has been observed in case of river Brahmaputra that wetted perimeter is two to three times the top width.



3) Most of the available gage discharge relations are developed for specific location. Due to high establishment cost the gauging locations has to be limited. In 623 km. length of river Brahmaputra, there are only three gauging sites. In such situations, the developed equation for gauge discharge can effectively be used for calculating the discharge corresponding to known gauge at any section of the river.

## CONCLUSION

---

Based on the present investigation, the following conclusions can be drawn:

- 1) Generally, the cross-sections are not available beyond the river boundary to the extent of flood plain because of economic reasons. The cross-sectional area and perimeter of flooded river could reasonably be obtained from the modeled simplified equations (1) and (2). The simplified equations for area and perimeter can be used for flood routing of river Brahmaputra without assuming the river prismatic or rectangular.
- 2) Braided rivers may be assumed as multi-channel channel flow, whereas Lacey's formula was for single-channel. Therefore Lacey's perimeter equation was thus not borne out by field data and hence perimeter for river Brahmaputra is two and a half times greater than that of the Lacey's perimeter.
- 3) On account of braiding, meandering and large suspended sediment in river Brahmaputra there is greater resistance to flow of water compared to Lacey's straight, single and relatively silt free channel. Due to these characteristics, flow velocity for river Brahmaputra is nearly half that of Lacey's velocity.
- 4) Due to reduced velocity in river Brahmaputra due to factor(2) the cross-sectional area has to be more to follow the law of conservation of mass. Hence area for river Brahmaputra is nearly 1.8 times that of Lacey's channel.

- 5) The river is free to move in lateral direction contrary to that of Lacey's channel whose dimensions are fixed and therefore to maintain the flow area the hydraulic depth in case of river has to be decreased. Hence hydraulic depth for river Brahmaputra is nearly 0.8 times that of Lacey's hydraulic depth.
- 6) Since the sediment concentration in river is much larger than the sediment concentration in artificial channels(Amongst the large rivers of the world, river Brahmaputra is second only to the Yellow river in China in the amount of sediment transport per unit of basin area (Goswami, 1983). The average suspended load of 402 million metric tons). Therefore to transport such a large amount of sediment, the river naturally acquires a greater slope. This probably may be the reason for slope of river Brahmaputra to be nearly six times greater than that for Lacey's slope.
- 7) The modeling procedure attempted to arrive at the equation for discharge of the river at any cross-section has been validated through the observed data sets, which substantiated the results and is in agreement with the desired accuracy. The Equation for gauge discharge curve developed in this research can effectively be used for flood forecasting of river Brahmaputra.
- 8) The gauge discharge relationship developed in this study is capable of calculating the discharge corresponding to known gauge at any section of the river.

## REFERENCES :

---

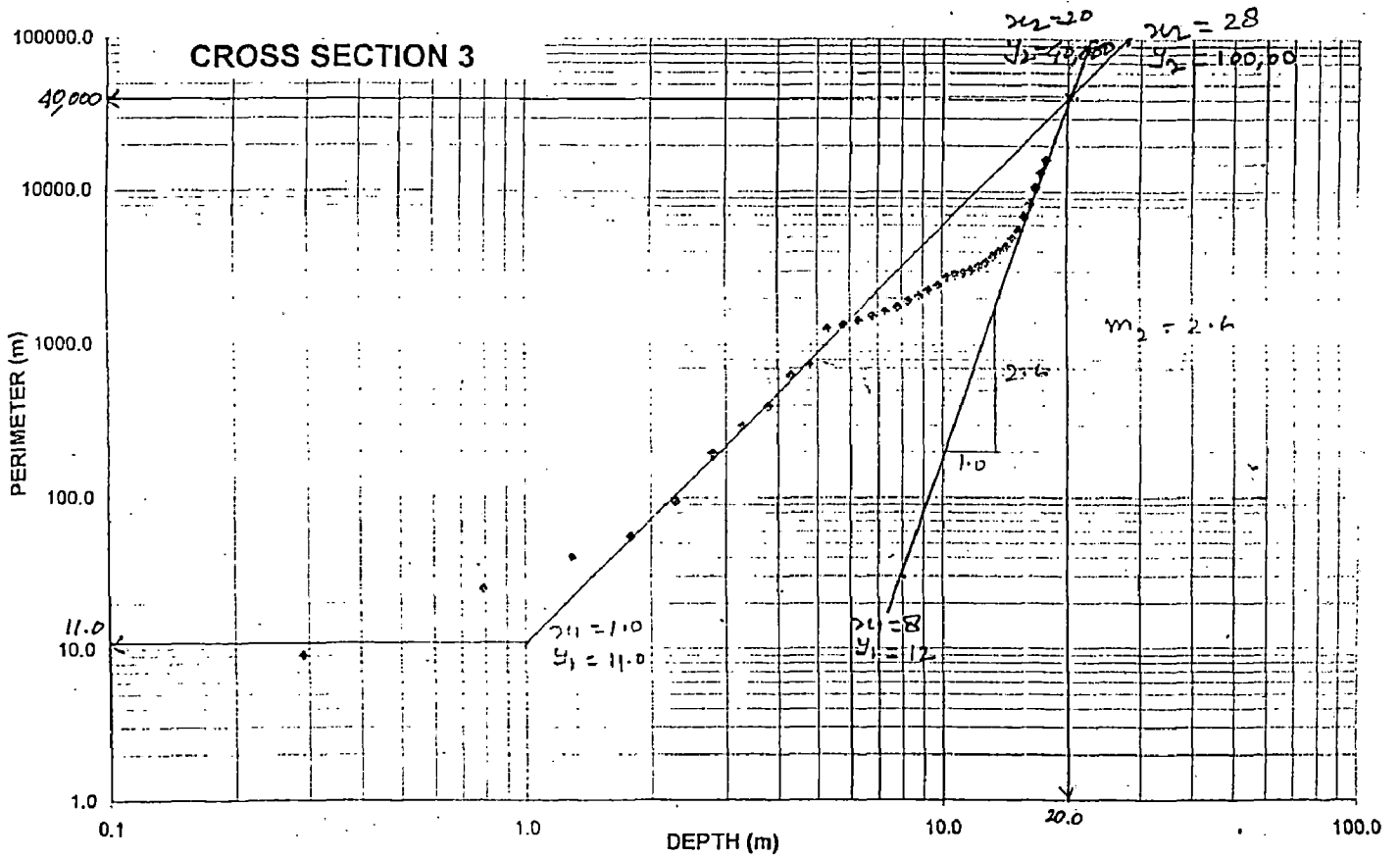
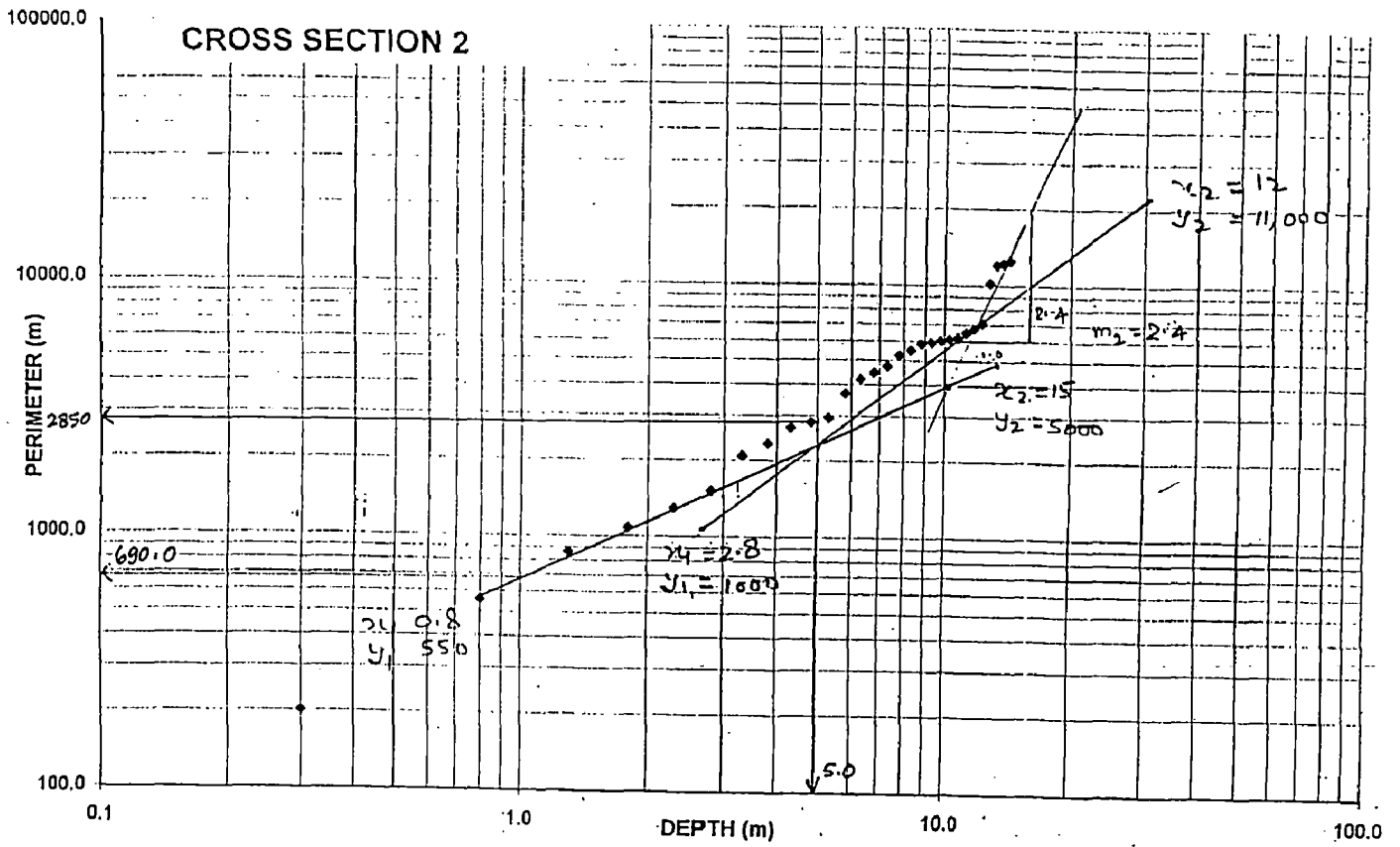
1. Anonymous, (1986), Master plan of Brahmaputra Basin, Part-I, Mainstream. Brahmaputra Board, Guwahati, pp.165.
2. Anonymous. 1986, Atlas of Brahmaputra Basin, Vol. 1 and 2, Brahmaputra Board, Ministry of Water Resources, Guwahati, India.
3. Barton, I.J. and Bathols, J.M., 1989, monitoring floods with AVHRR, Remote sensing of Environment, 30, 89-94
4. Baumann, P., 1999, Flood analysis: 1993 Mississippi Flood. URL <http://www.research.umbc.edu/~tbenja1/baumann/mod2.html>.
5. Brahmaputra Board, Ministry of Water Resources, Govt. of India, (1986), "Atlas of Brahmaputra Basin", Vol. I.
6. Brahmaputra Board, Ministry of Water Resources, Govt. of India, (1986), "Atlas of Brahmaputra Basin", Vol. II.
7. Datta B. and Singh V. P., (2004), Hydrology, The Brahmaputra Basin Water Resources, Kluwer Academic Publication, The Netherlands, pp. 139-195.
8. Frazier, P. and Page, K., (2000), Water body detection and delineation with Landsat TM data, Photogrametric Engineering and Remote Sensing, Vol. 66, No. 12, December 2000.
9. Goswami, D. C., (1998), Flood Studies in India, Geol. Soc. of India, Bangalore, pp. 53-75.
10. Goswami, D.C. and Das, P.J. 2000, Report on some characteristics of high flow and low flow in the Brahmaputra River, India, Guwahati University, Guwahati, India.
11. Goswami, D.C., 1998, Fluvial regime and Flood Hydrology of the Brahmaputra River Assam, In: Kale V. S. (ed.) Flood studies in India, Geol. Soc. India, Memoir 41, pp. 53-75

12. Goswami, S. D., (1983). "*Brahmaputra River Assam (India) -Suspended Sediment Transport, Valley Aggradation and Basin Denudation*". Ph.D. Thesis, Johns Hopkins Univ., Maryland, pp. 199.
13. Islam, M. and Kimiteru Sado, 2000, Flood hazard assessment in Bangladesh using NOAA AVHRR data with GIS, *Hydrological Processes*, 14, 605-620, 2000
14. Lacey, G. 1929-1930, Stable channel in alluvium. *Proc. Inst. of Civil Engrs.*, London, Vol. 229, pp. 259-285.
15. Lacey, G. 1933-1934, Uniform flow in alluvial rivers and canals. *Proc. Inst. of Civil Engrs.*, London, Vol. 237, pp. 421-453.
16. Lacey, G. 1958, Flow in channels with sandy mobile beds. *Proc. Inst. of Civil Engrs.*, London, Vol. 9, pp. 145-164.
17. Lacey, G., (1930), Stable channels in alluvium, *Proceedings, Institution of Civil Engineers*, Vol. 229, pp. 259-384.
18. Lacey, G., (1946), A general theory of flow-in alluvium, *Journal of the Institution of Civil engineering*, London, Vol.27, 16-47, Vol.28, pp. 425-451.
19. Lacey, G., (1958), Flow in alluvial channels with sand mobile beds. *Proceedings, Institution of Civil Engineers*, London, Vol. 9, pp. 146-164.
20. Lin, C., 1989, Applying meteorological satellite information to monitor waterlogging in Heilongjiang Province, *Remote sensing information*, 24-28.
21. Liu, Z., F.Huang and E.Wan, 2002, Dynamic monitoring and damage evaluation of flood in north-west Jilin with remote sensing, *International Journal of Remote Sensing*, Vol. 23, No. 18, 3669-3679.
22. Mohapatra, P.K. and R.D.Singh, (2003), Flood management in India, *Natural Hazards* 28, 131-143, 2003, Kluwer Academic Publishers, The Netherlands.
23. Rahman, Md. Munsur and Haque, M. A., (2003). "Scour Estimation at Bridge Site: Modification and Application of Lacey Formula", *International Journal of Sediment Research*, Vol. 18, No. 4, pp. 333-339.

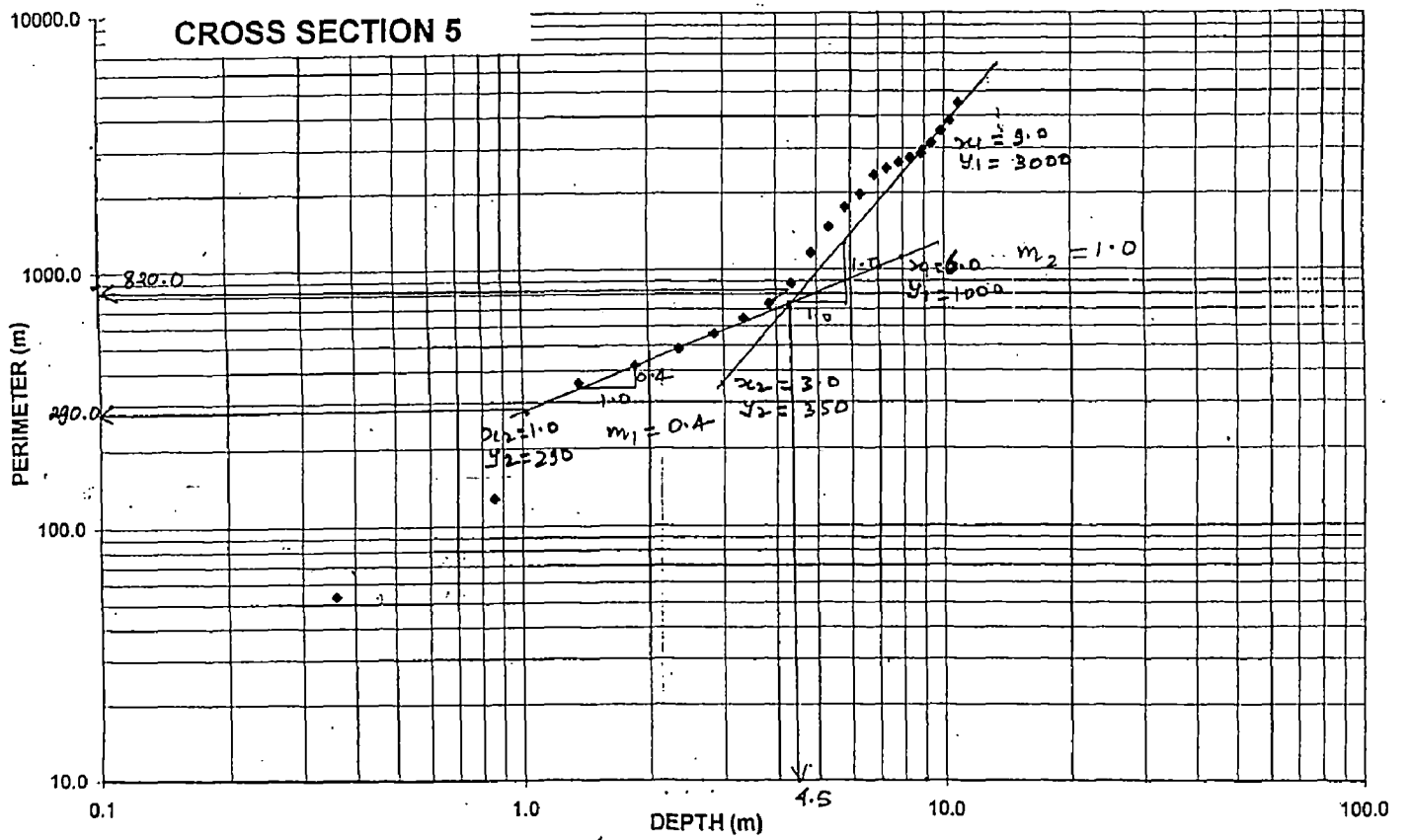
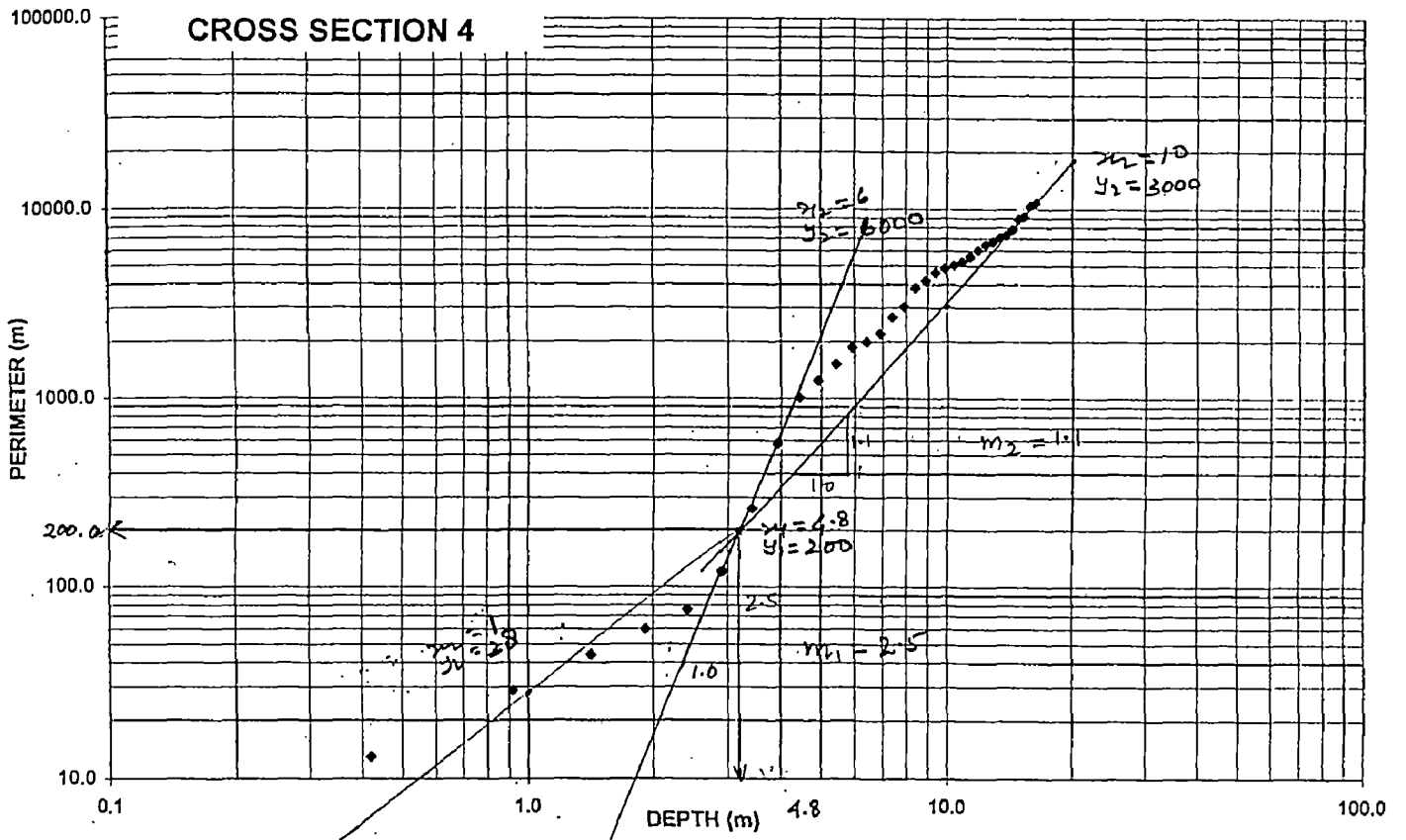
24. Sanders R., and Tabuchi S., 2000, Decision support system for flood risk analysis for river Thames, United Kingdom, *Photogrammetric Engineering and Remote Sensing Journal*, Vol. 66, No. 10.
25. Sheng, Y., and Xiao, Q., 1994, Water identification in cloud-contaminated NOAA/AVHRR Imagery, *Remote Sensing of Environment in China*, 9, 247-255
26. Sheng, Y., Su, Y. and Xiao, Q., 1998, Challenging the cloud contamination problem in flood monitoring with NOAA/AVHRR imagery, *Photogrammetric Engineering and Remote Sensing*, 64, 191-198.
27. Singh, V., P., (2003), "Theories of Hydraulic Geometry", *International Journal of Sediment Research*, Vol. 18, No. 3, pp. 196-218.
28. Smith, L.C., 1997, Satellite remote sensing of river inundation area, stage, and discharge: A review, *Hydrological Processes*, 11:1427-1439.
29. Swamee, P., K., (2000), "Stable channel objective function", *International Journal of Sediment Research*, Vol. 15 No. 4, 2000 pp. 434-439.
30. Verdin, J.P., 1996, Remote sensing of ephemeral water bodies in western Niger, *International Journal of Remote Sensing*, 17, 733-748.
31. Wang, Y., J. D. Colby and K. A. Mulcahy, 2002, An efficient method for mapping flood extent in a coastal flood plain using Landsat TM and DEM data, *Int. J. Remote Sensing*, 2002, Vol. 23, No. 18, 3681-3696
32. WAPCOS, (1993), *Morphological studies of river Brahmaputra*, New Delhi.
33. Winsnet, D. R., McGinnis, D.F., and Pritchard, J.A., 1974, Mapping of the 1973 Mississippi river floods by NOAA-2 satellite, *Water Resources Bulletin*, 10, 1040-1049.
34. Xiao, Q., and Chen, W., 1987, Songhua River monitoring with metrological satellite imagery, *Remote Sensing Information*, 37-41.

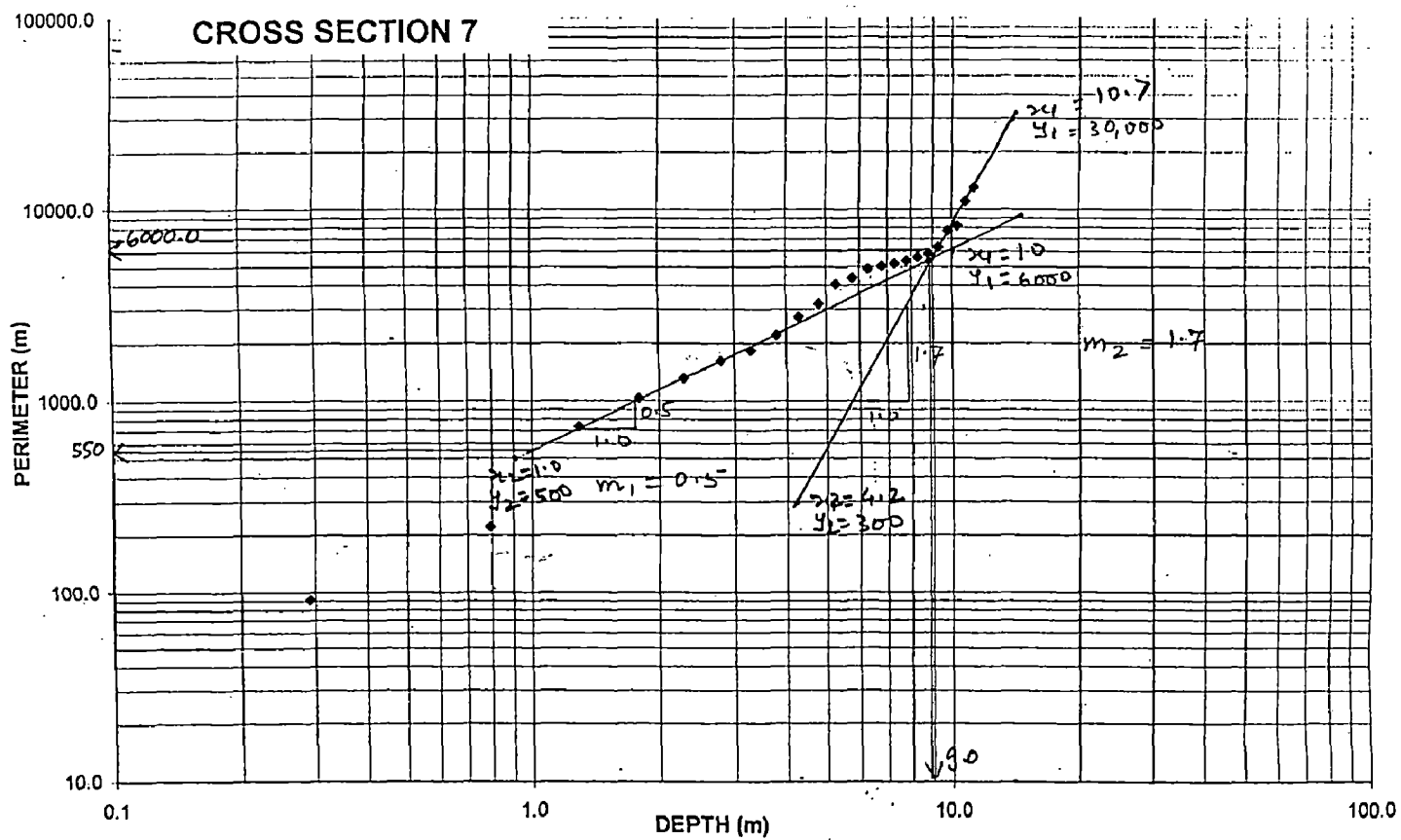
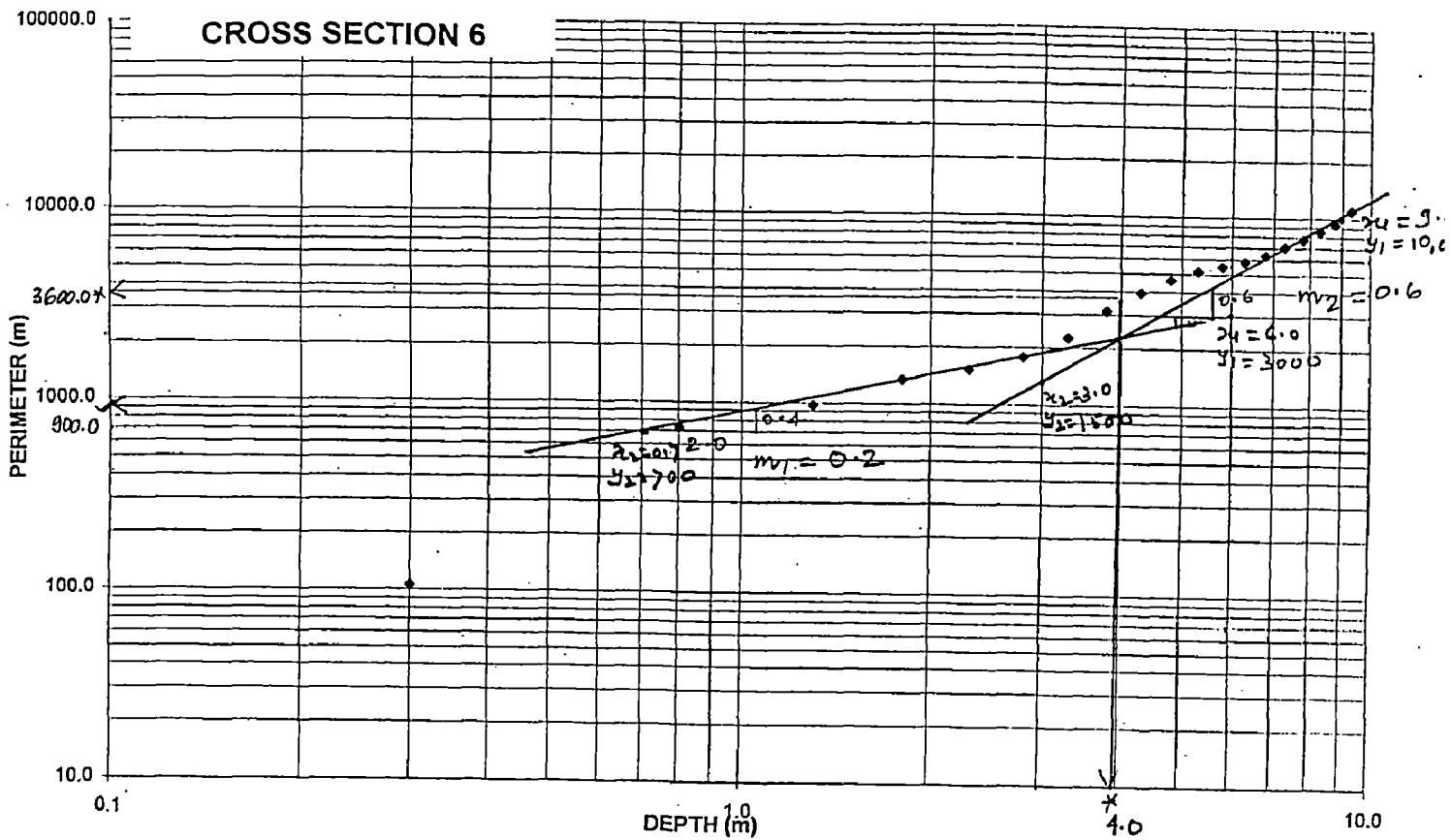
**APPENDIX A**  
**PLOT OF PERIMETER VS DEPTH**  
**FOR FINDING PARAMETER OF PERIMETER EQUATION**

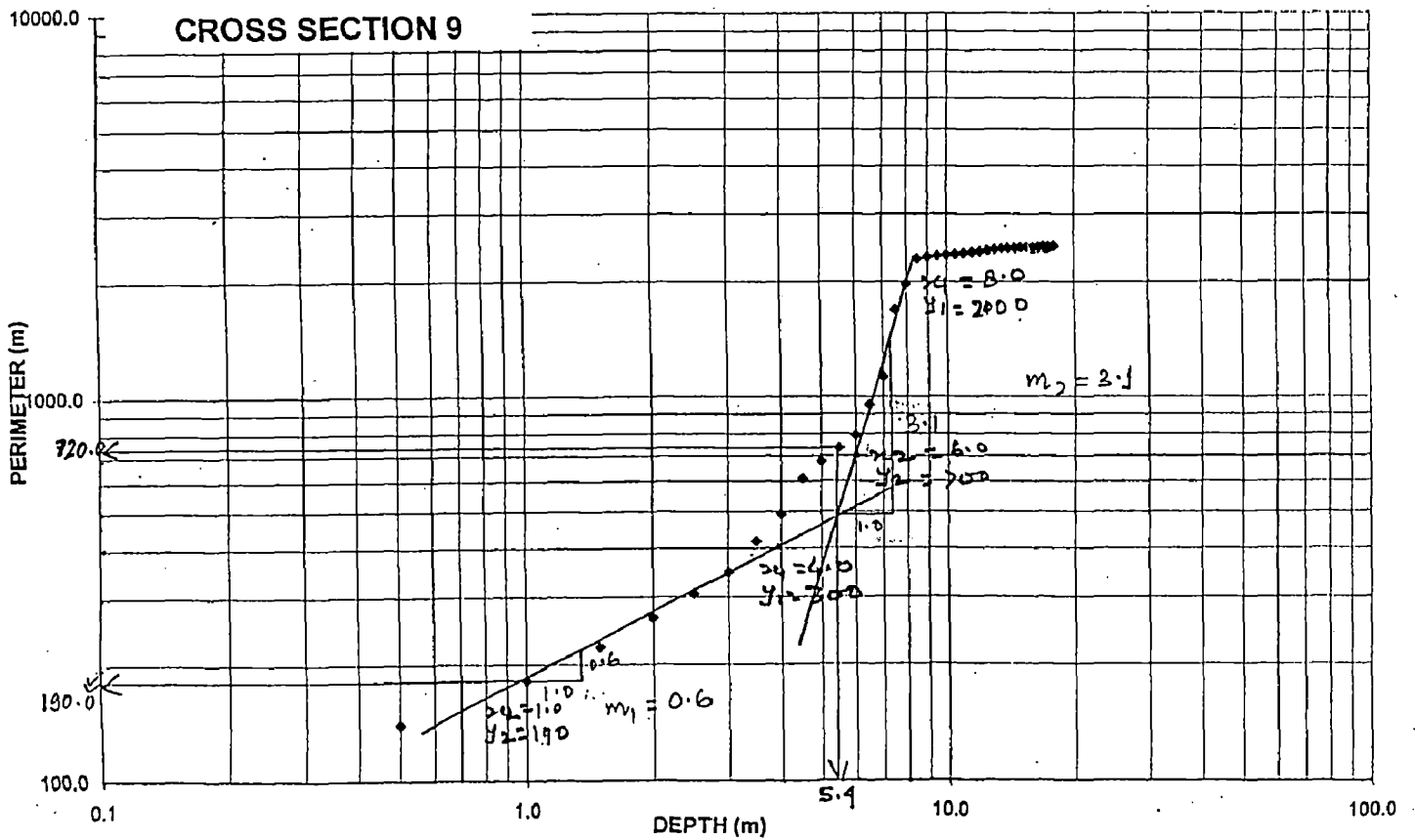
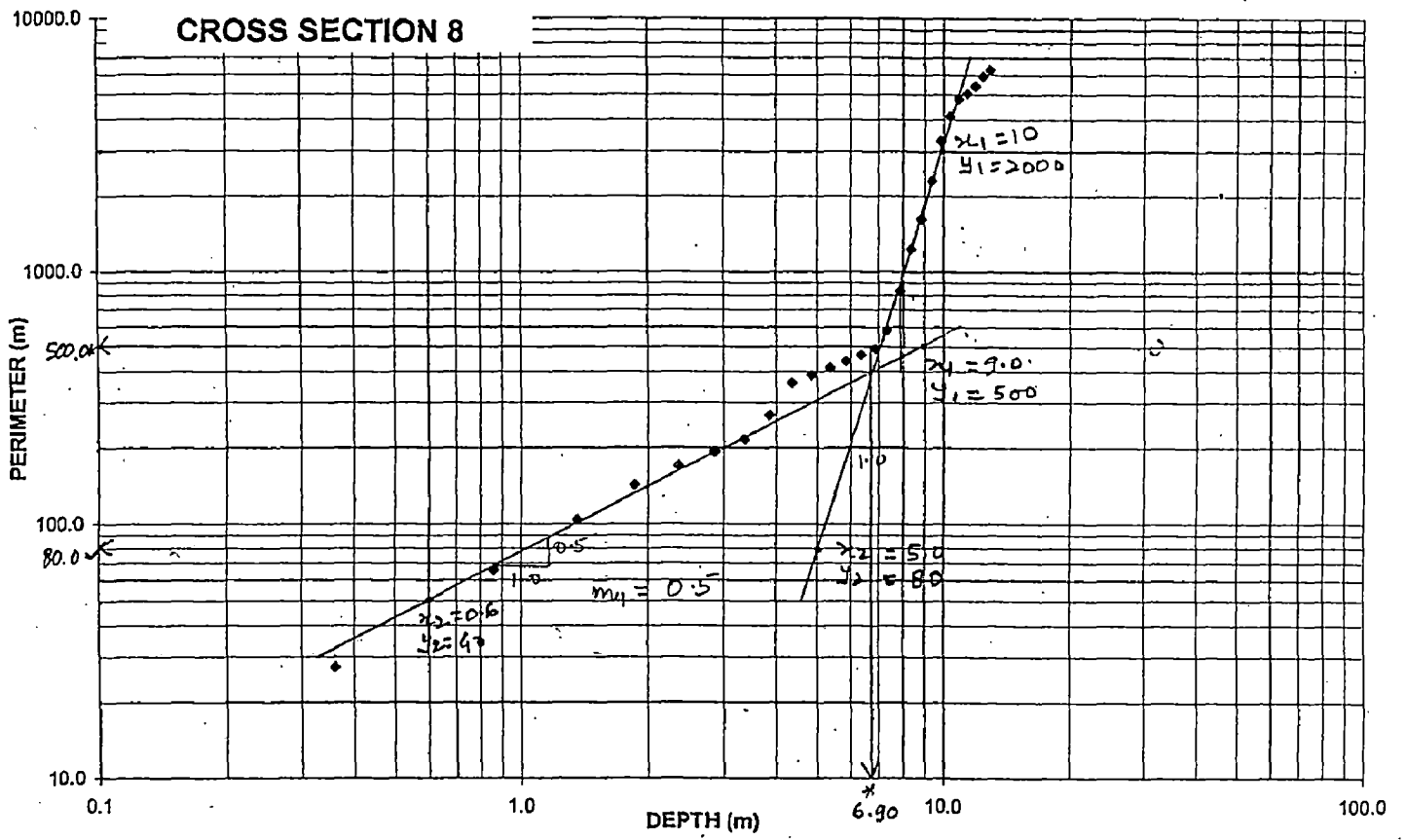
---

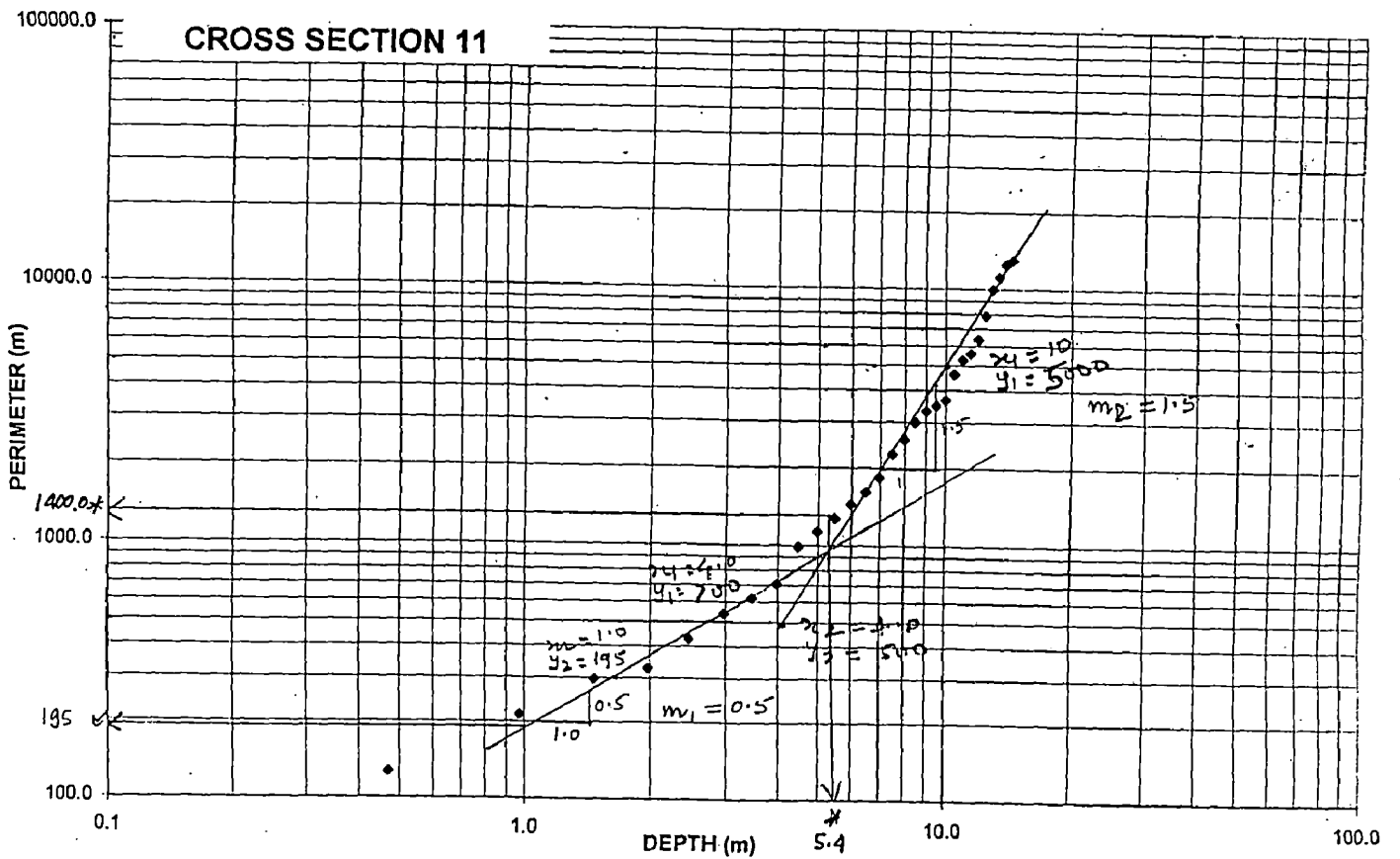
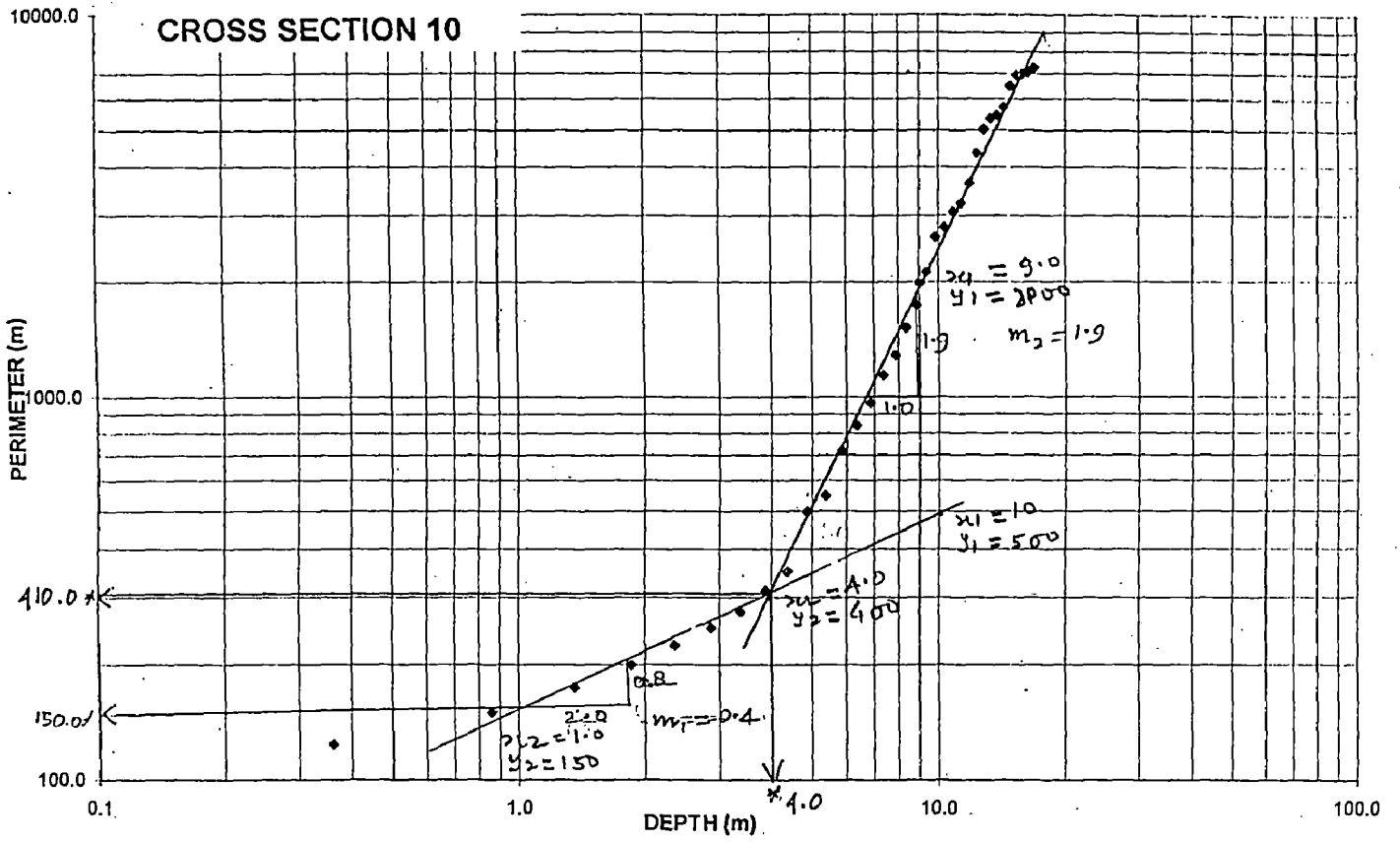


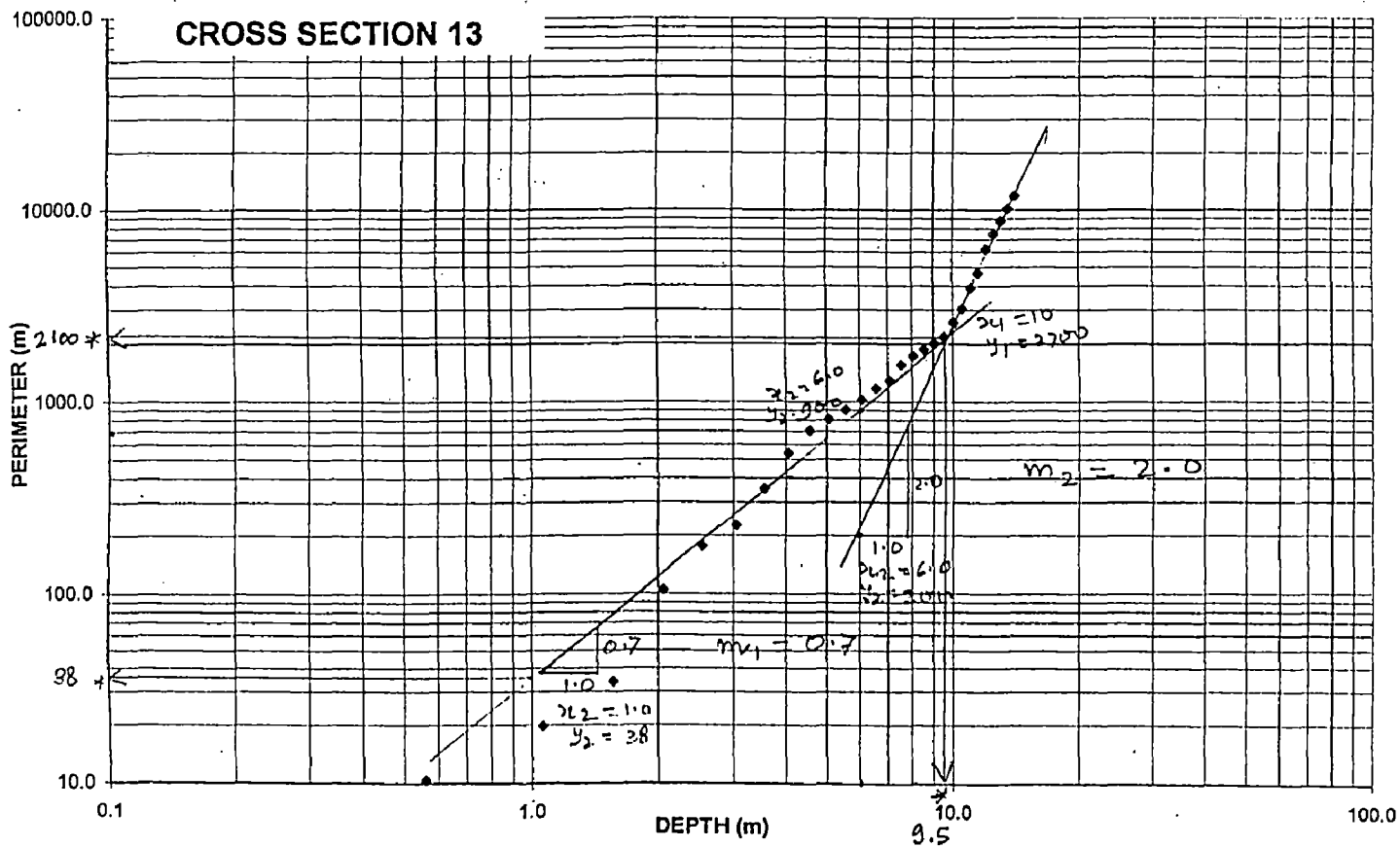
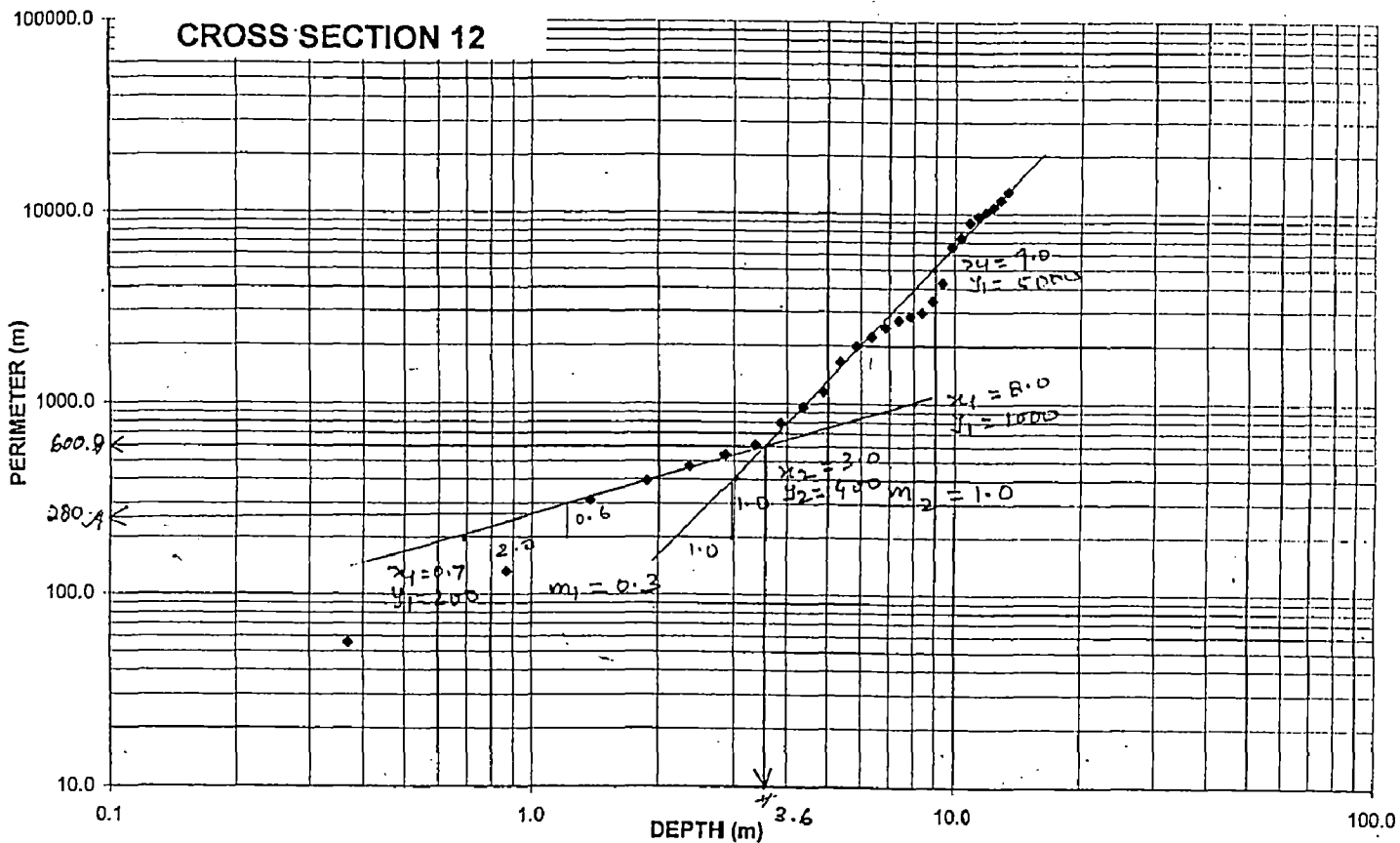


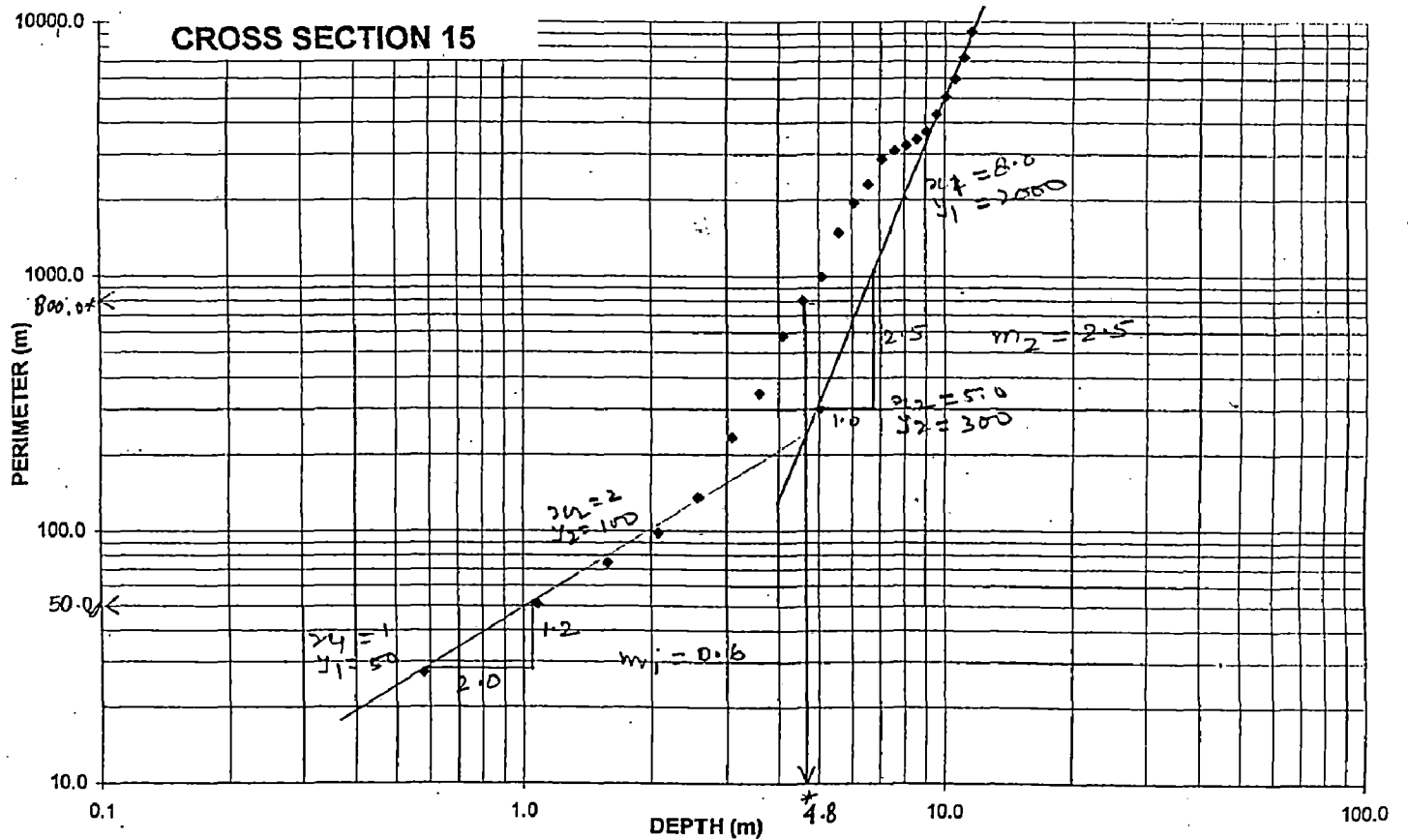
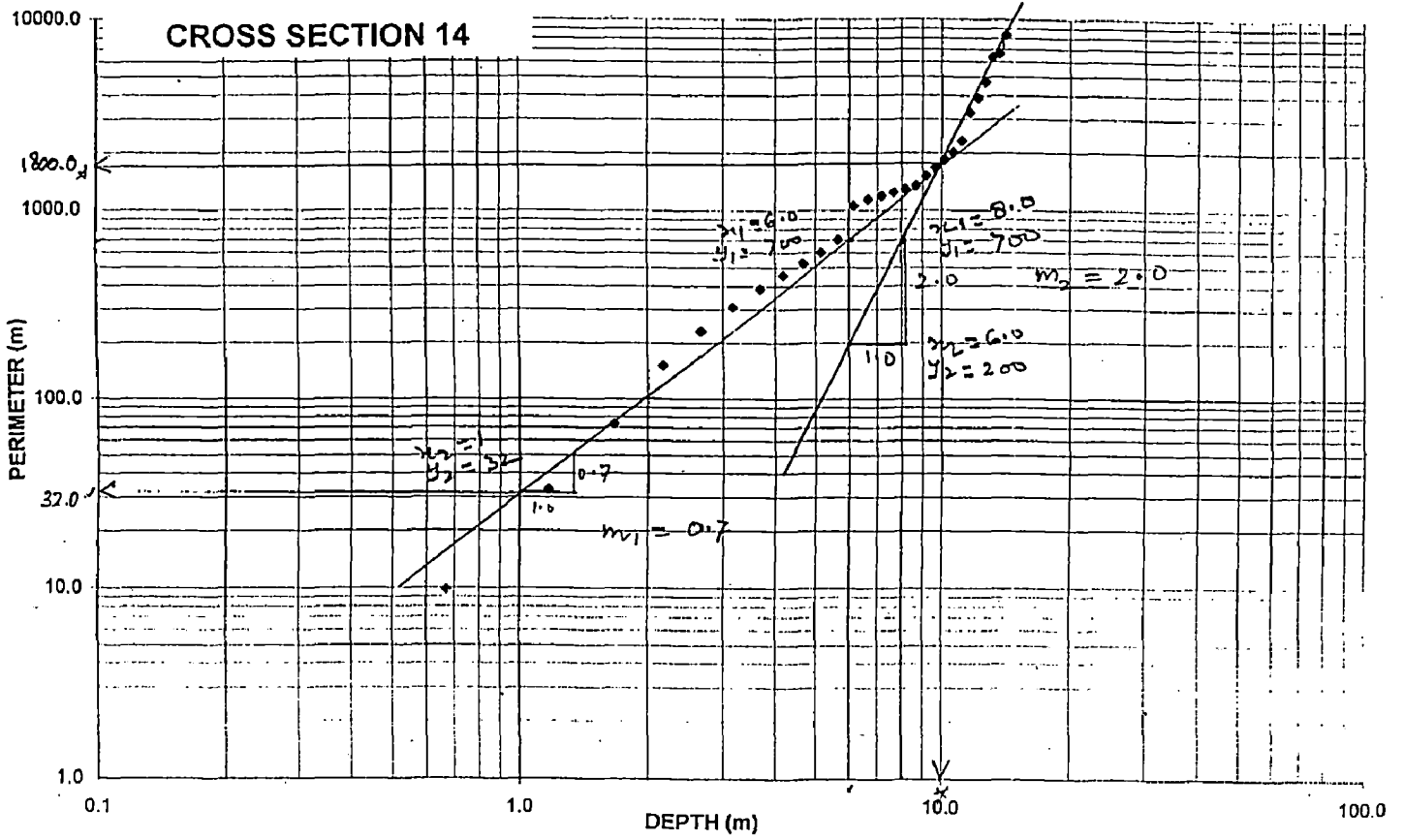


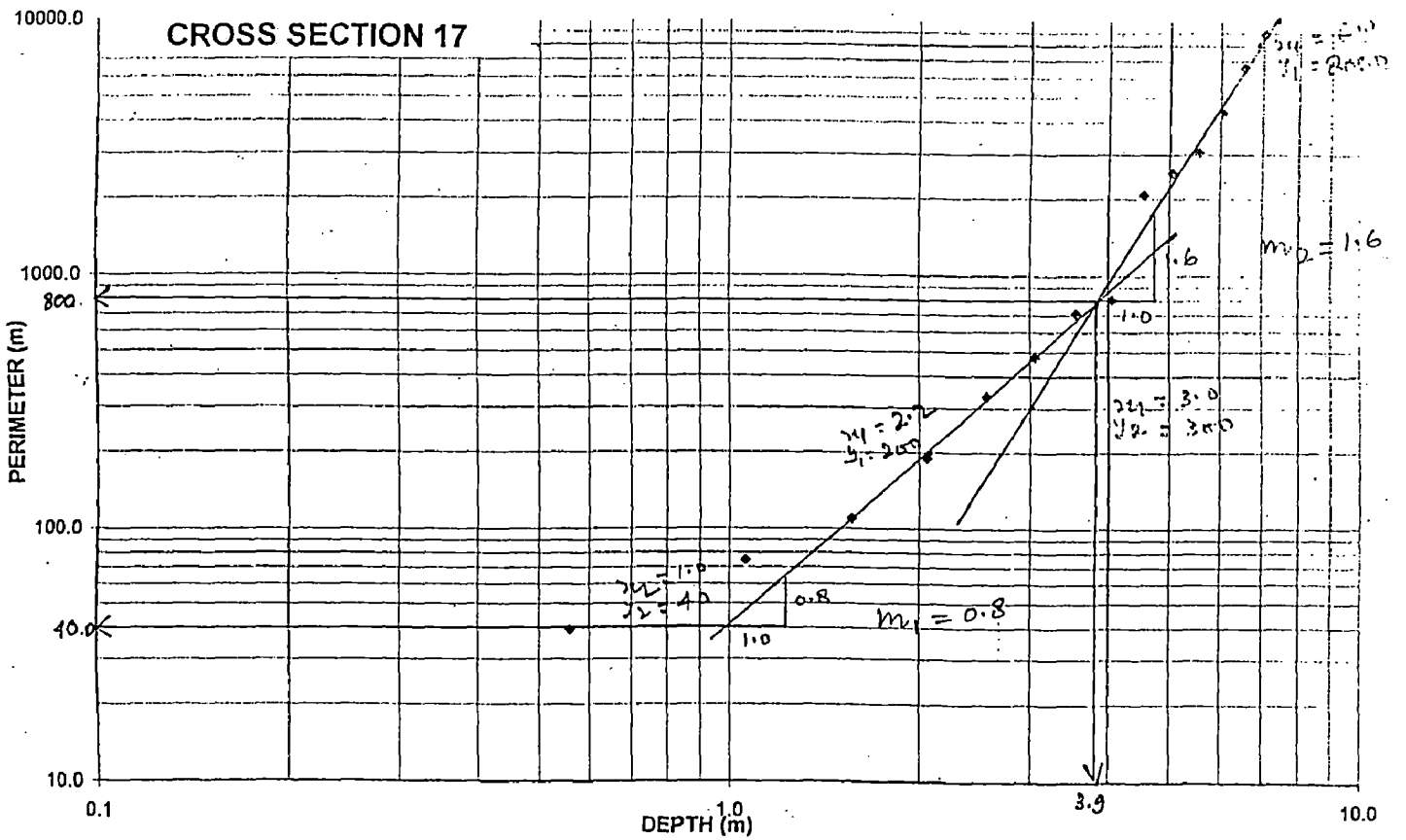
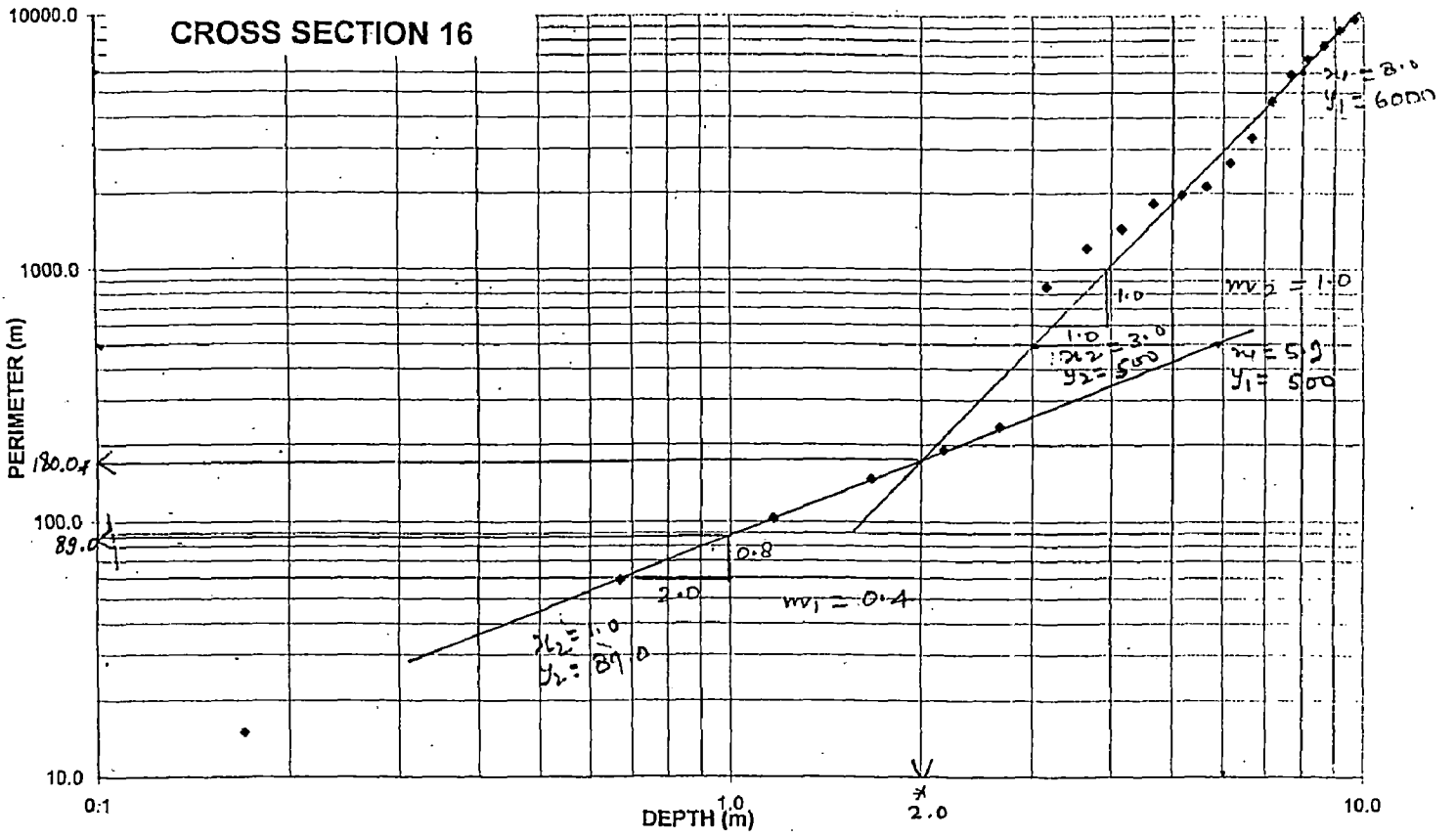


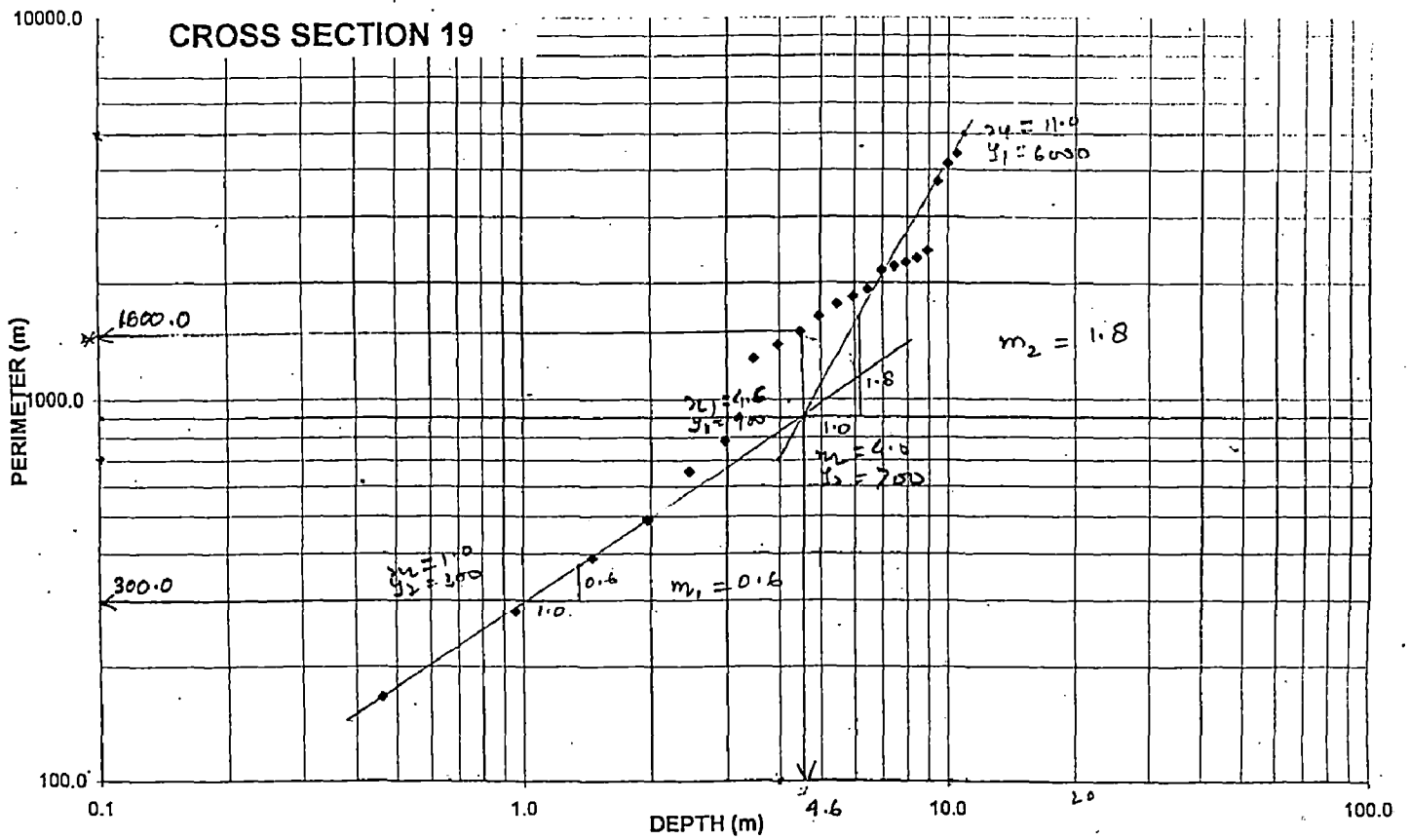
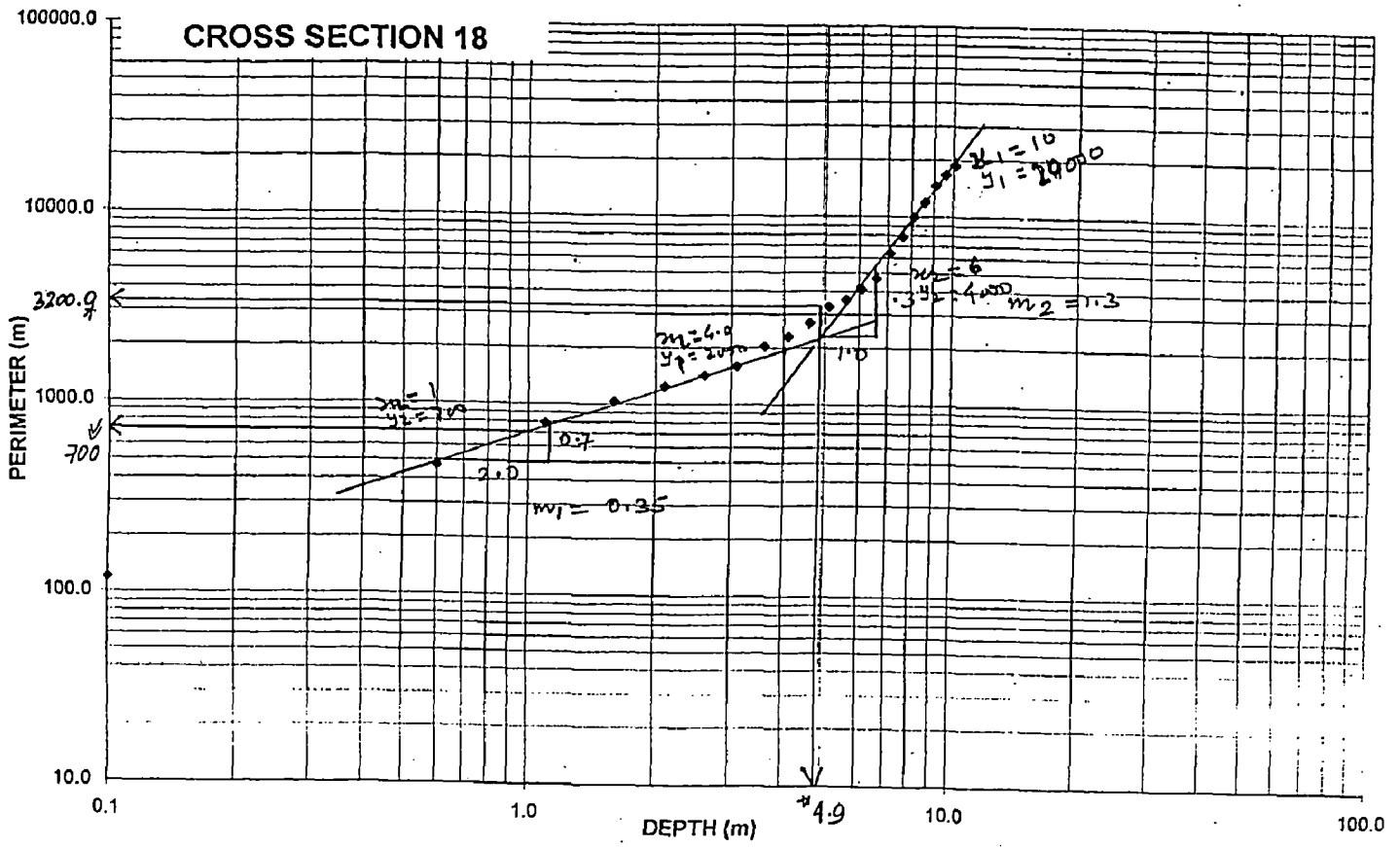




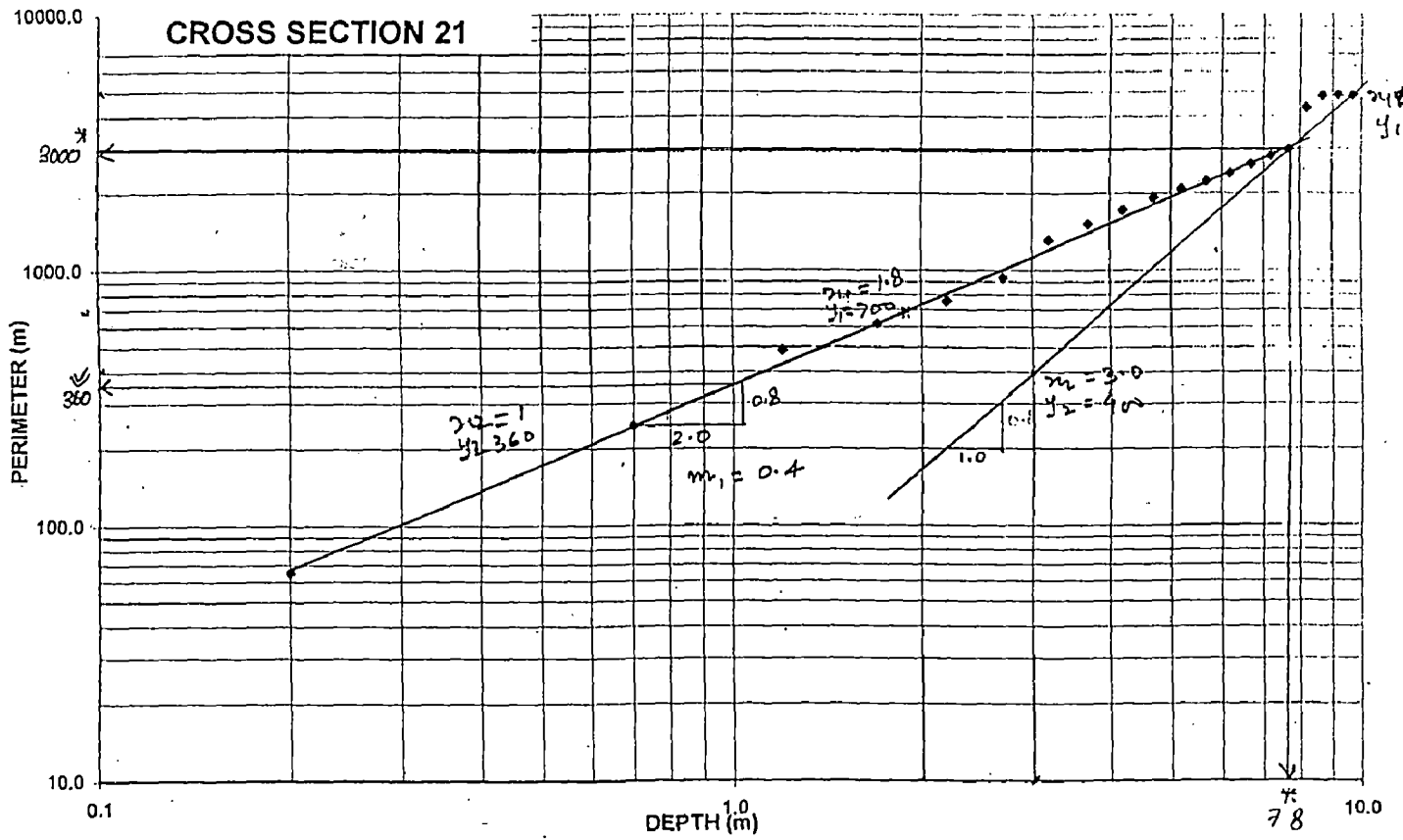
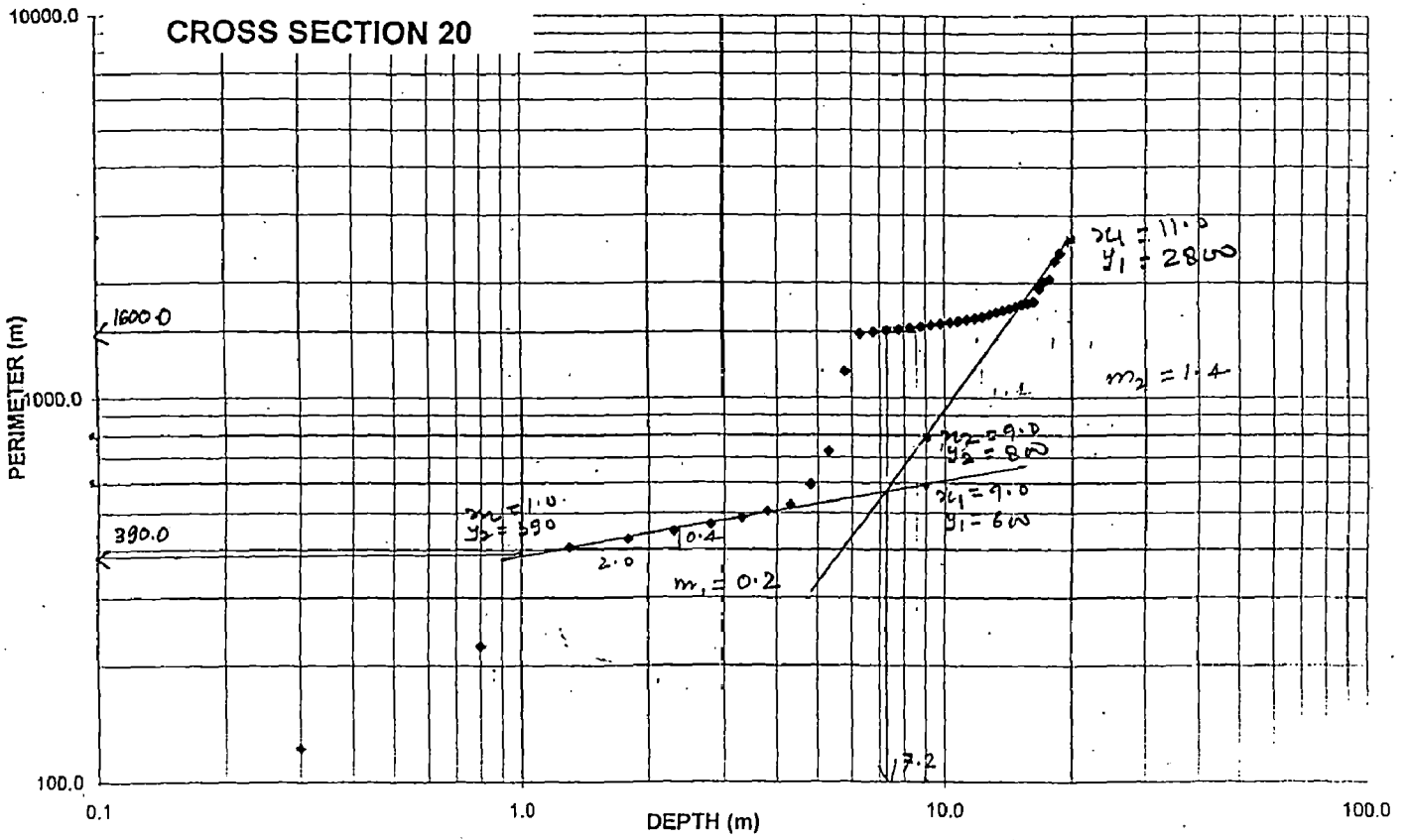


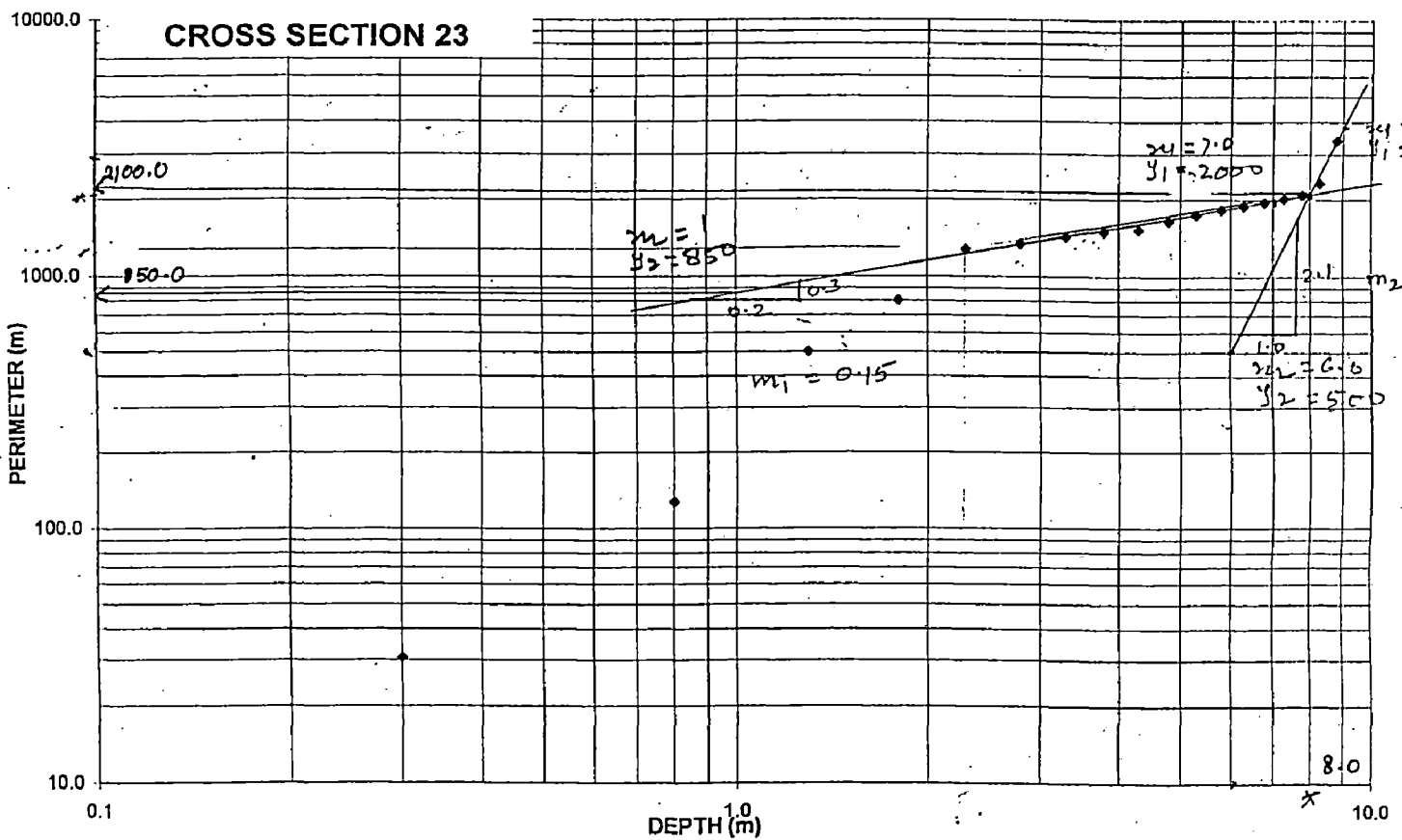
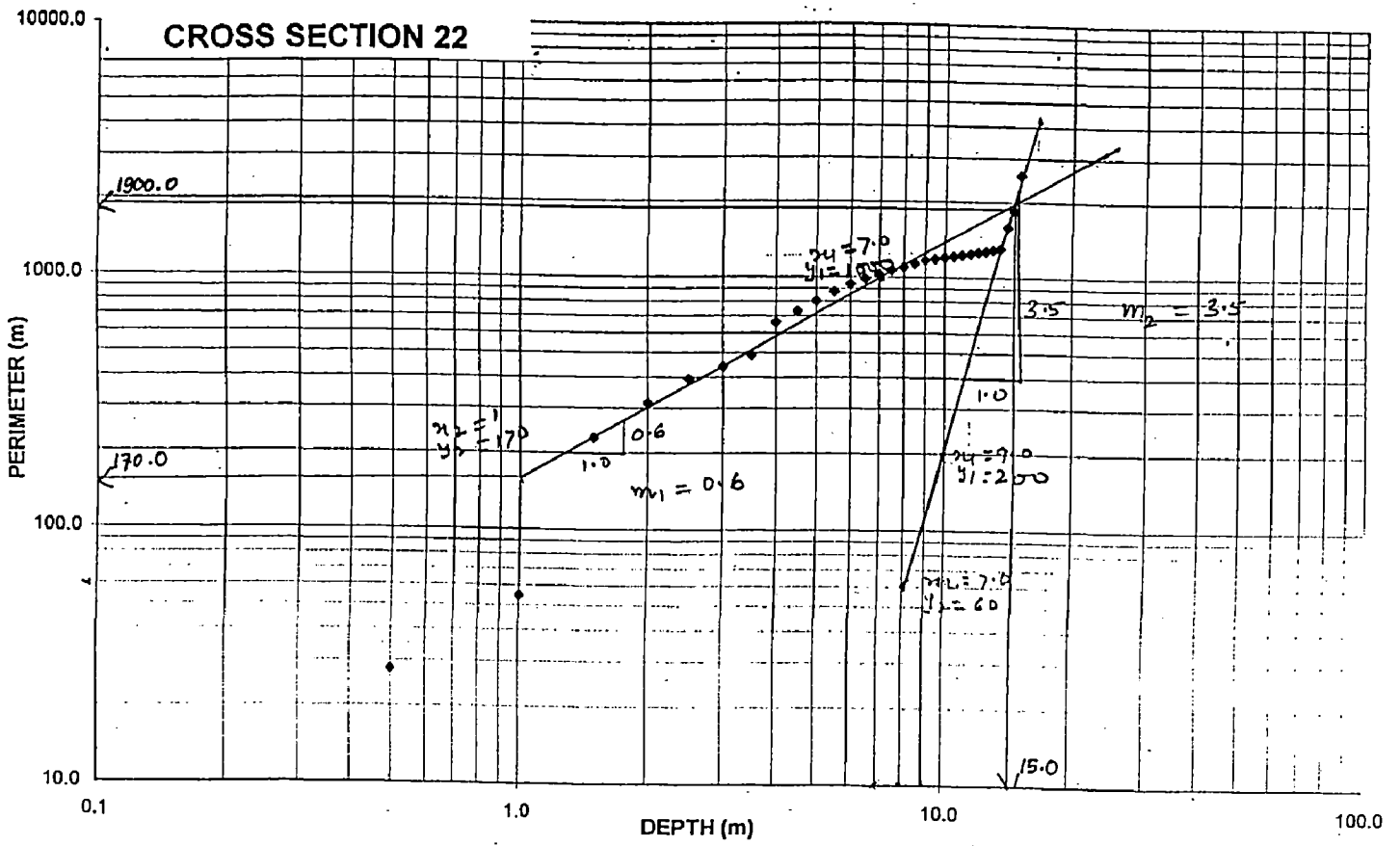


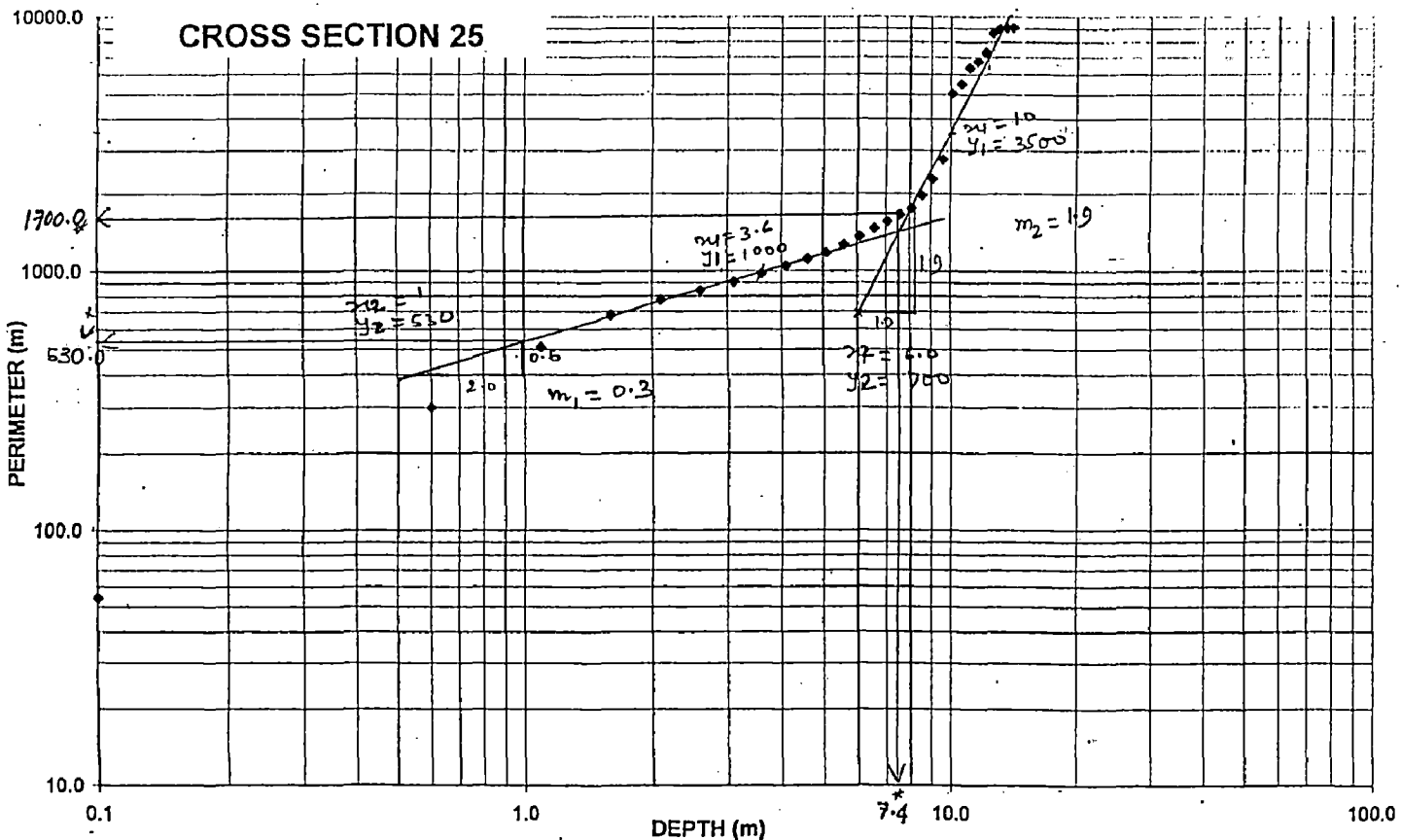
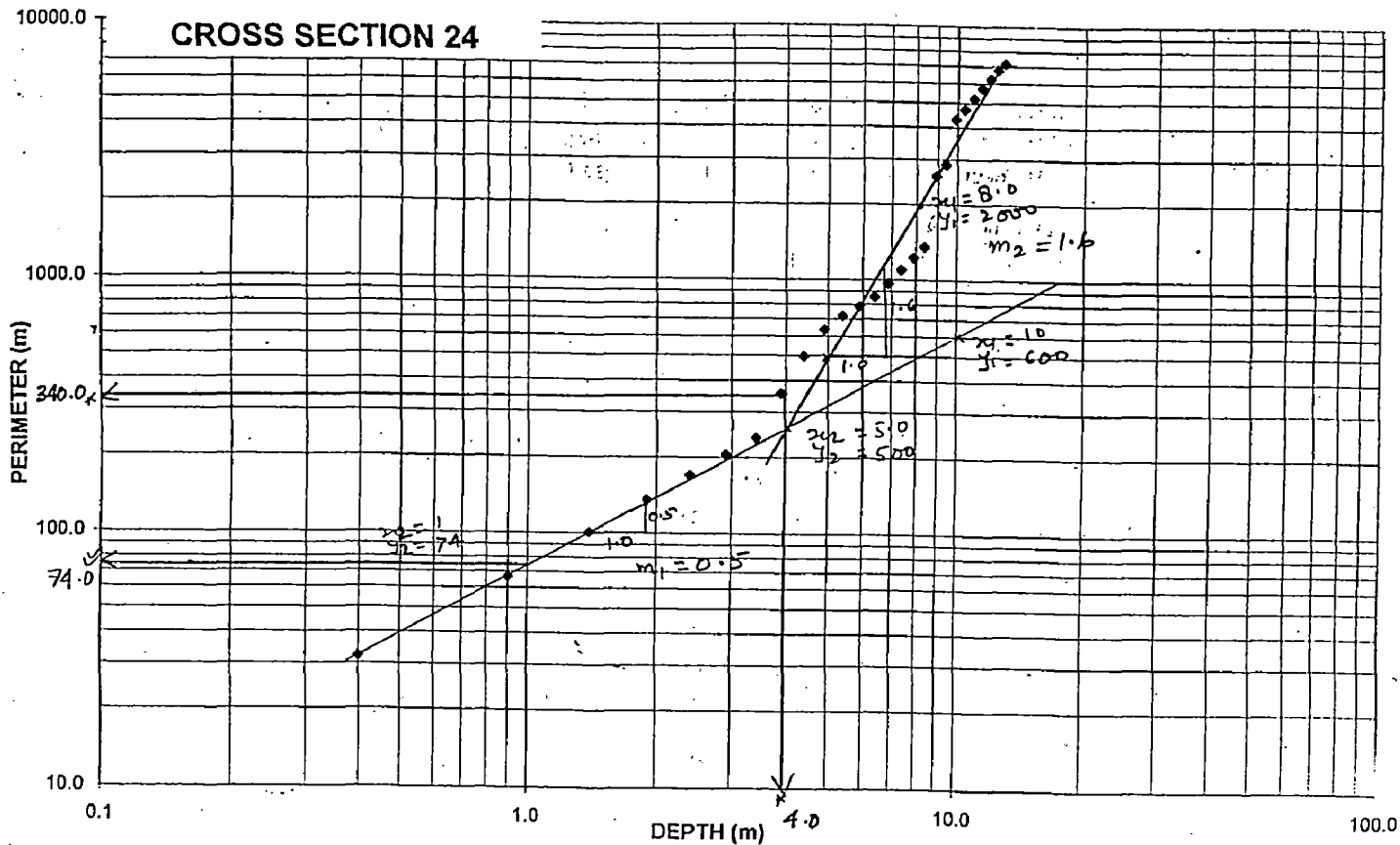


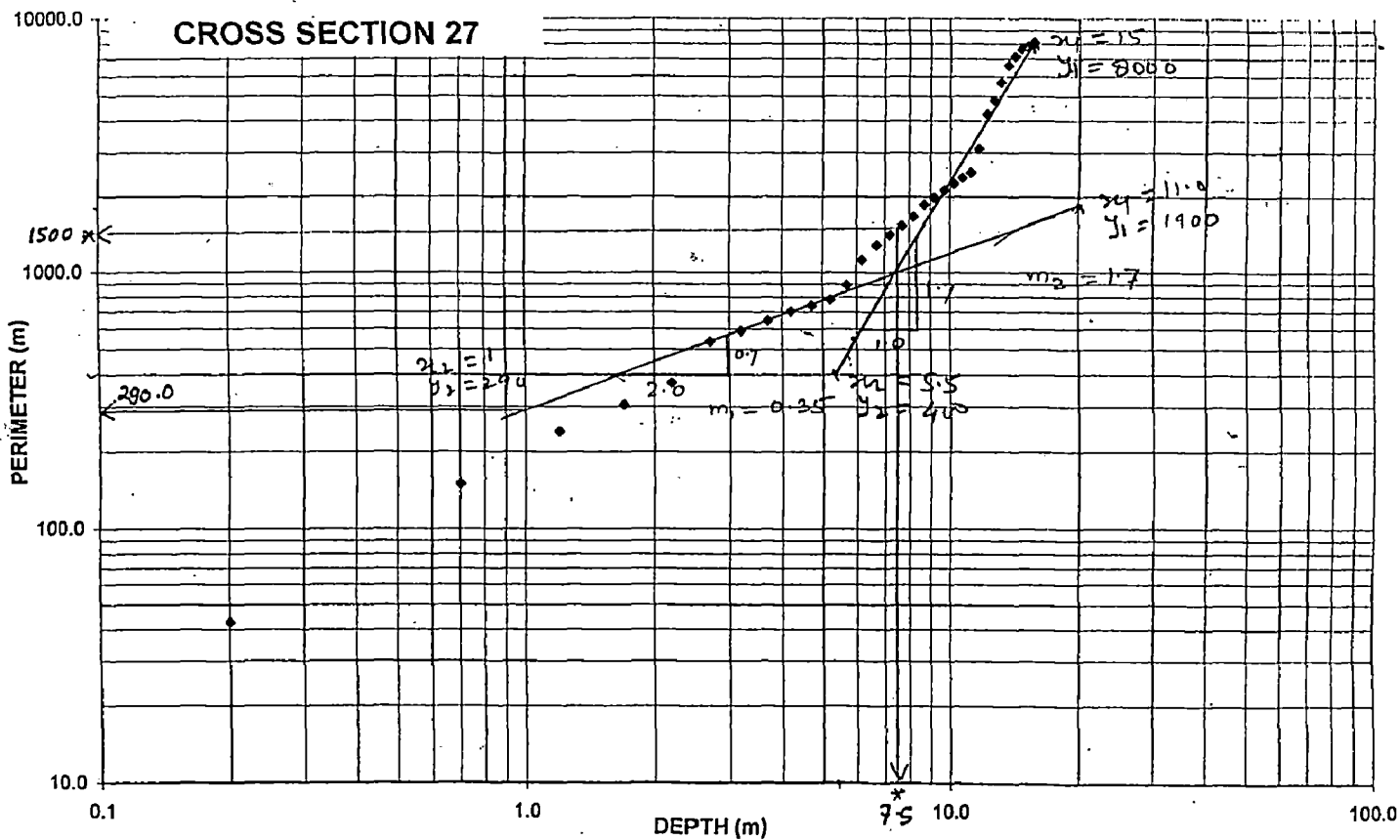
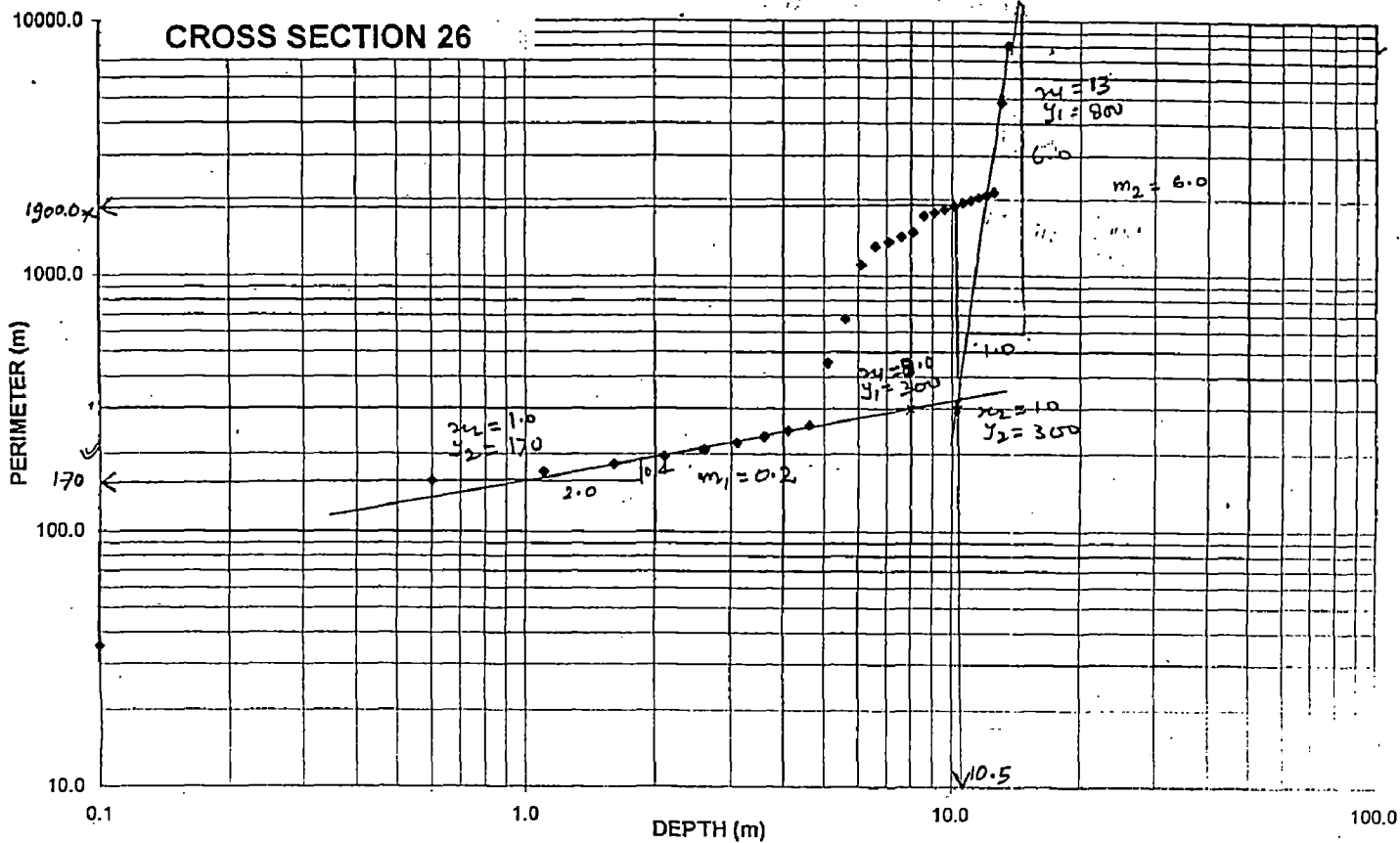


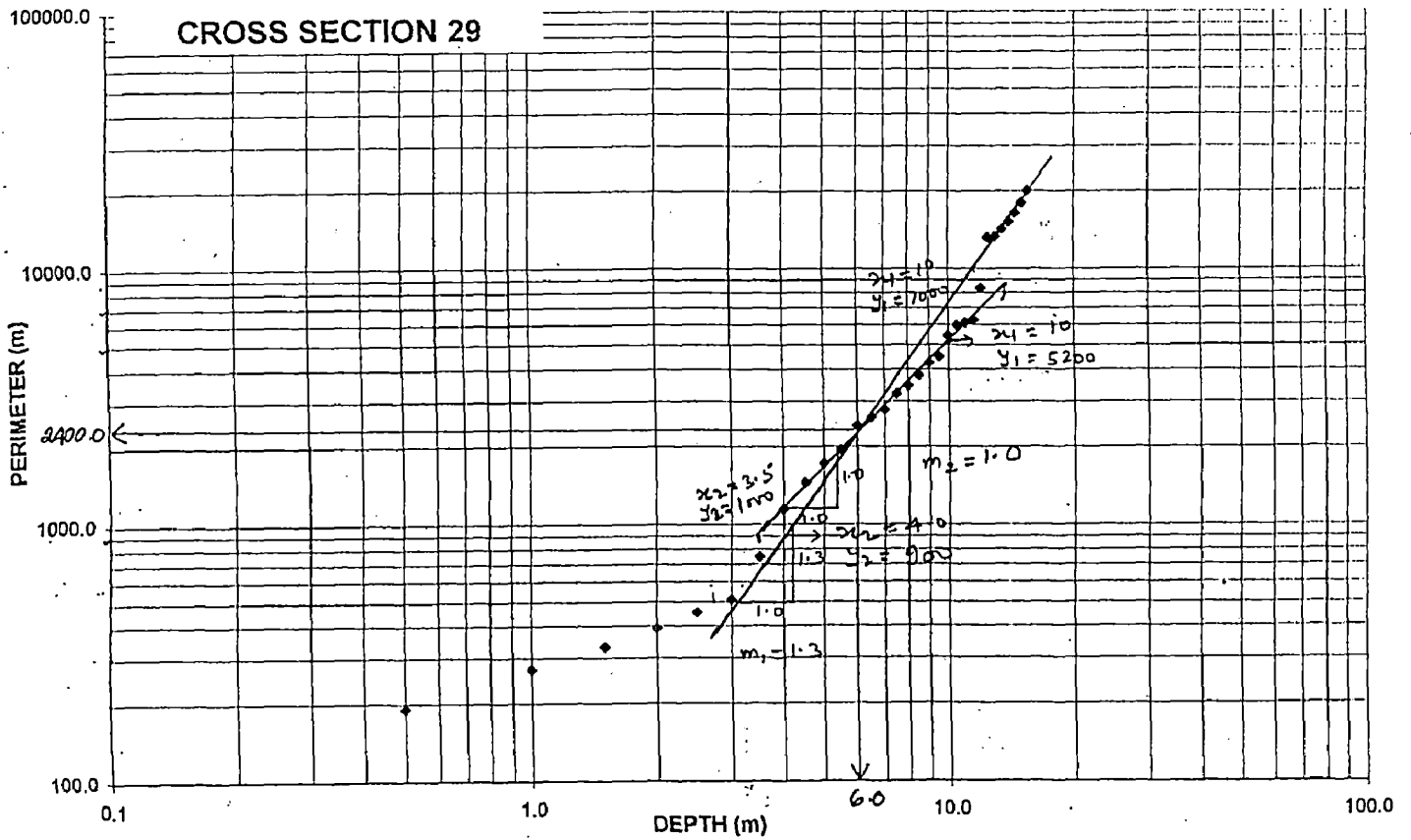
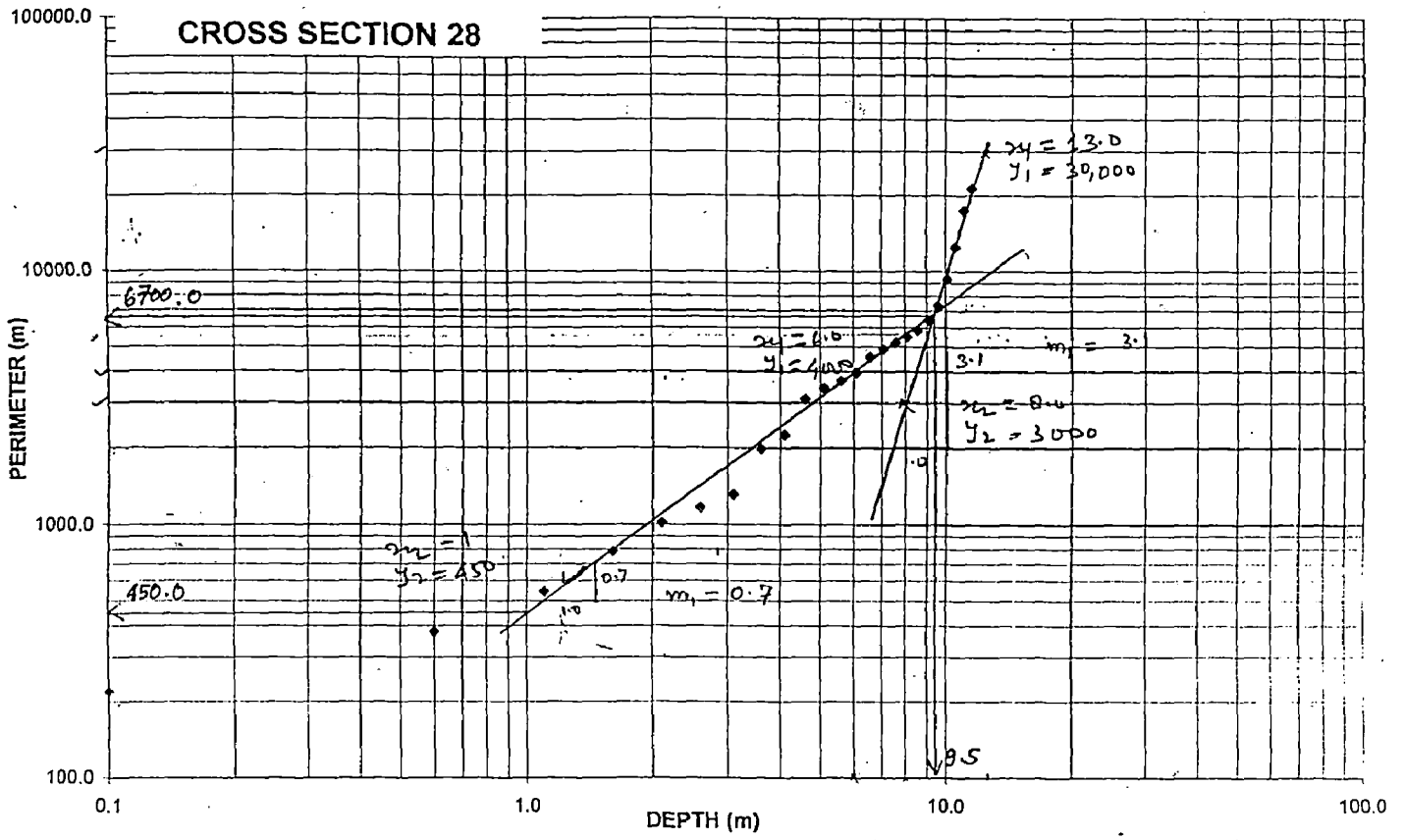


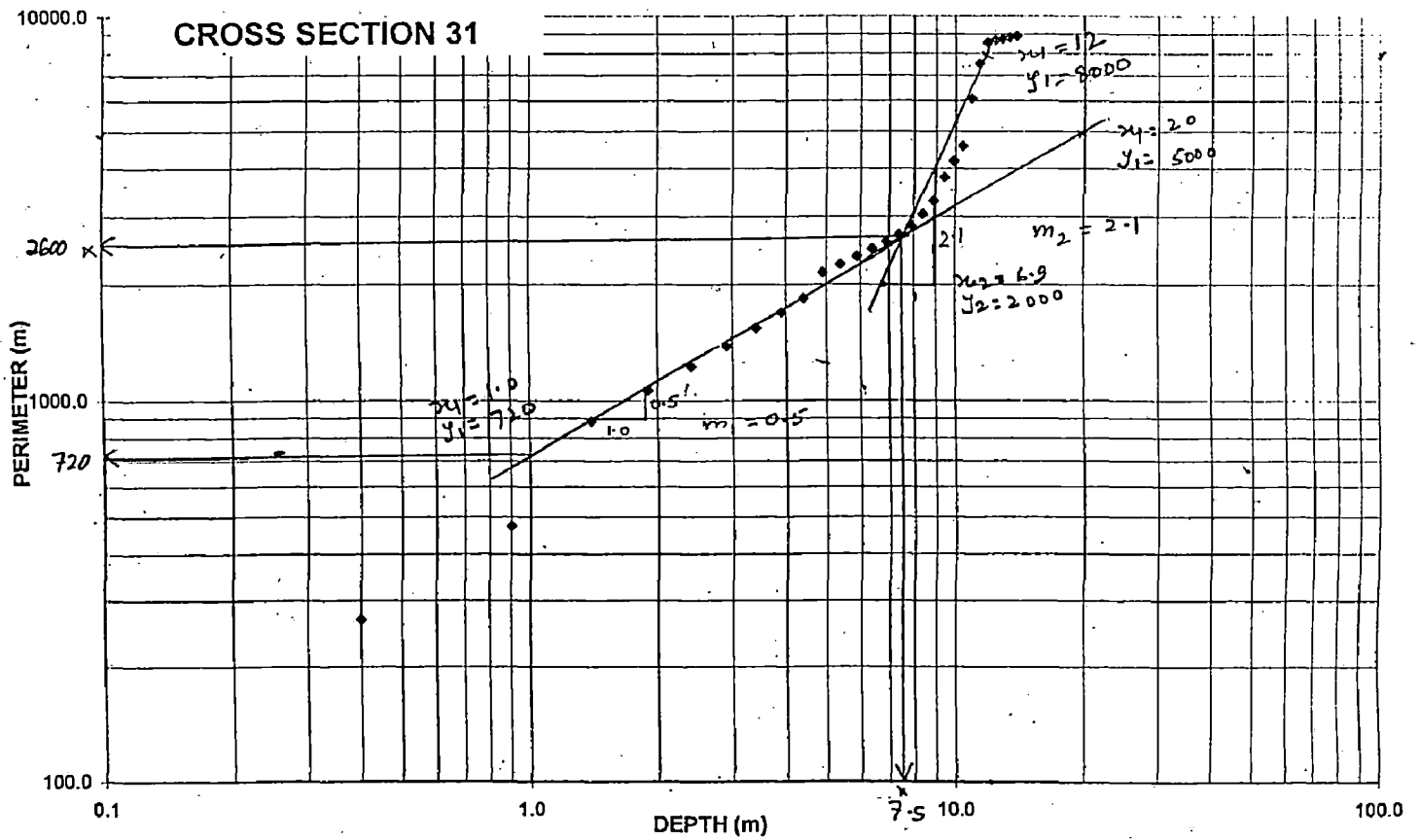
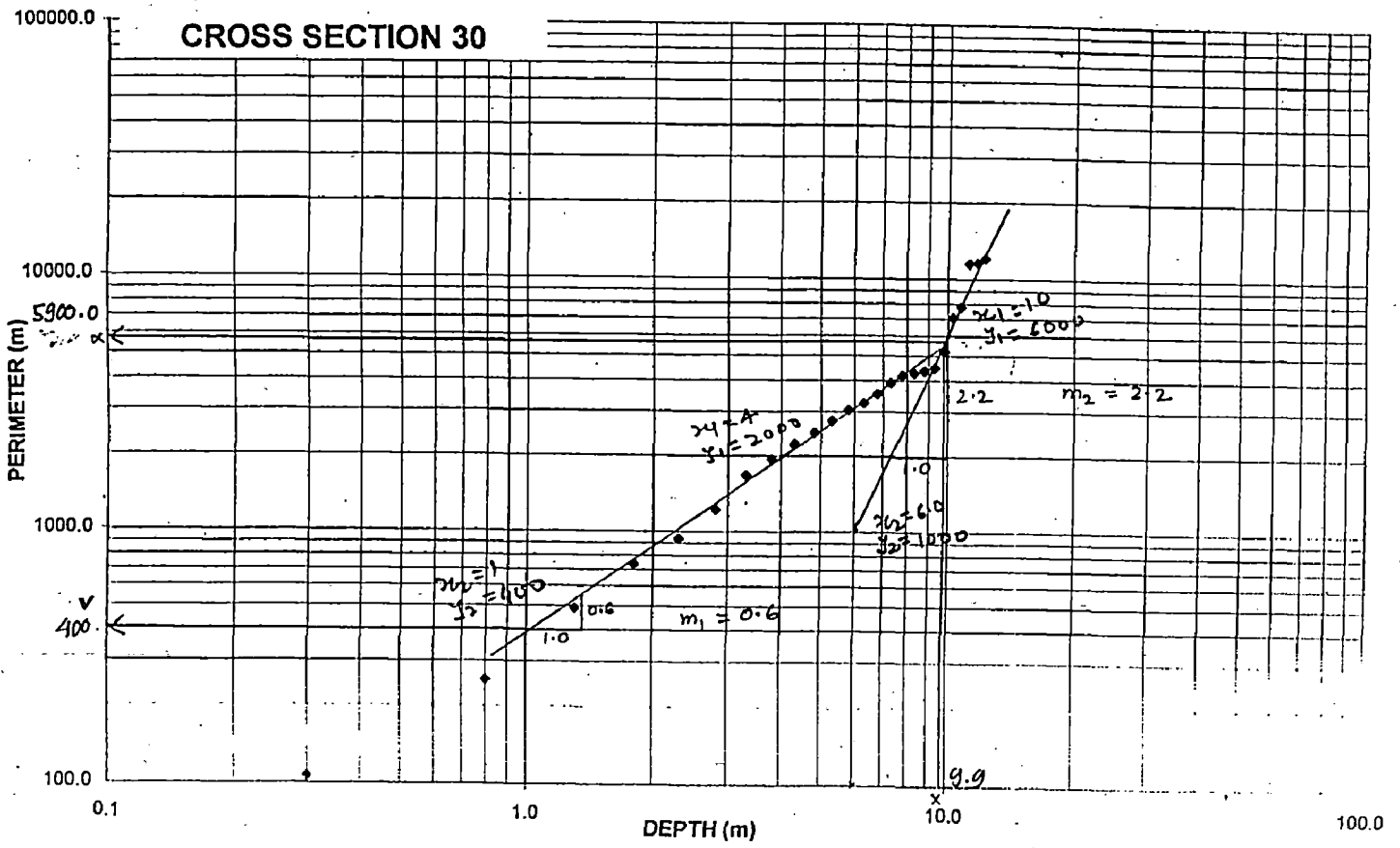


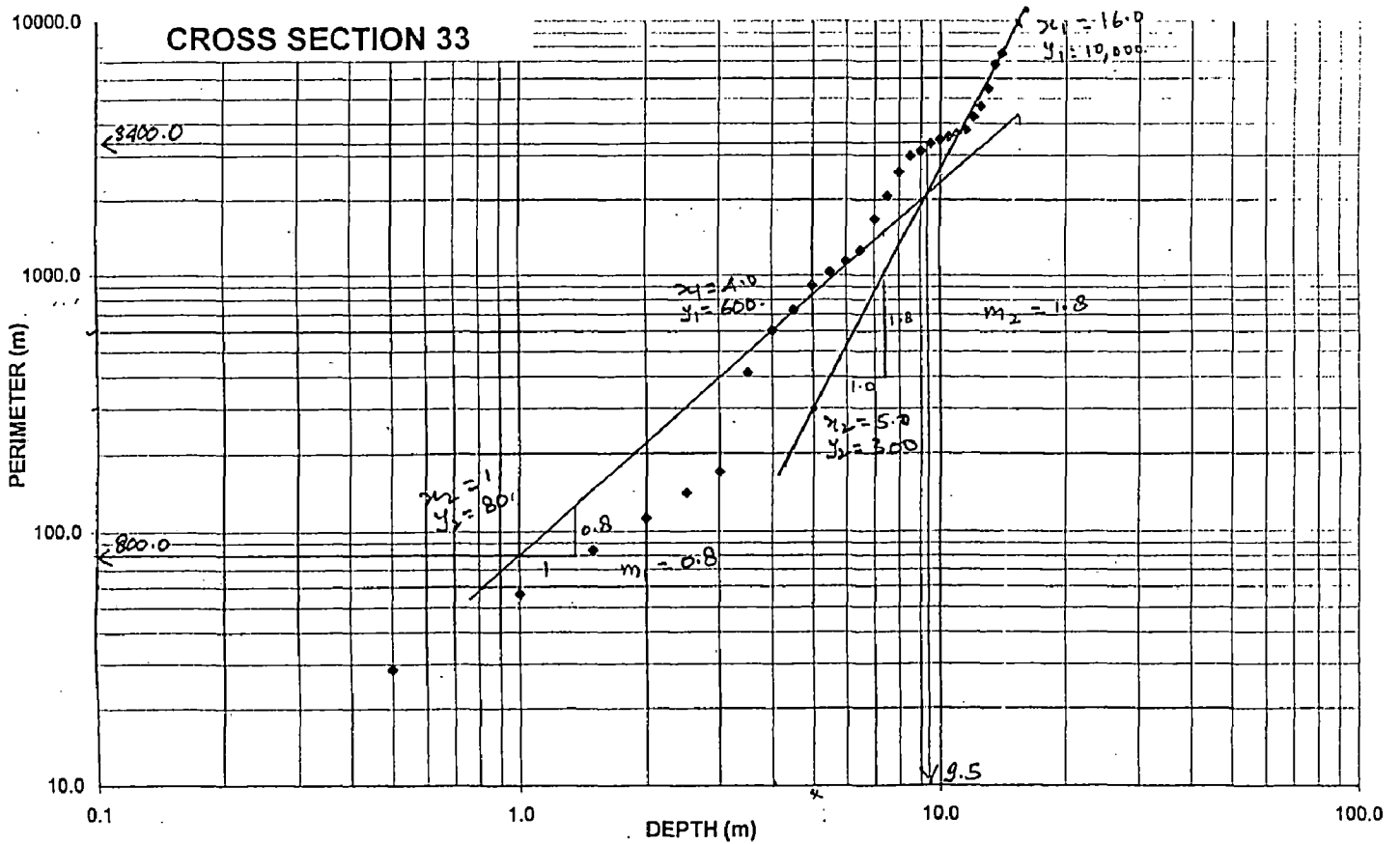
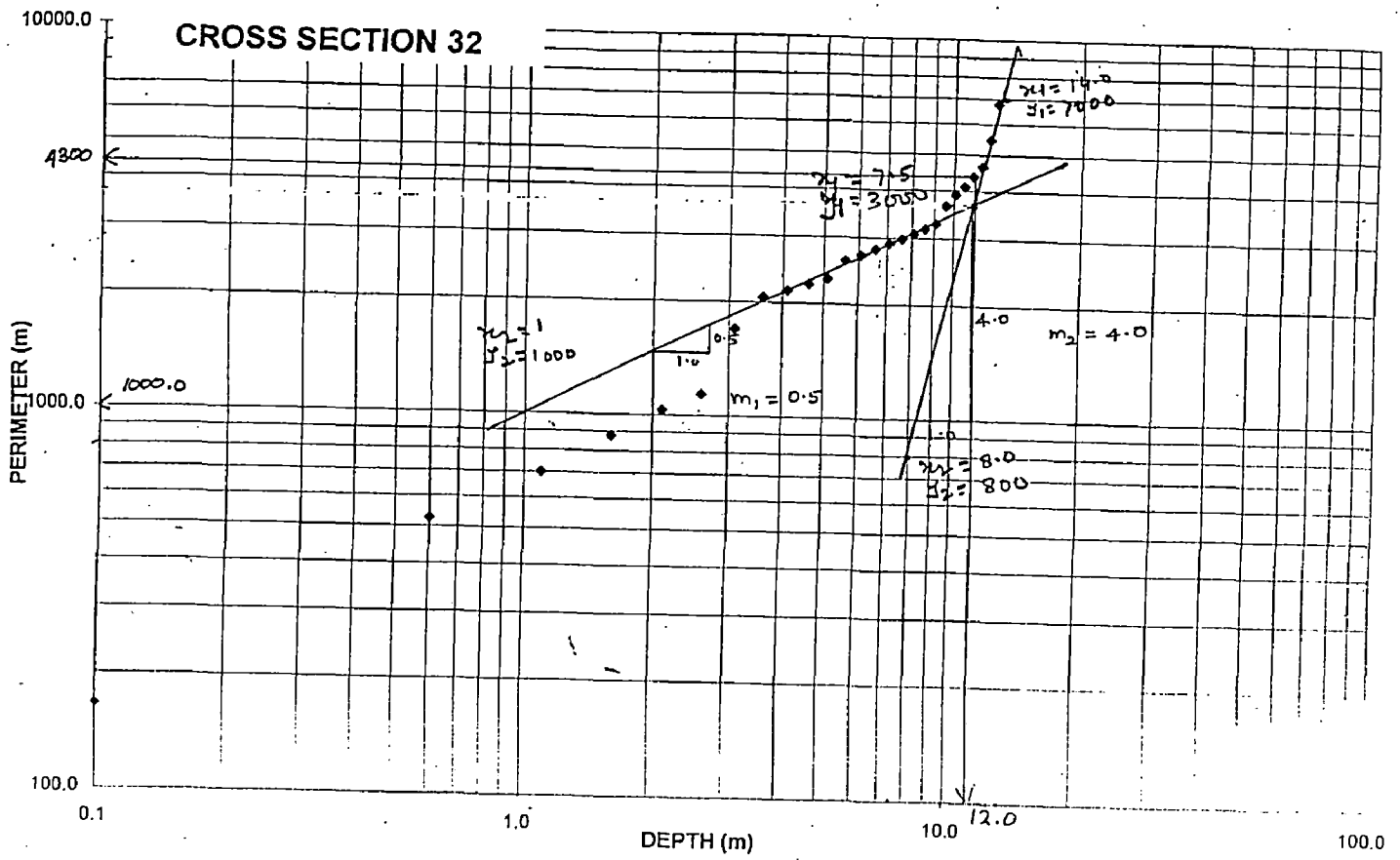


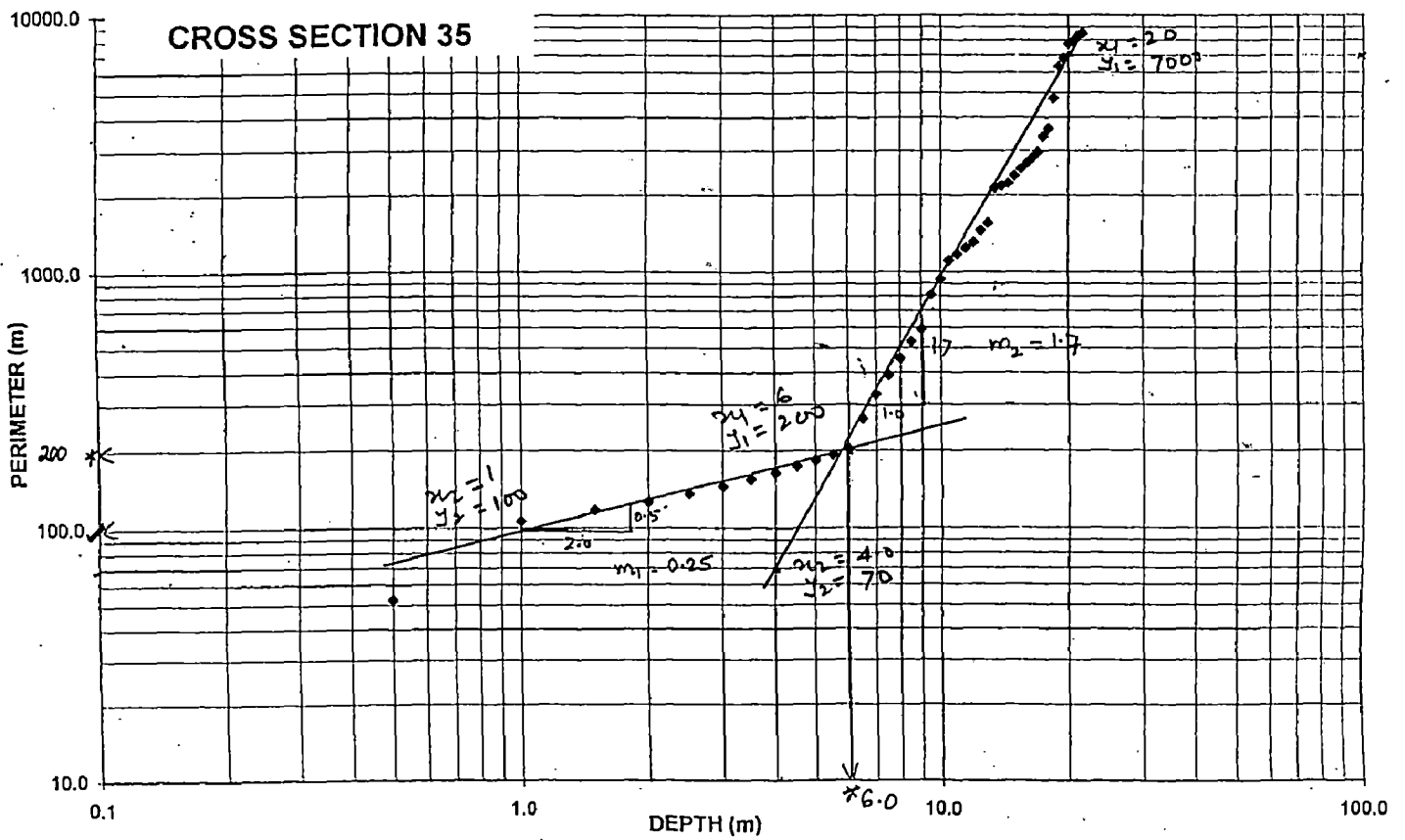
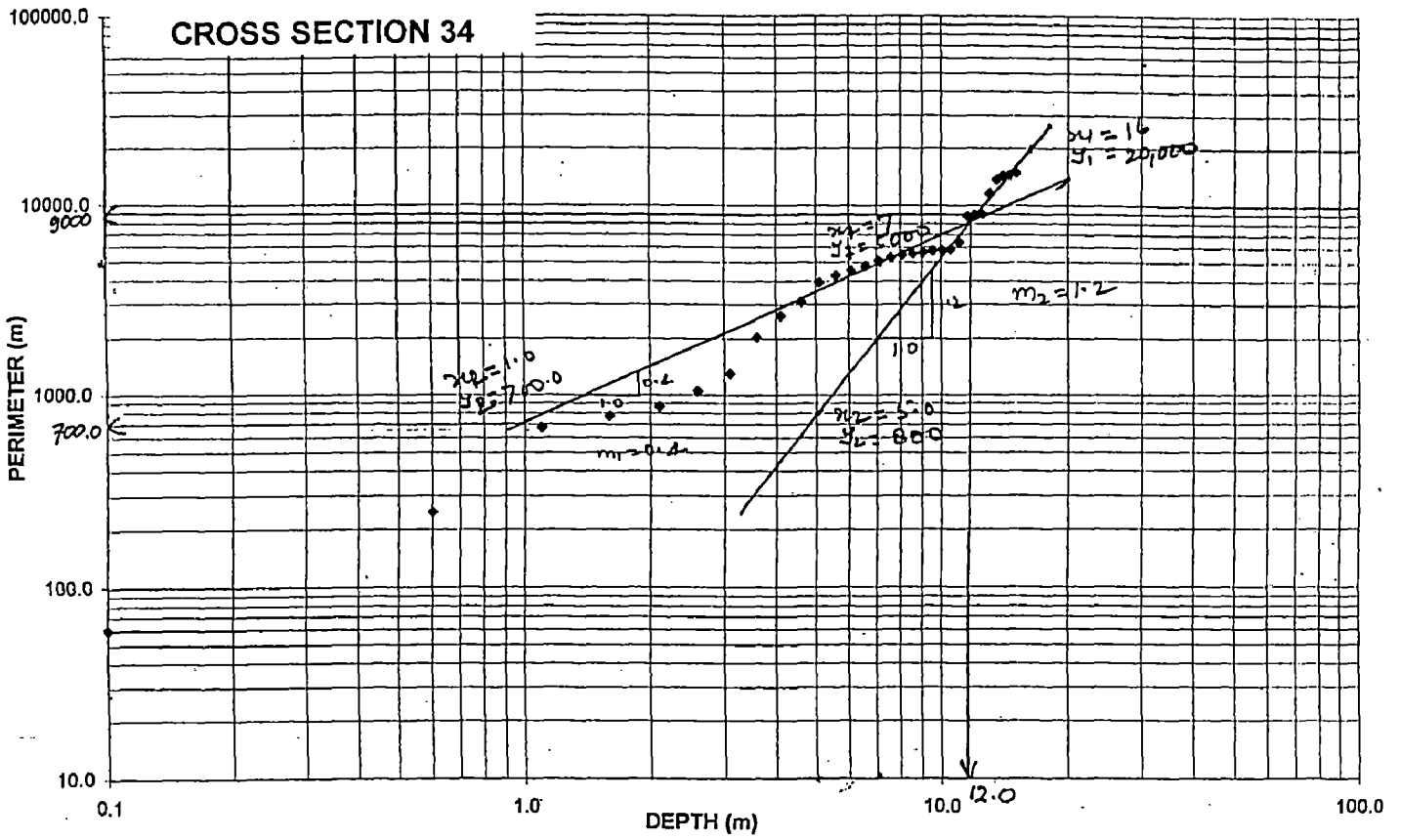




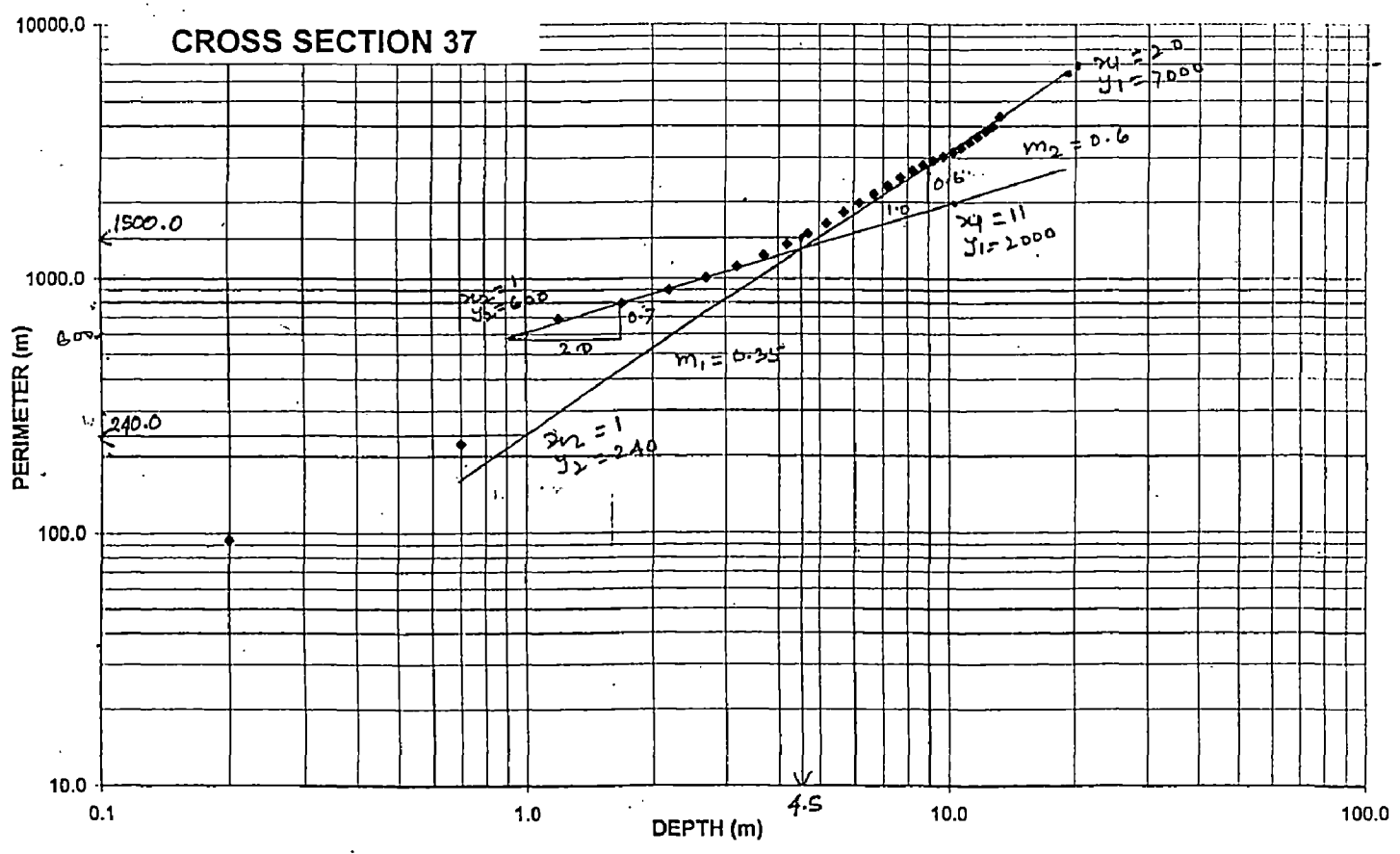
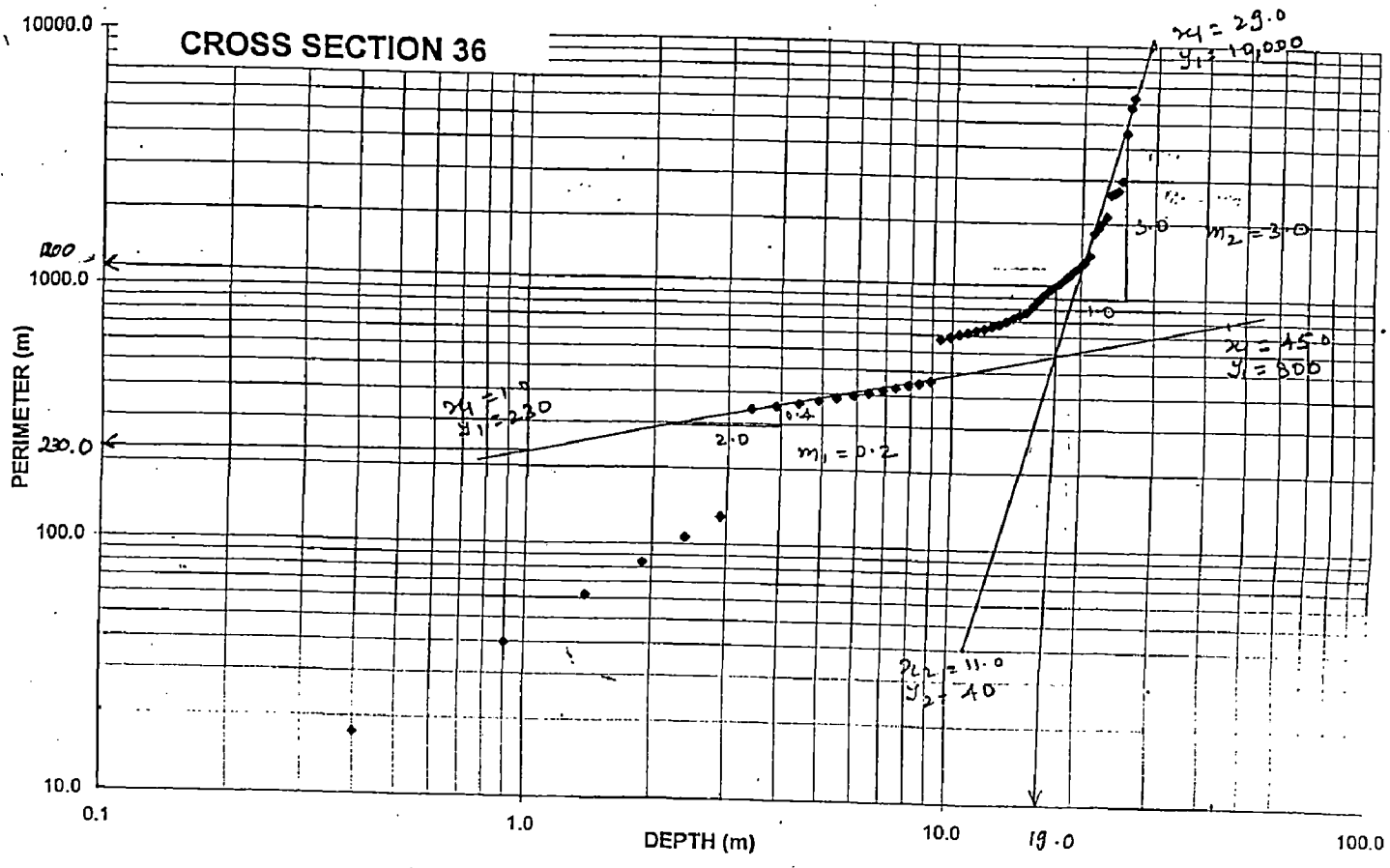


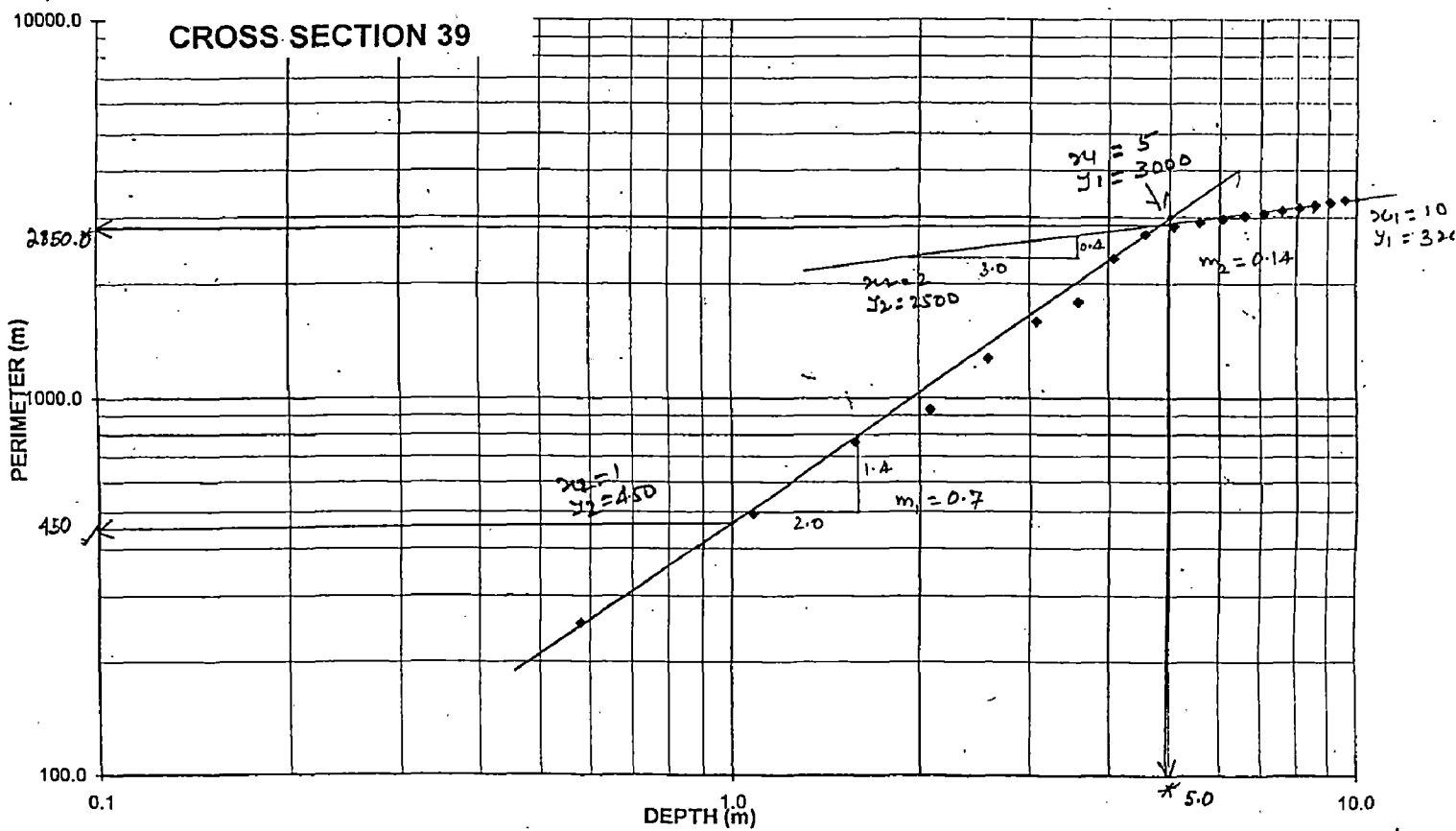
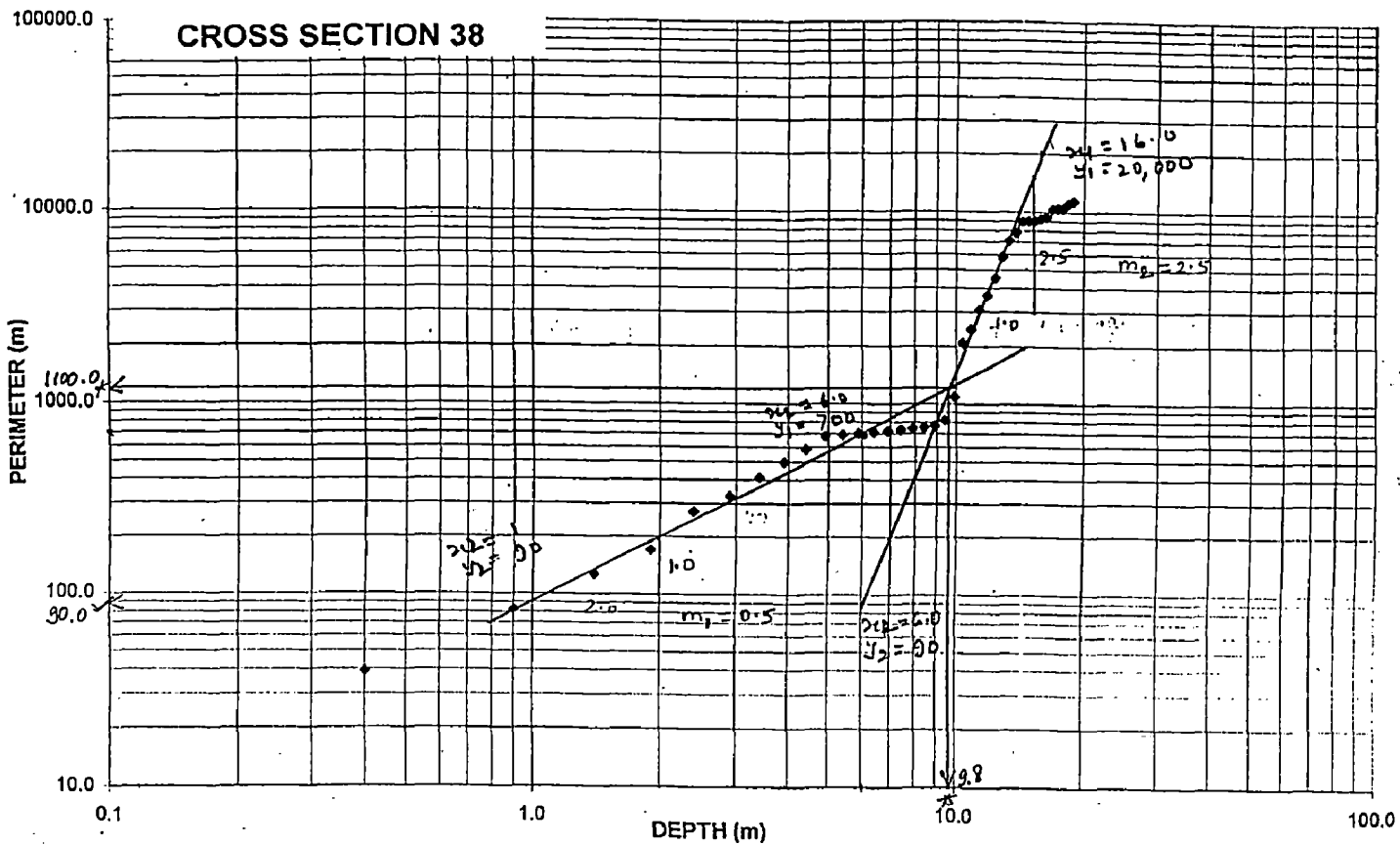


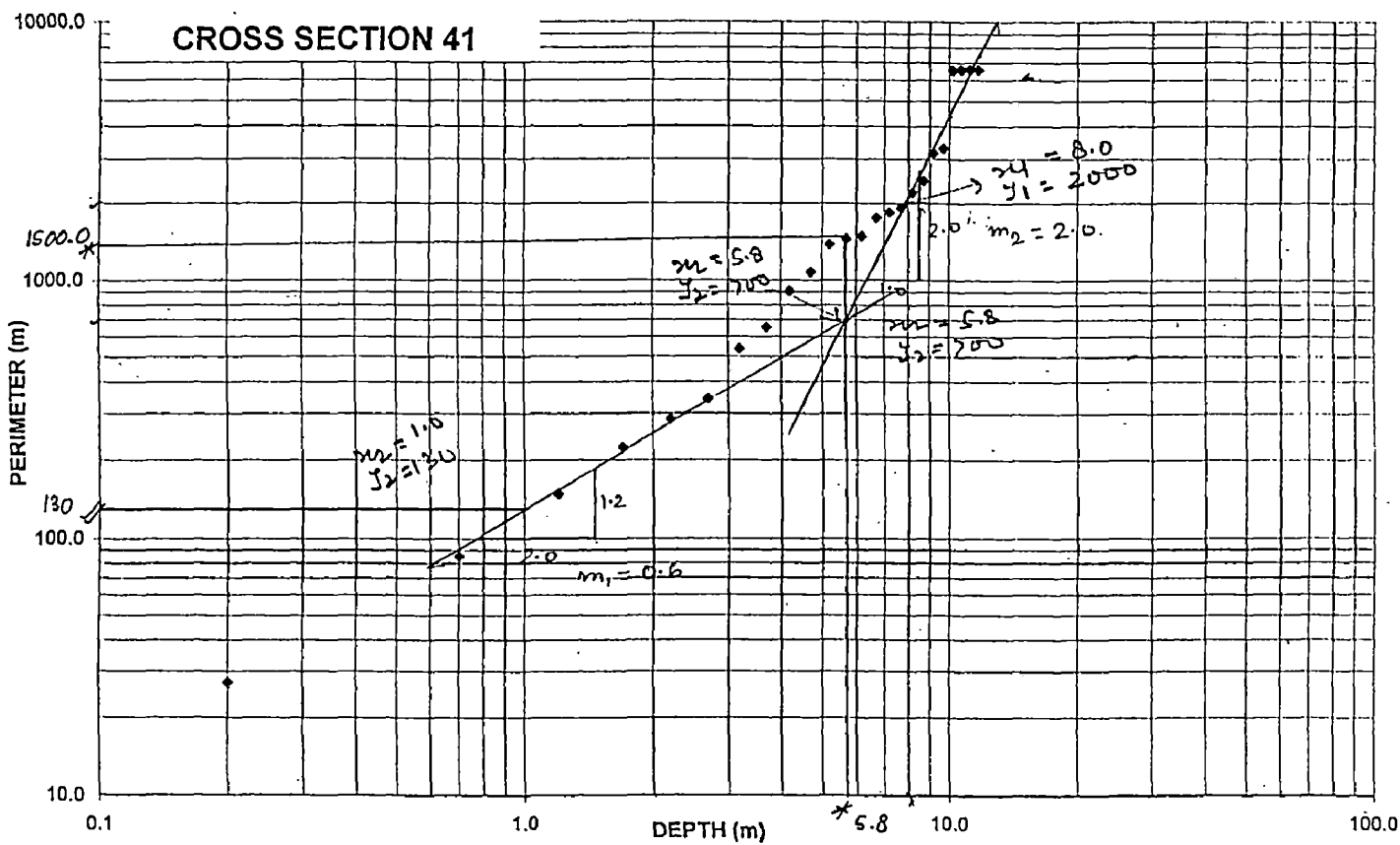
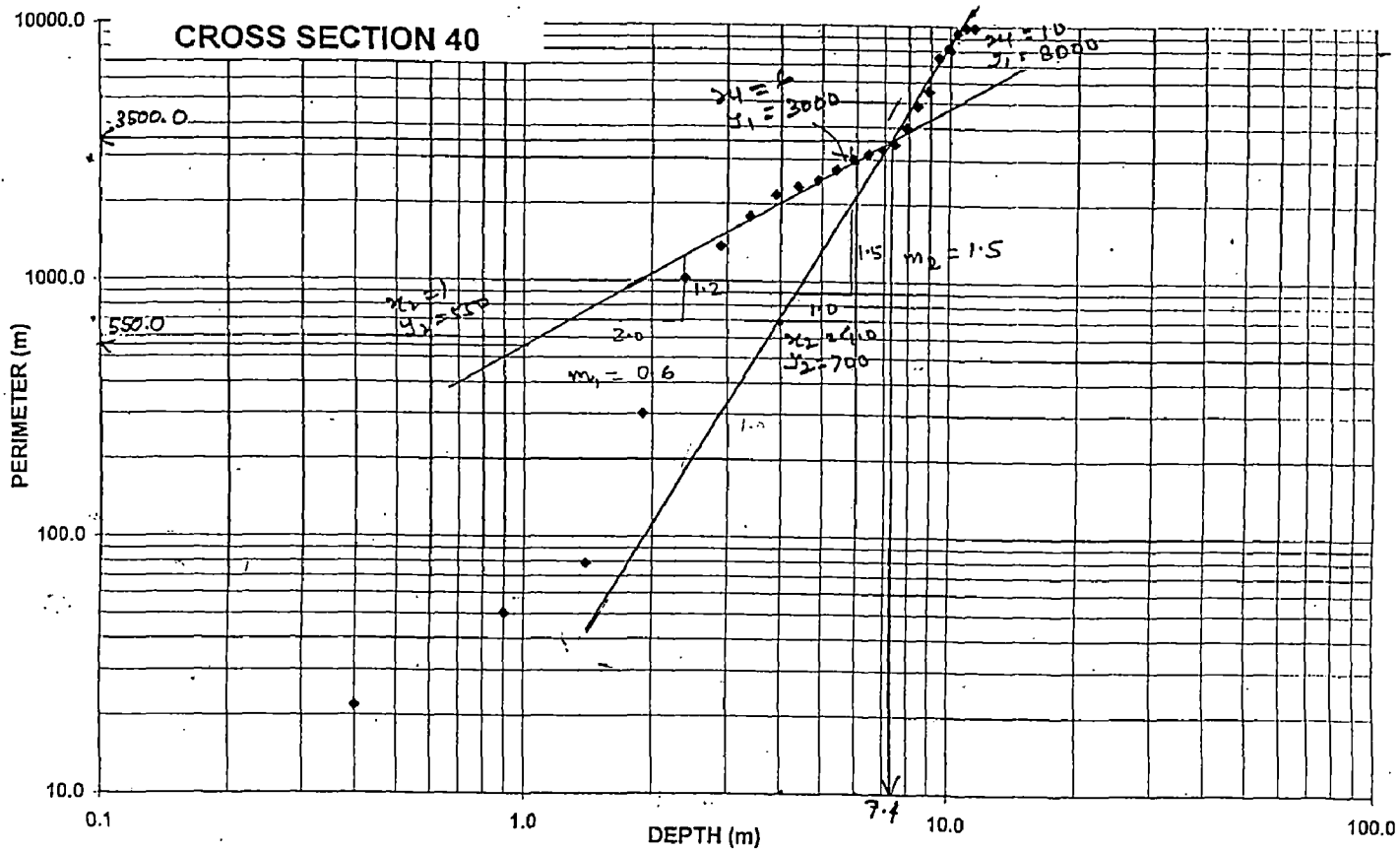


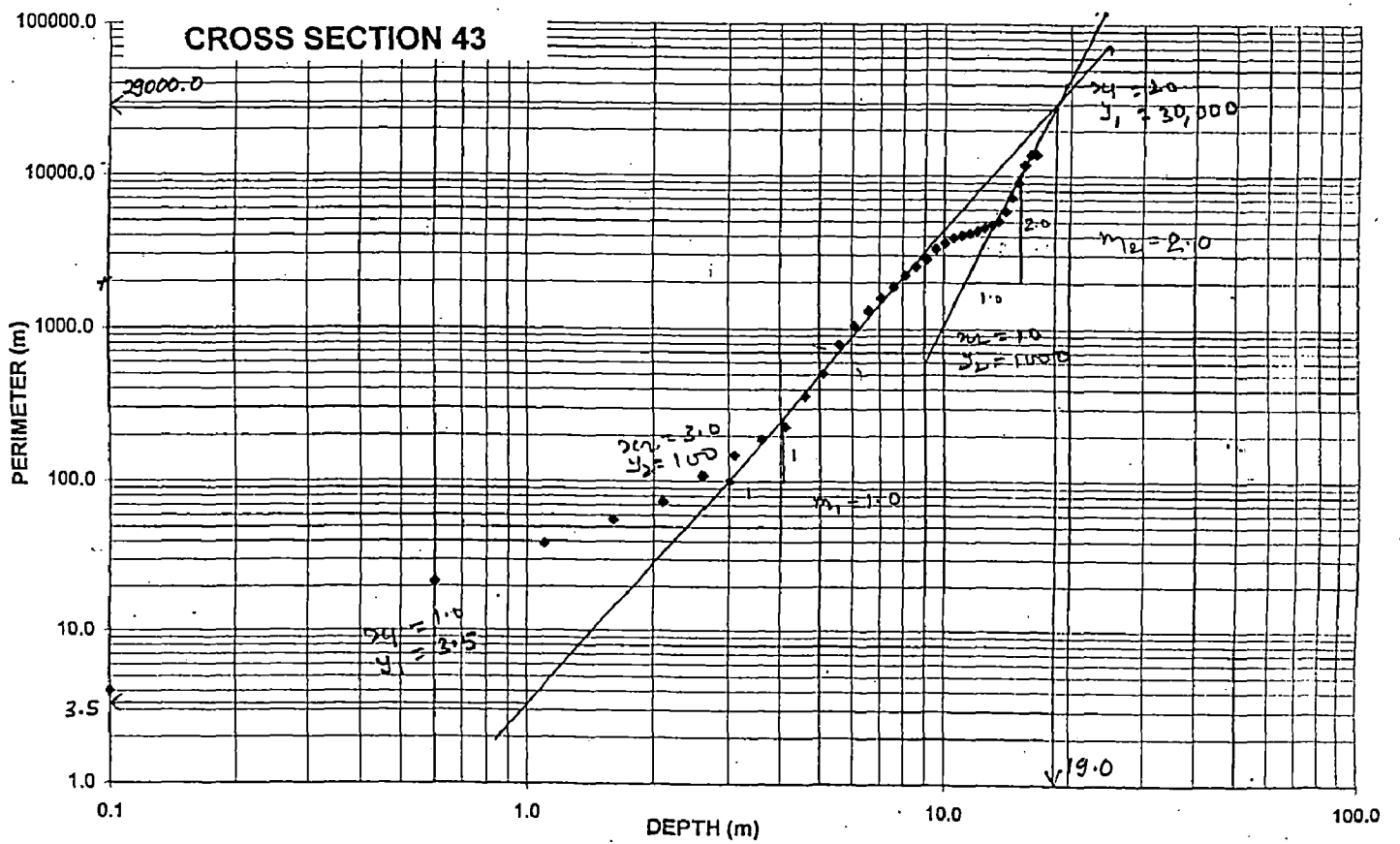
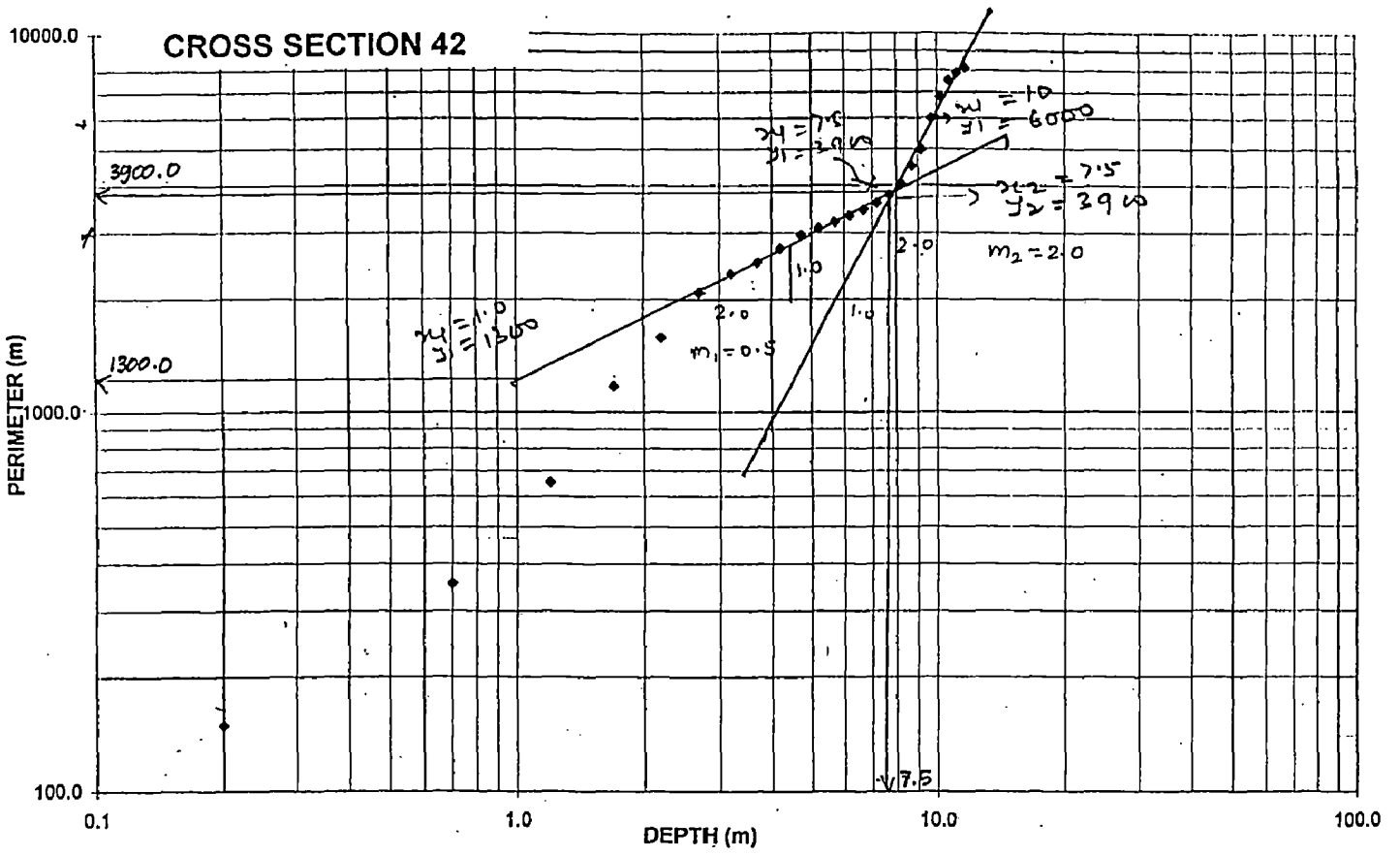


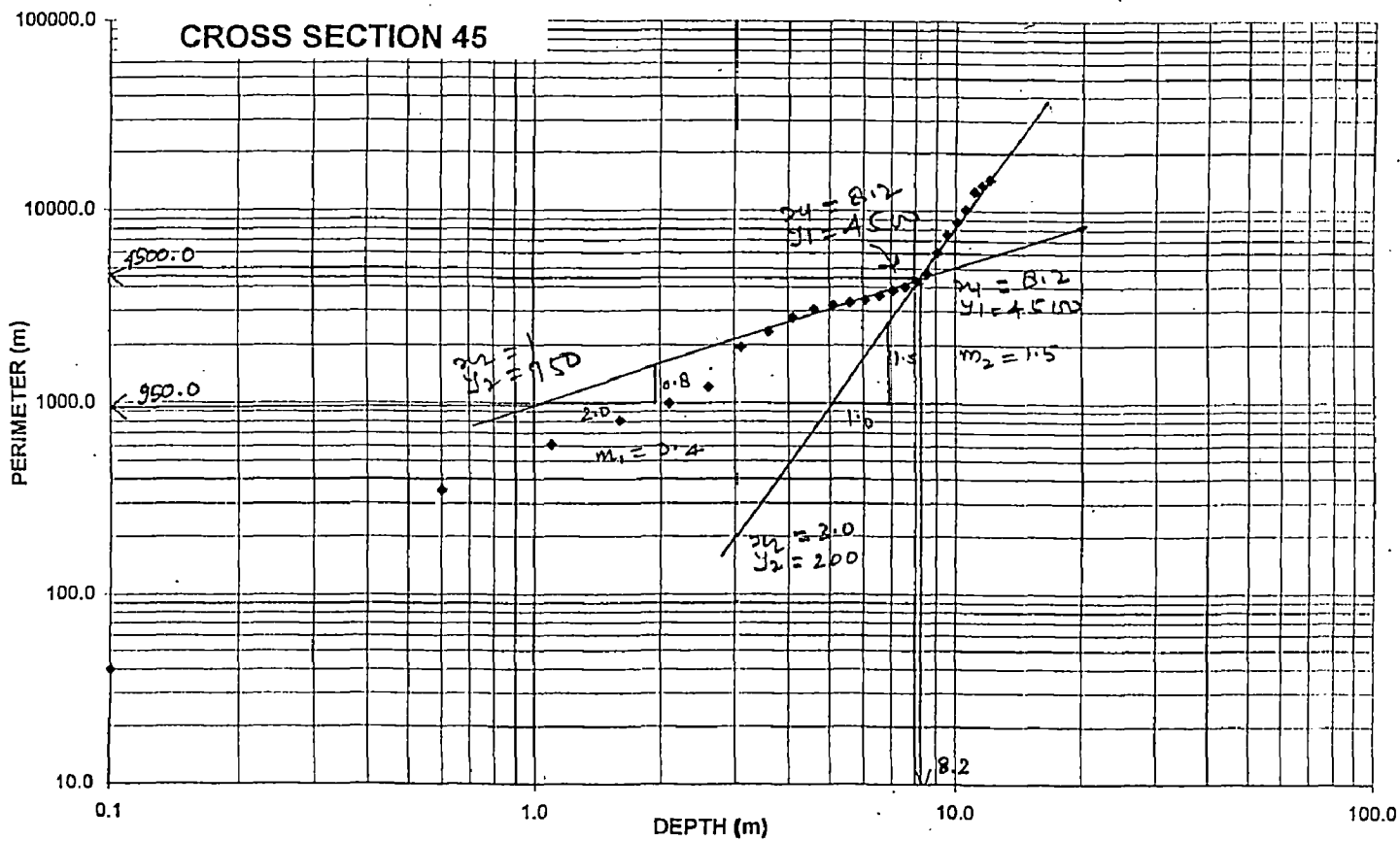
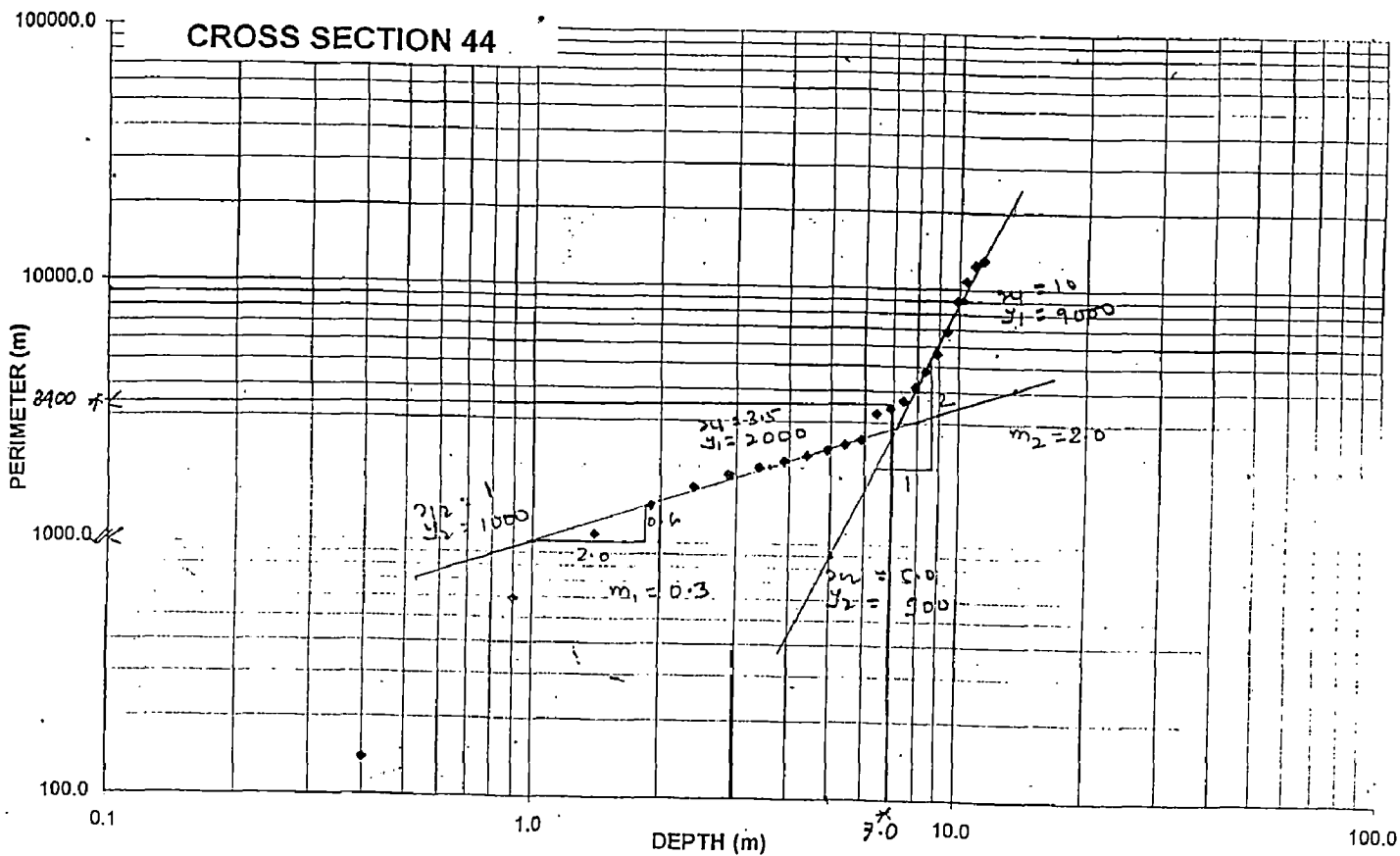


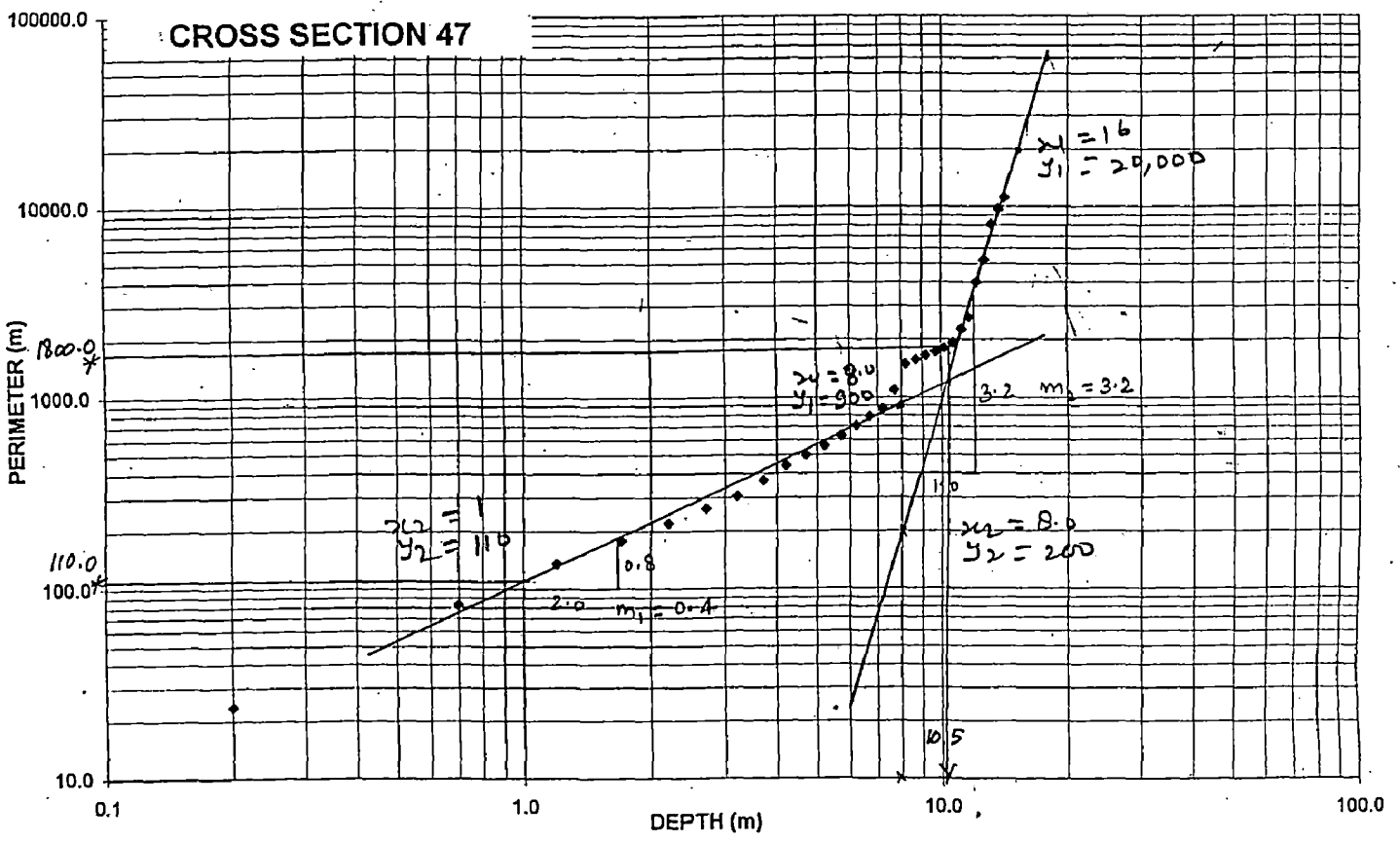
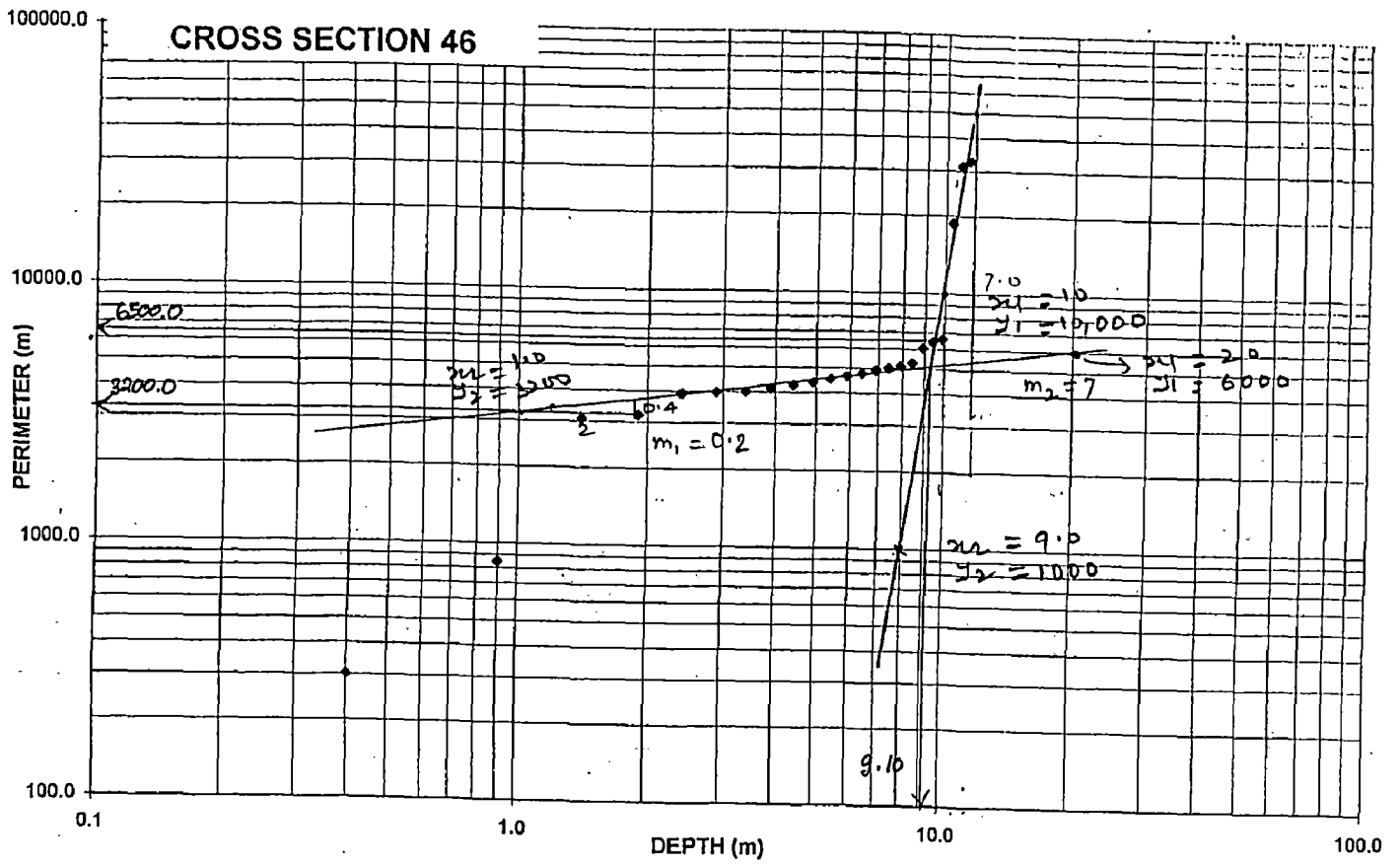


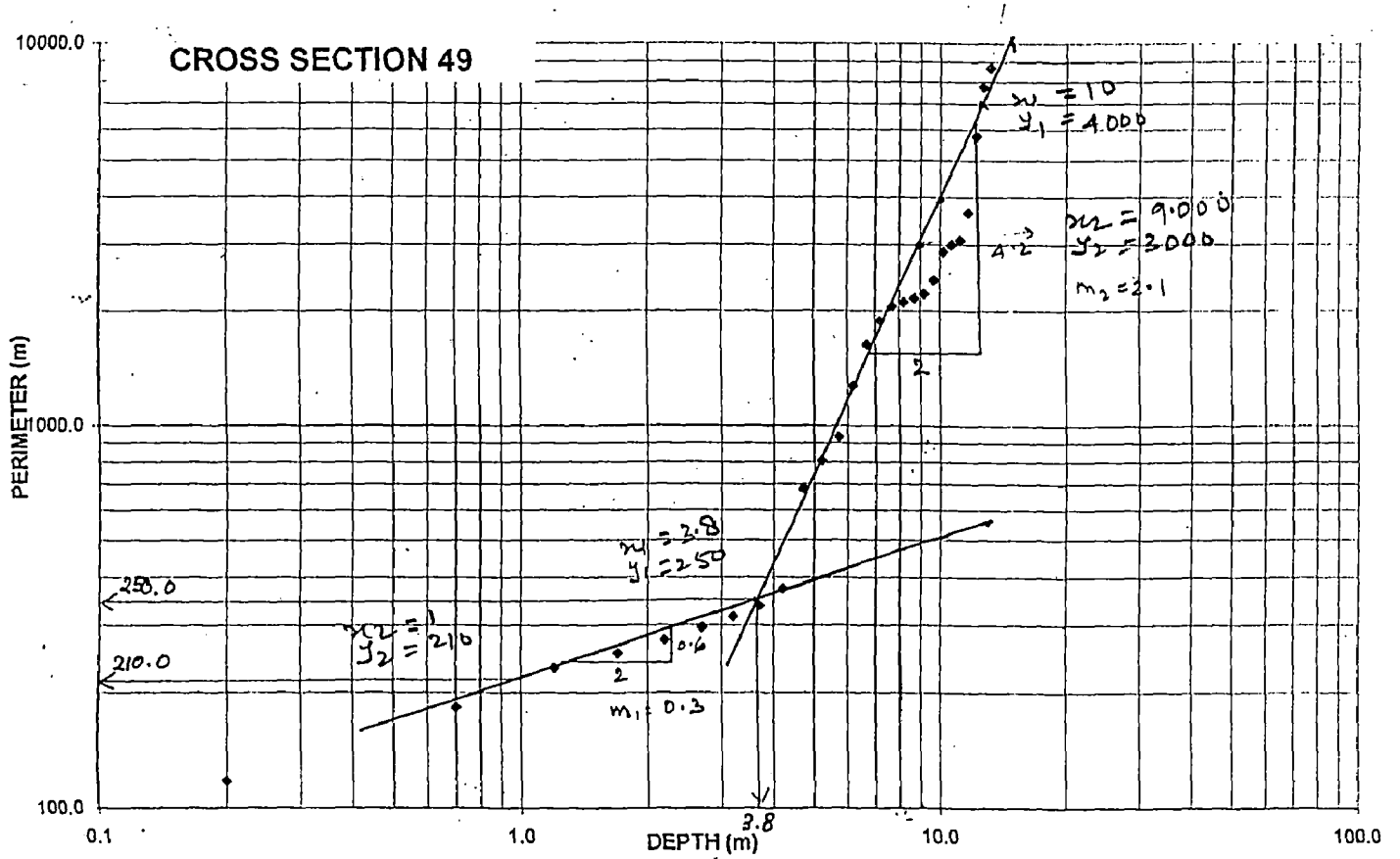
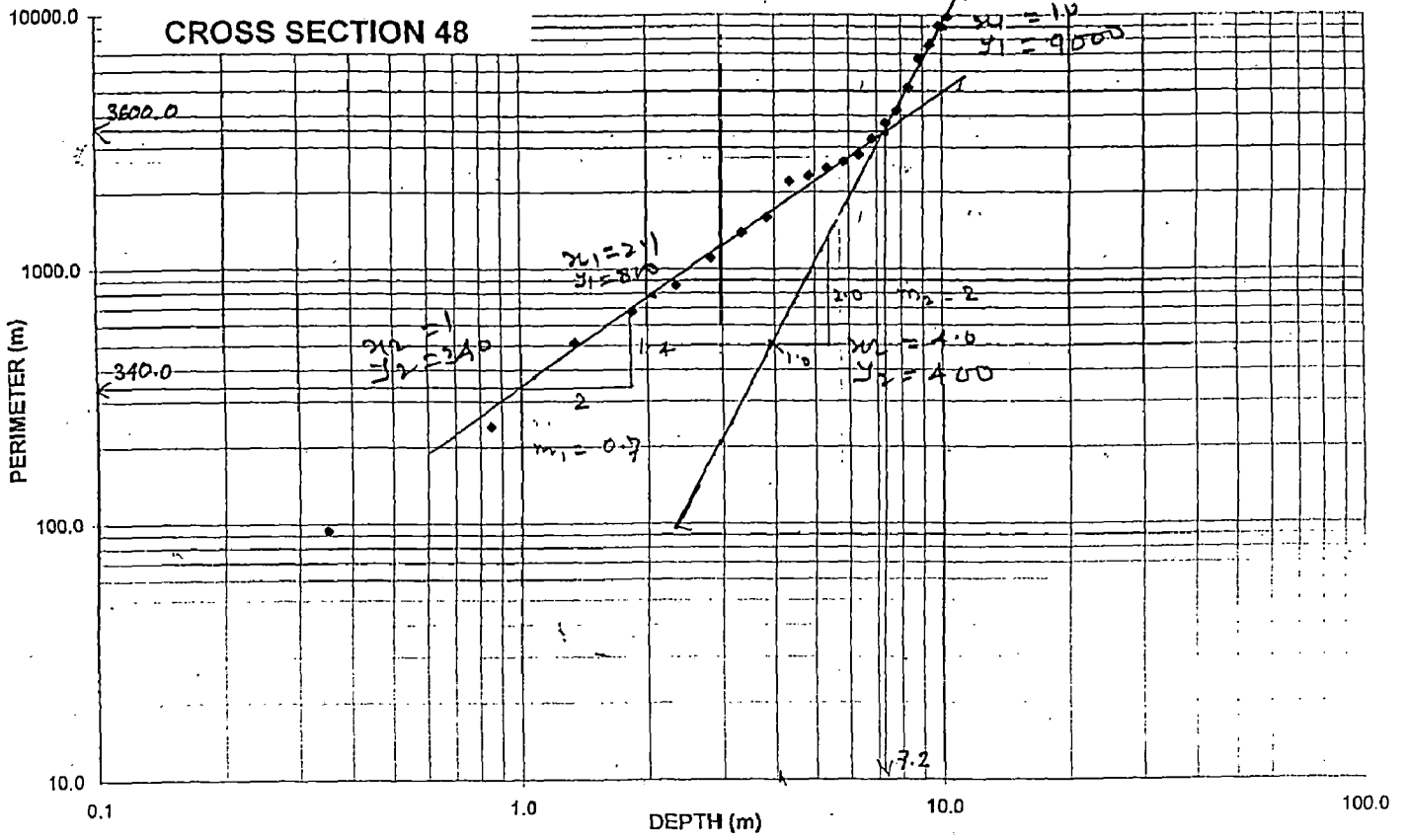


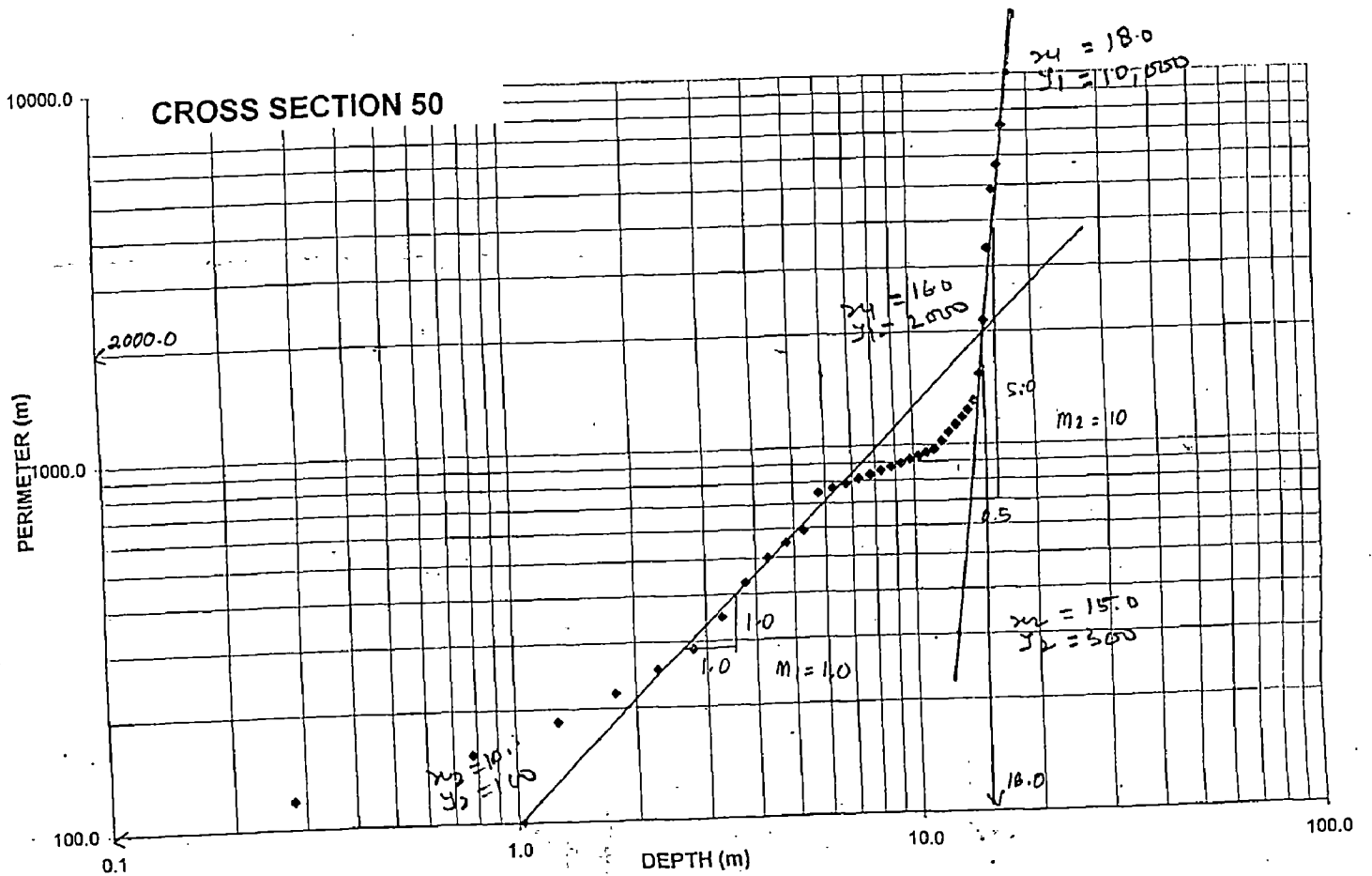
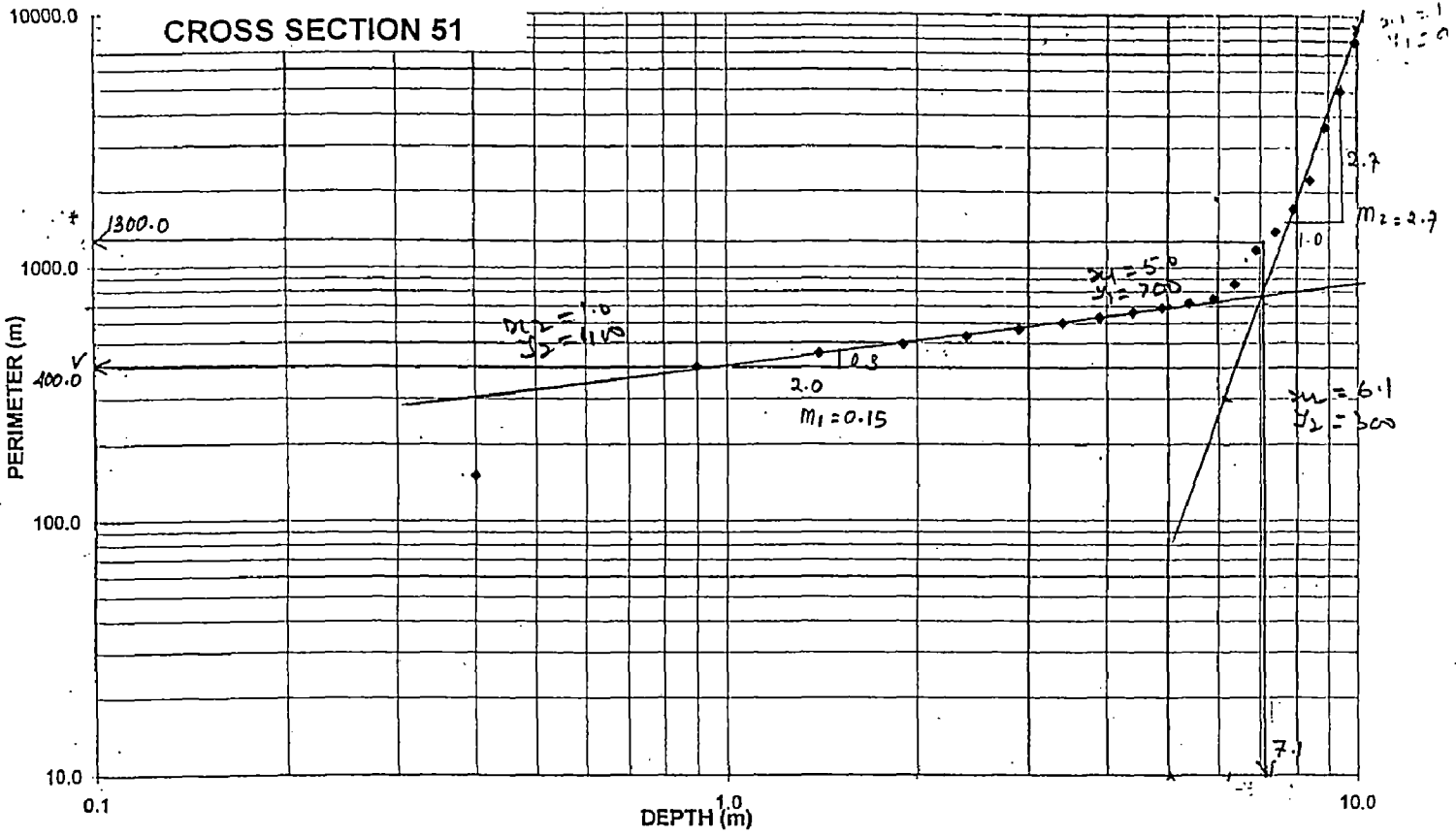




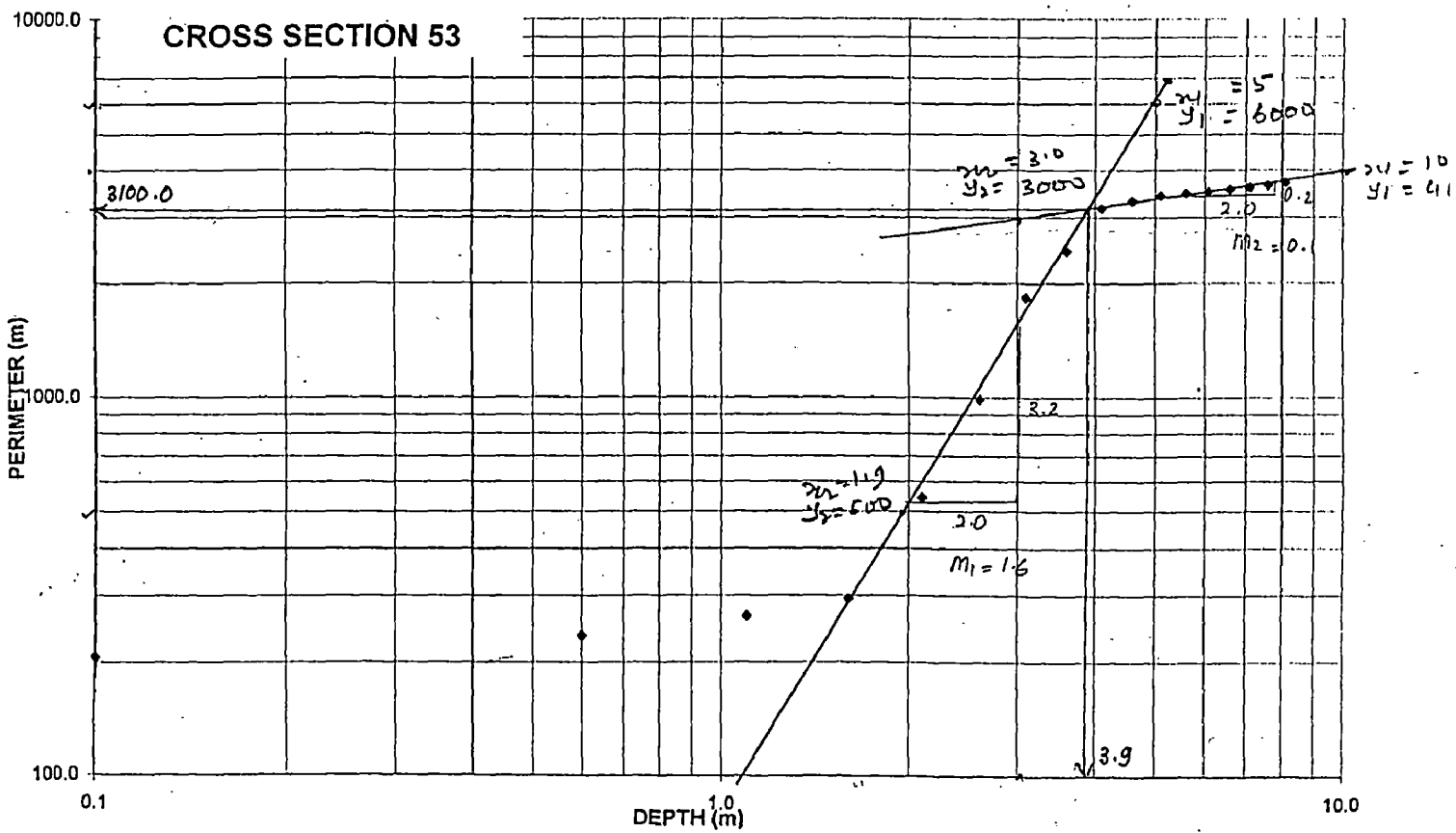
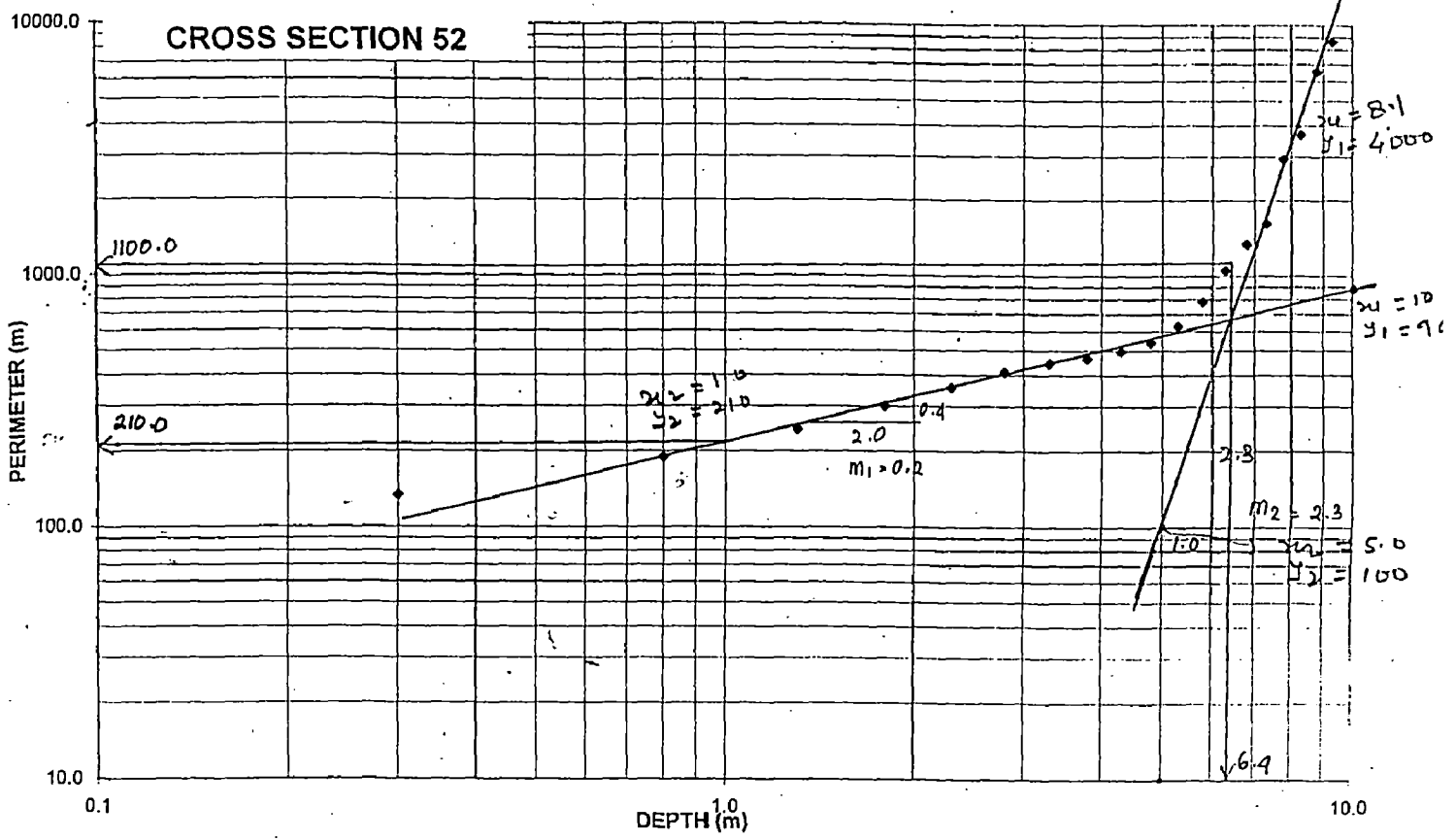


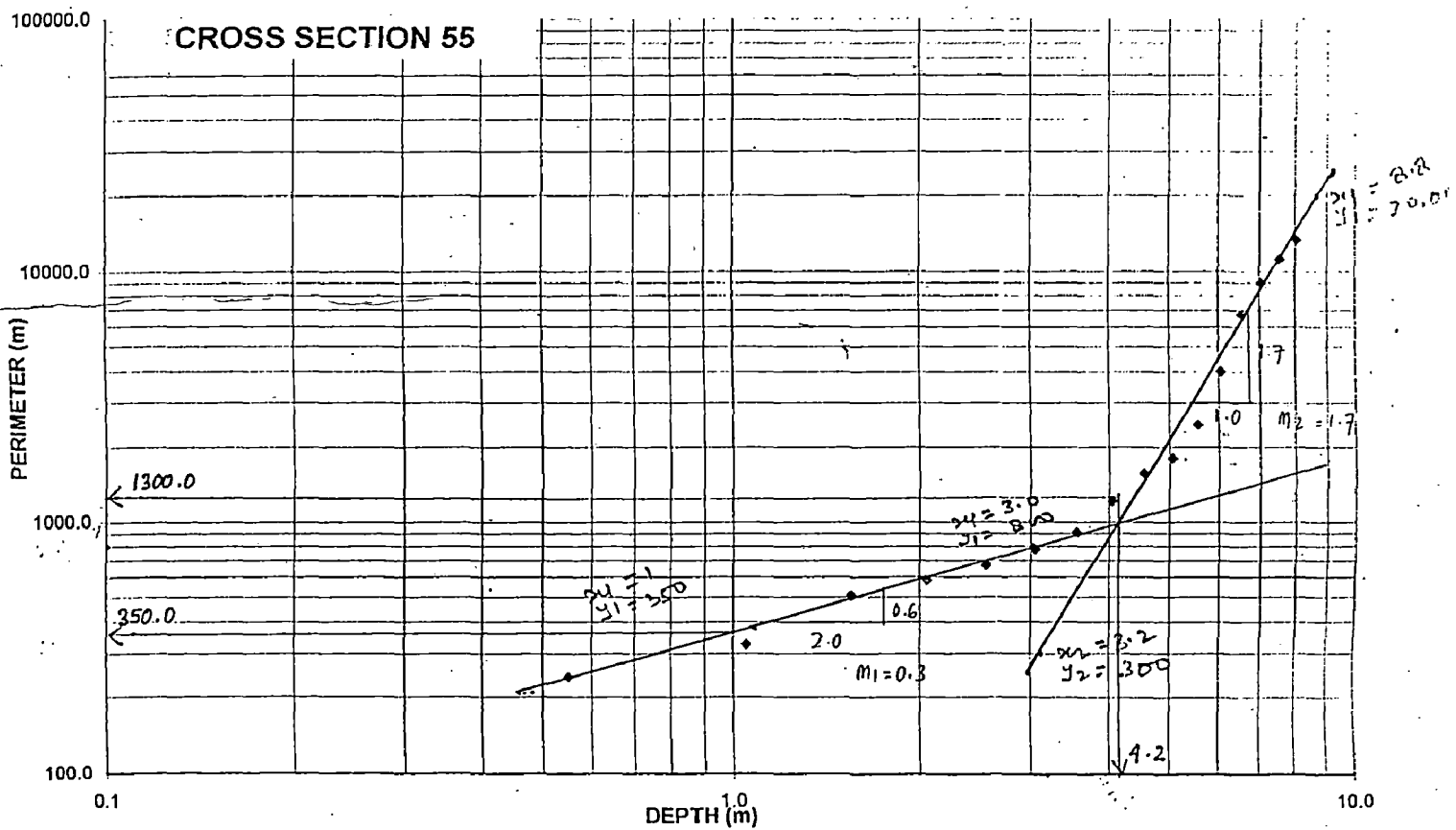
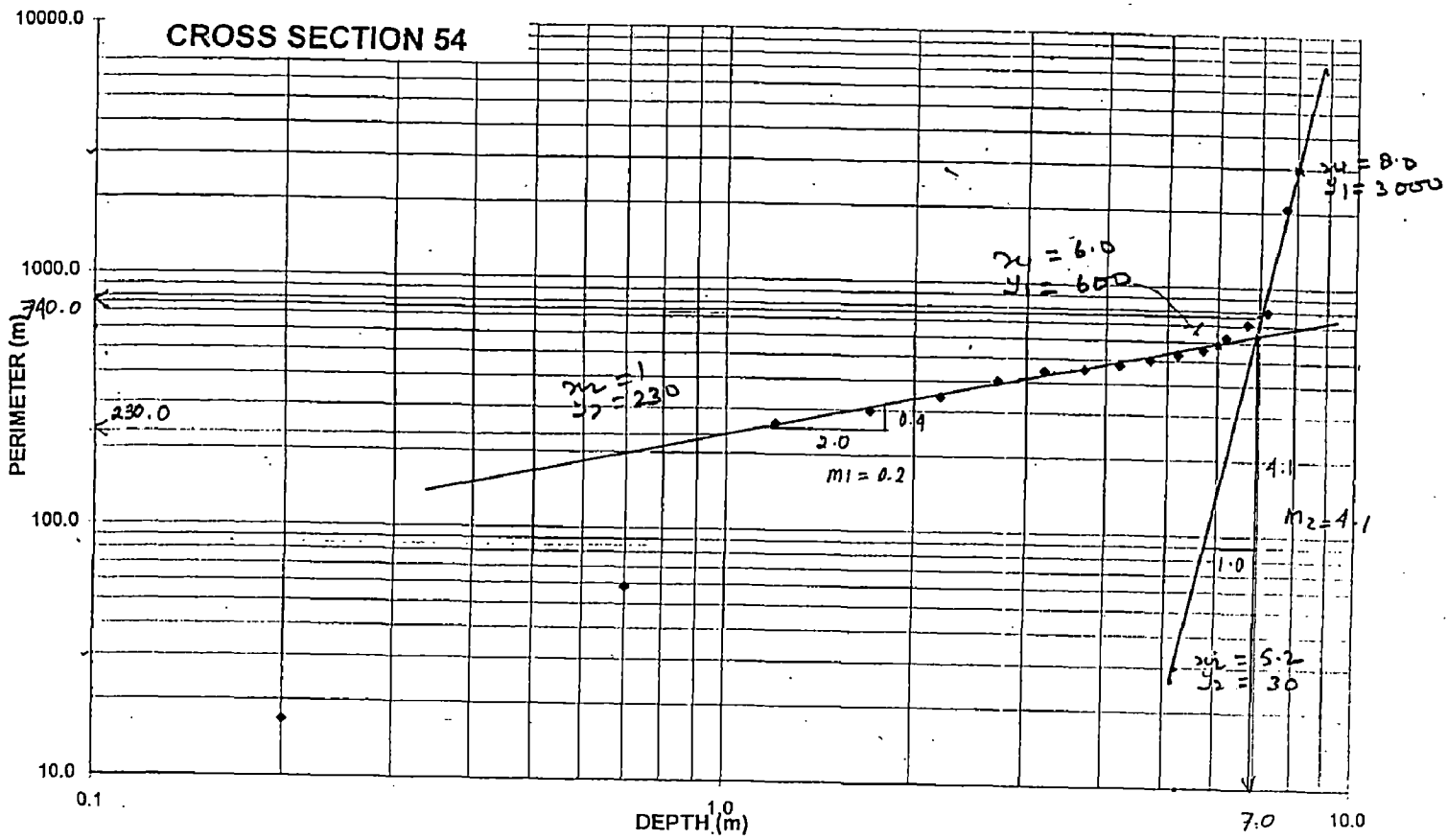


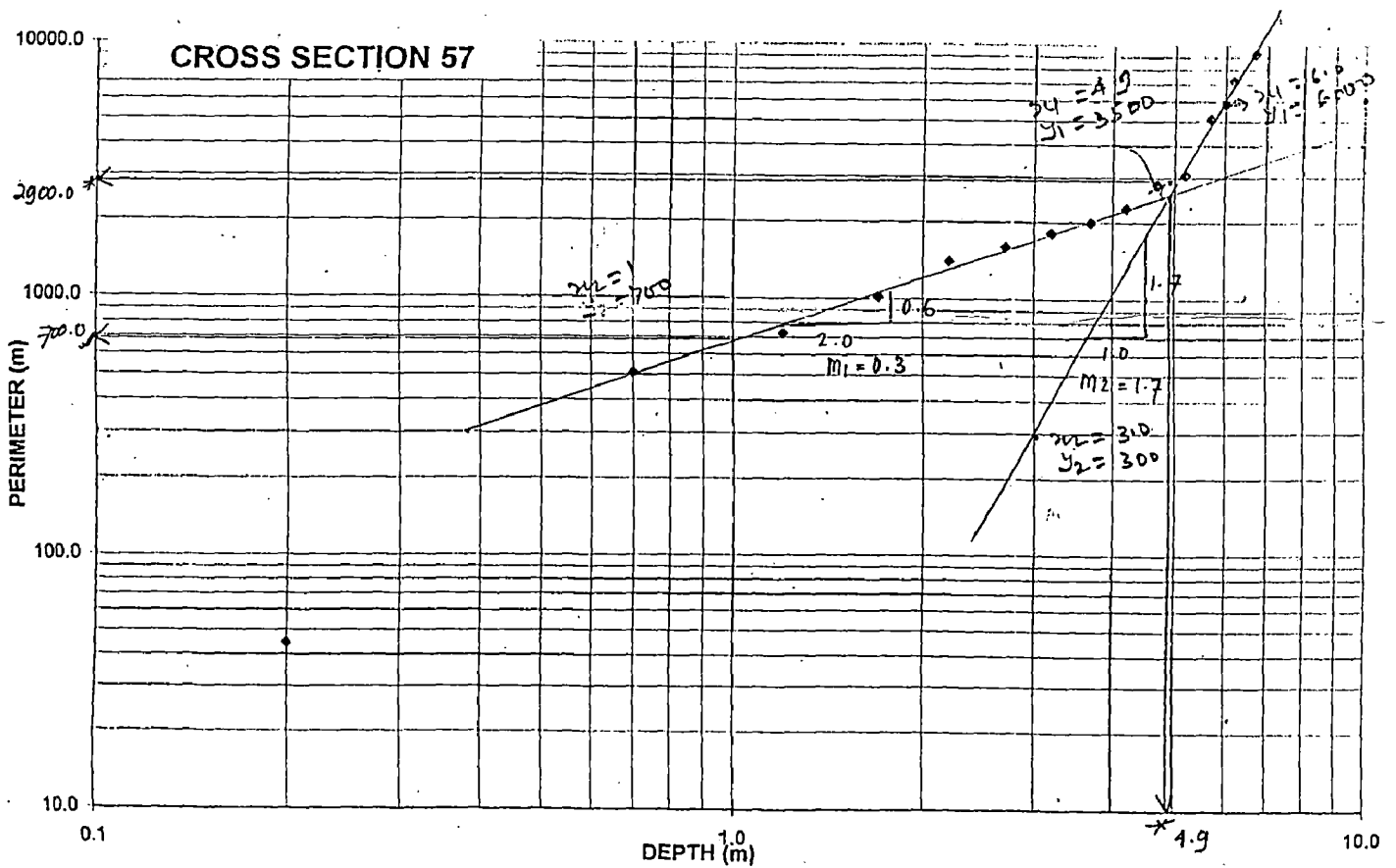
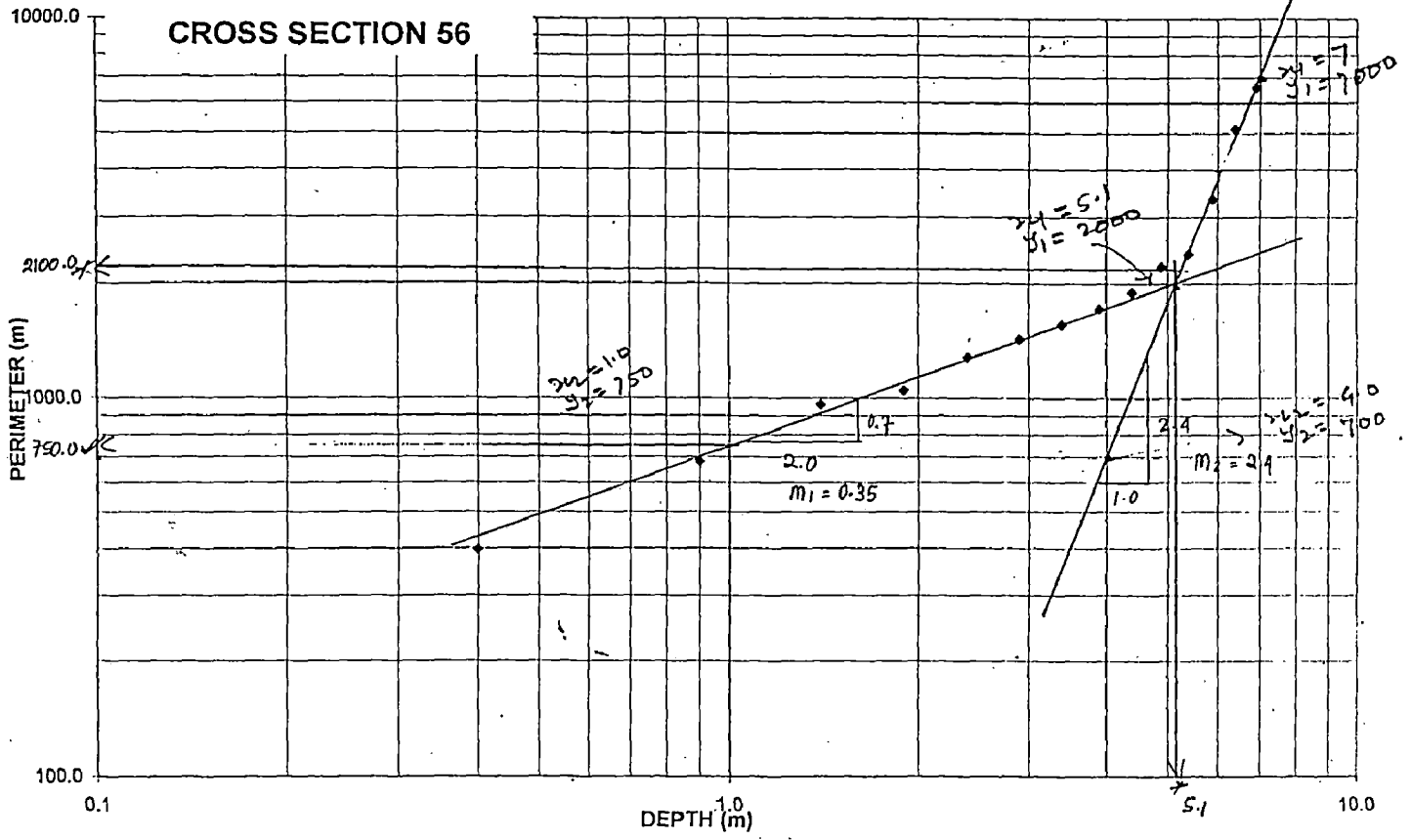


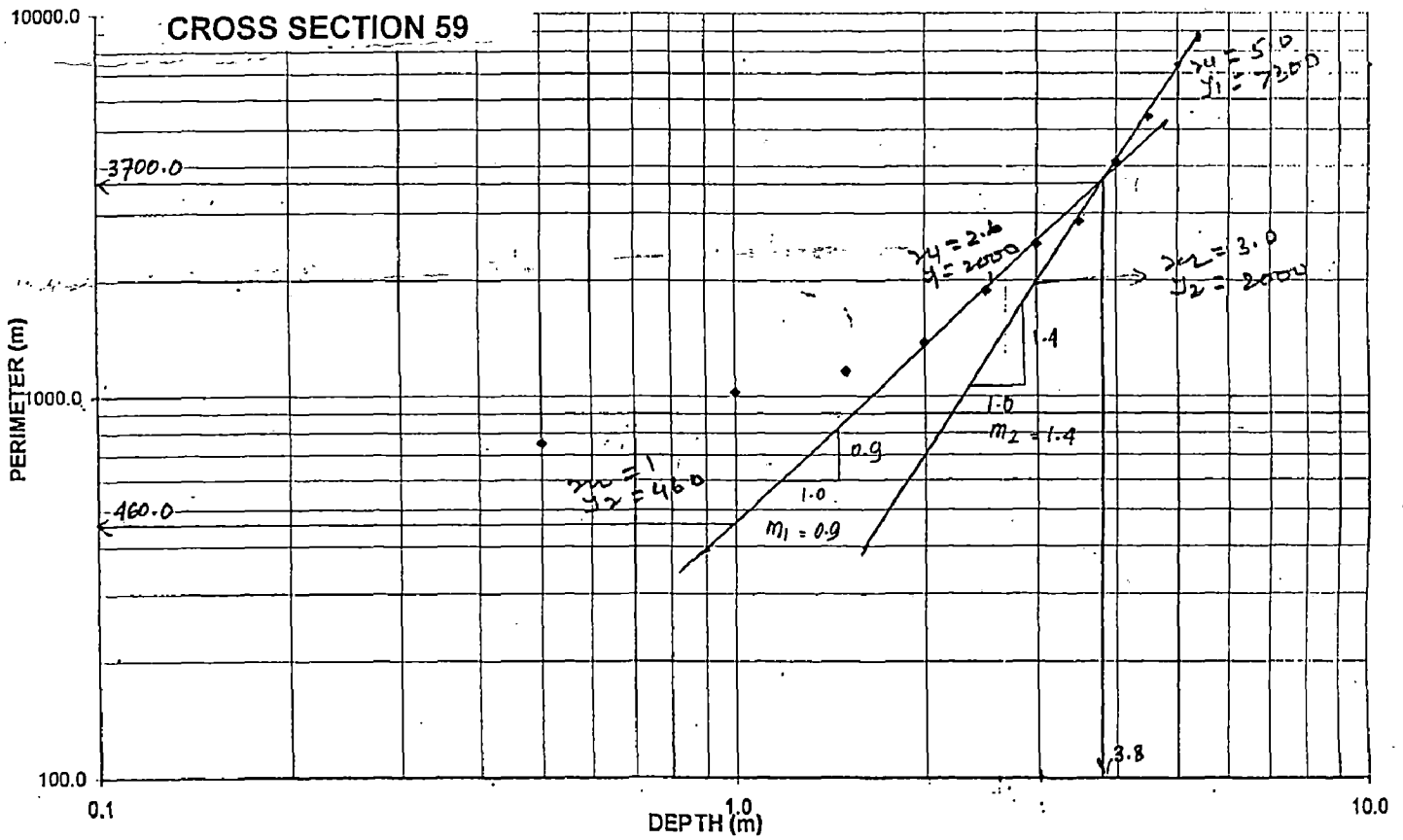
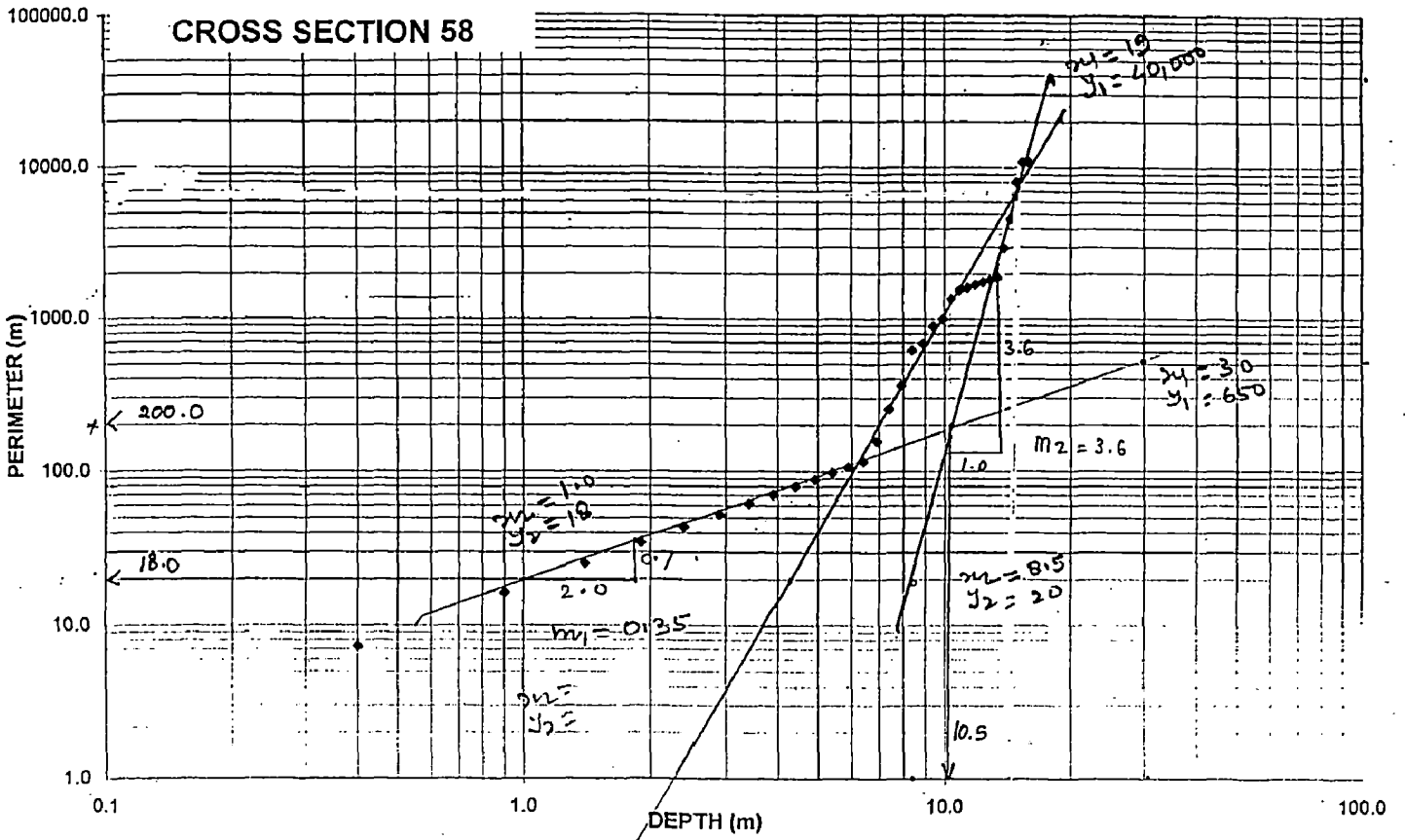


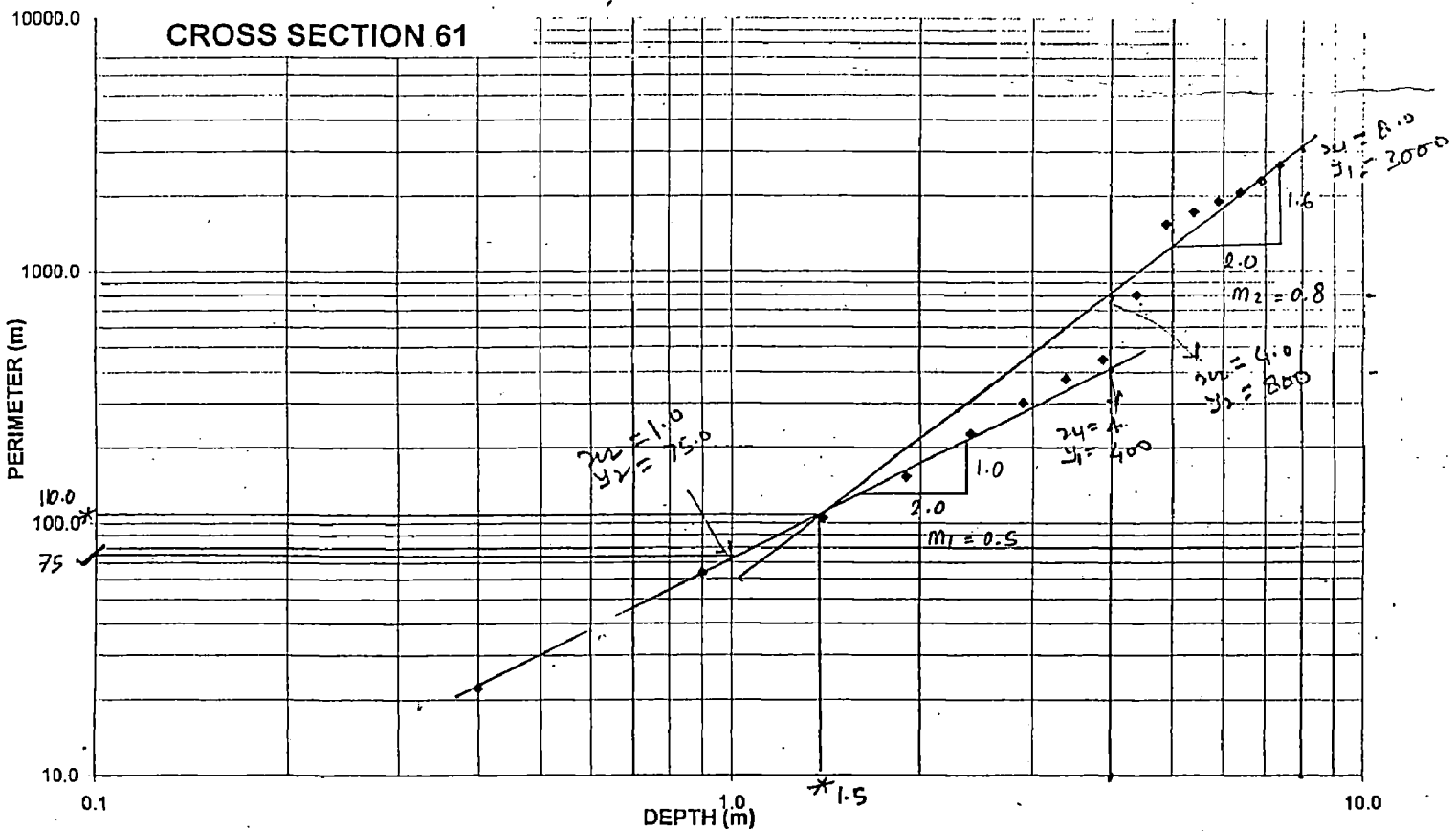
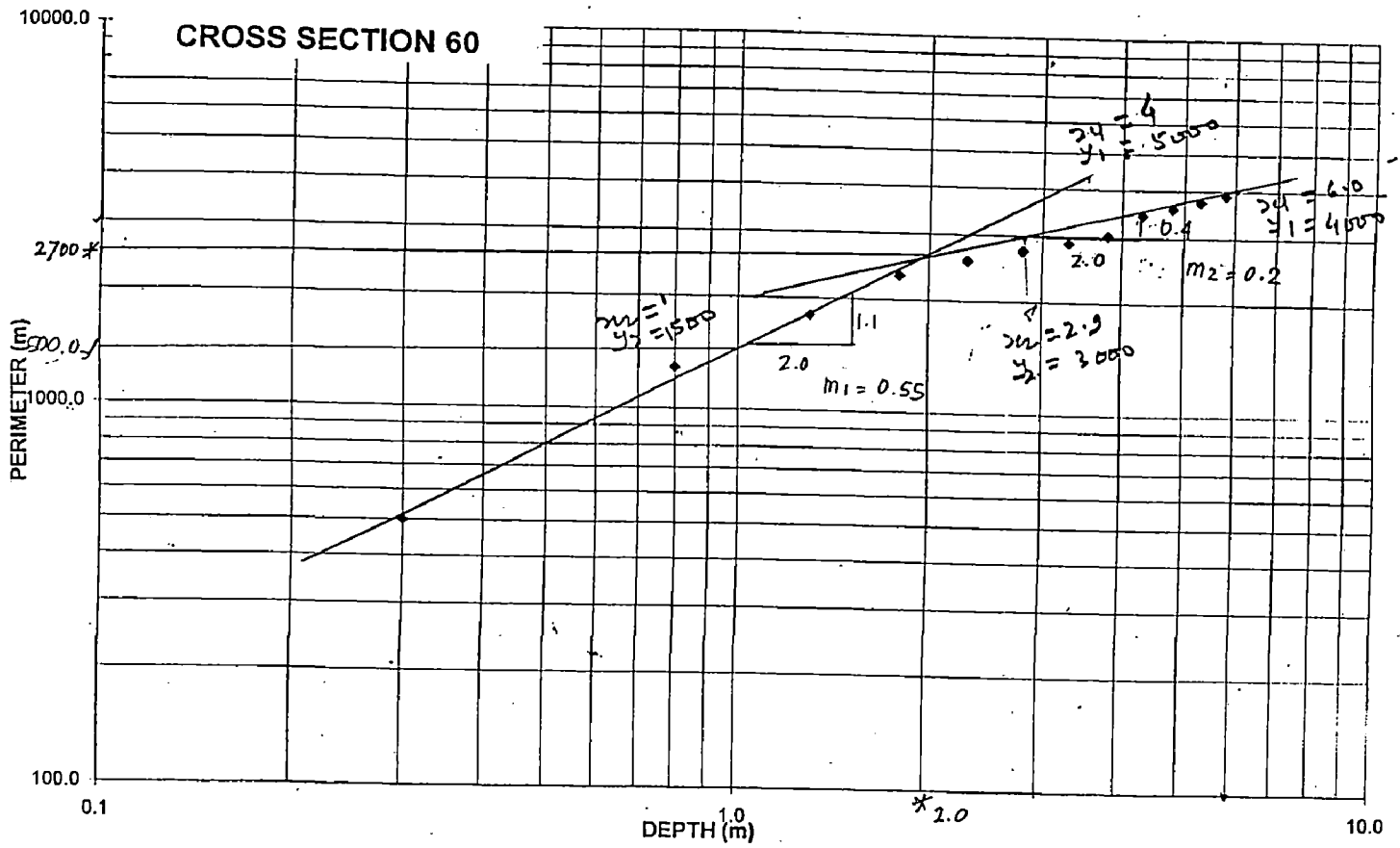


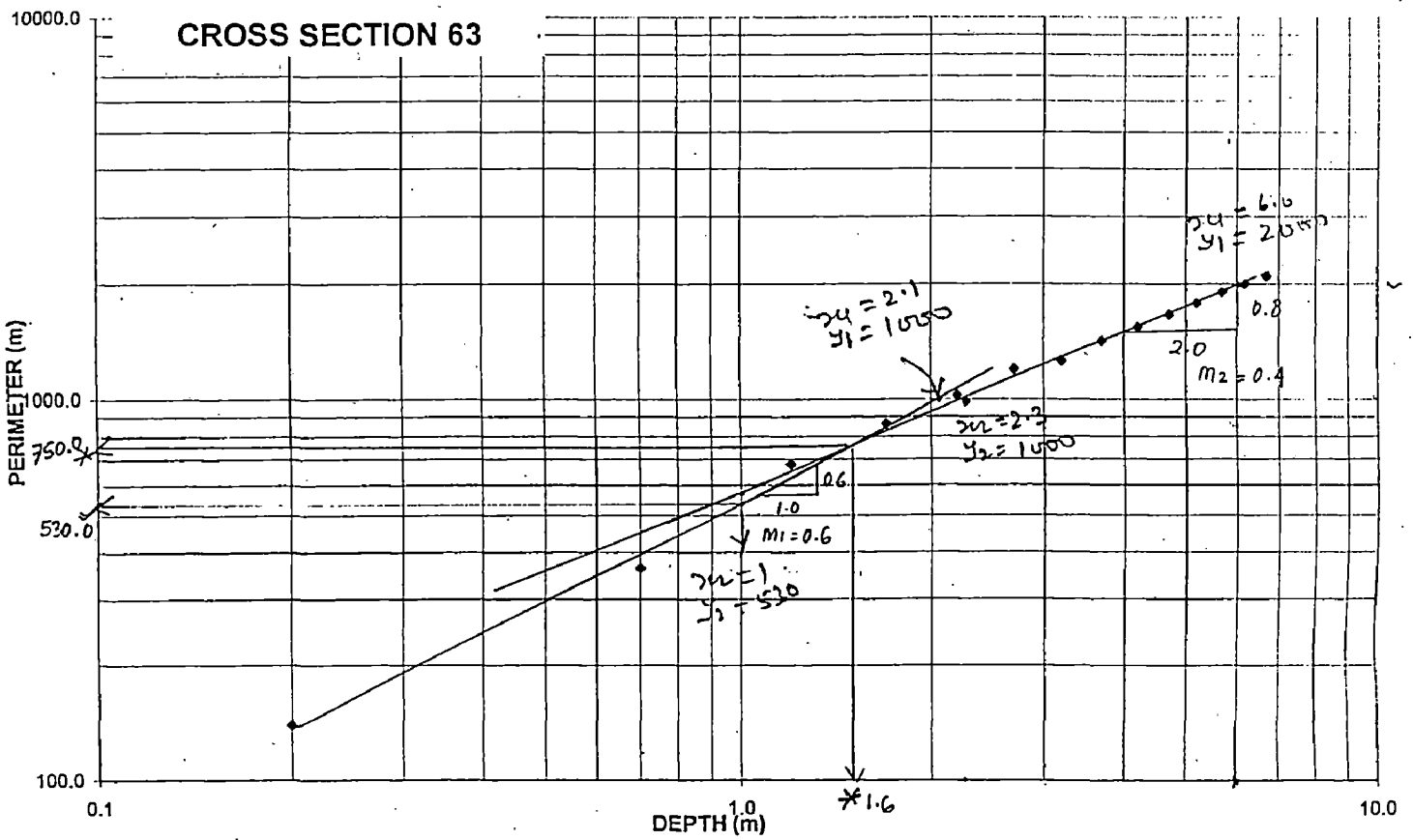
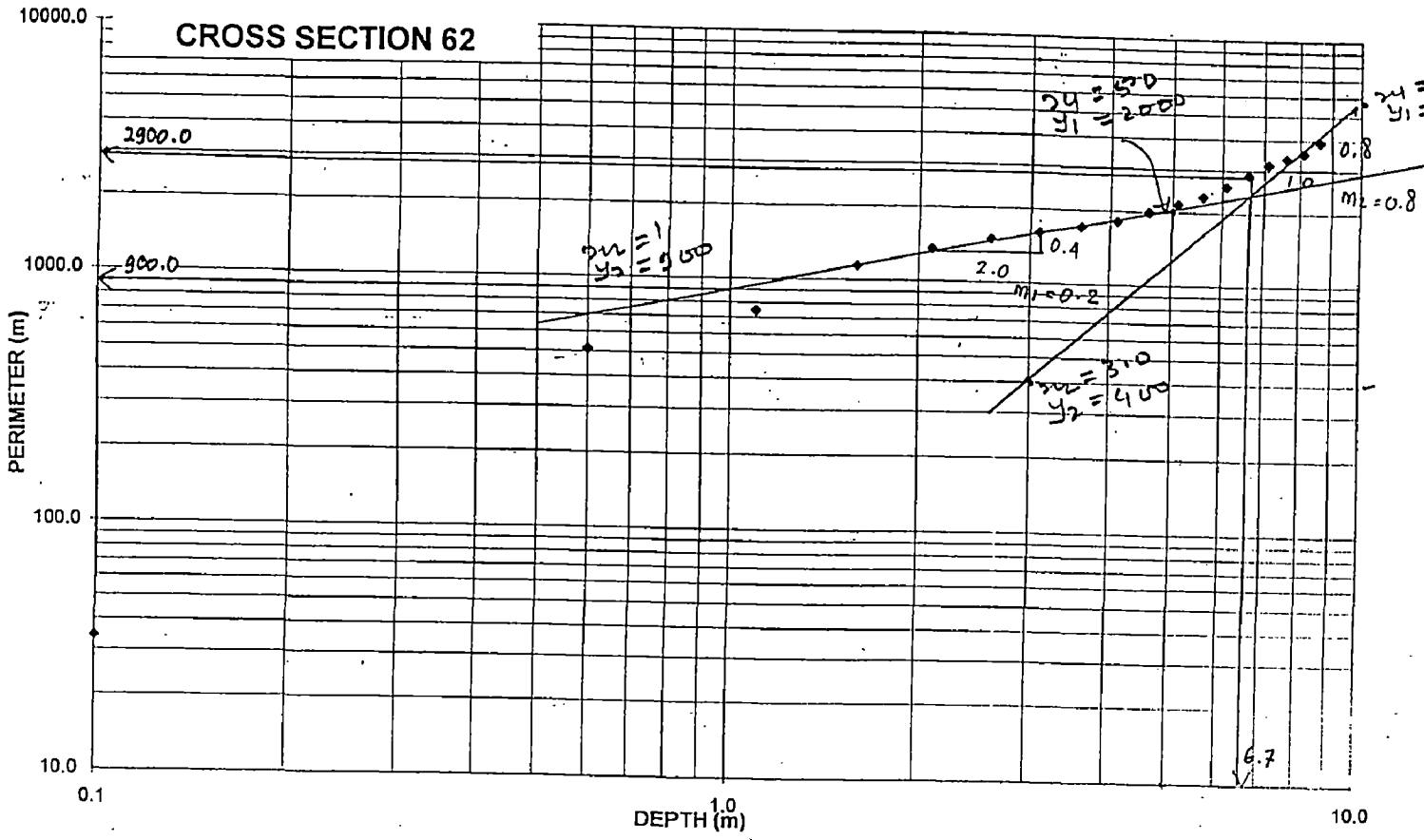


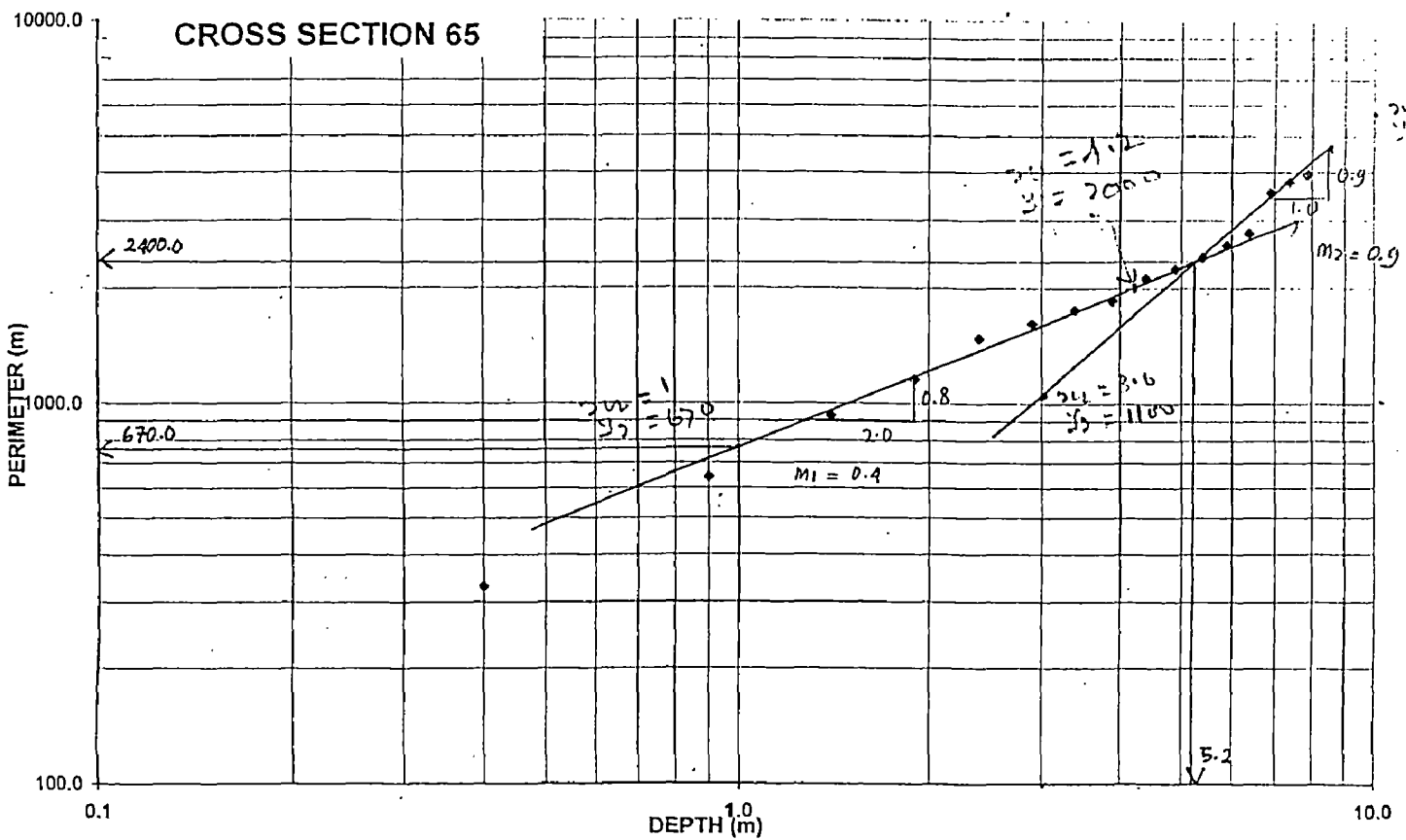
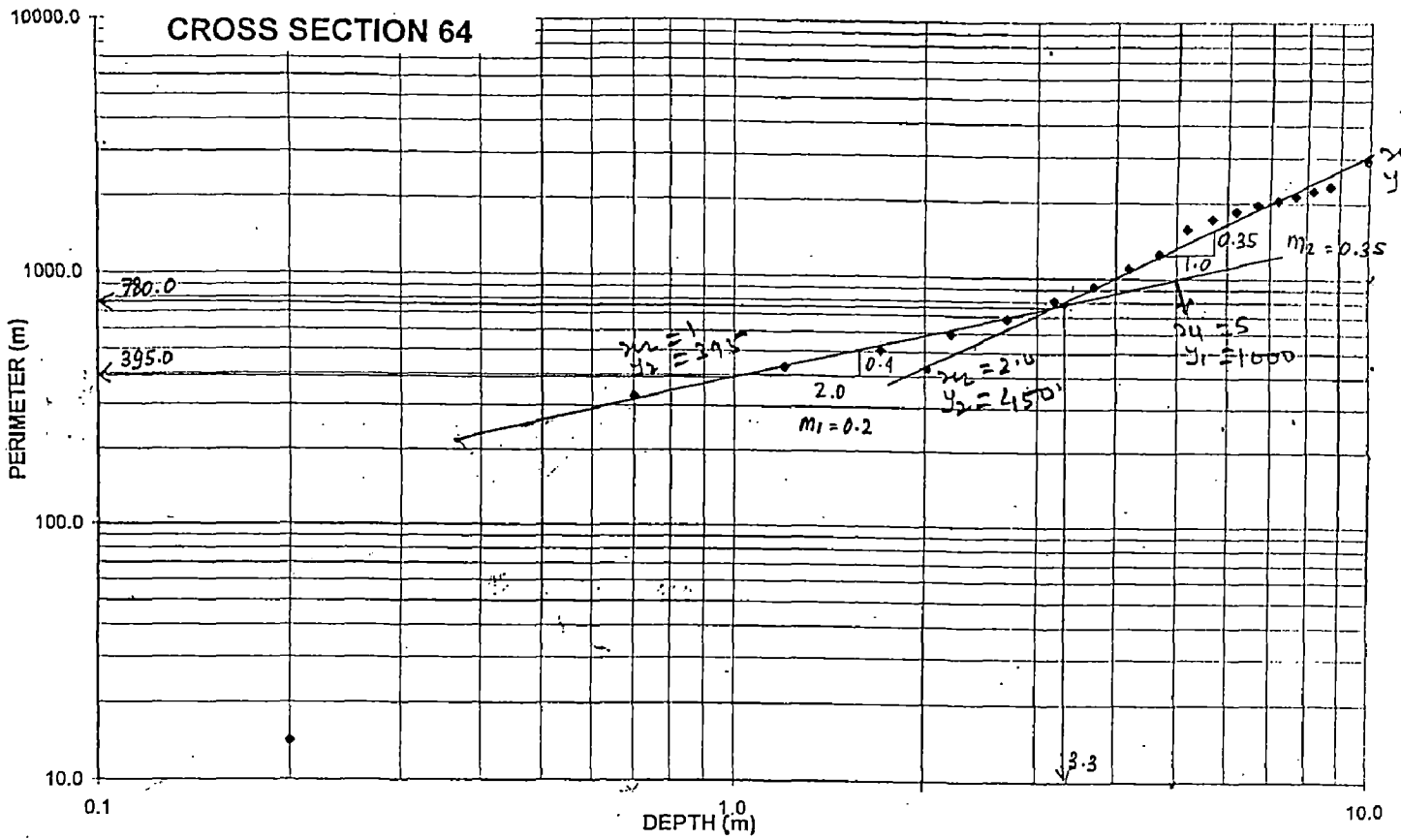








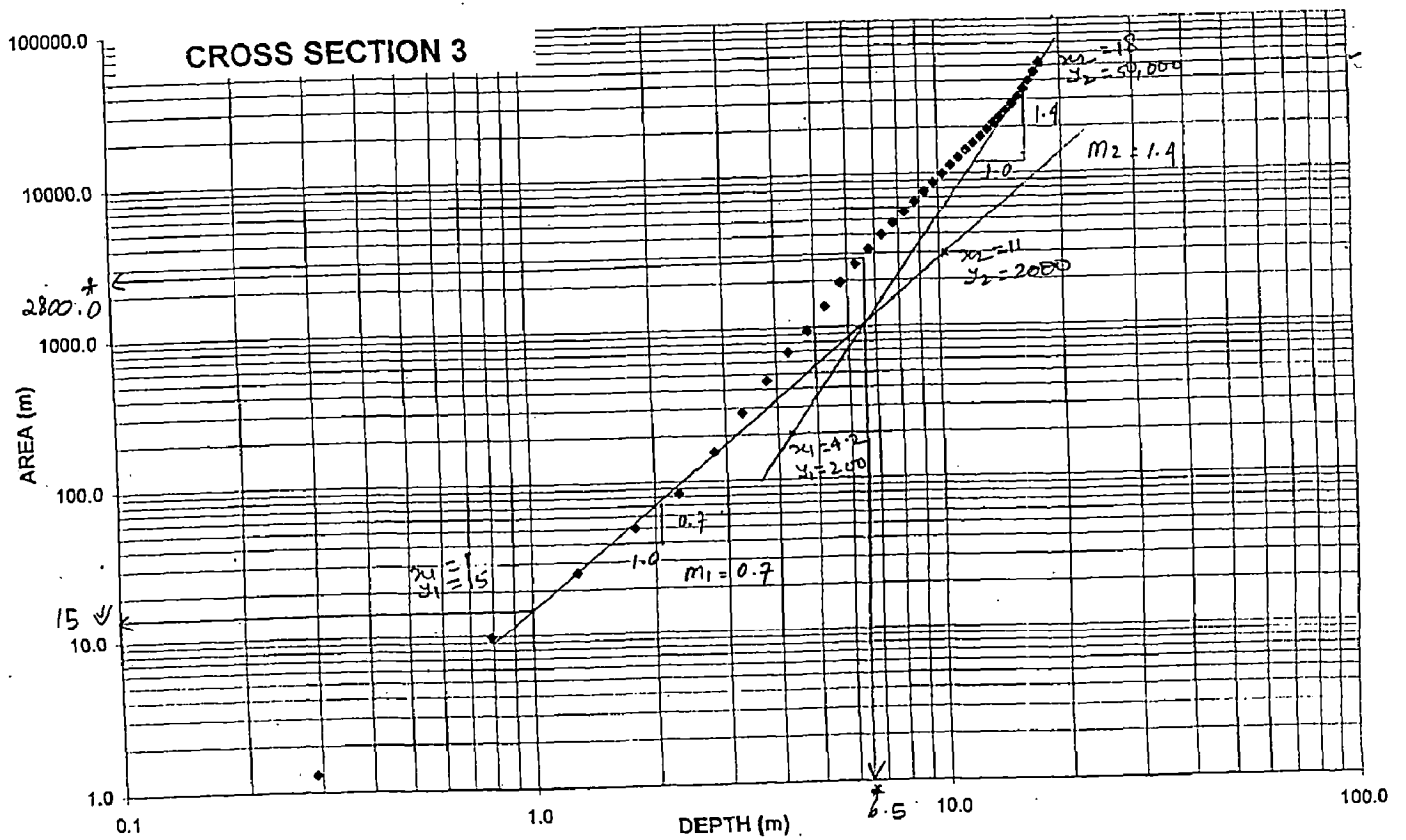
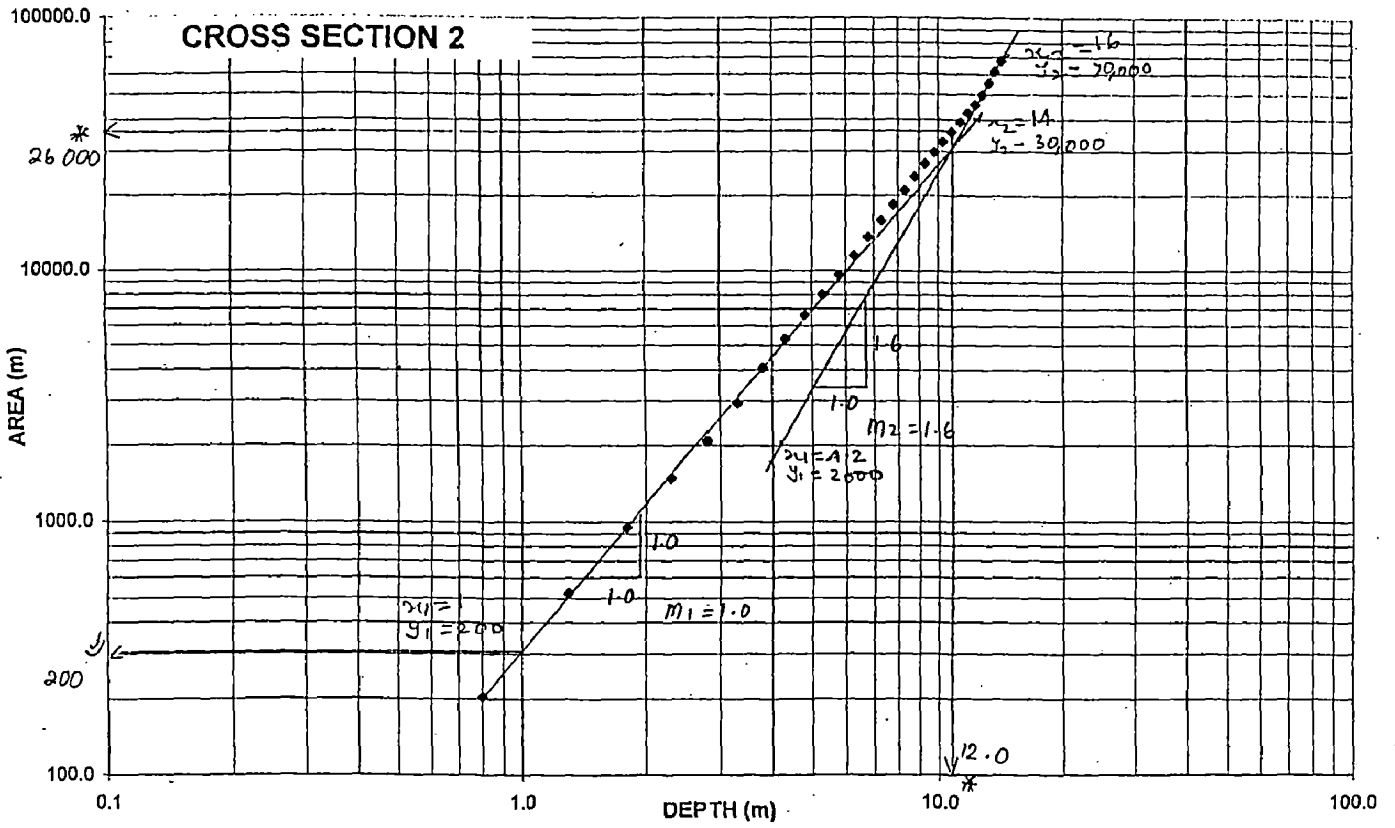


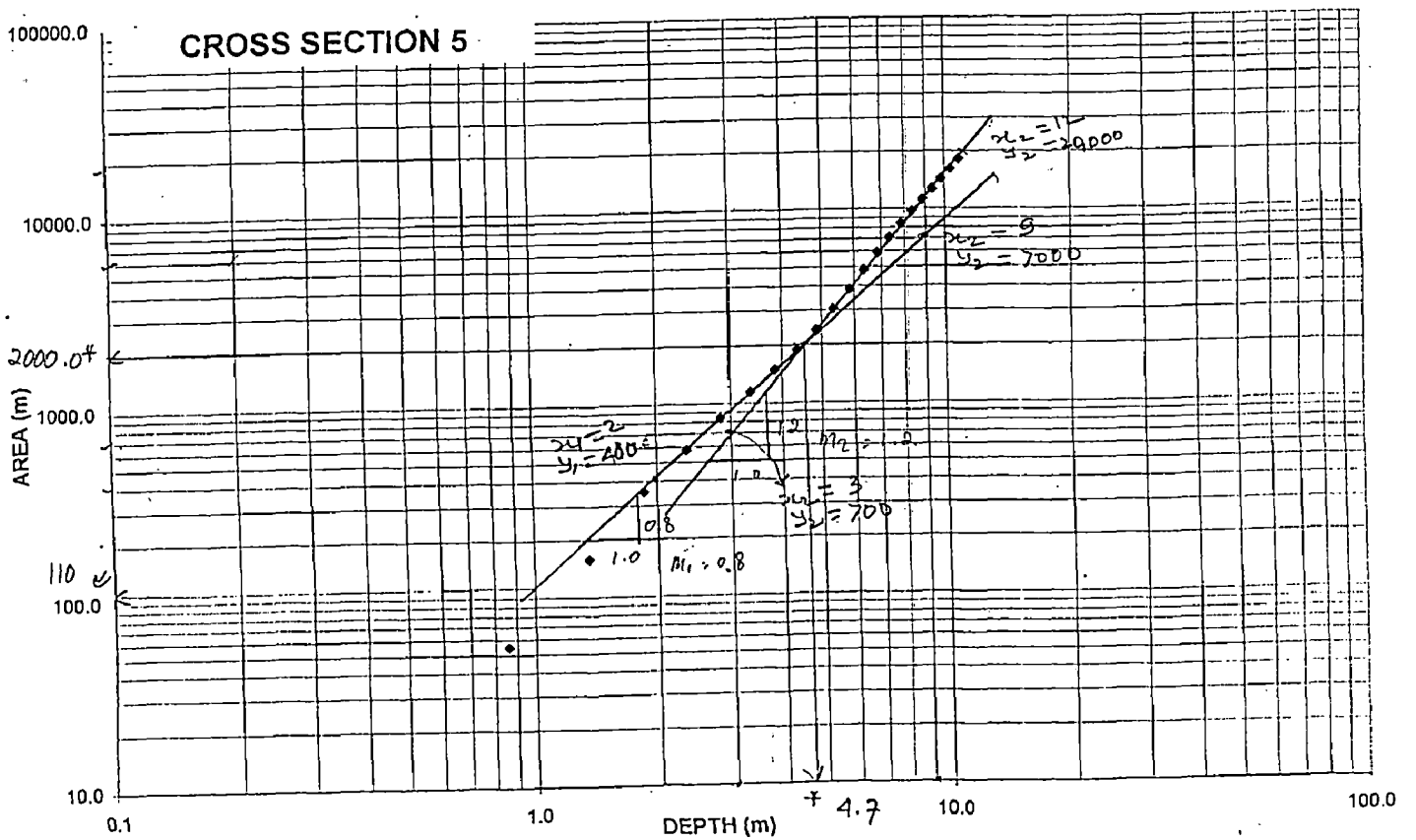
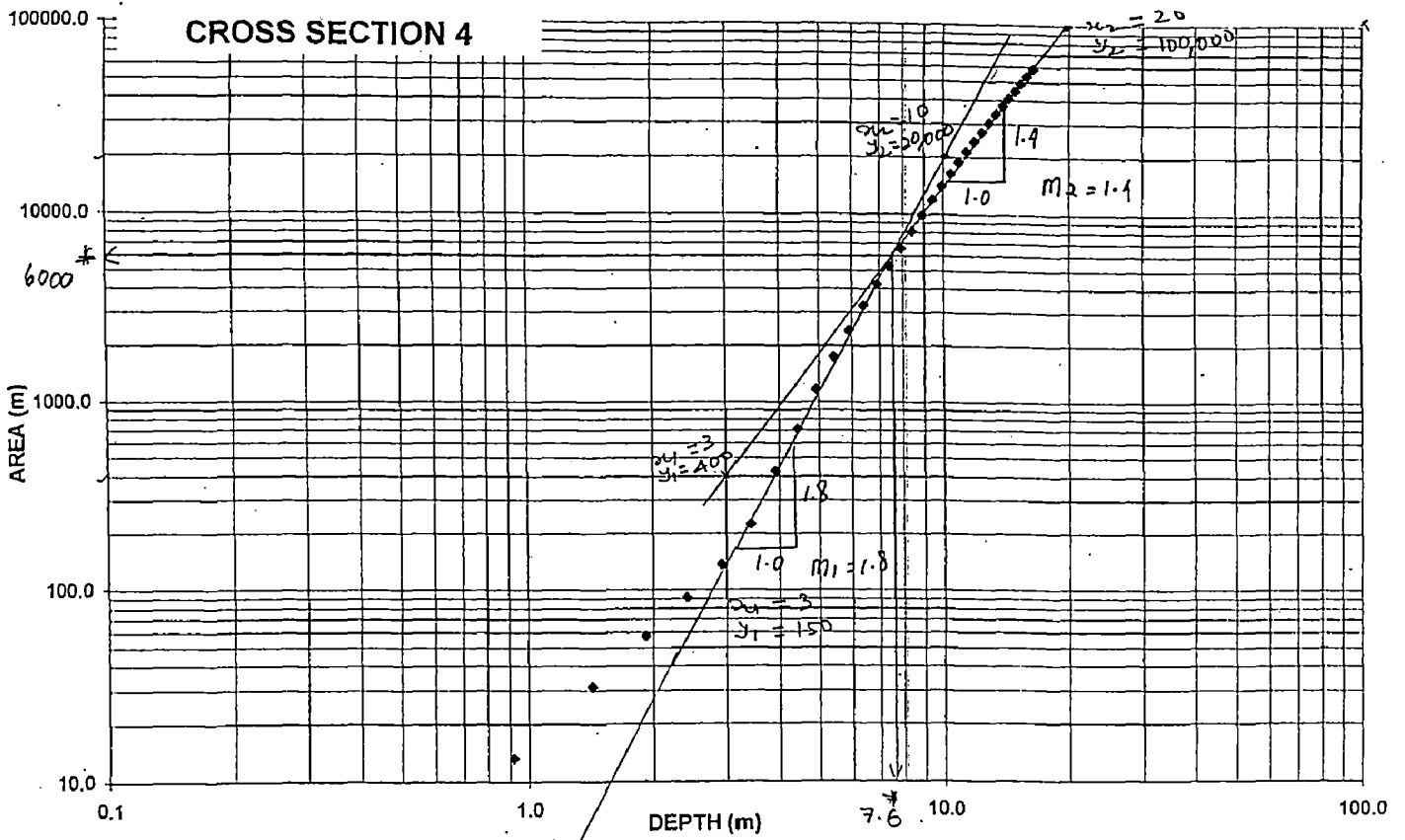


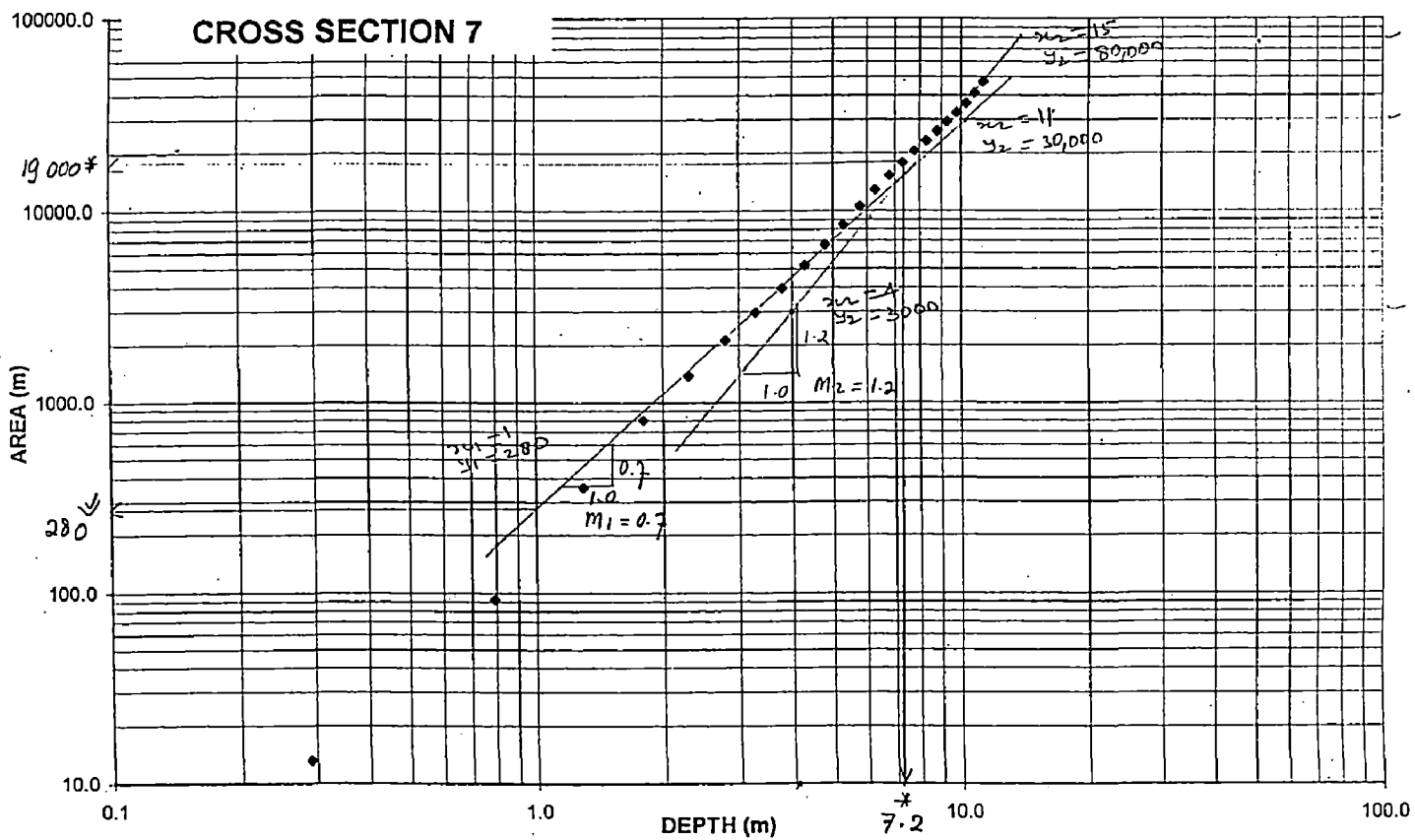
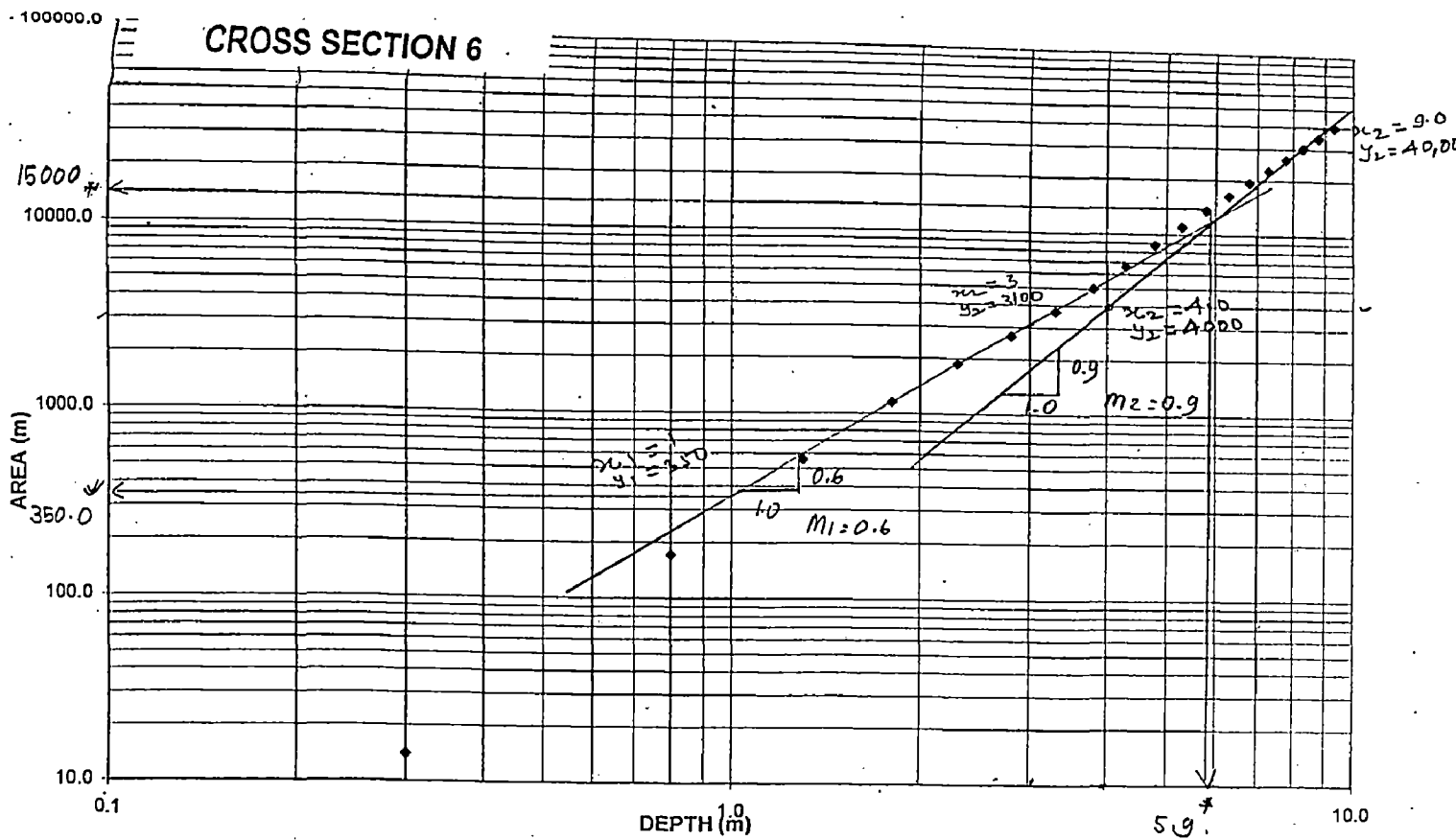
**APPENDIX B**  
**PLOT OF AREA VS DEPTH**  
**FOR FINDING PARAMETER OF AREA EQUATION**

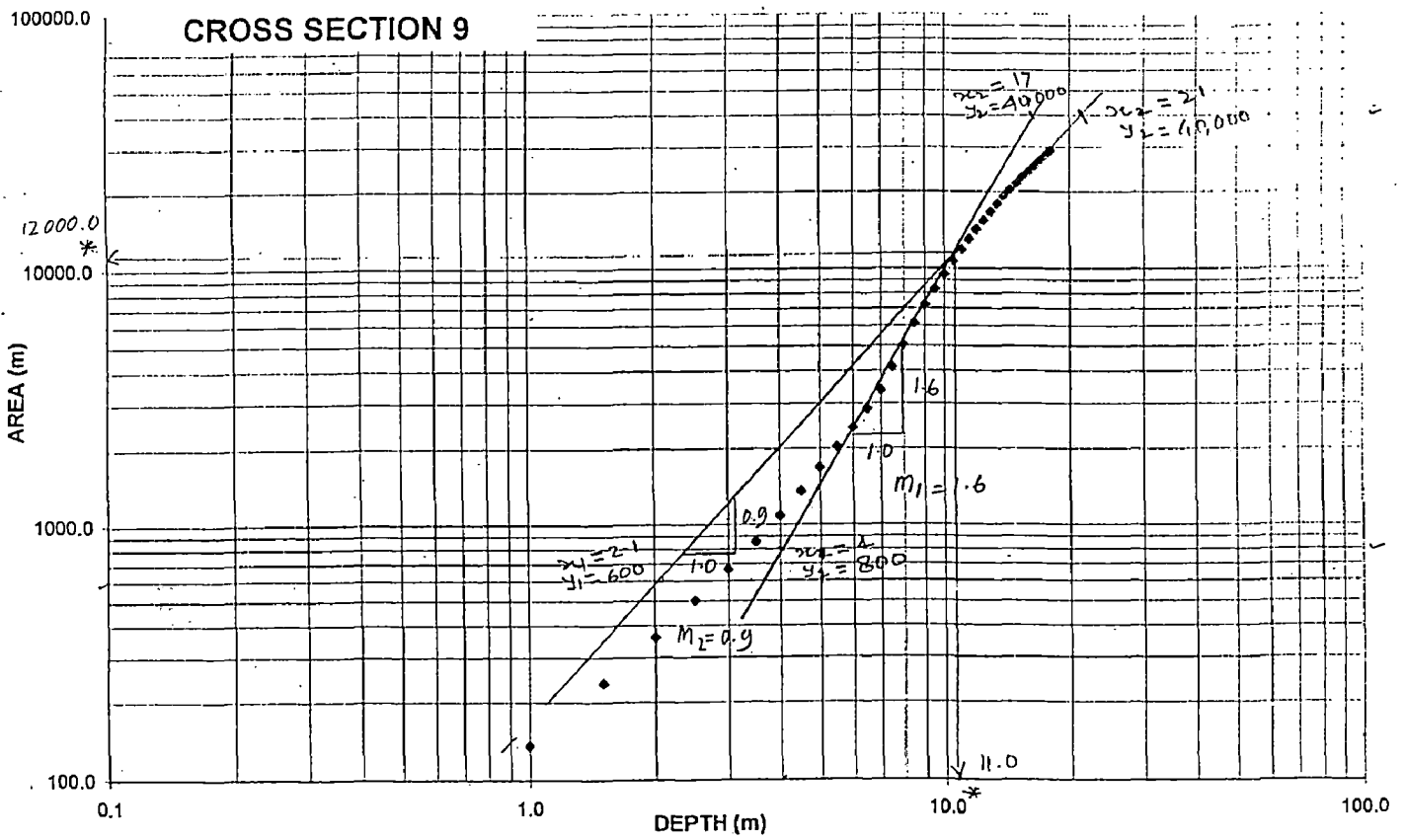
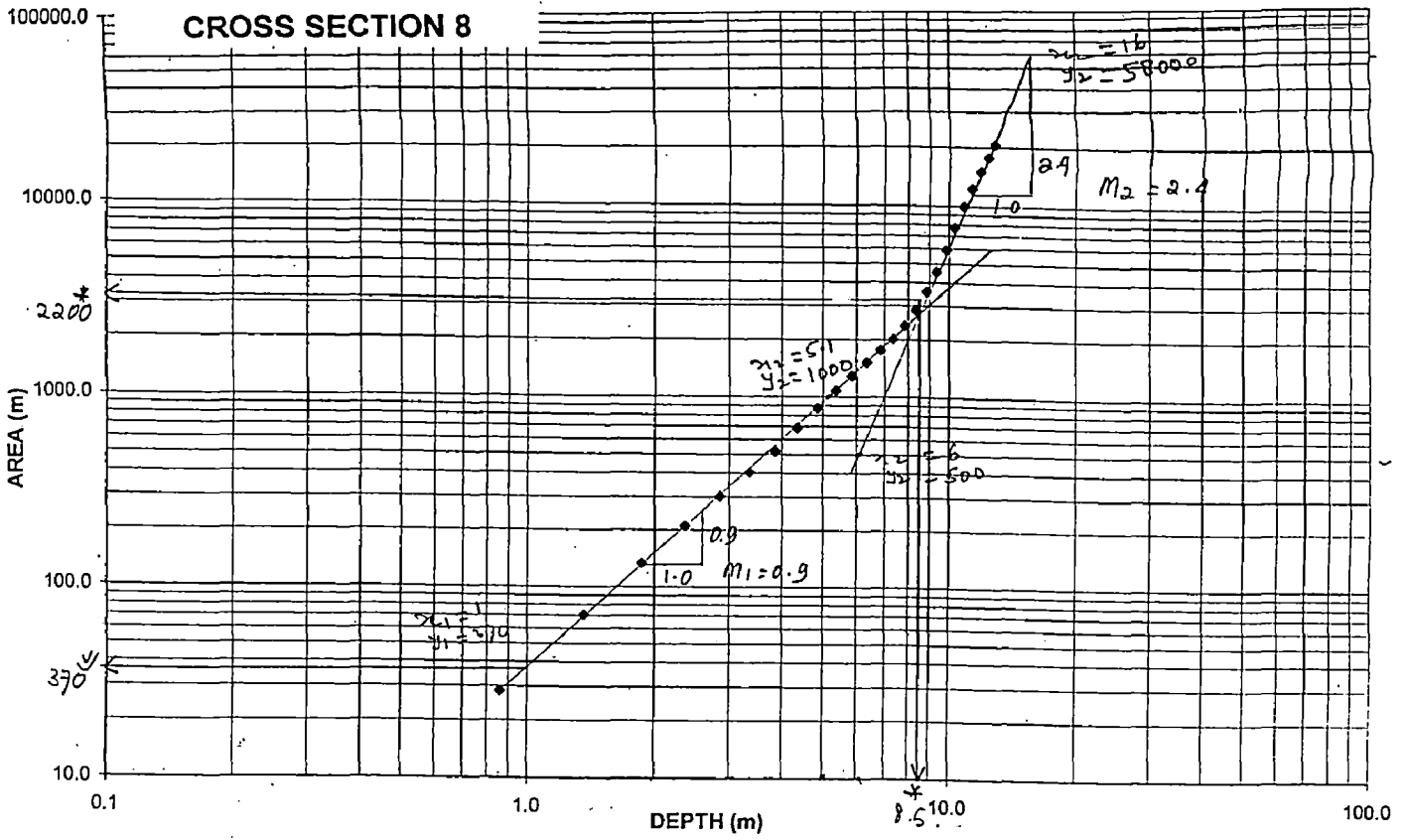
---



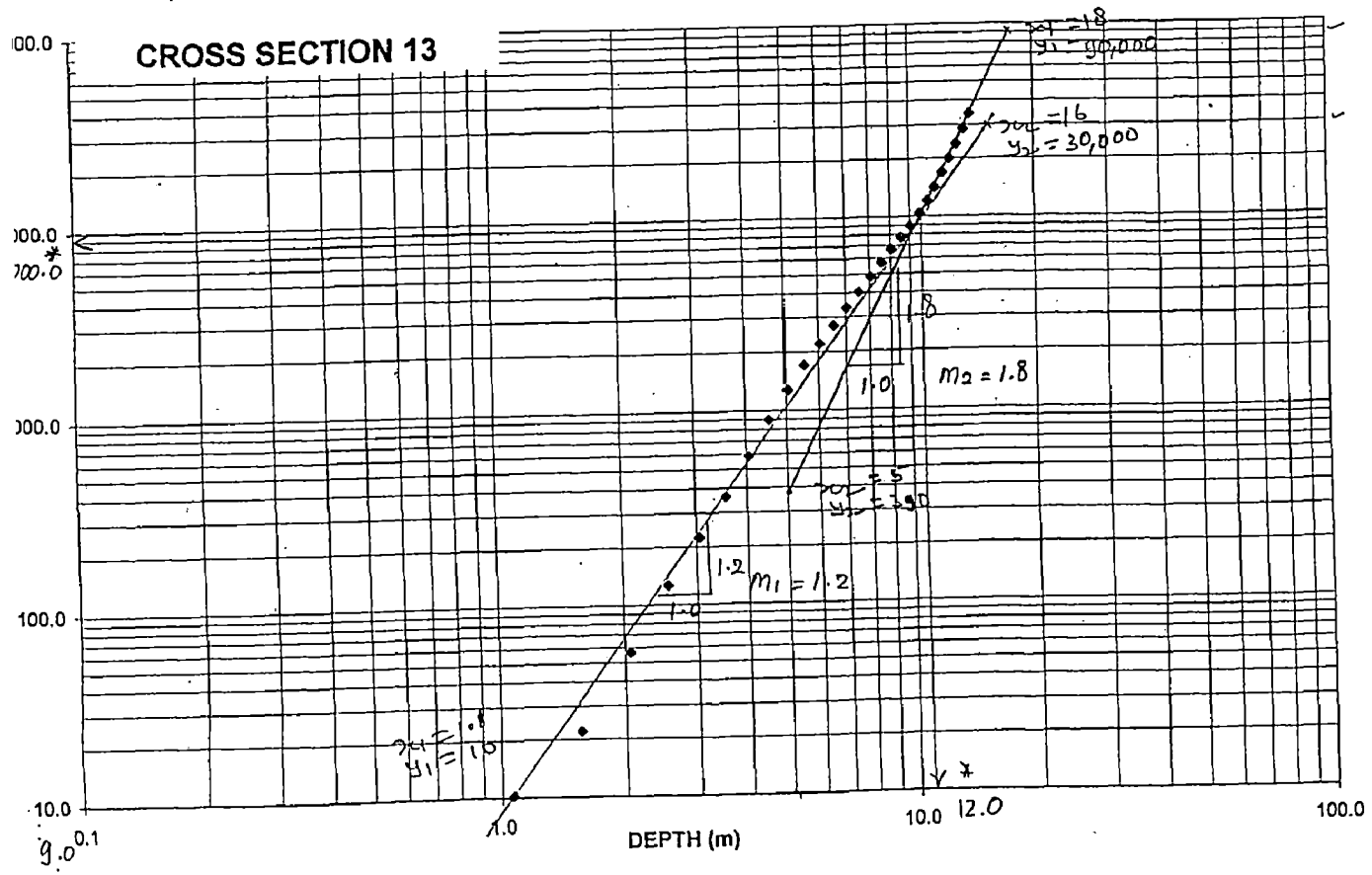
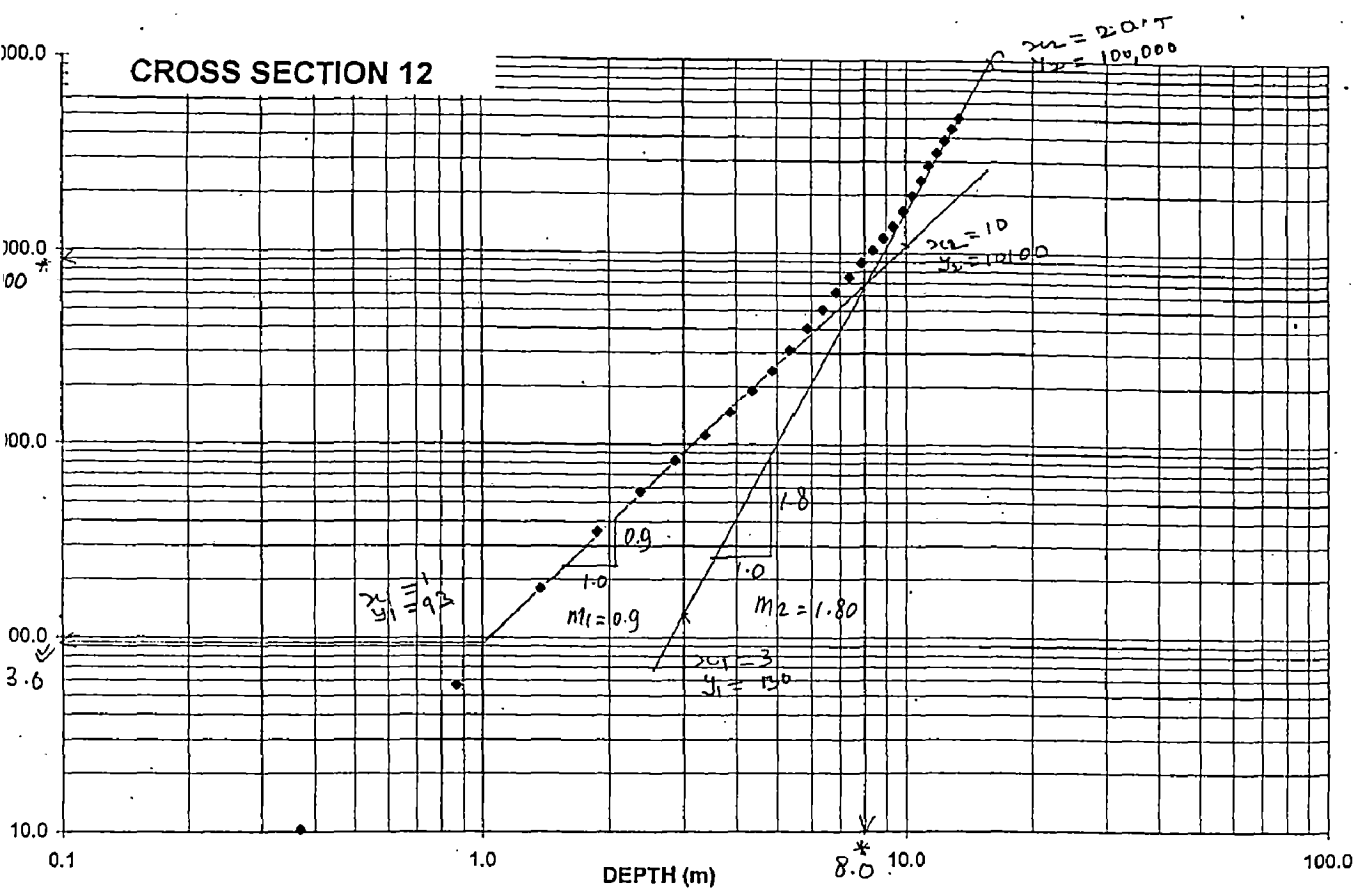


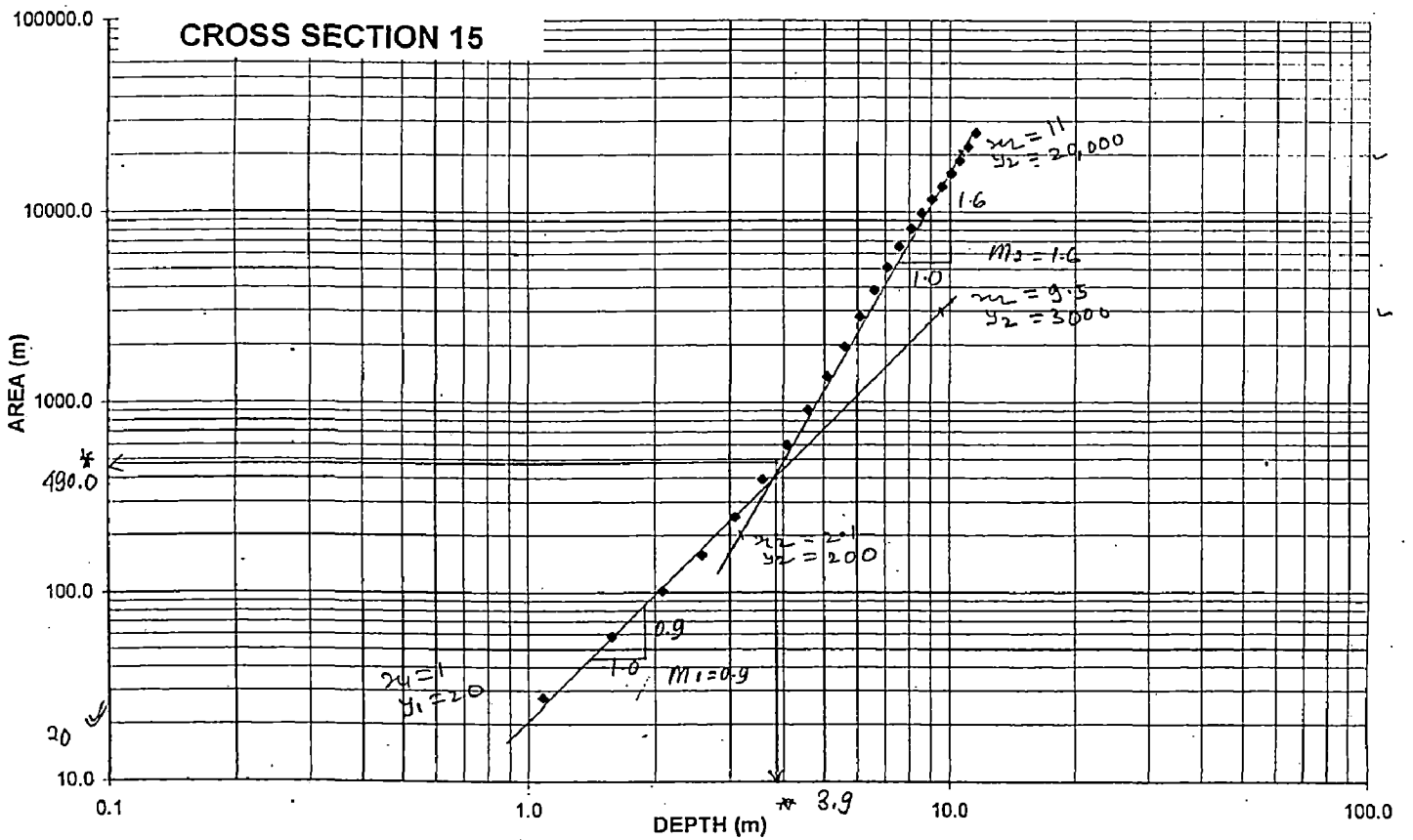
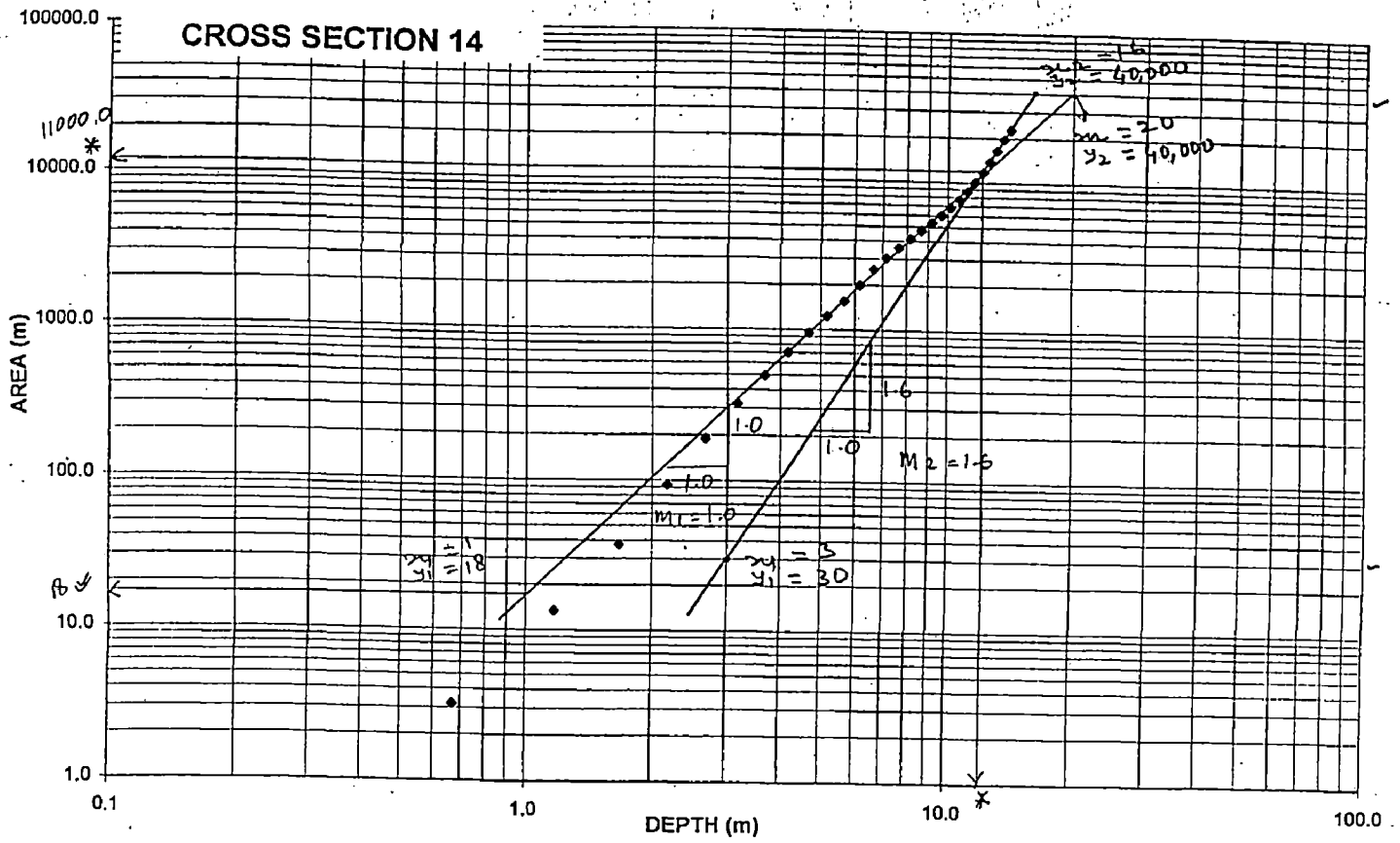


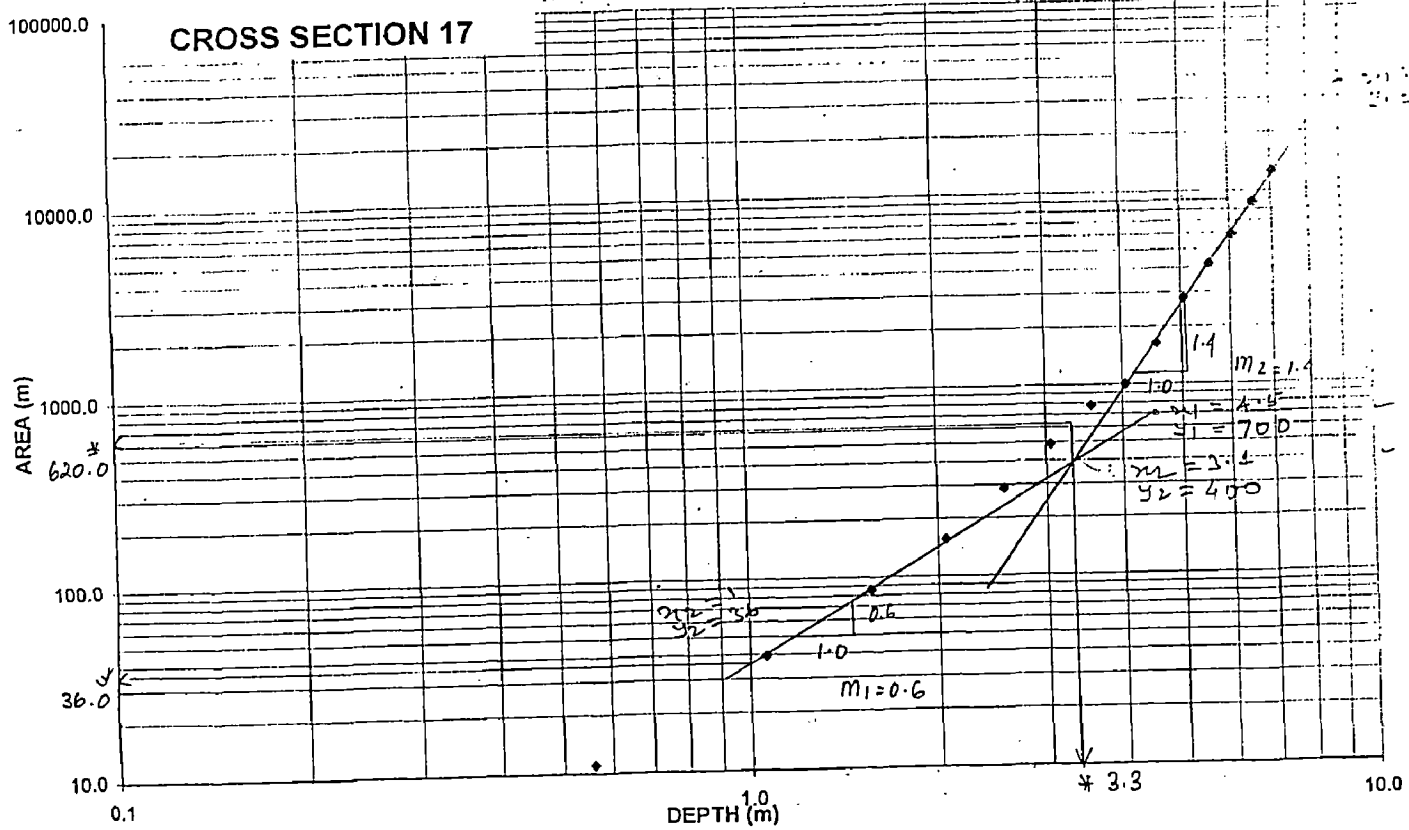
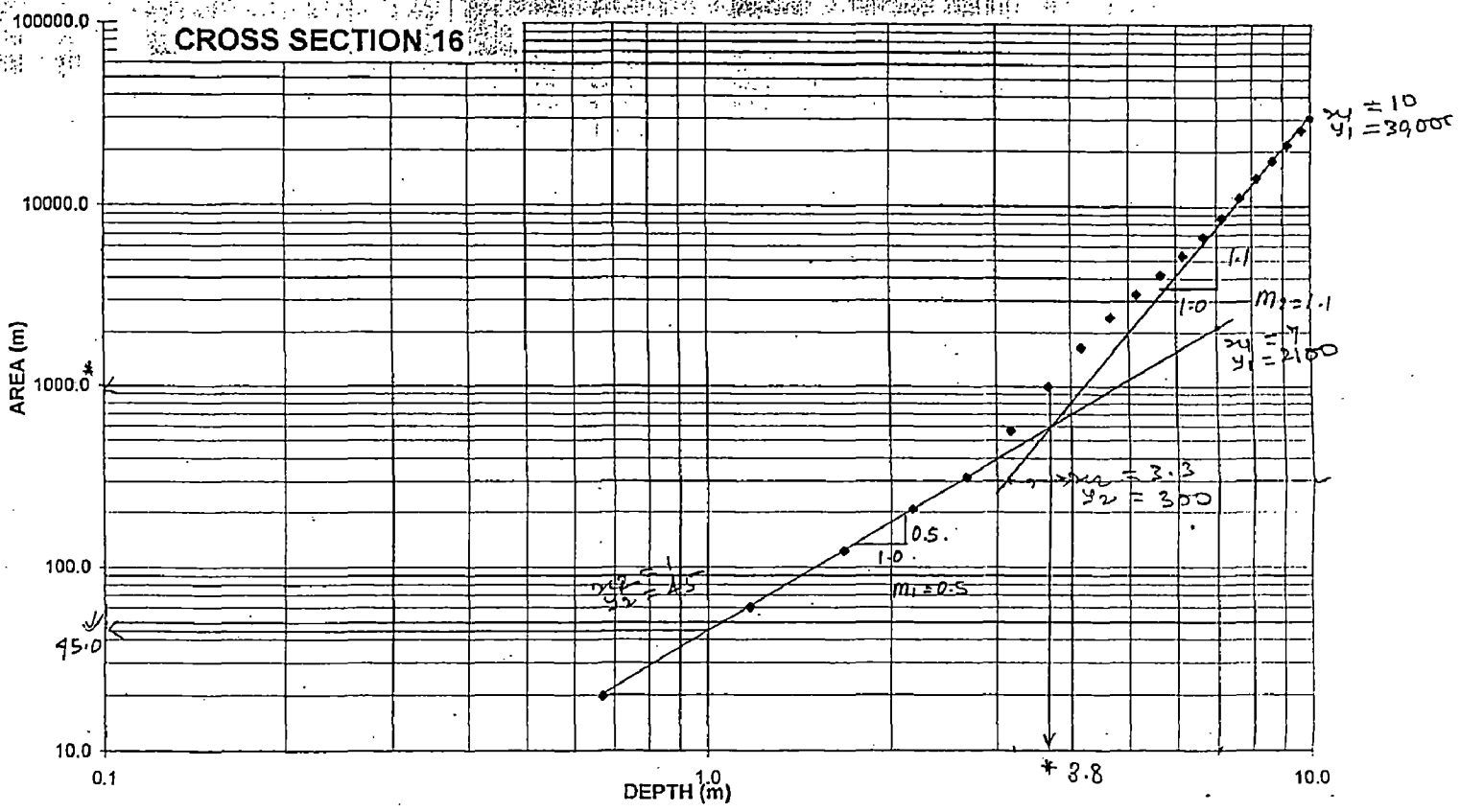




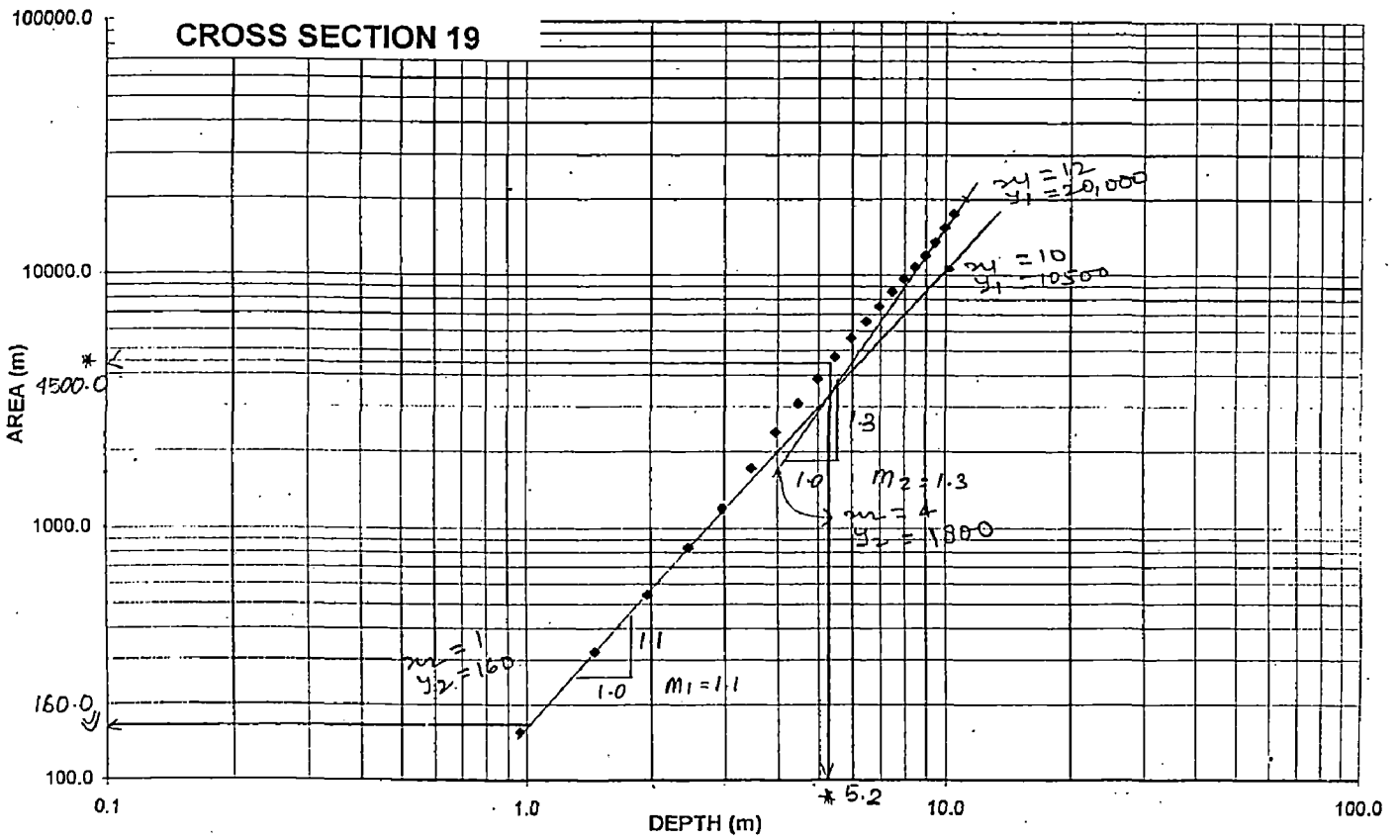
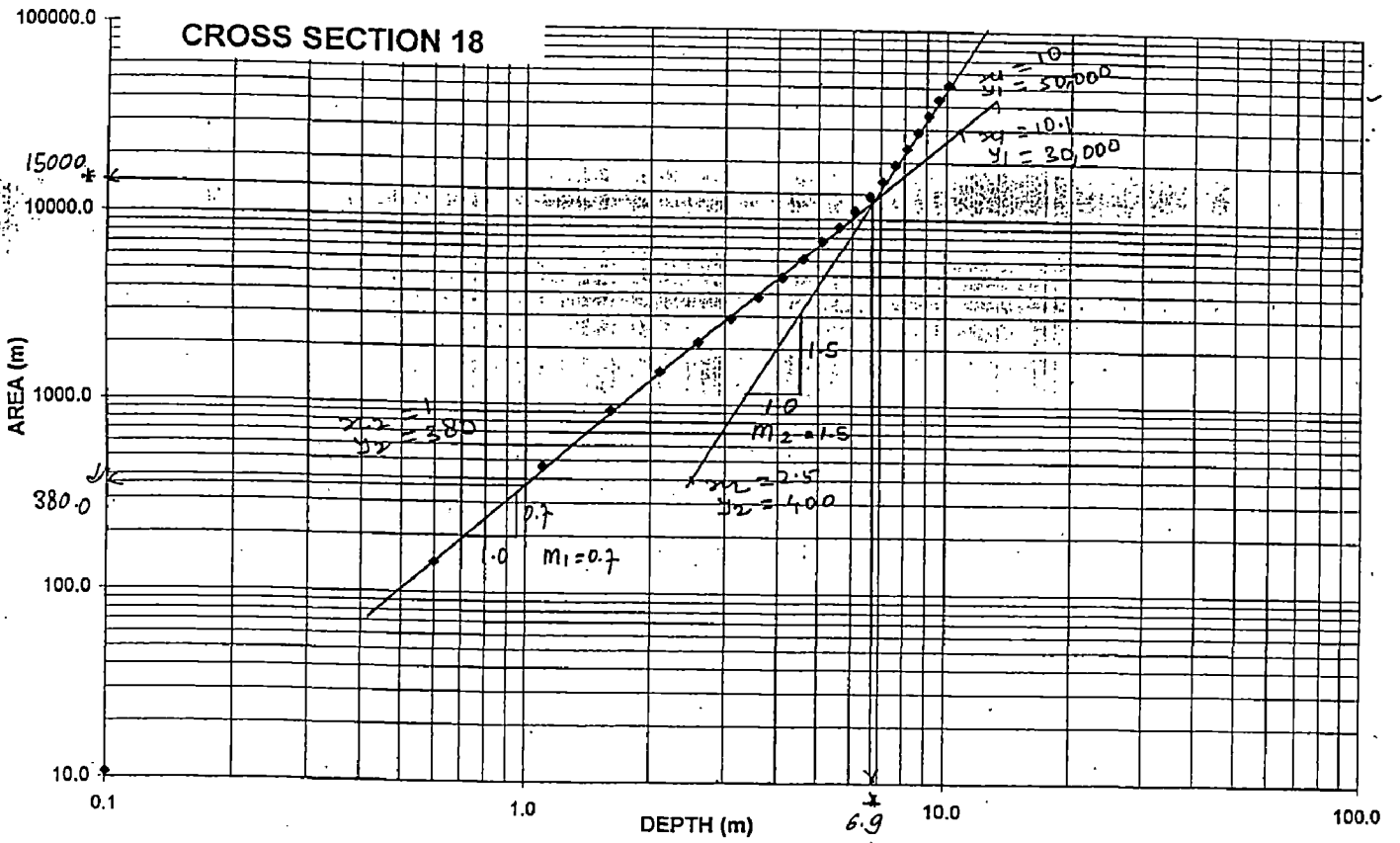


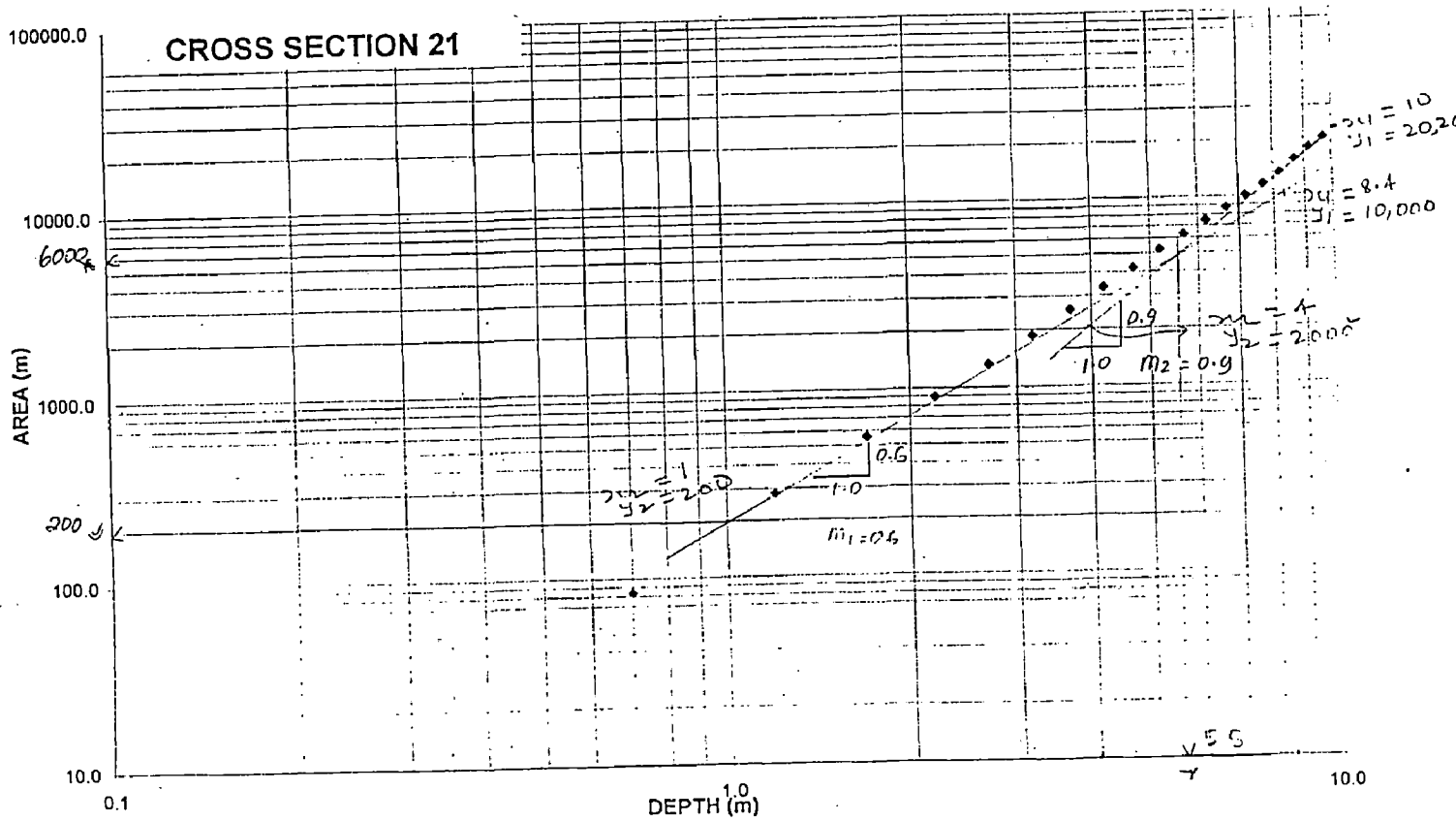
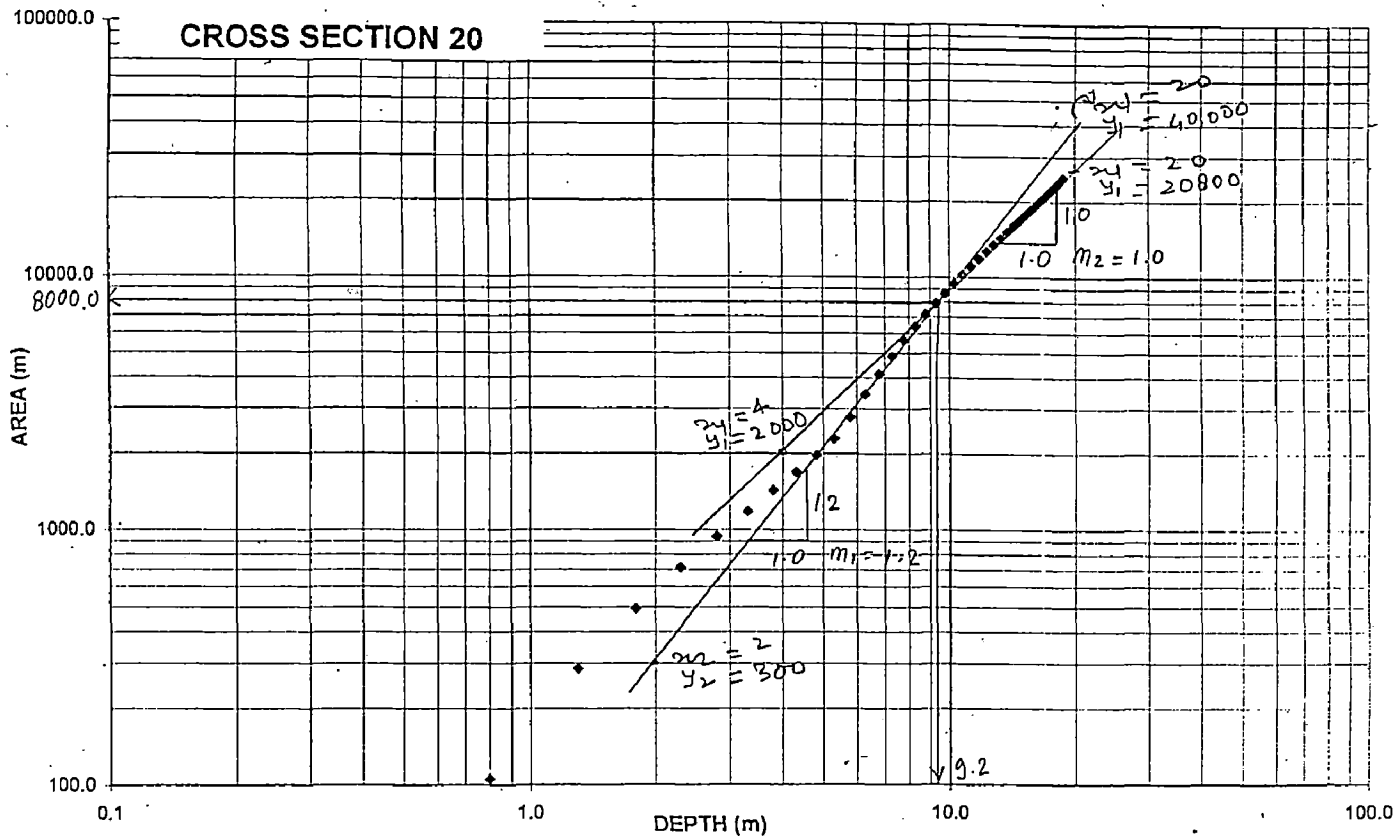


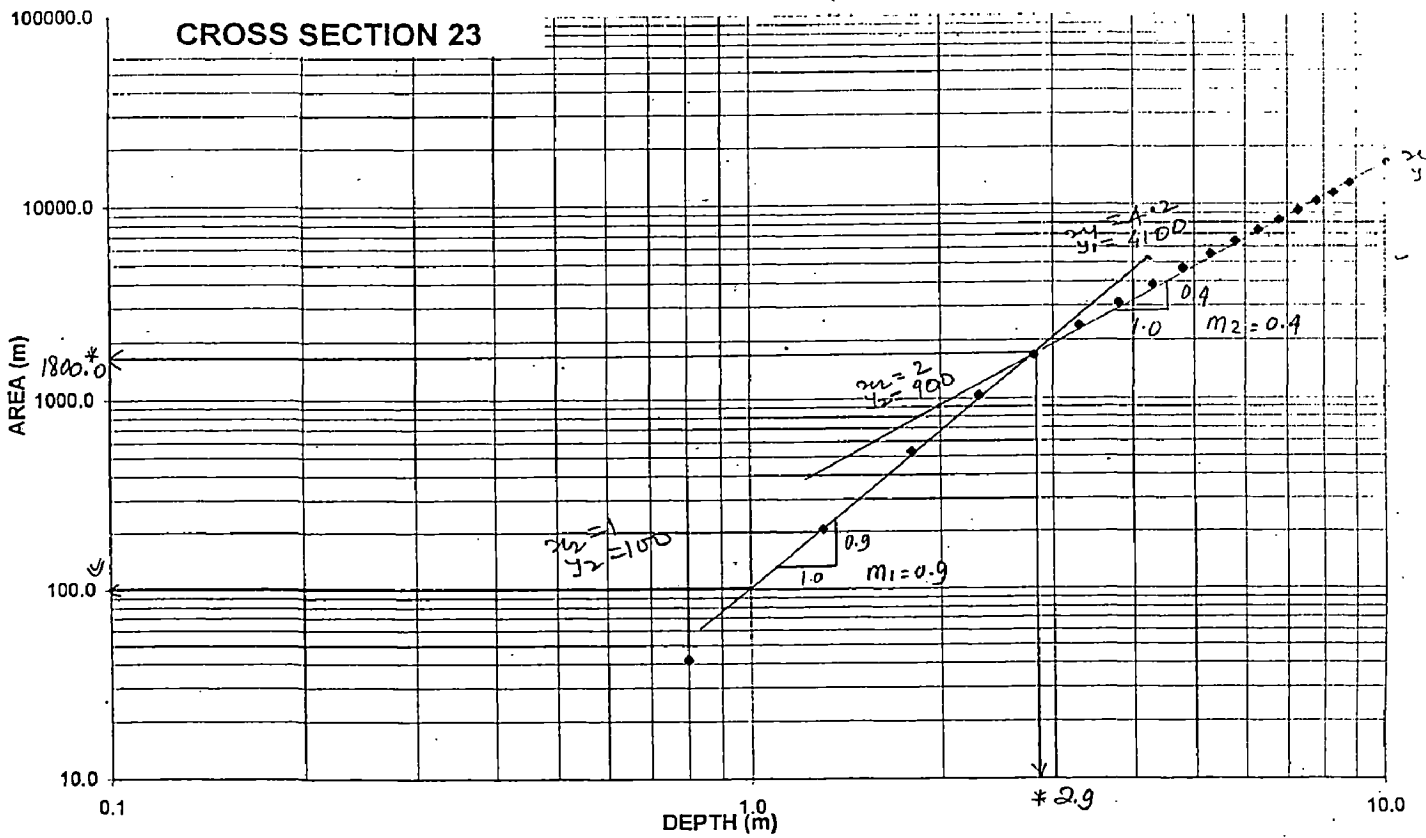
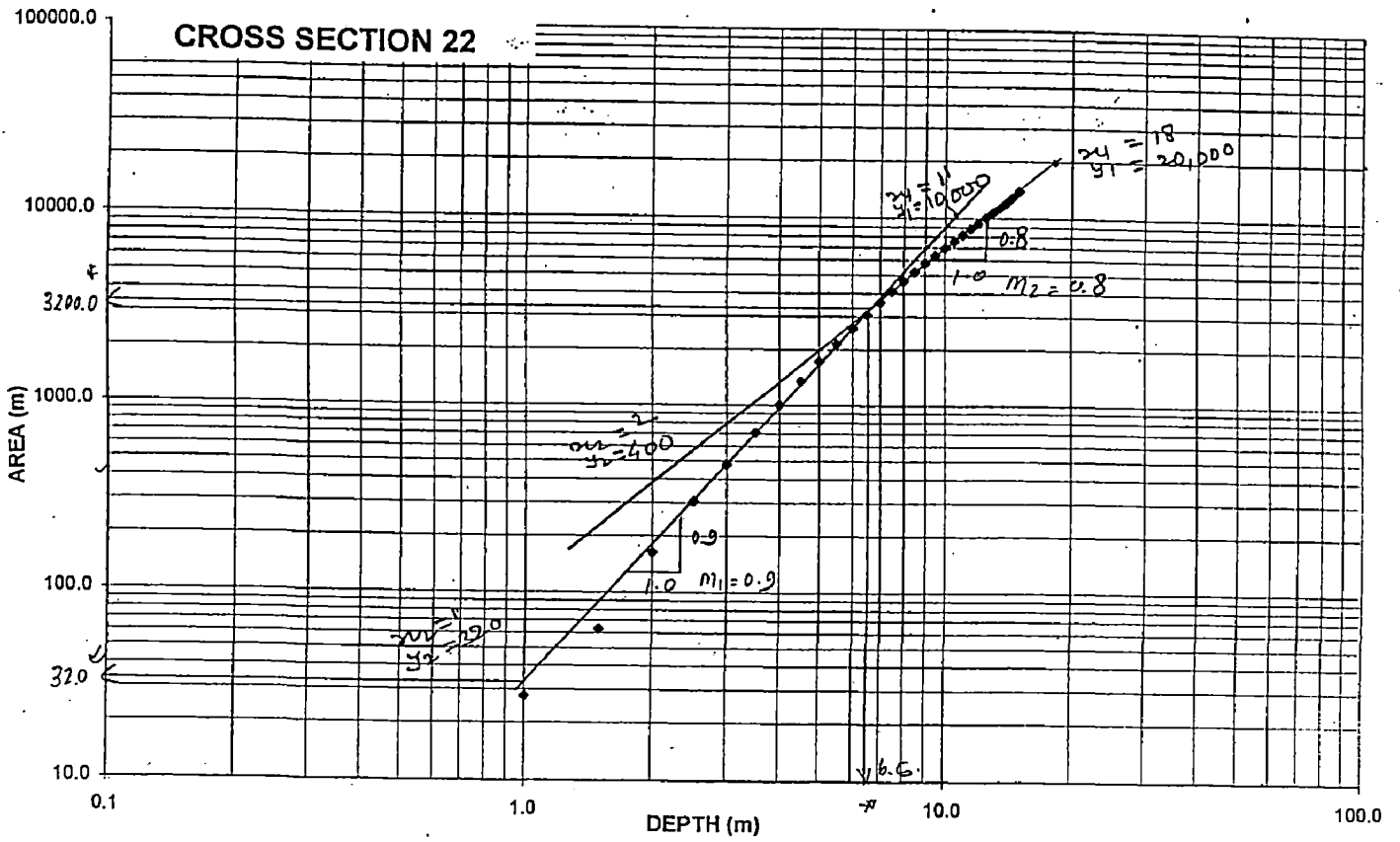


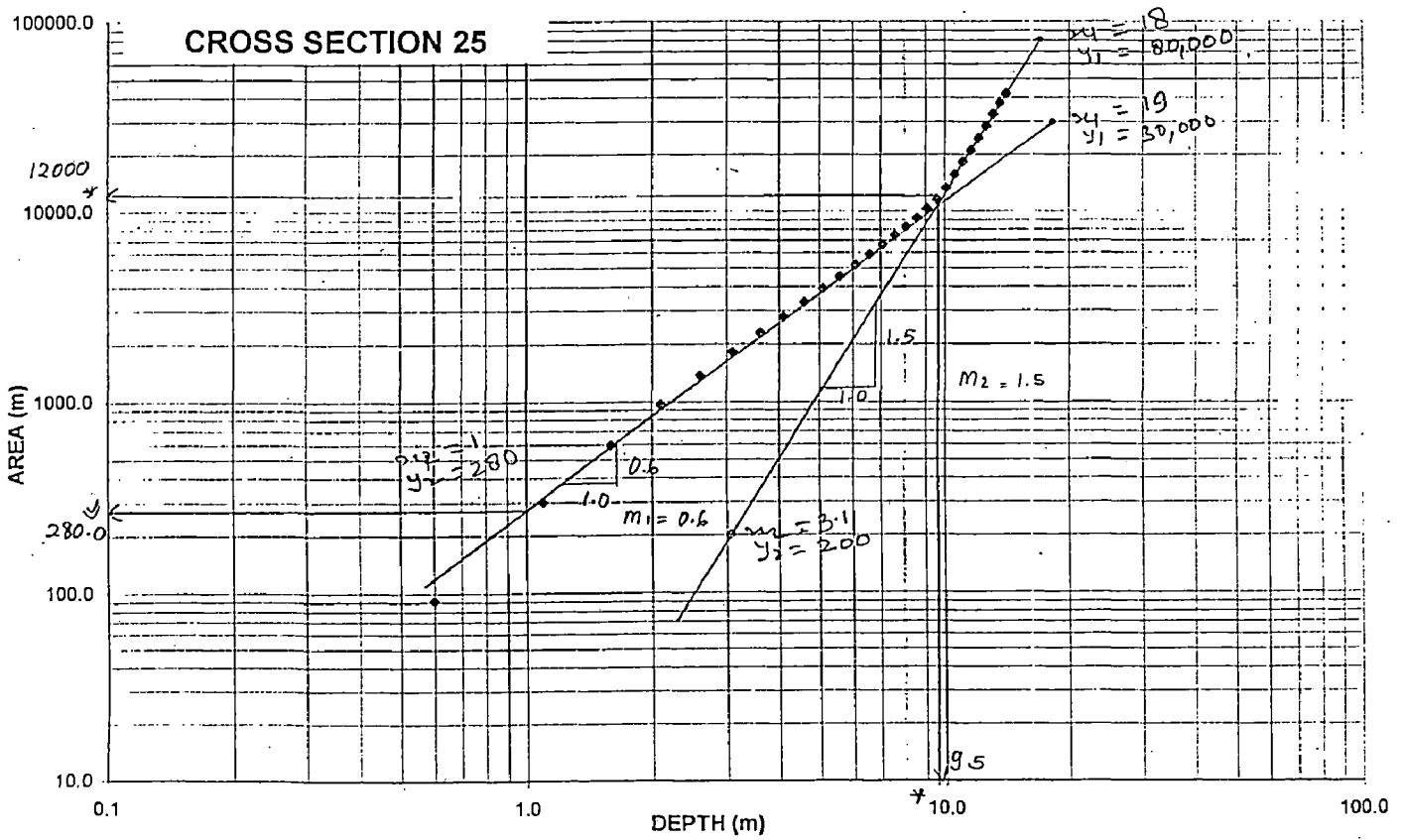
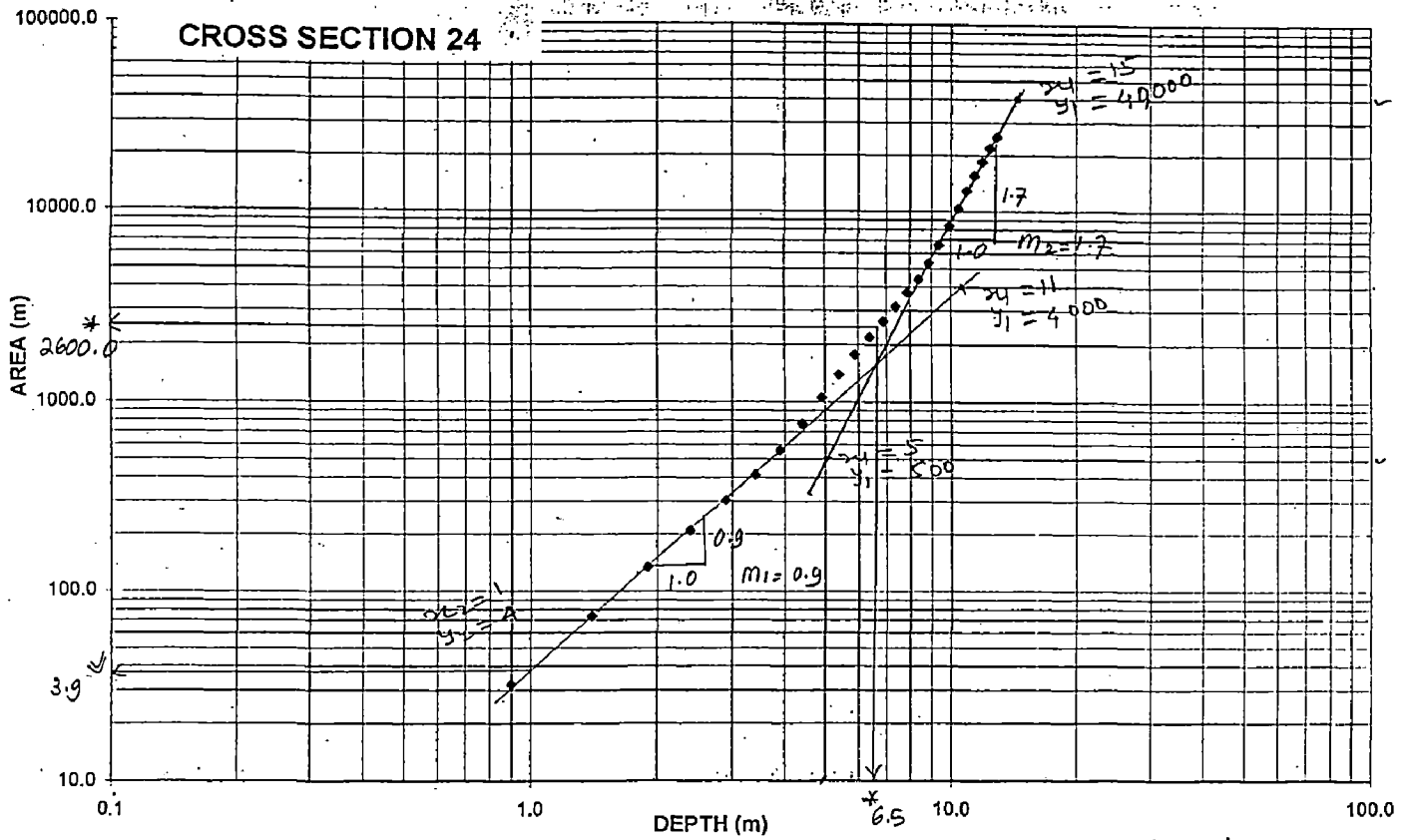


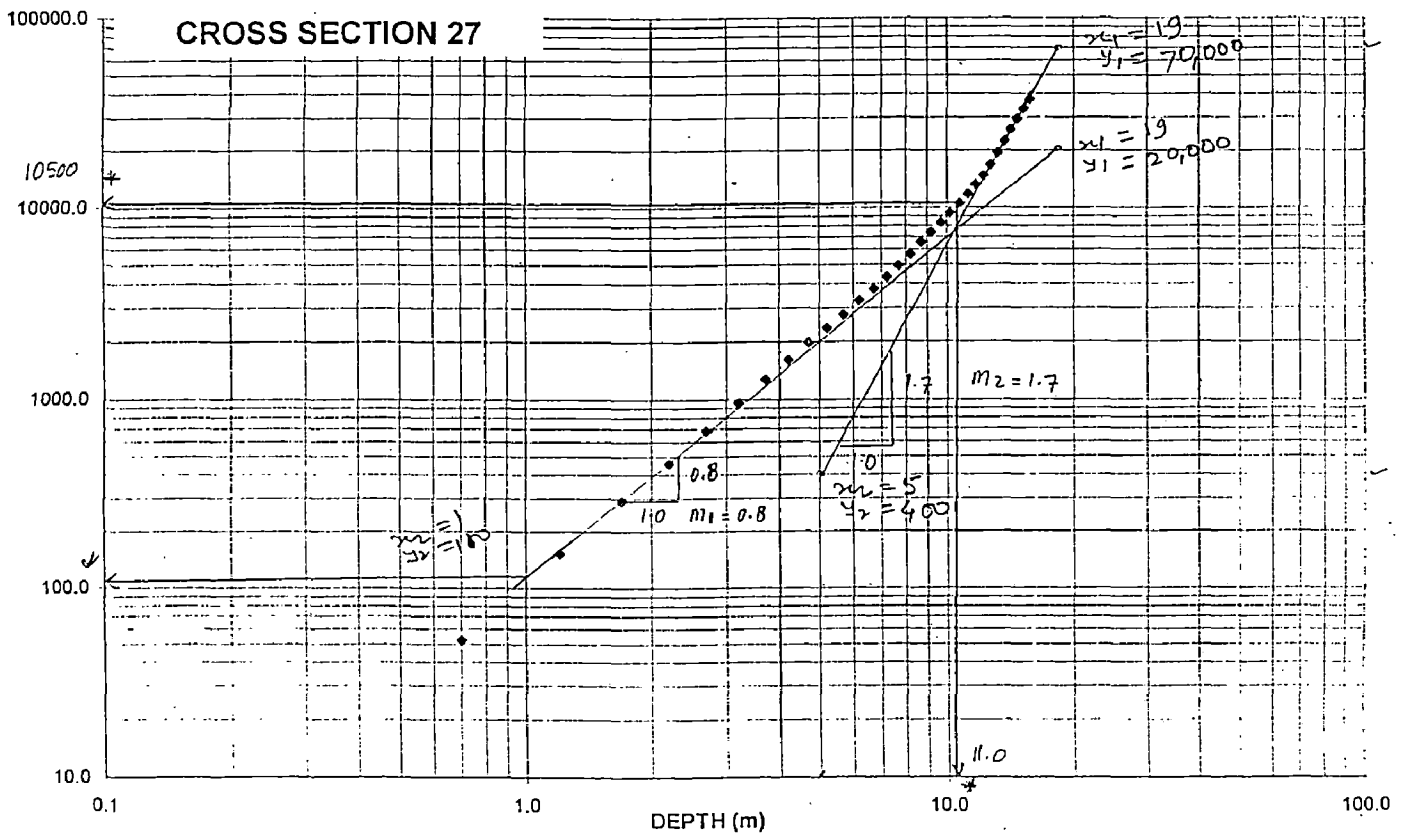
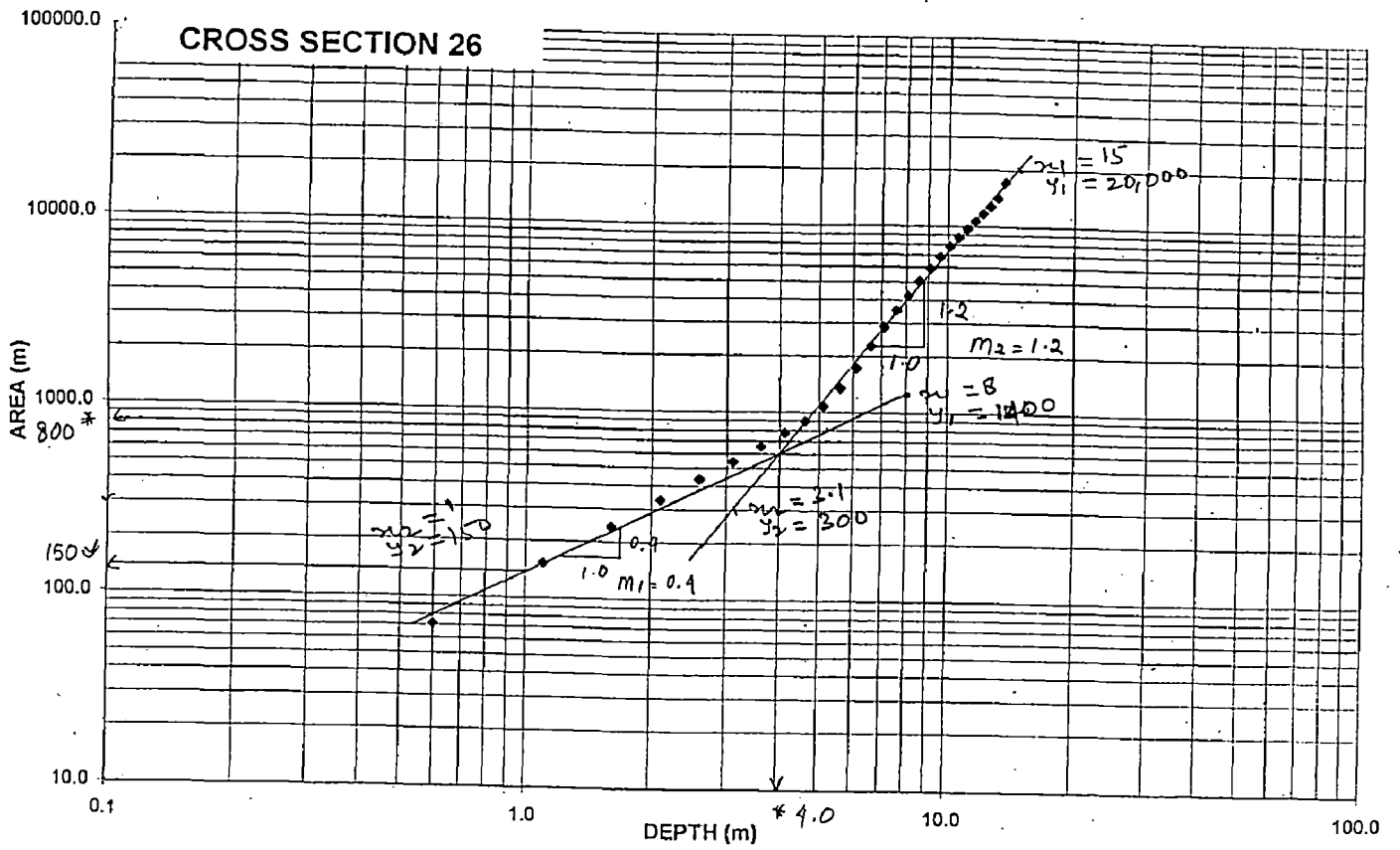


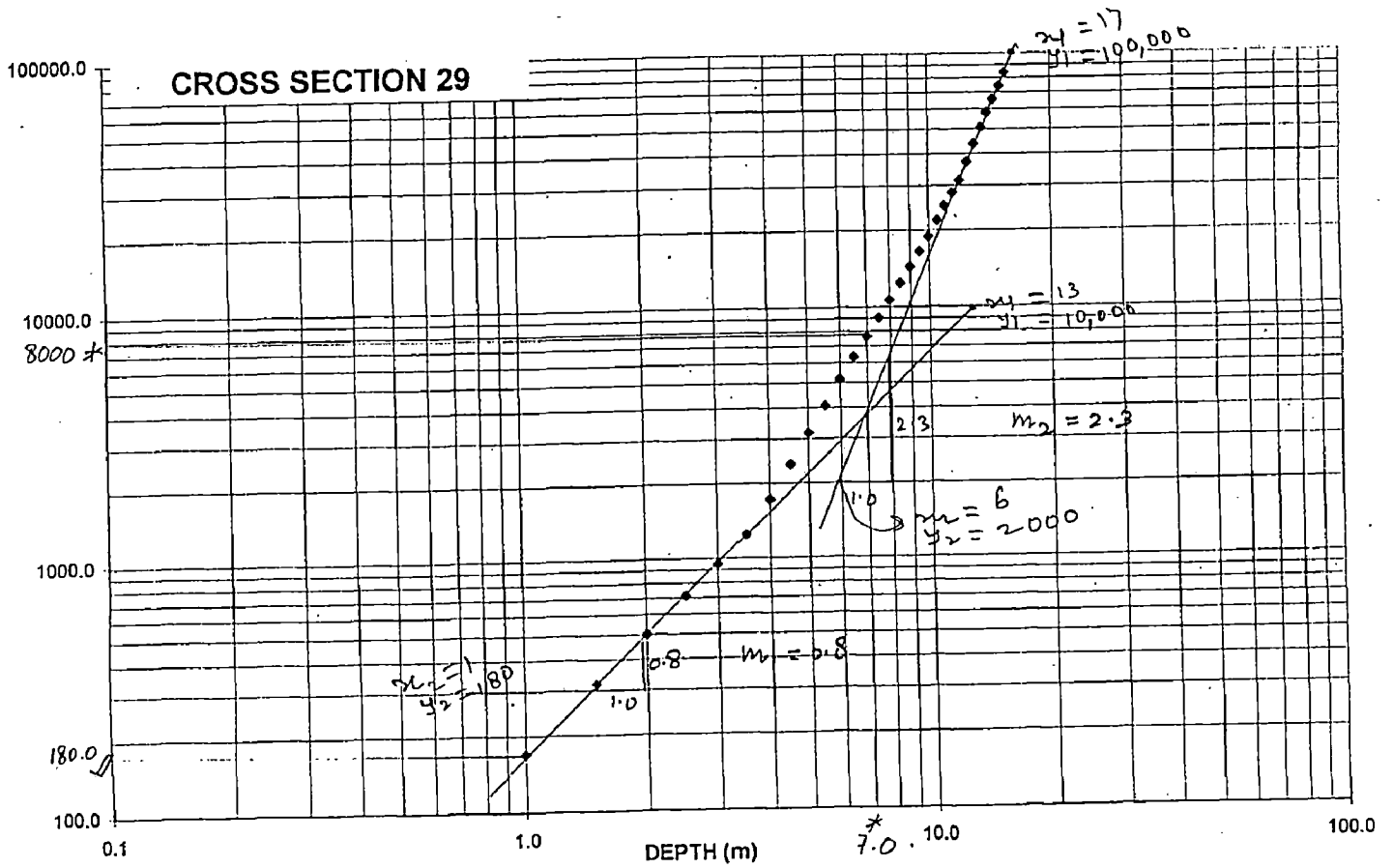
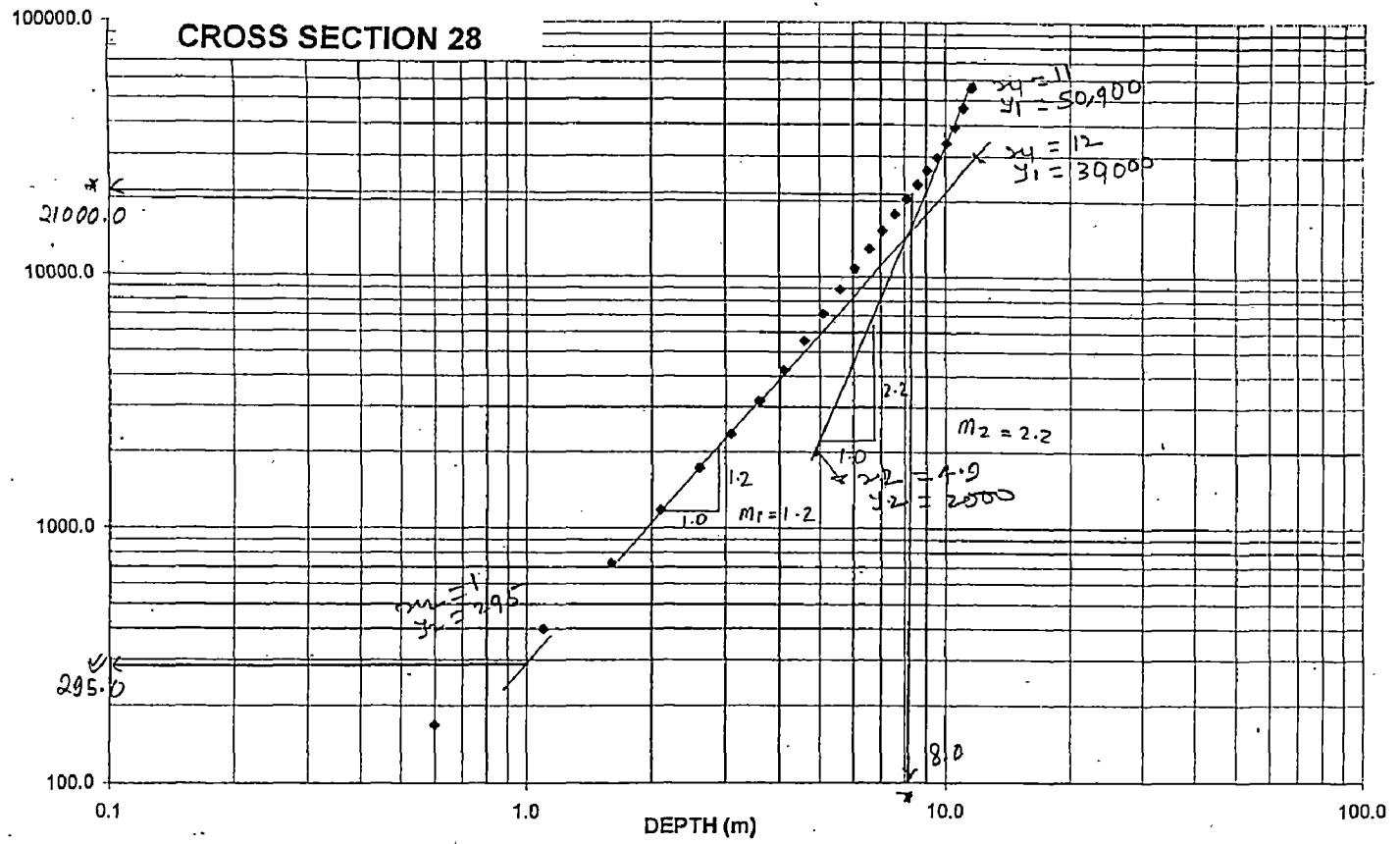


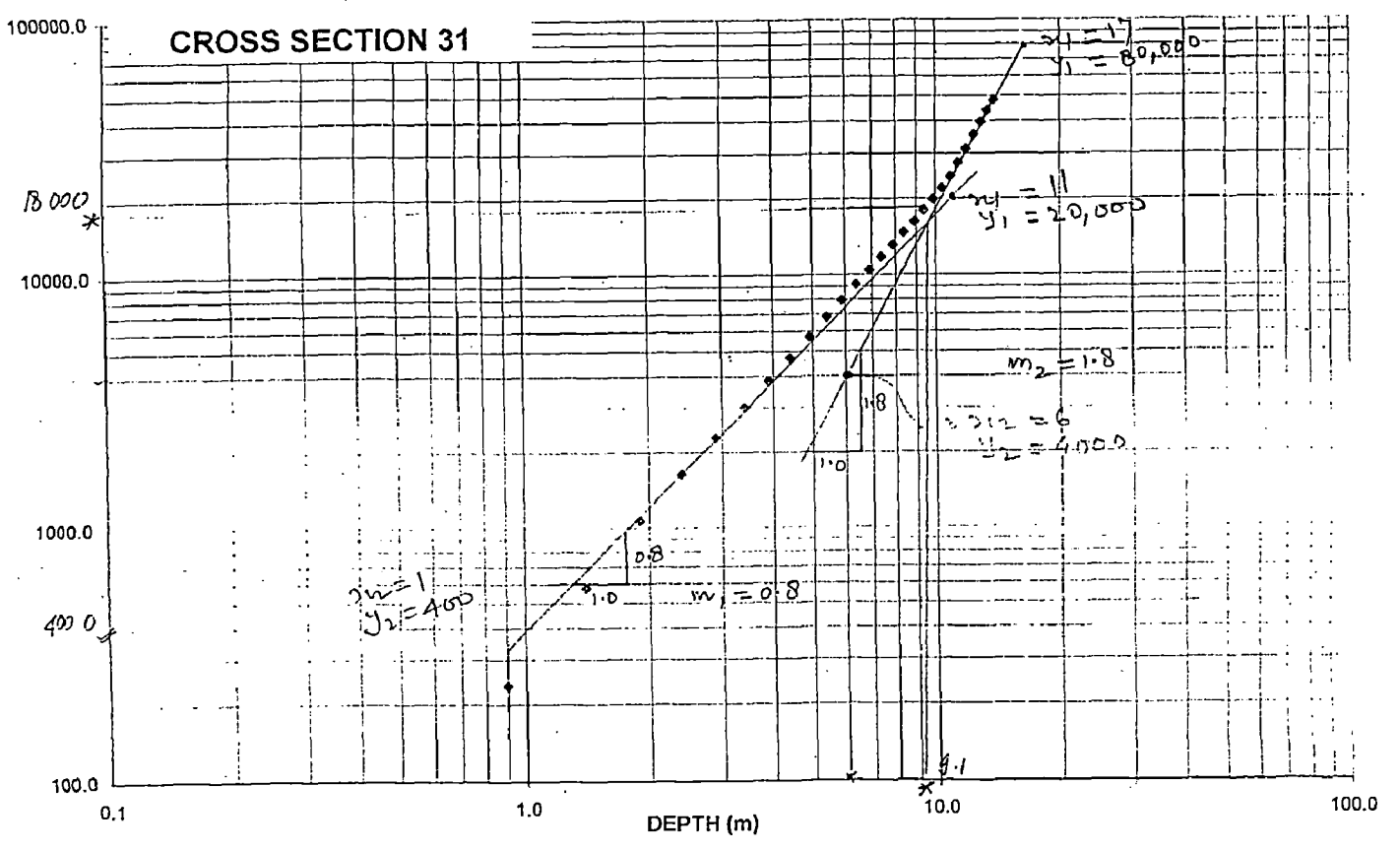
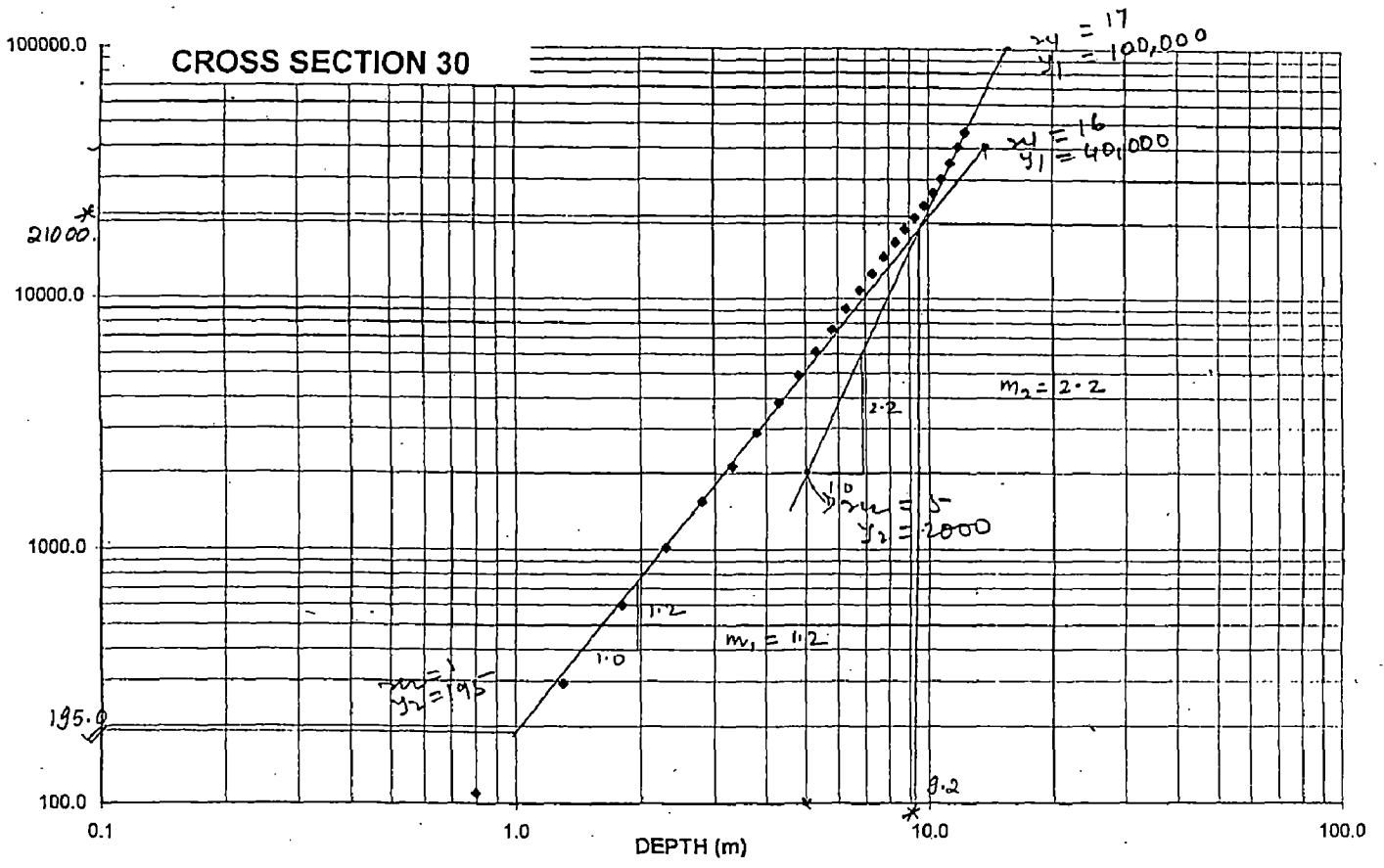


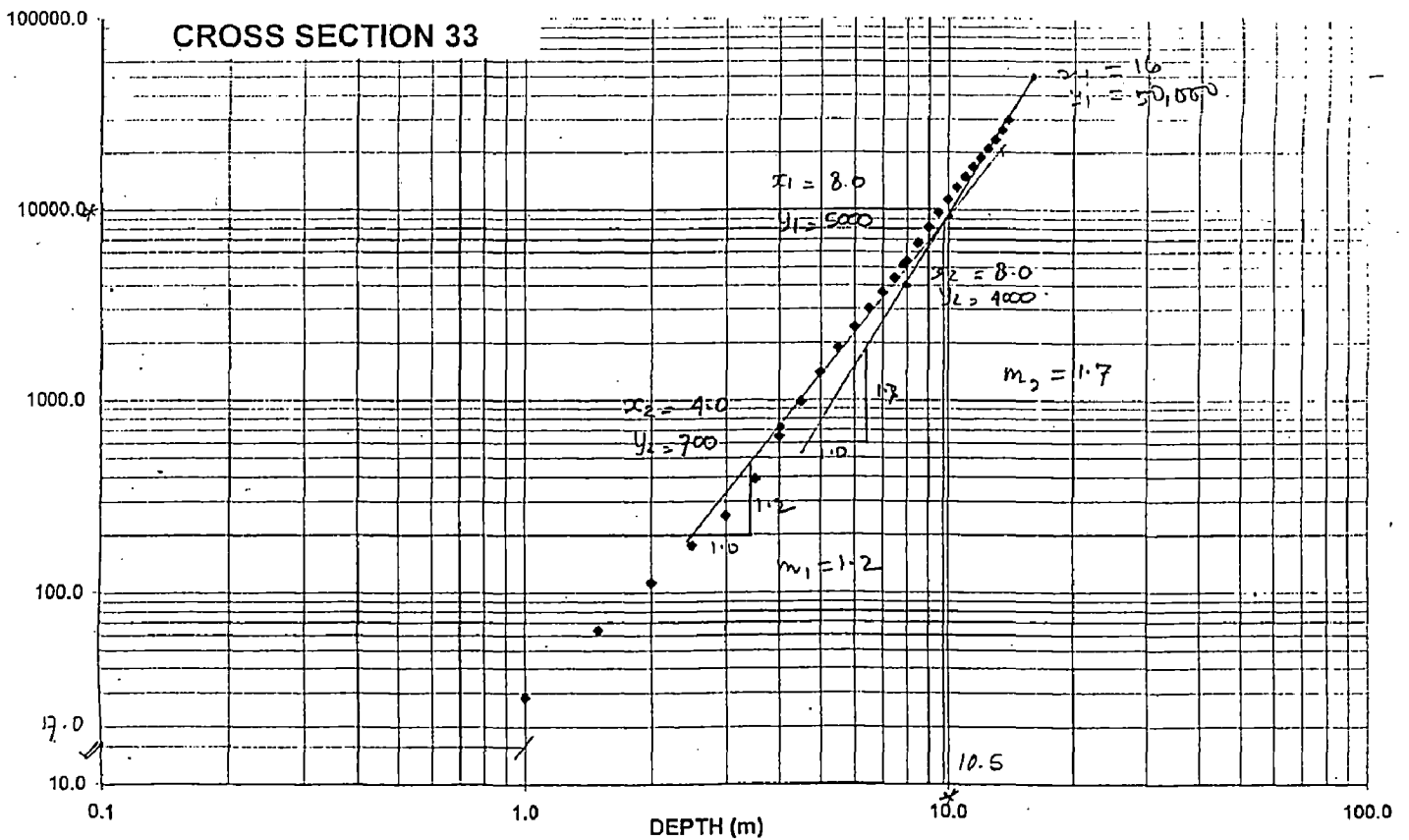
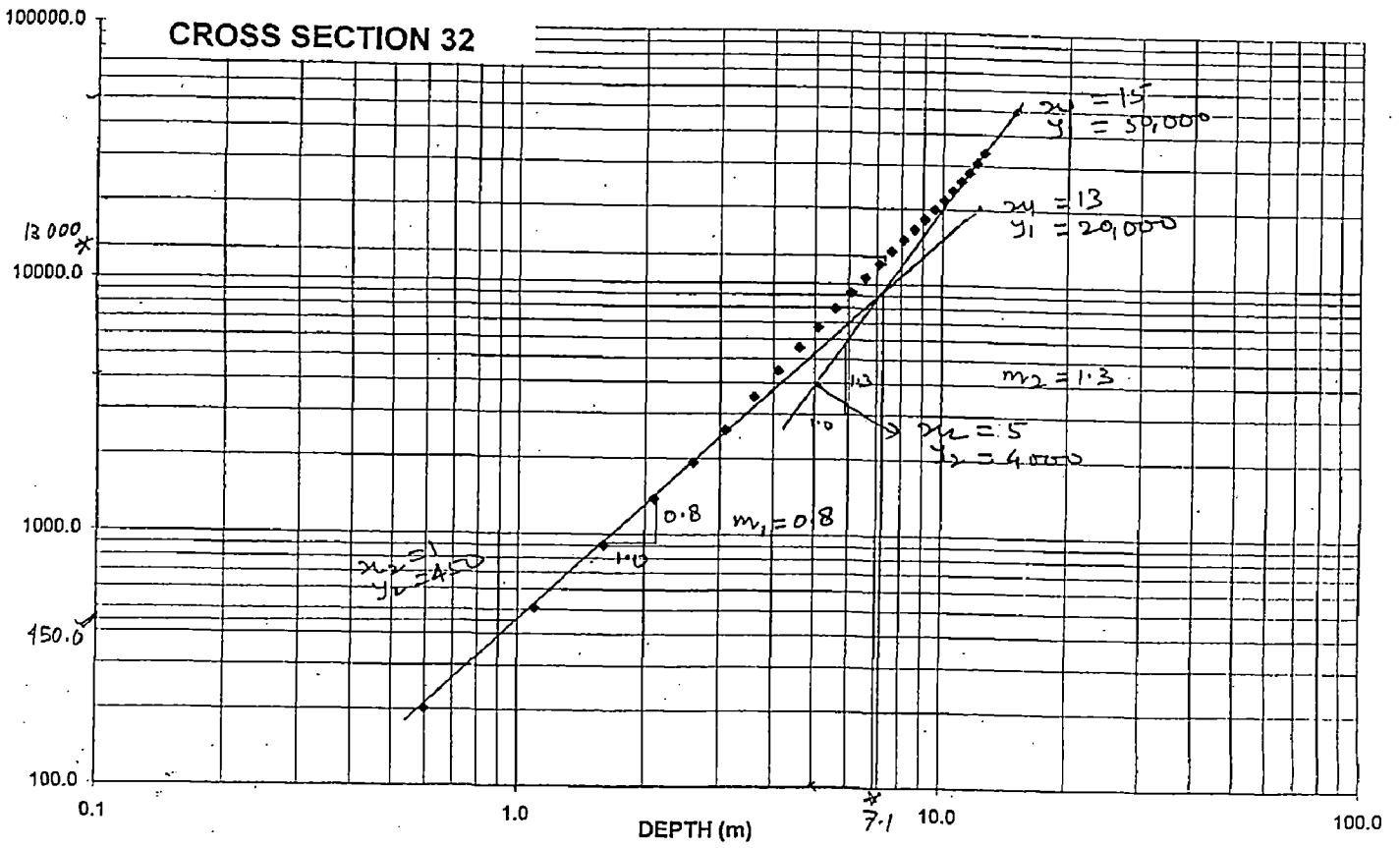




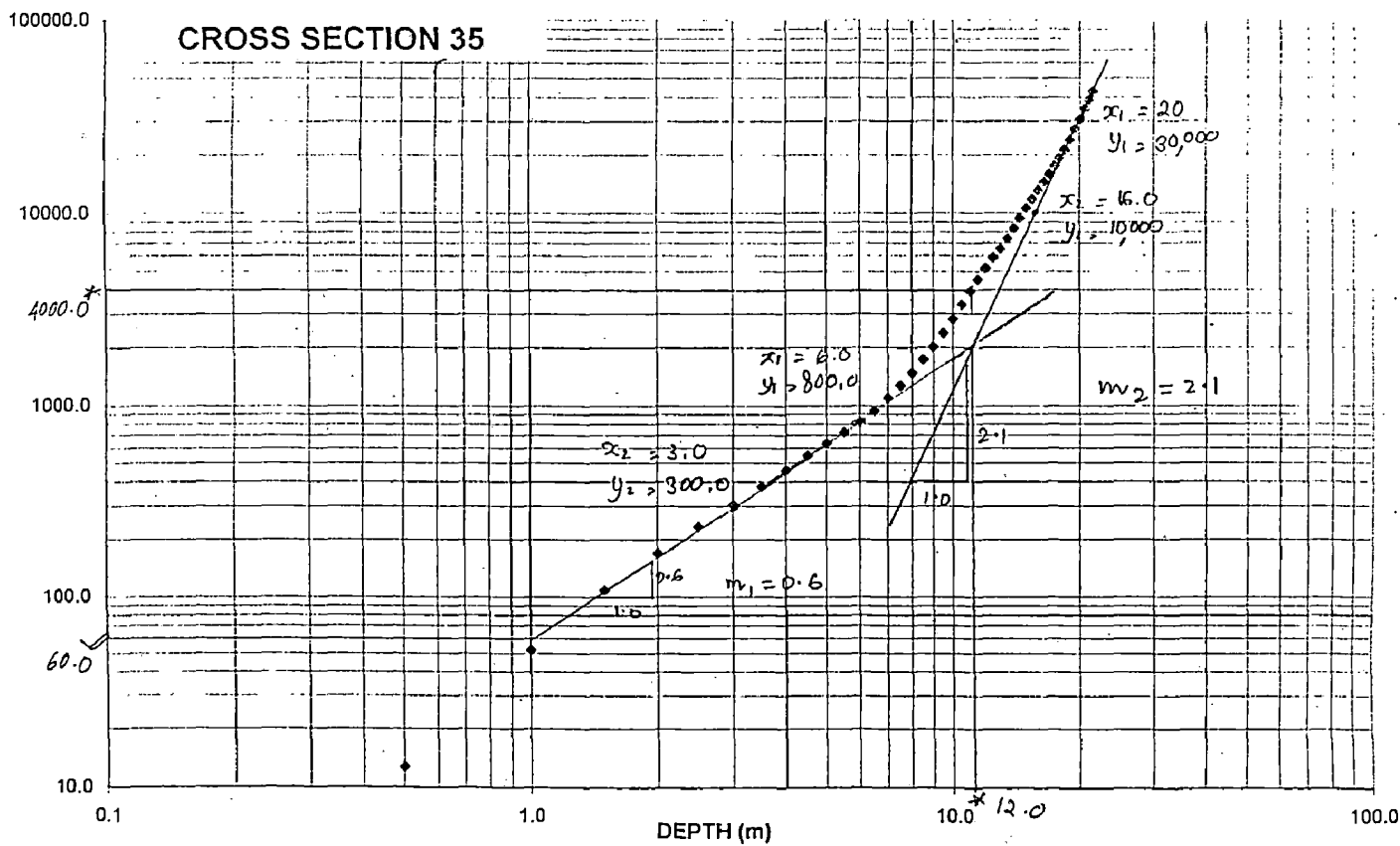
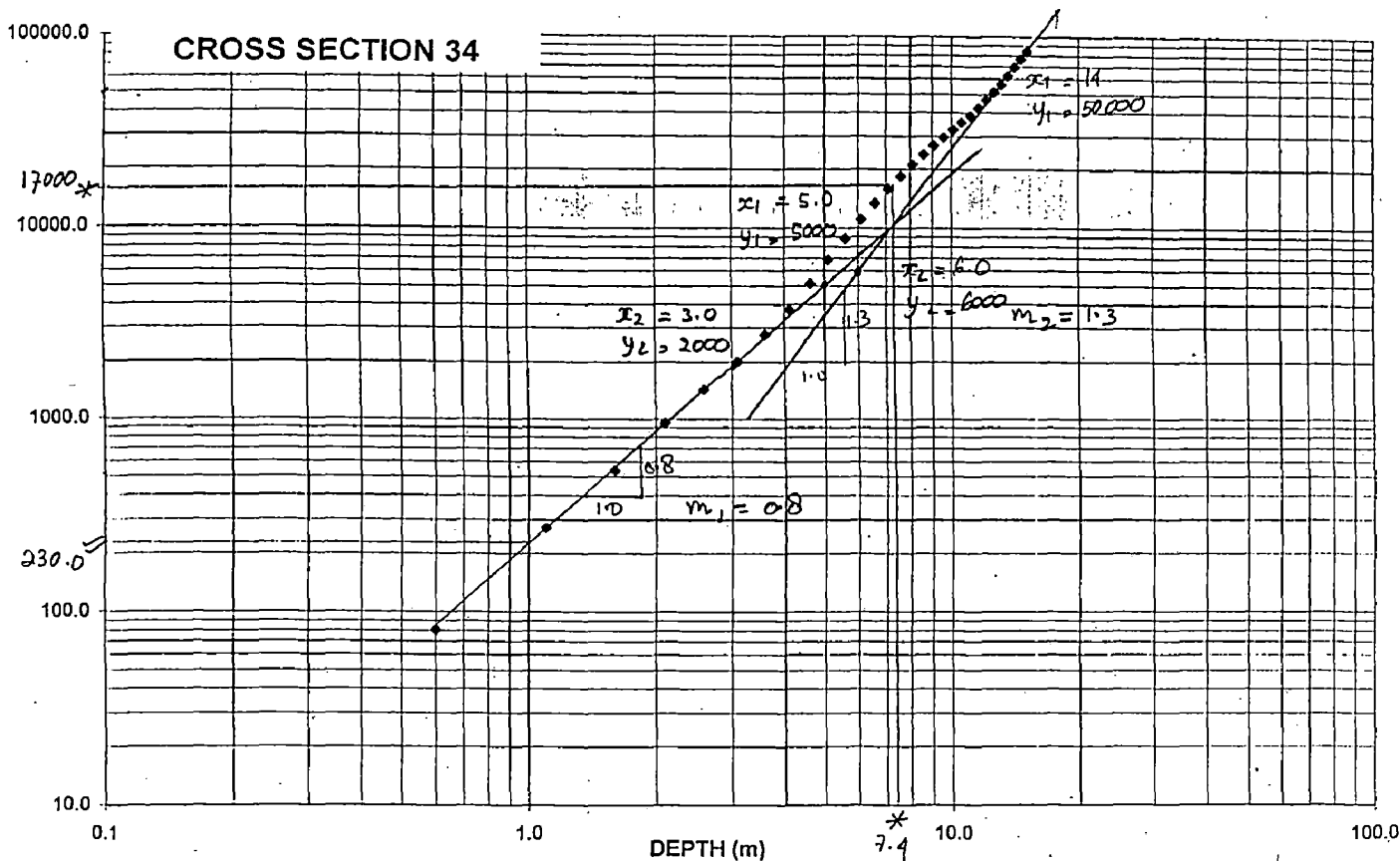


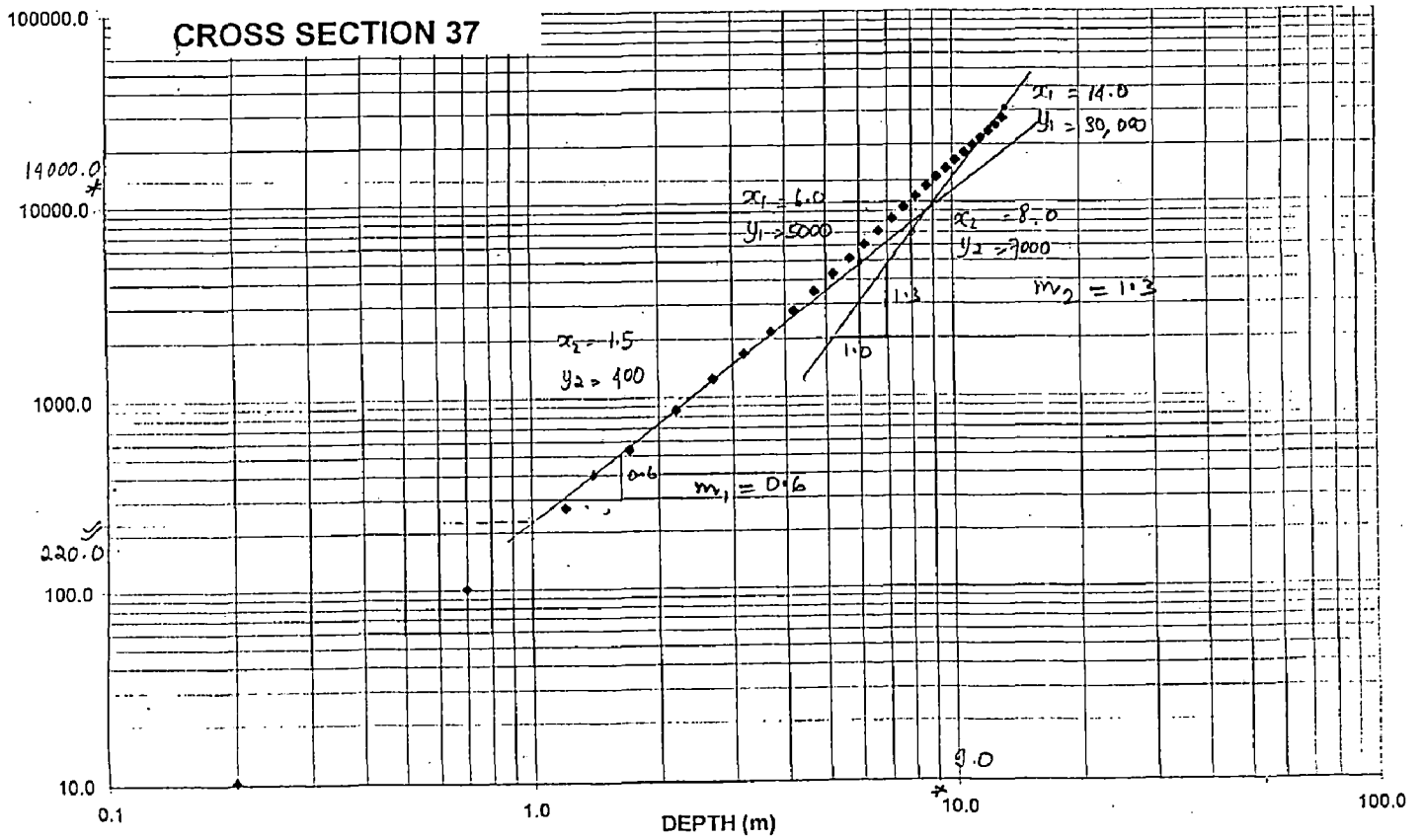
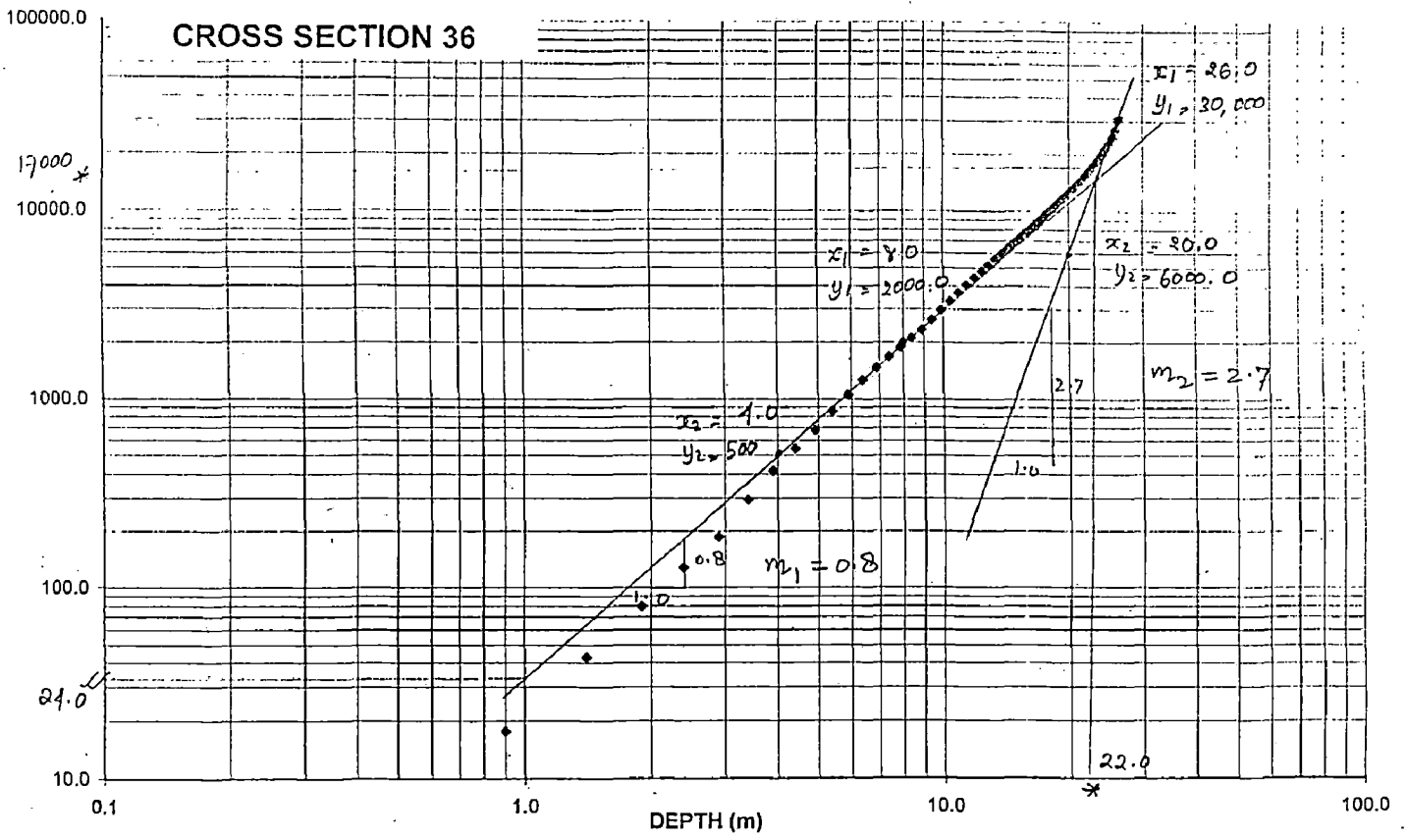


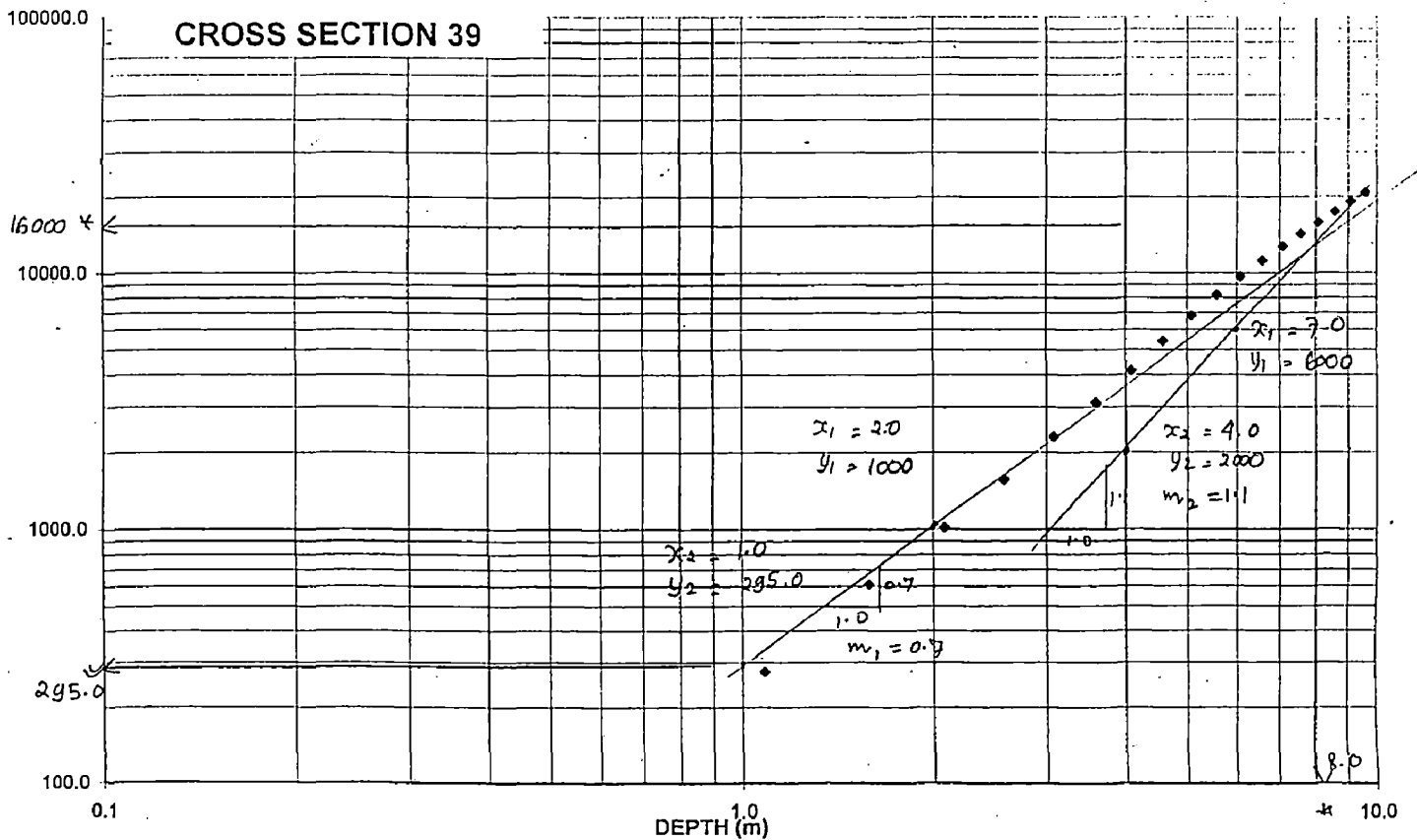
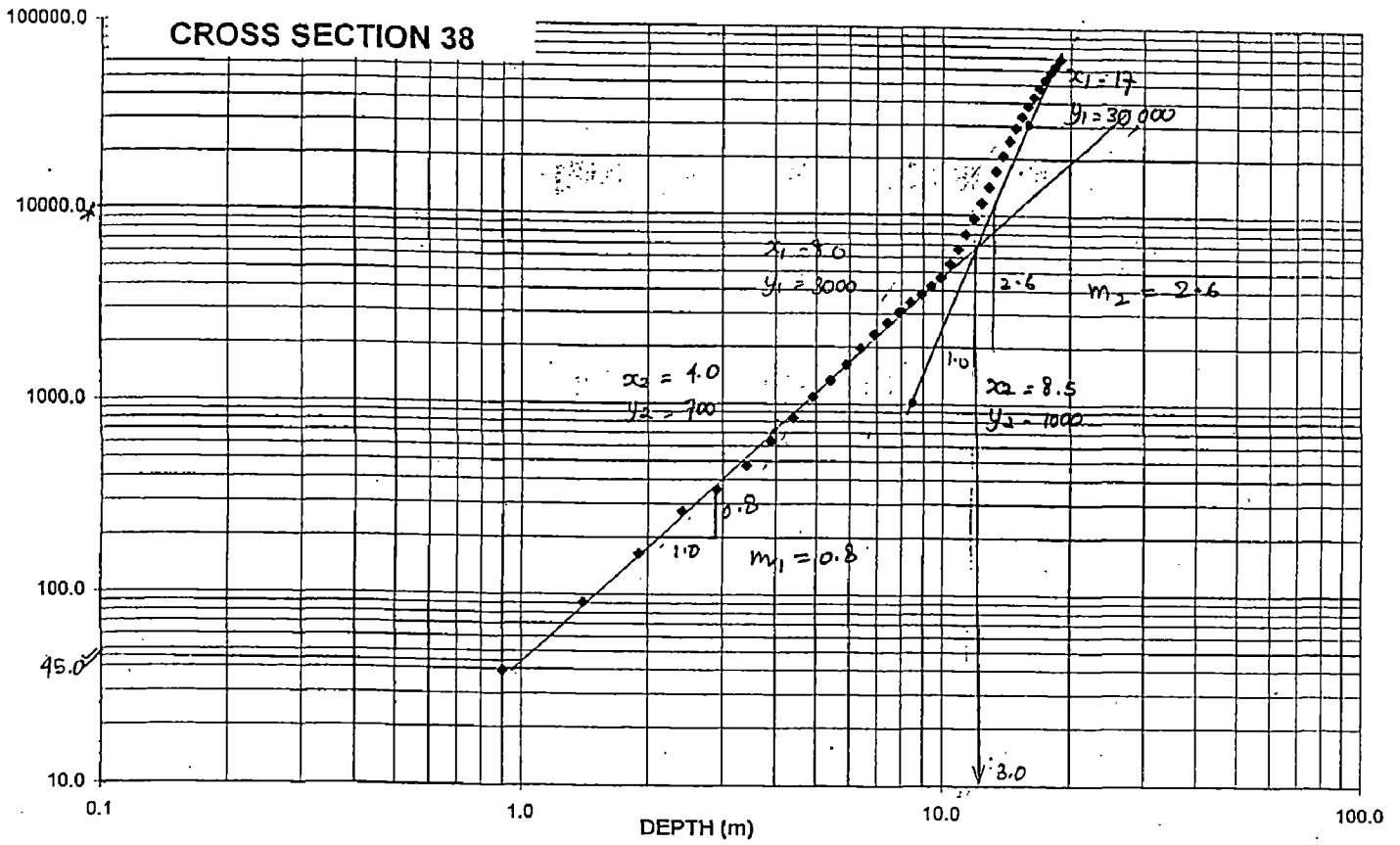




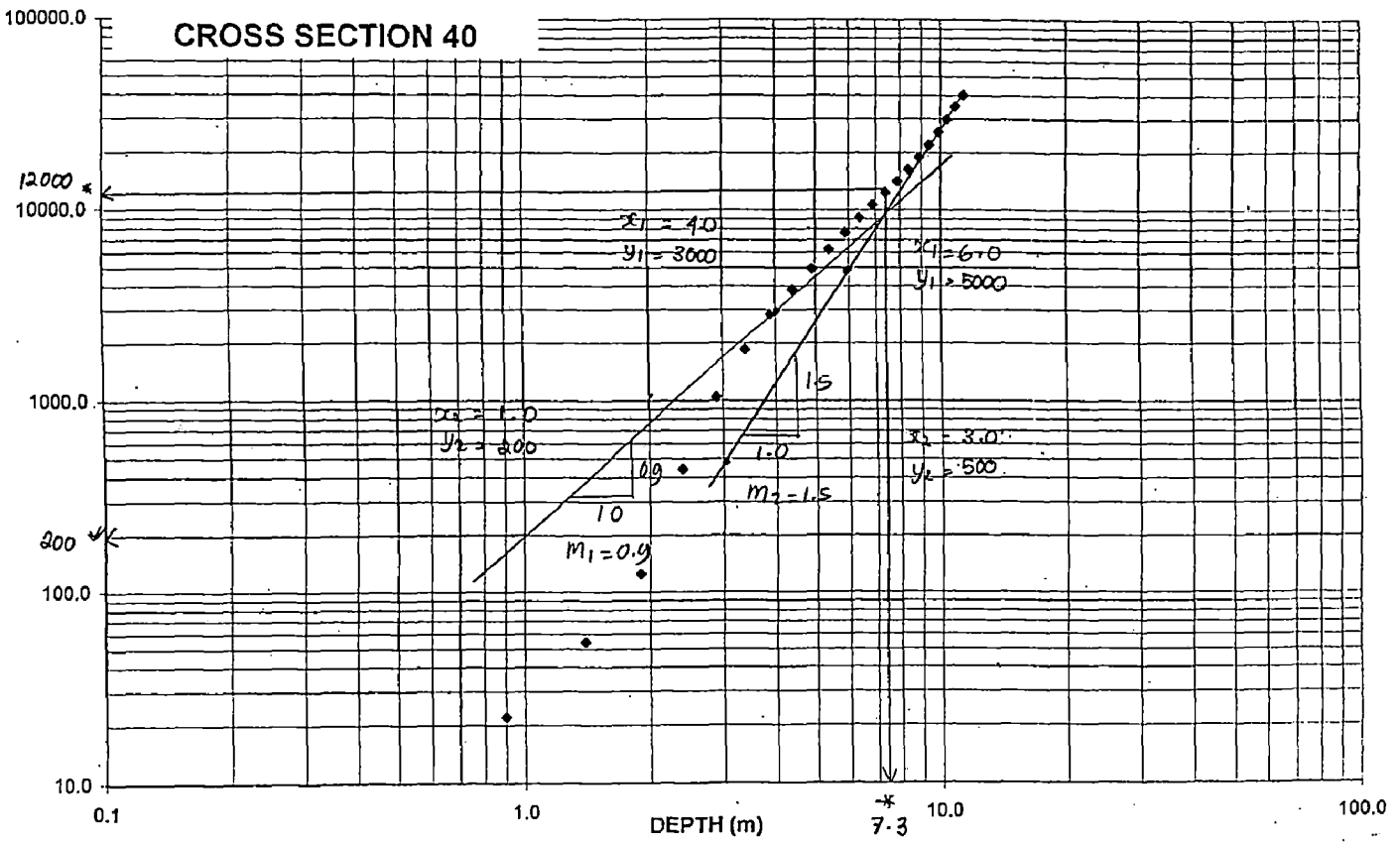




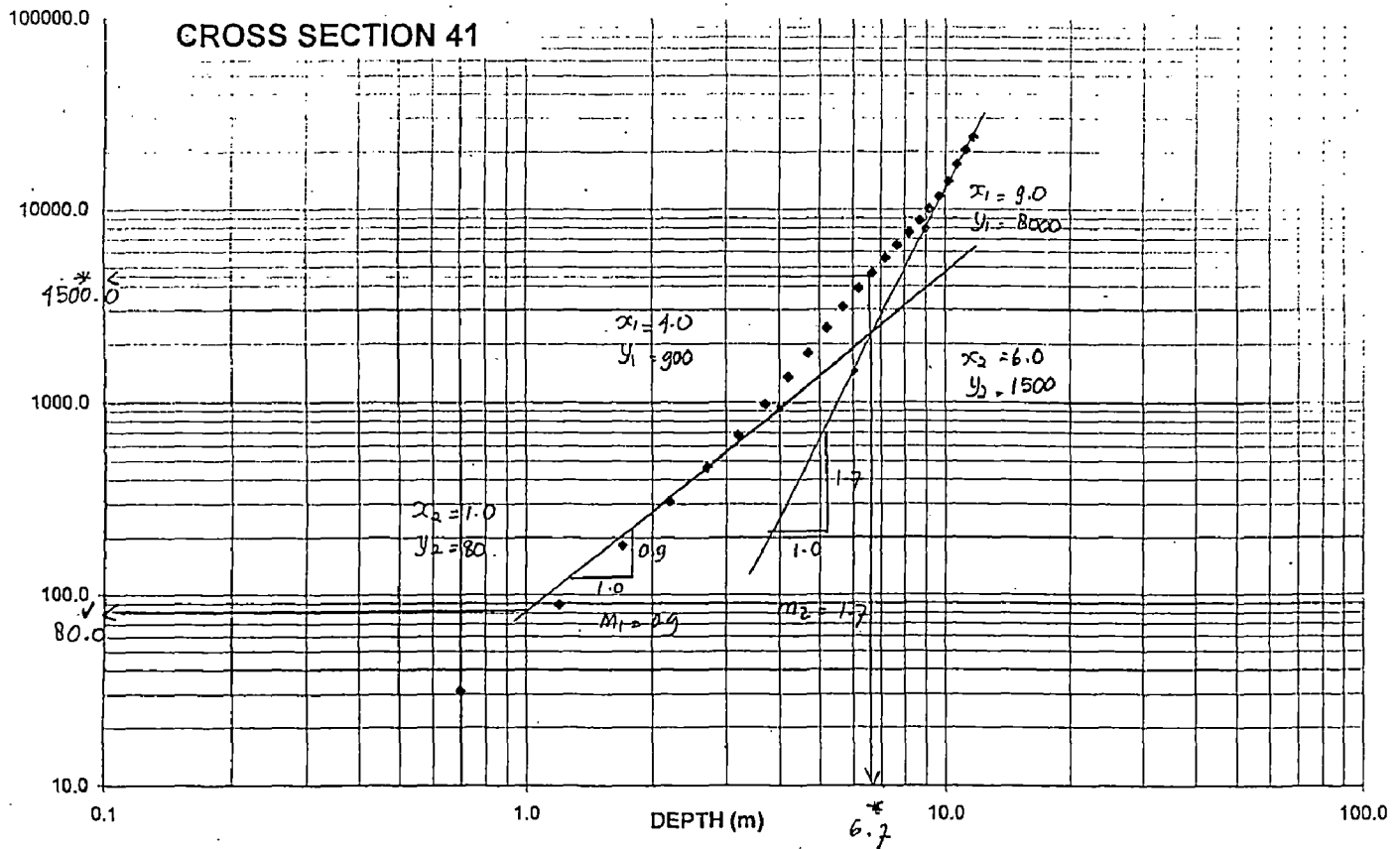


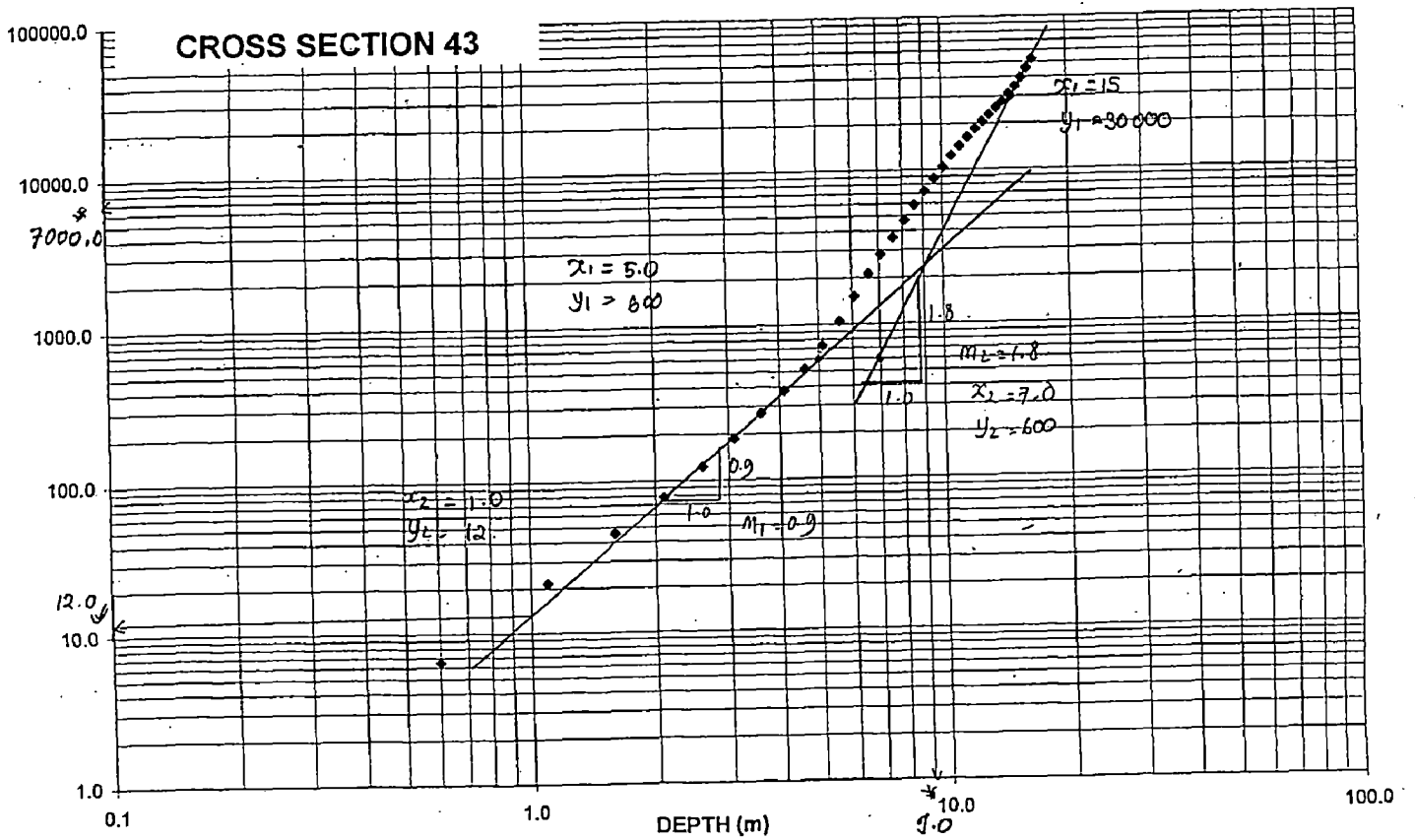
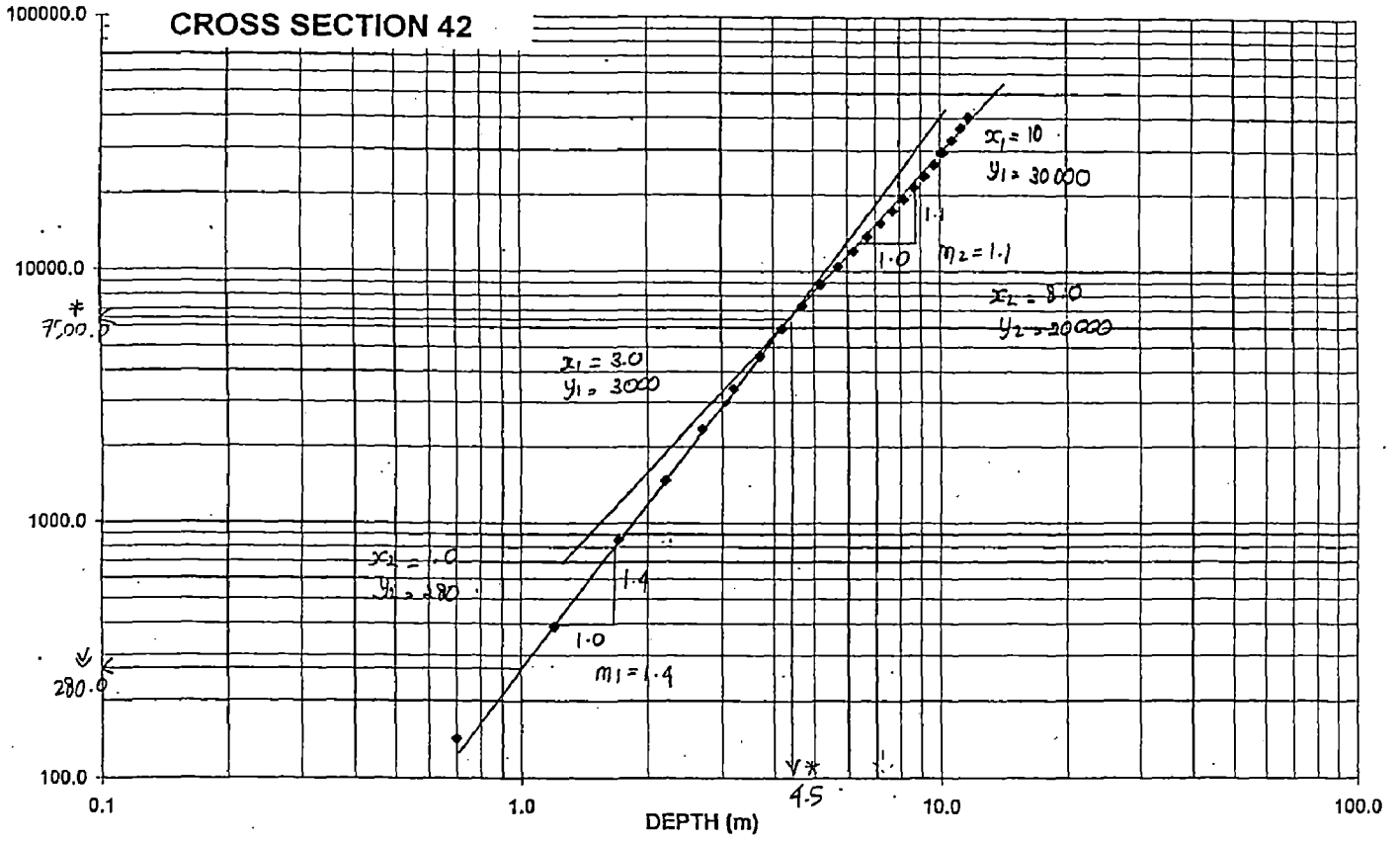


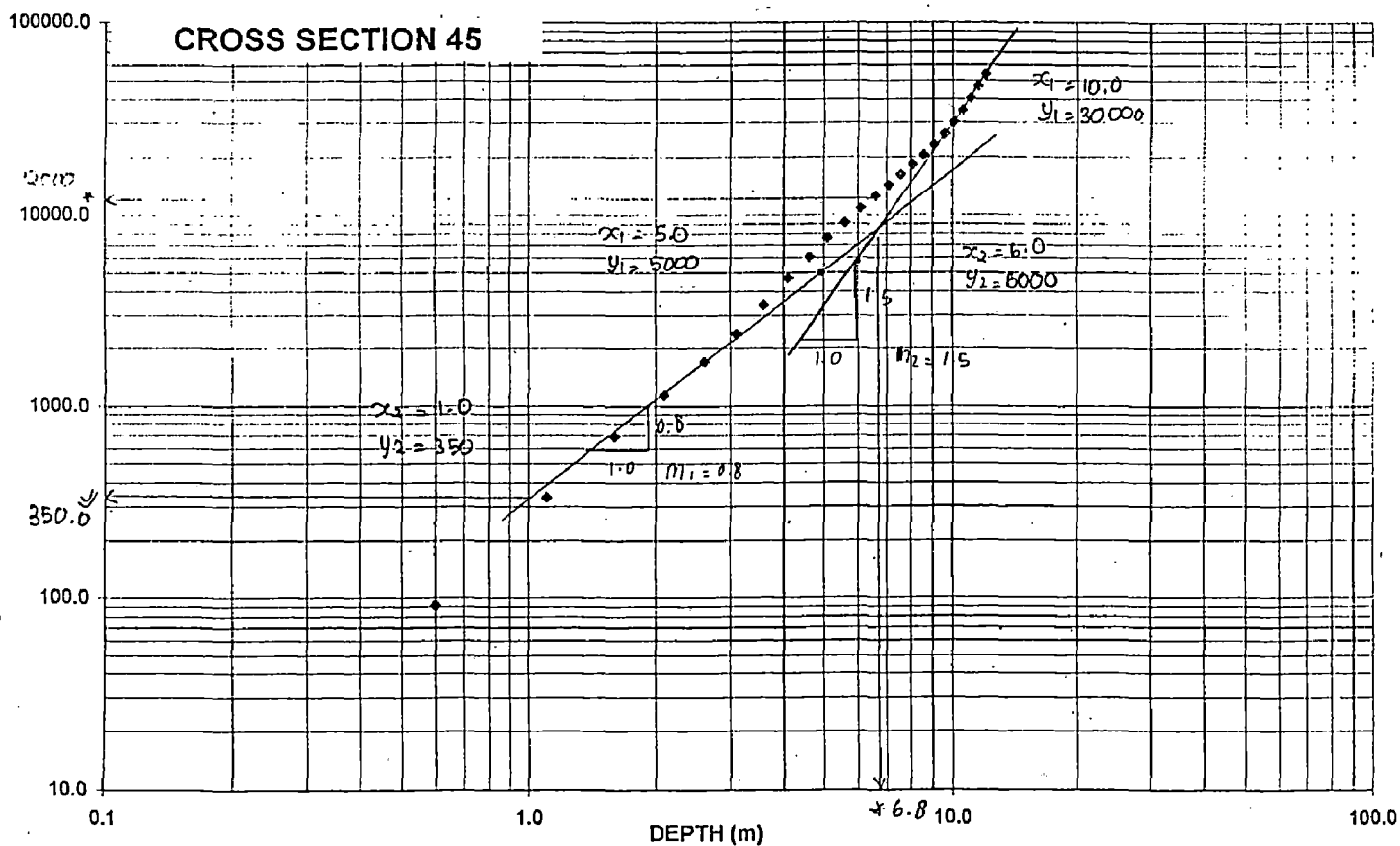
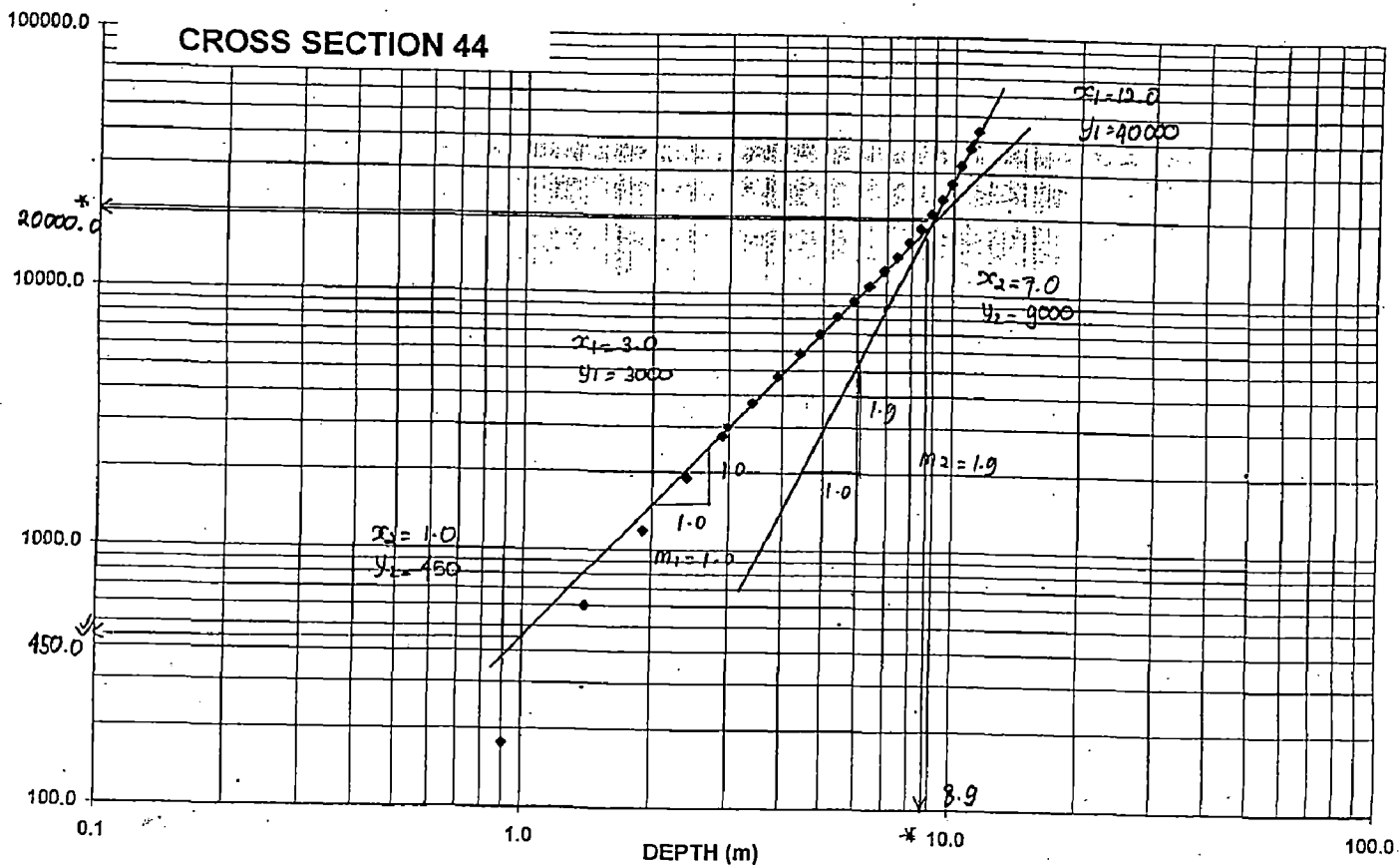
### CROSS SECTION 40

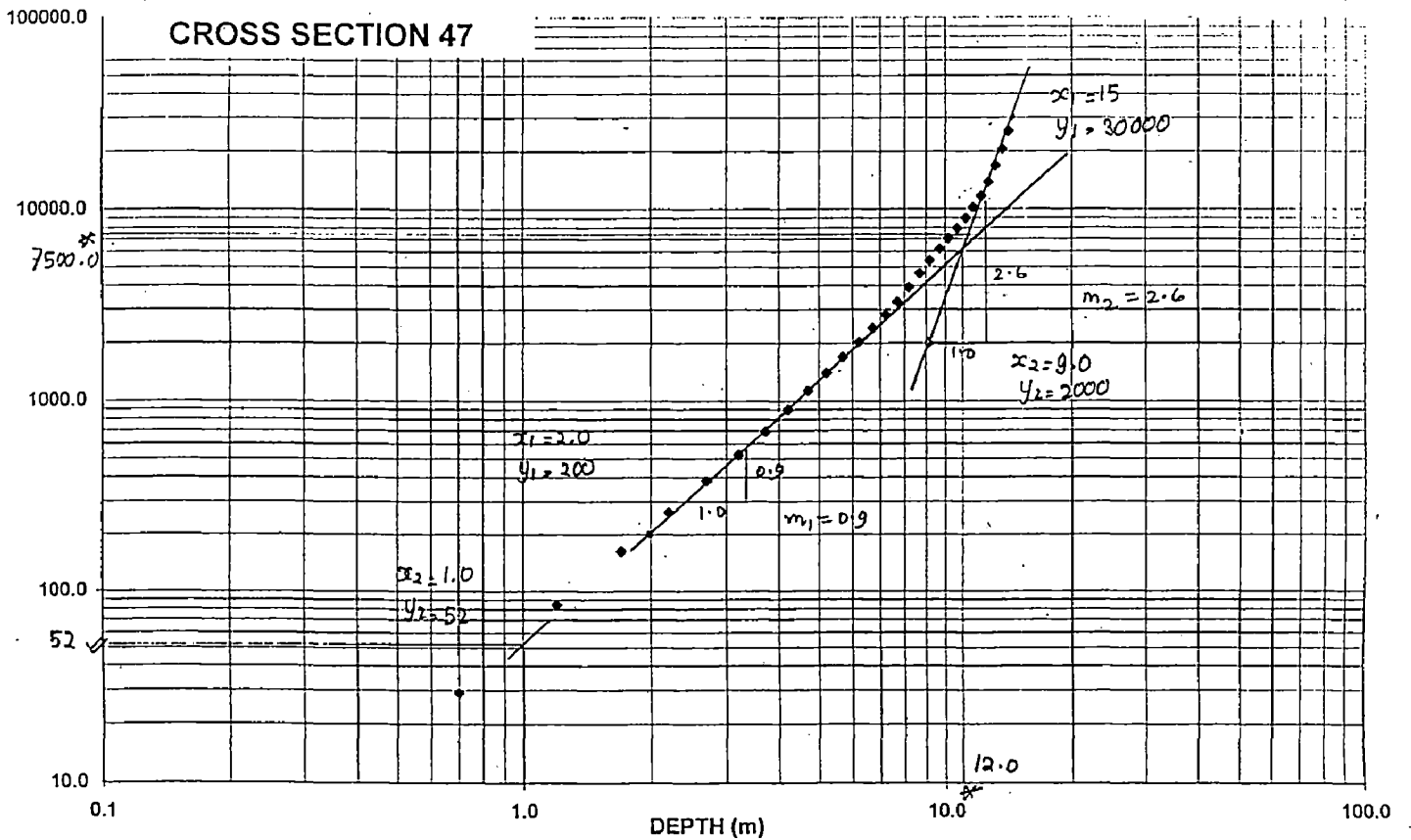
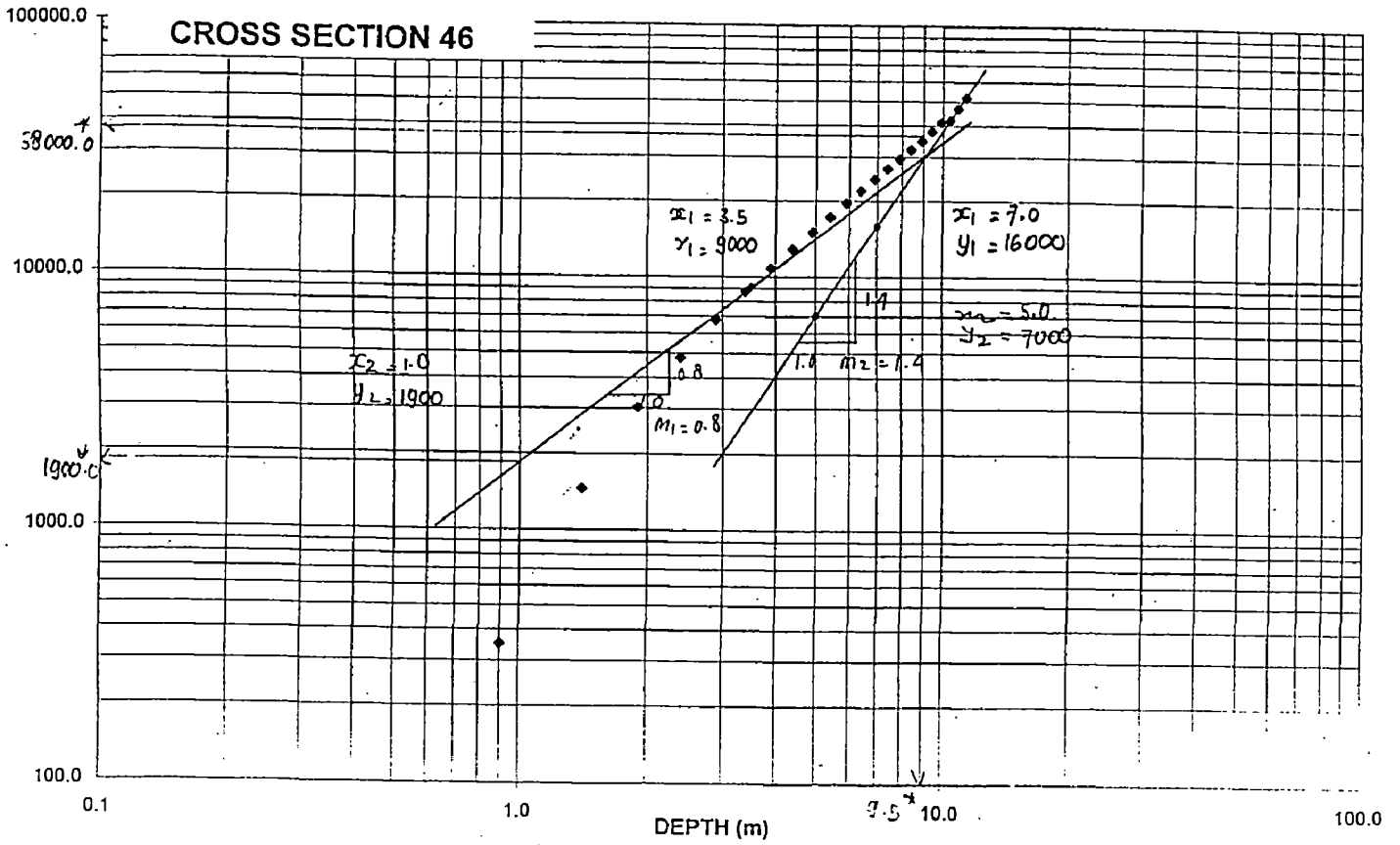


### CROSS SECTION 41

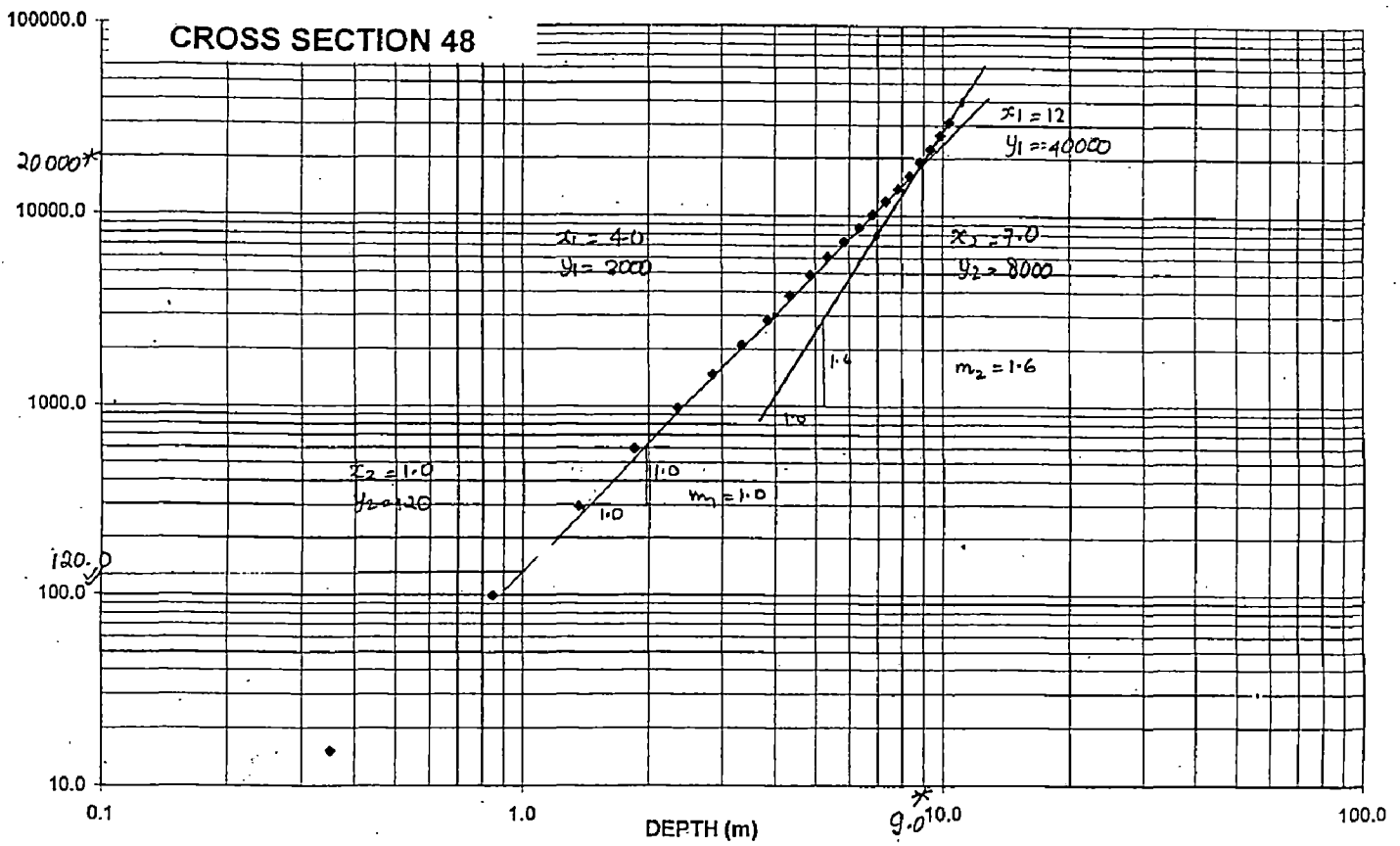




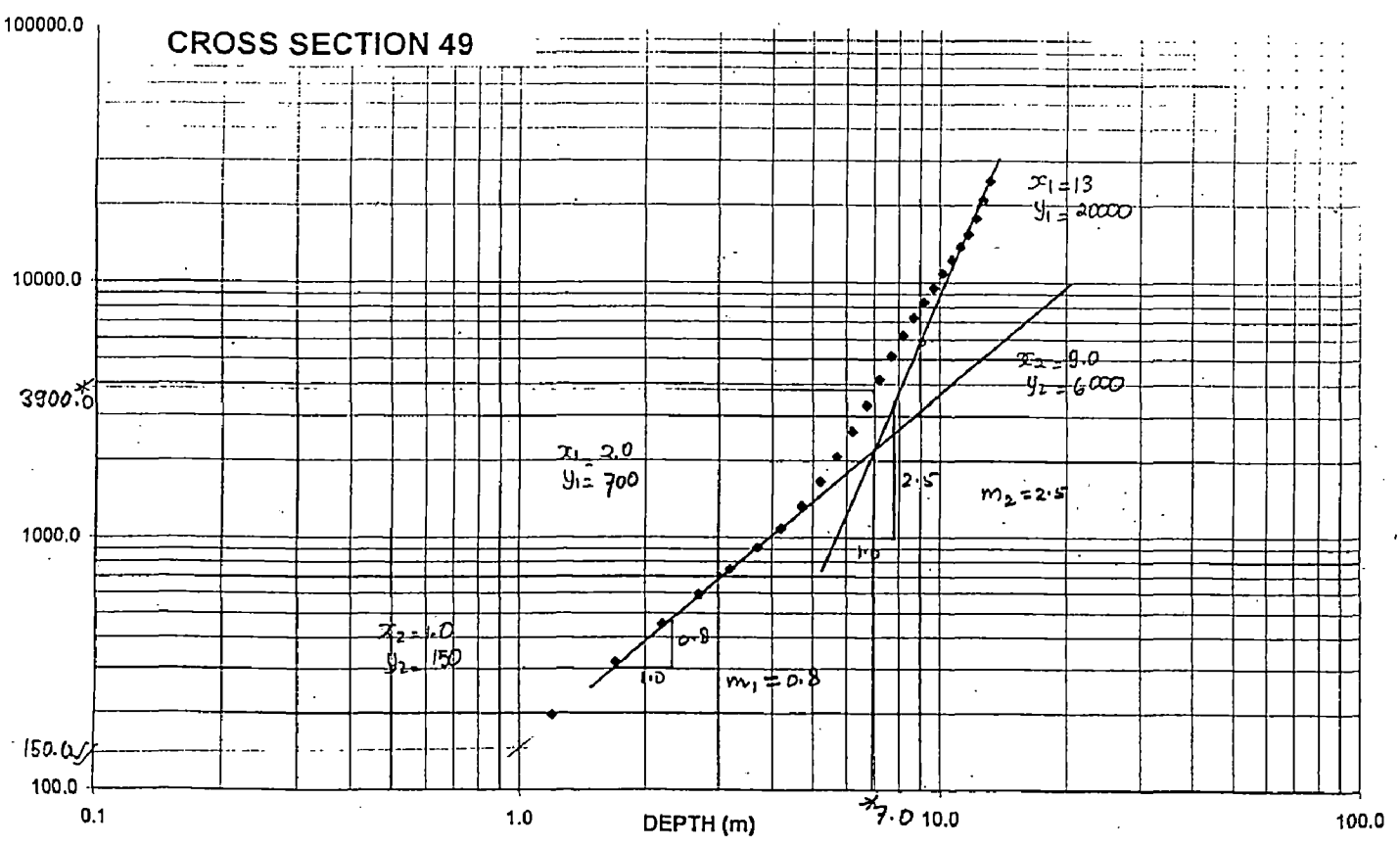




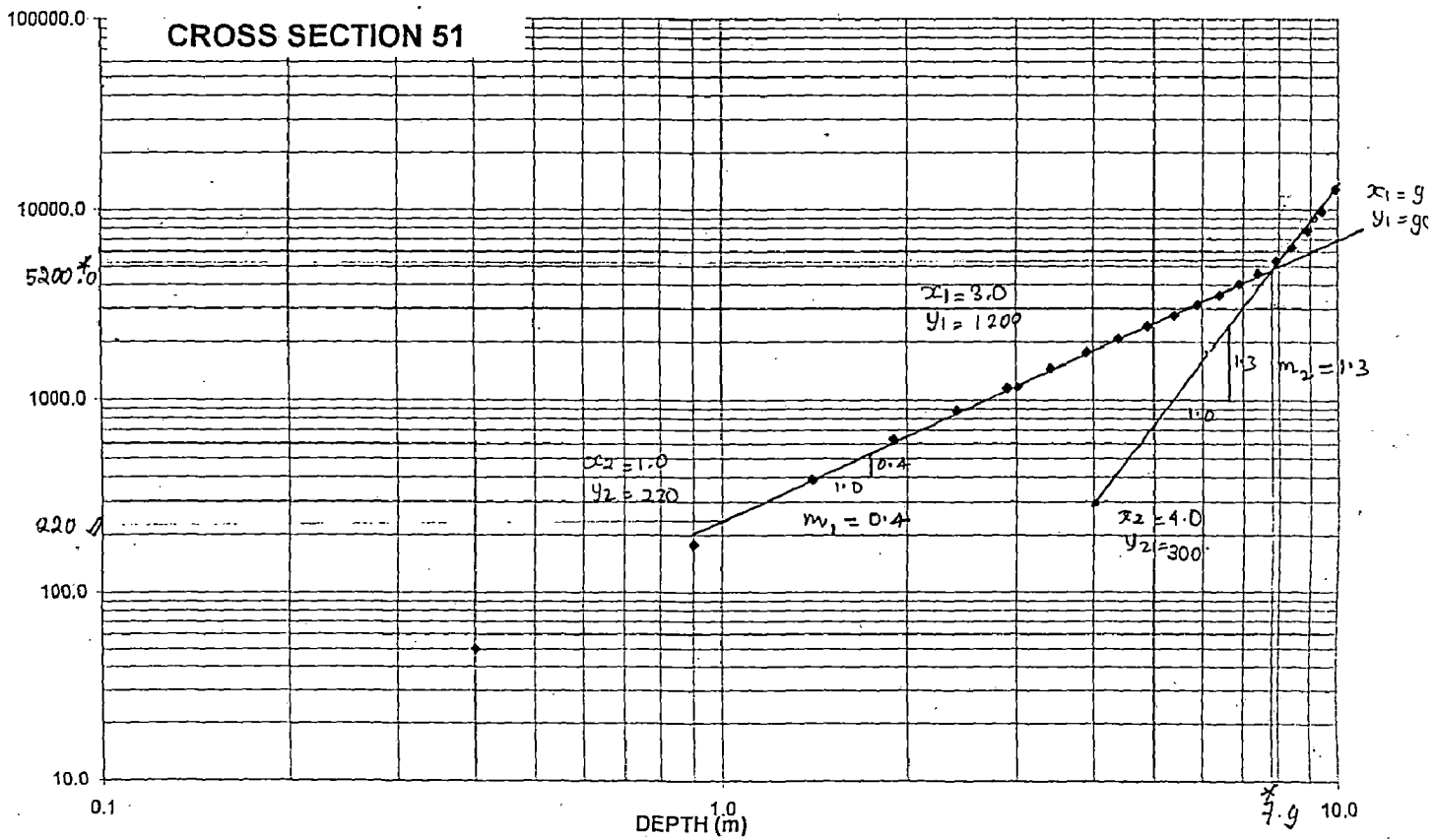
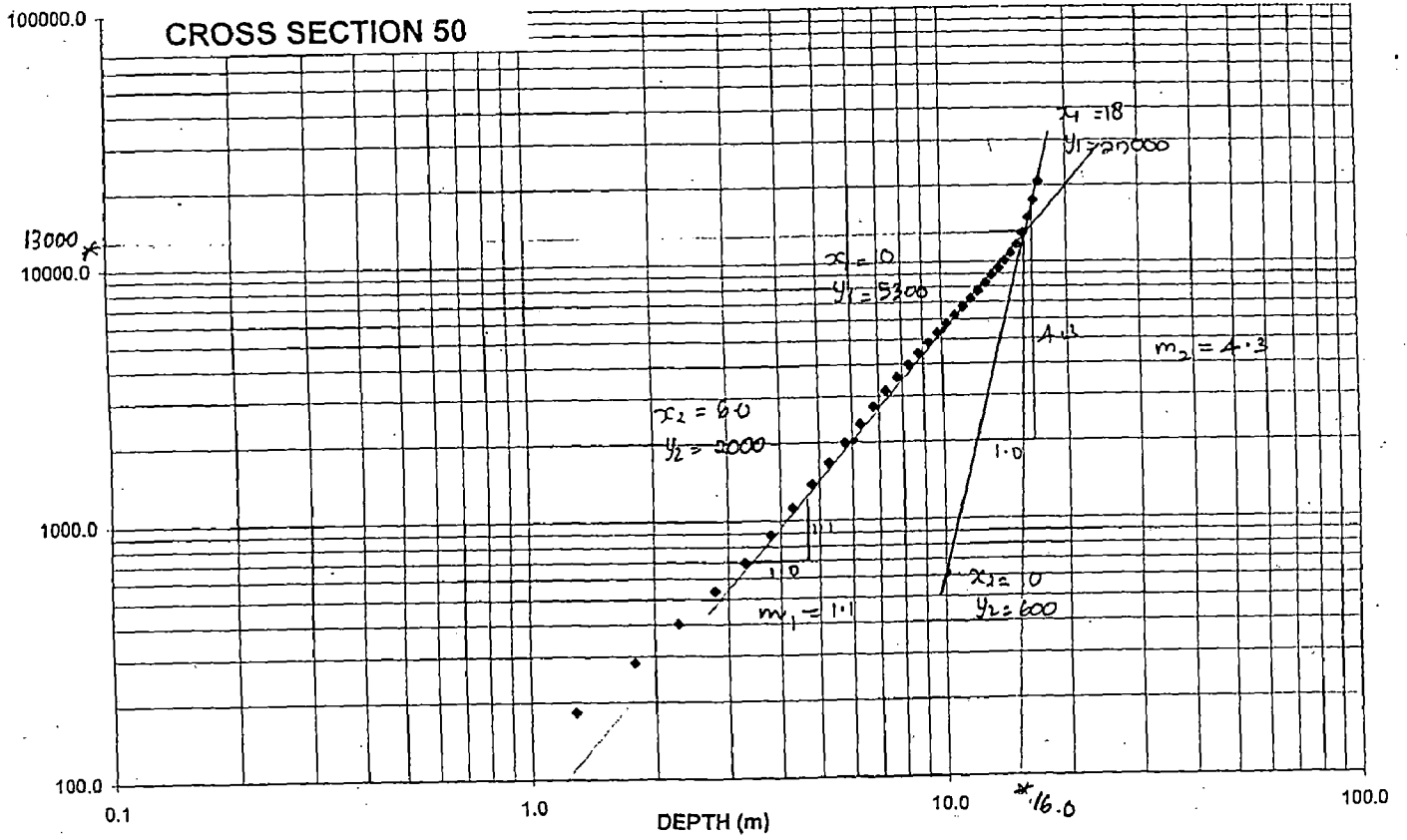
### CROSS SECTION 48

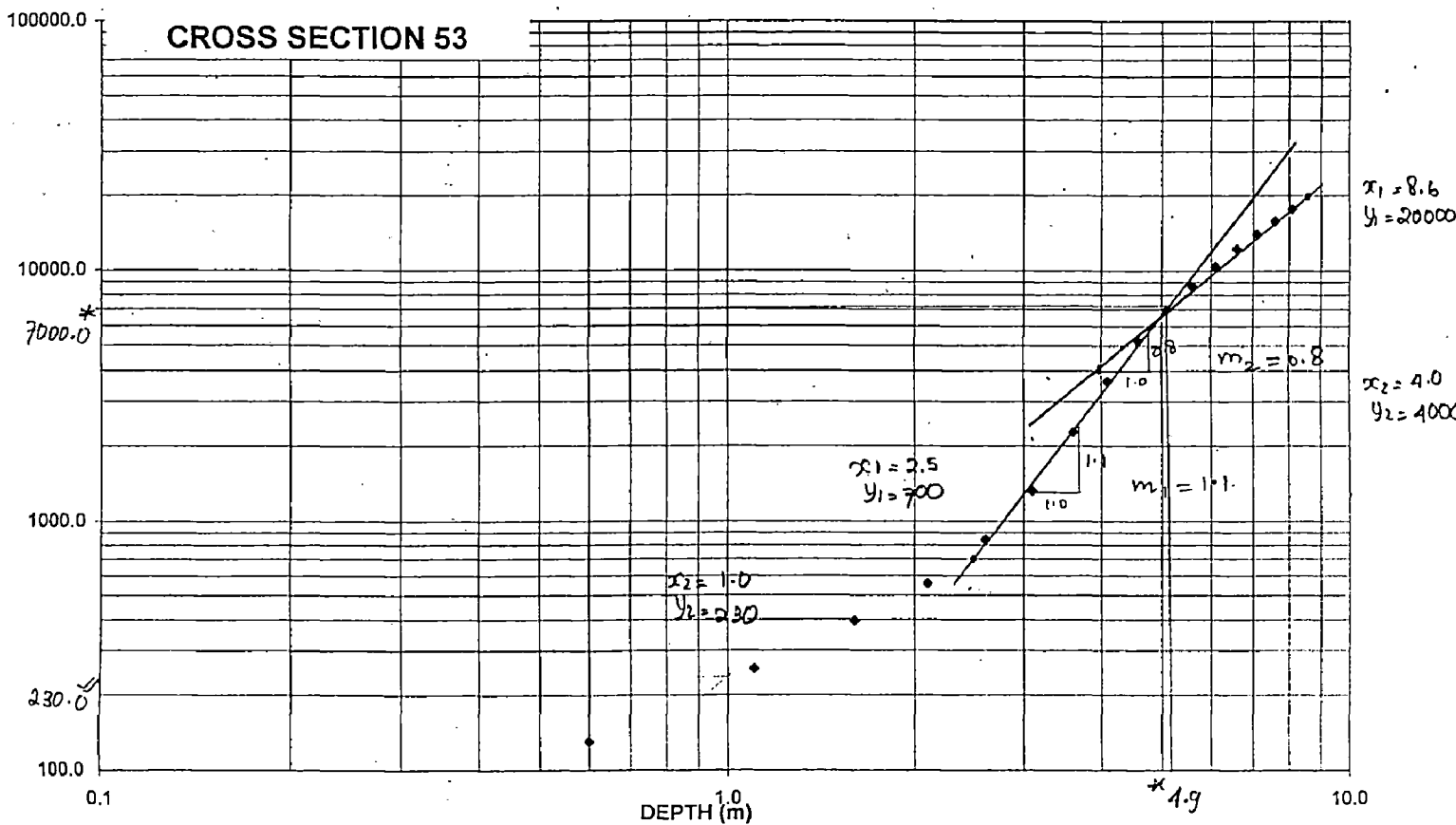
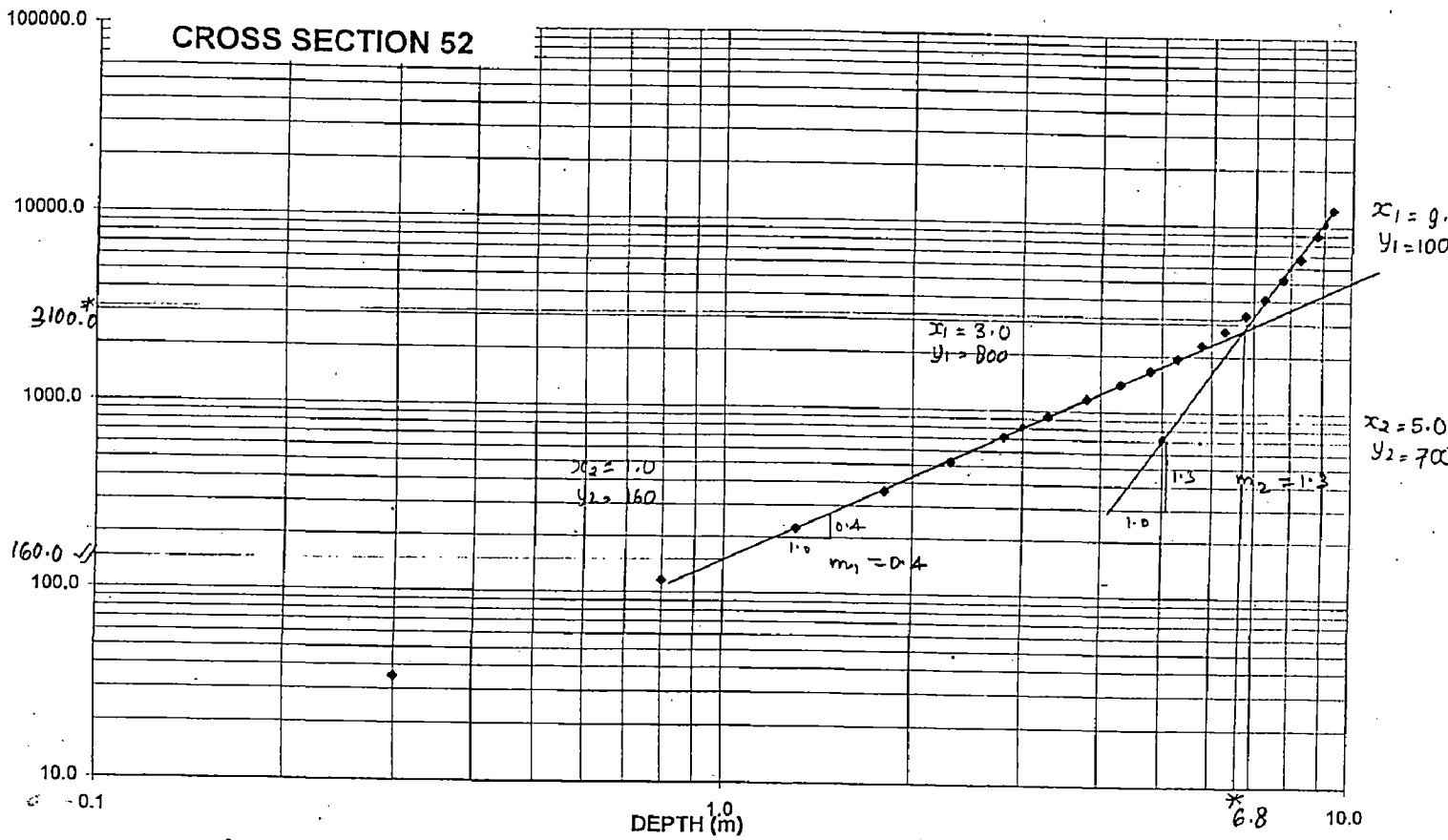


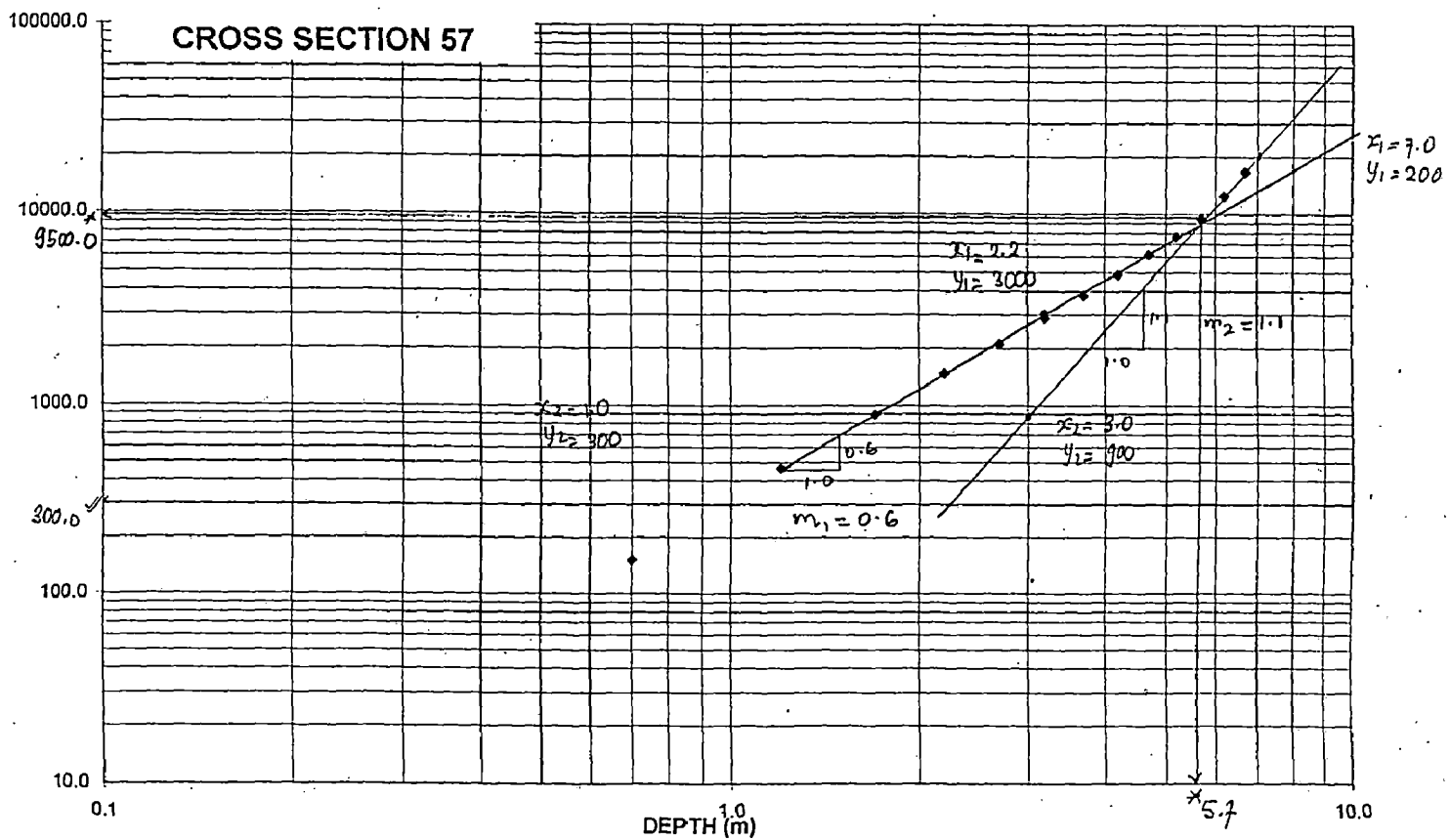
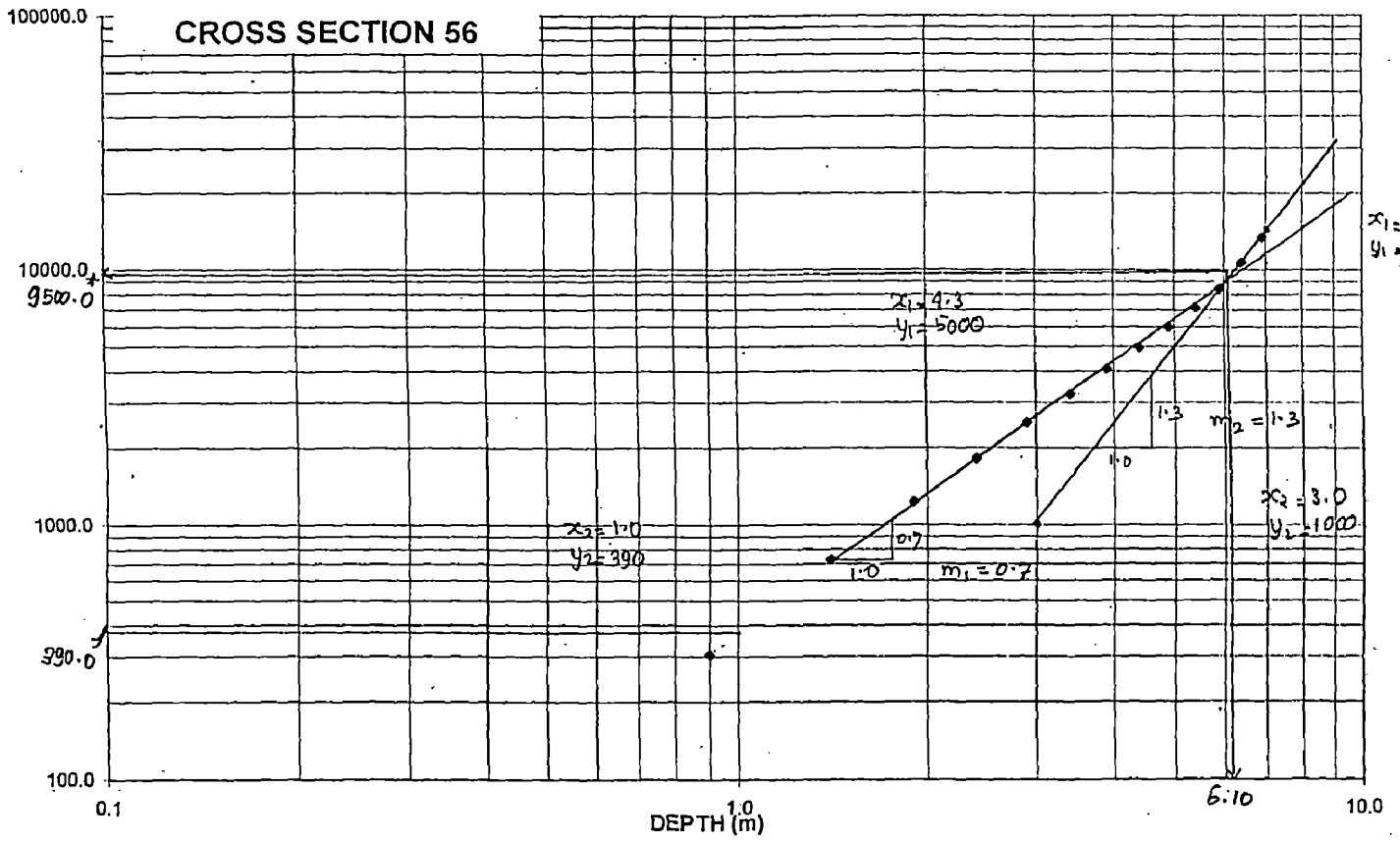
### CROSS SECTION 49

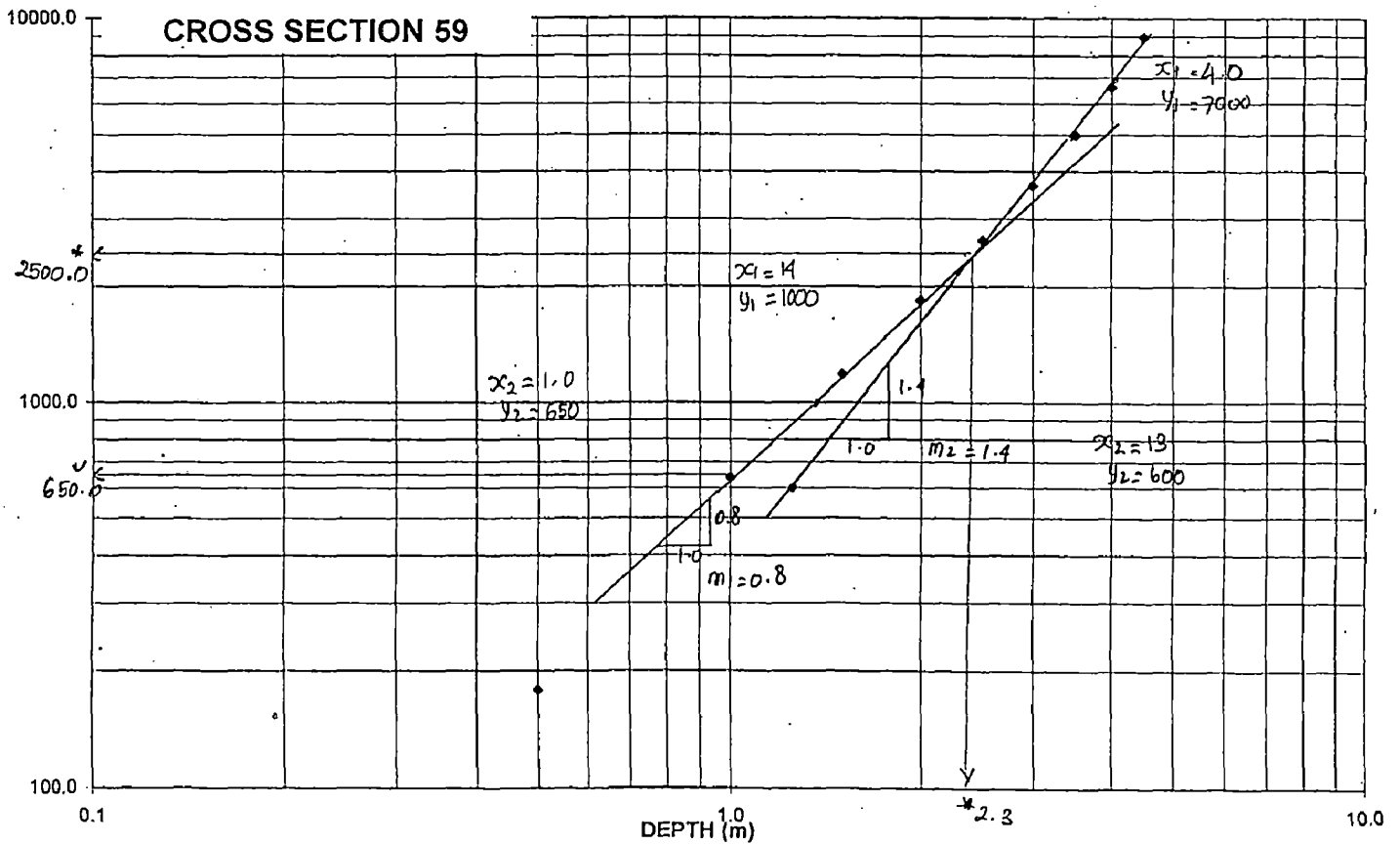
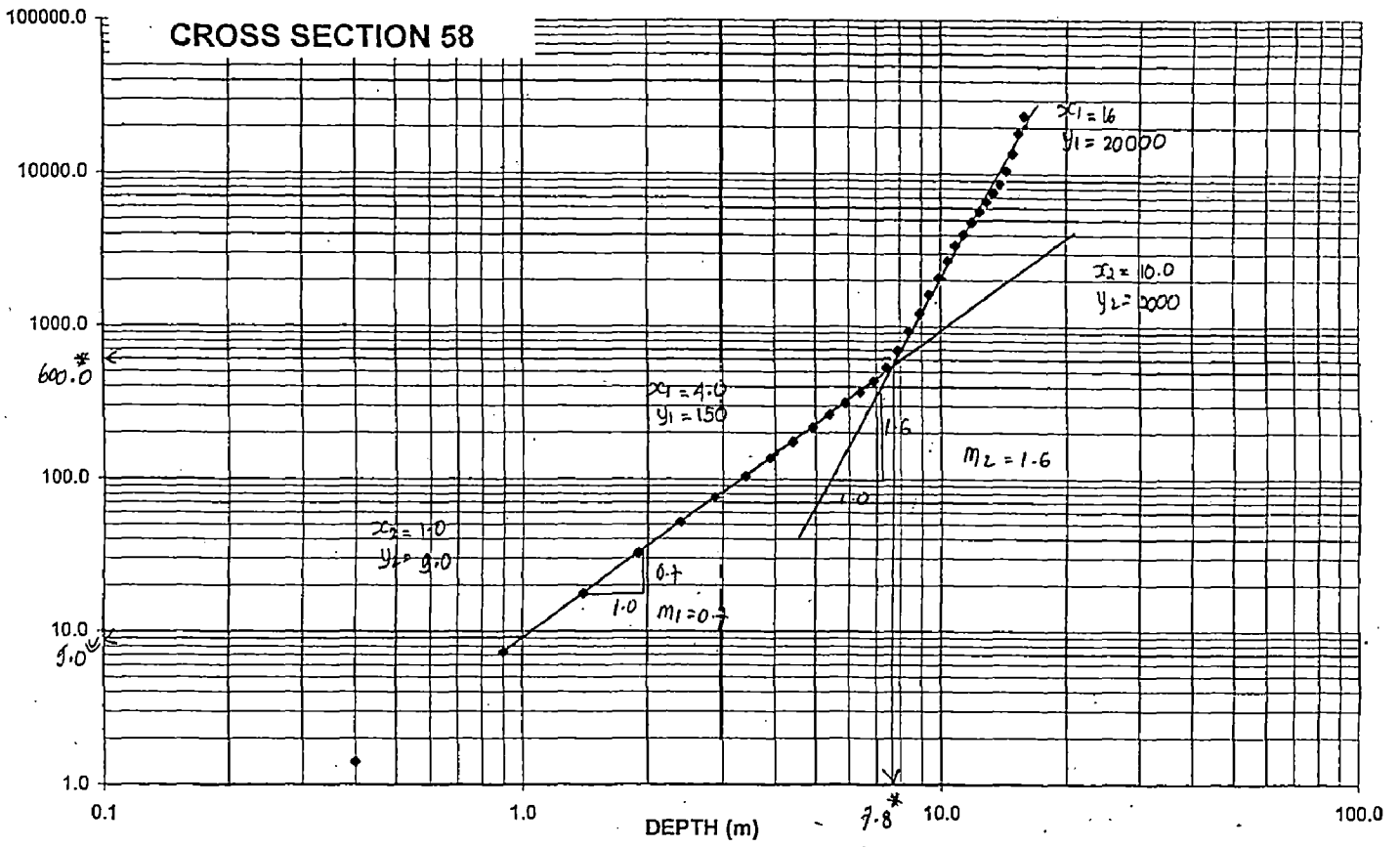


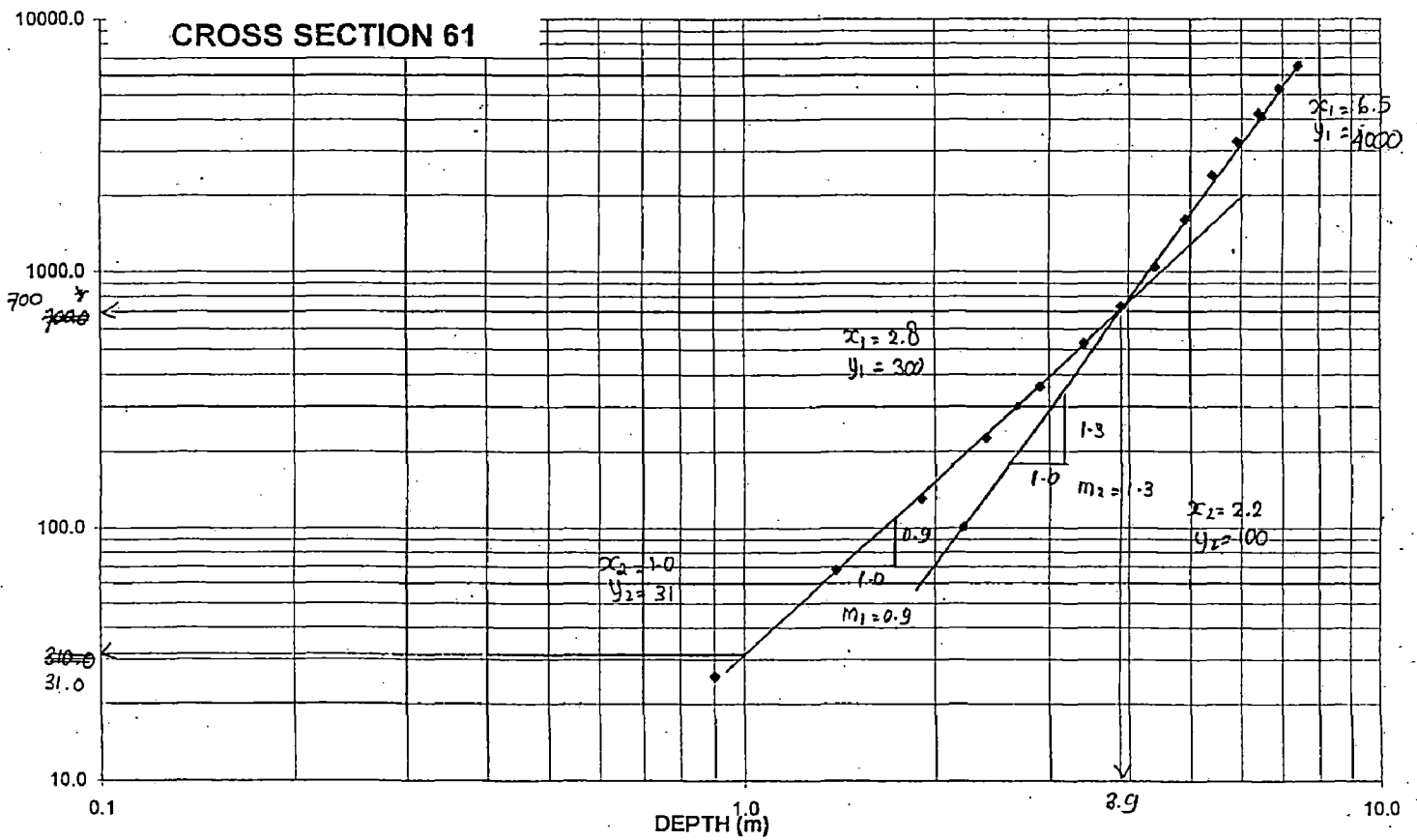
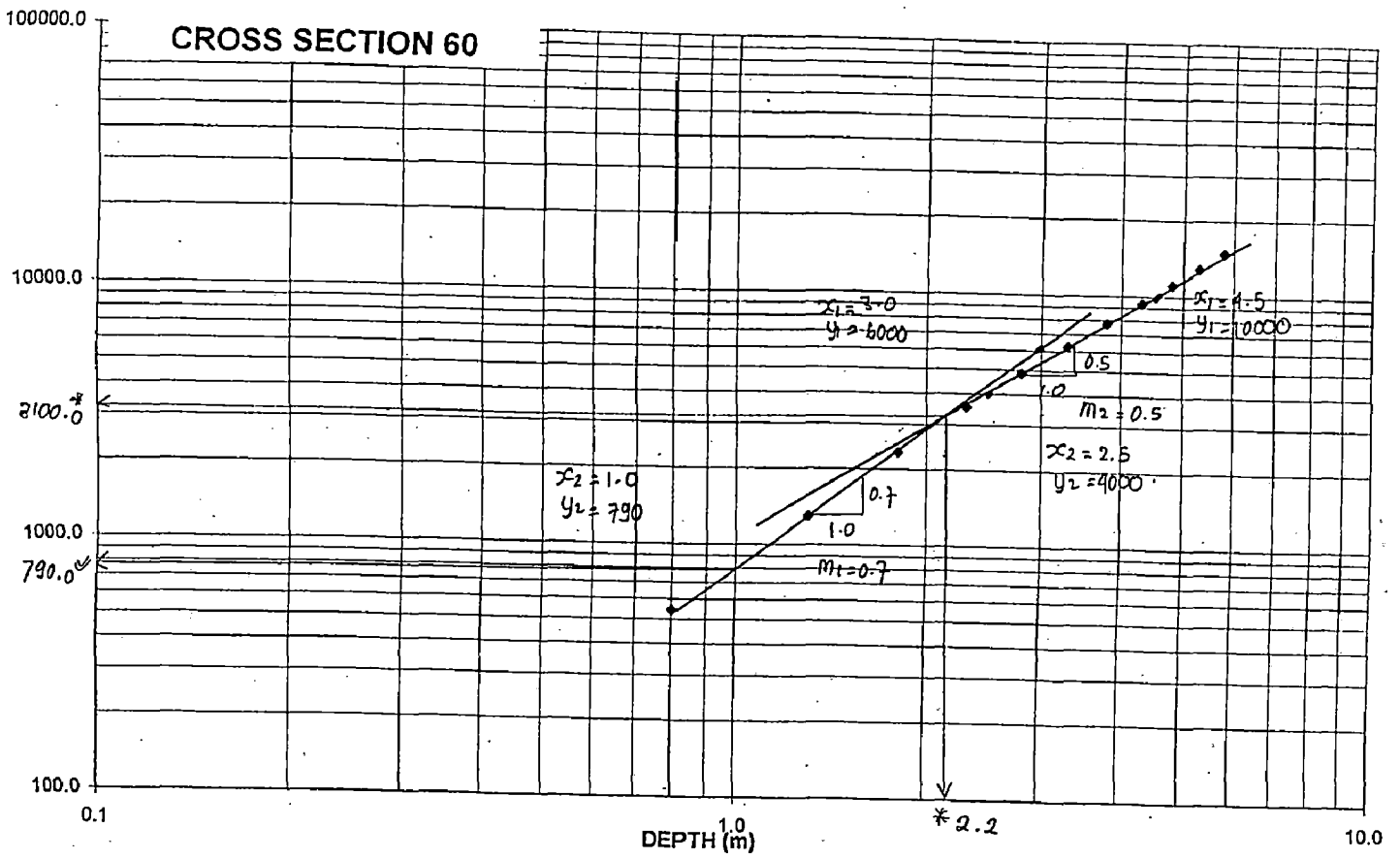


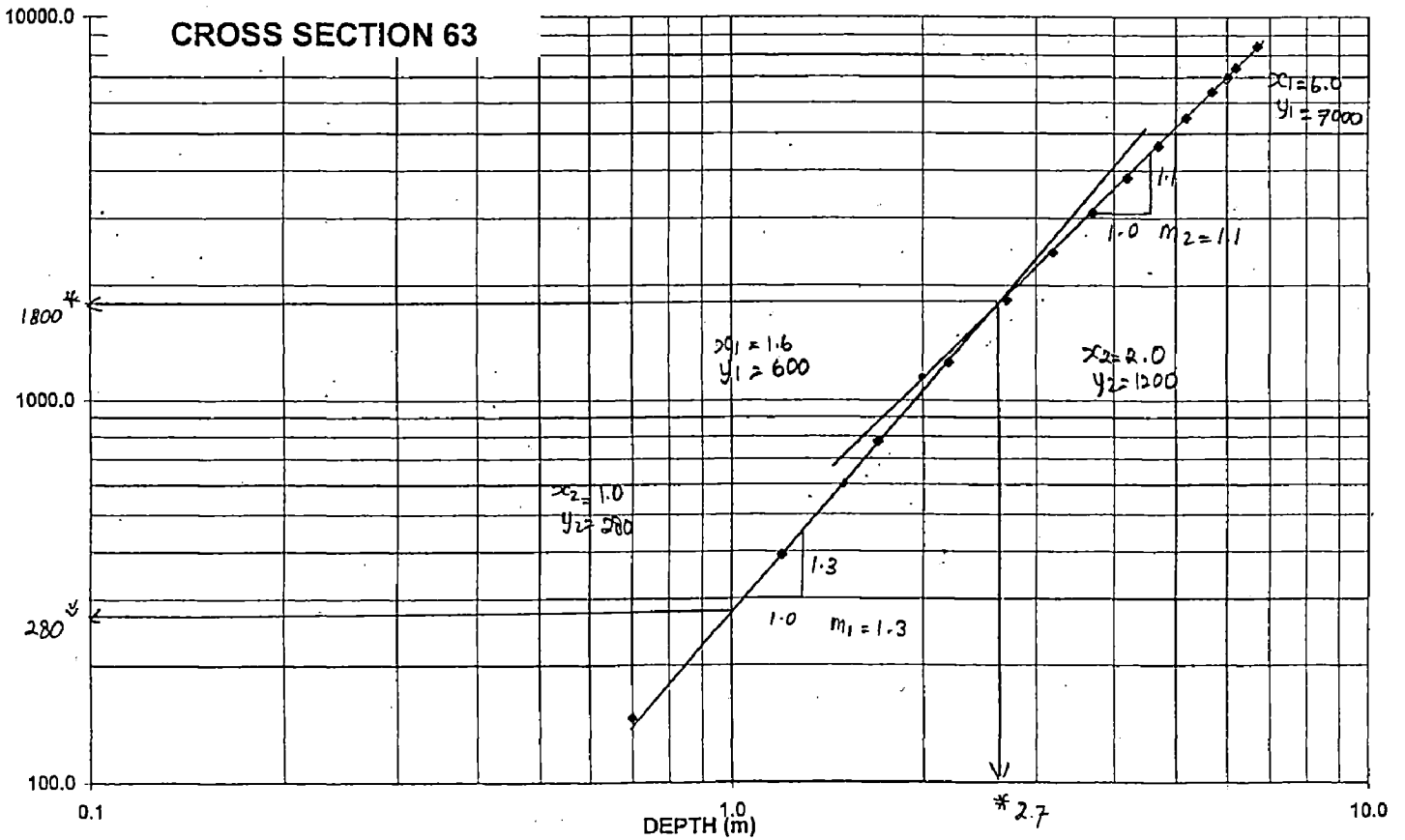
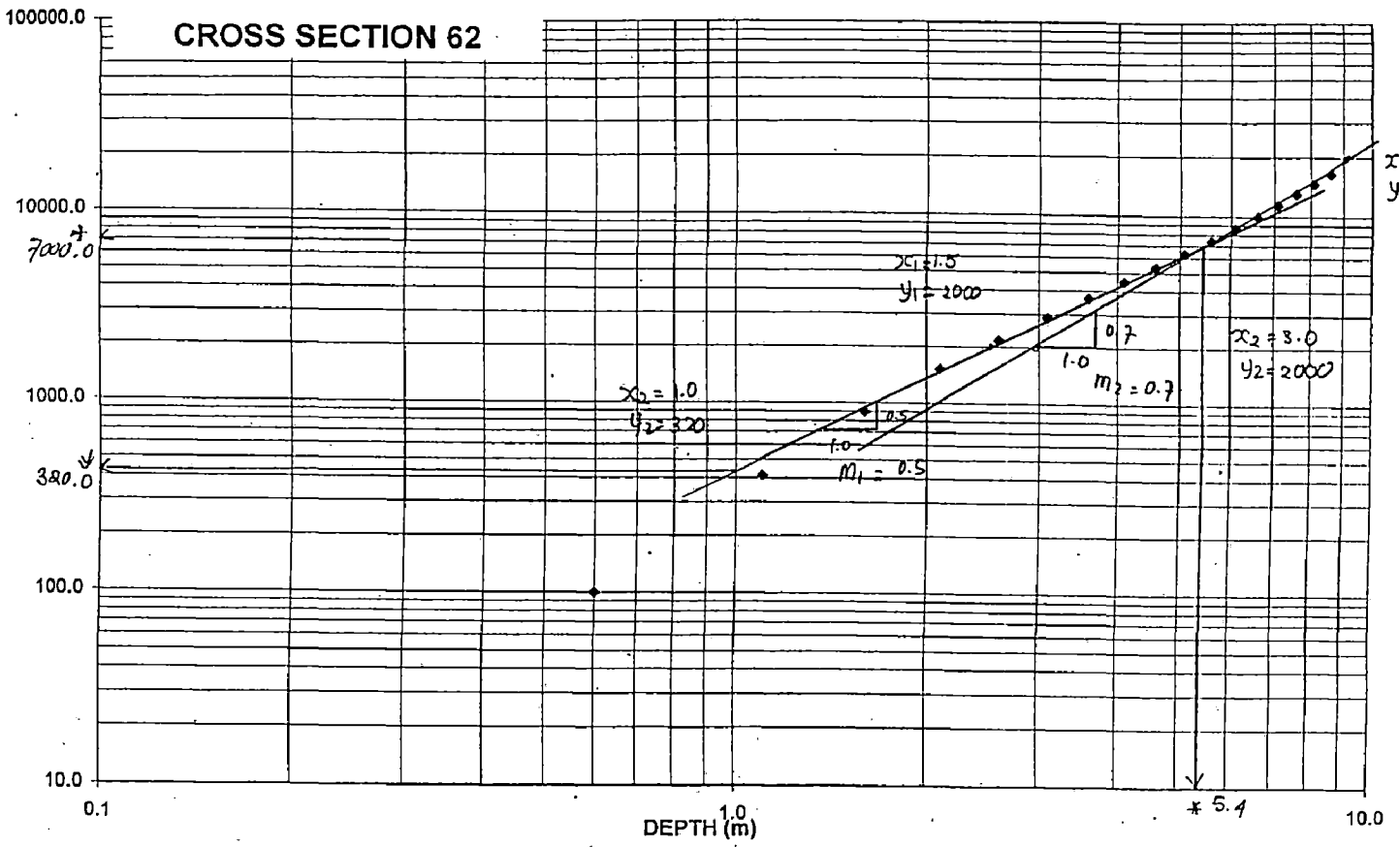


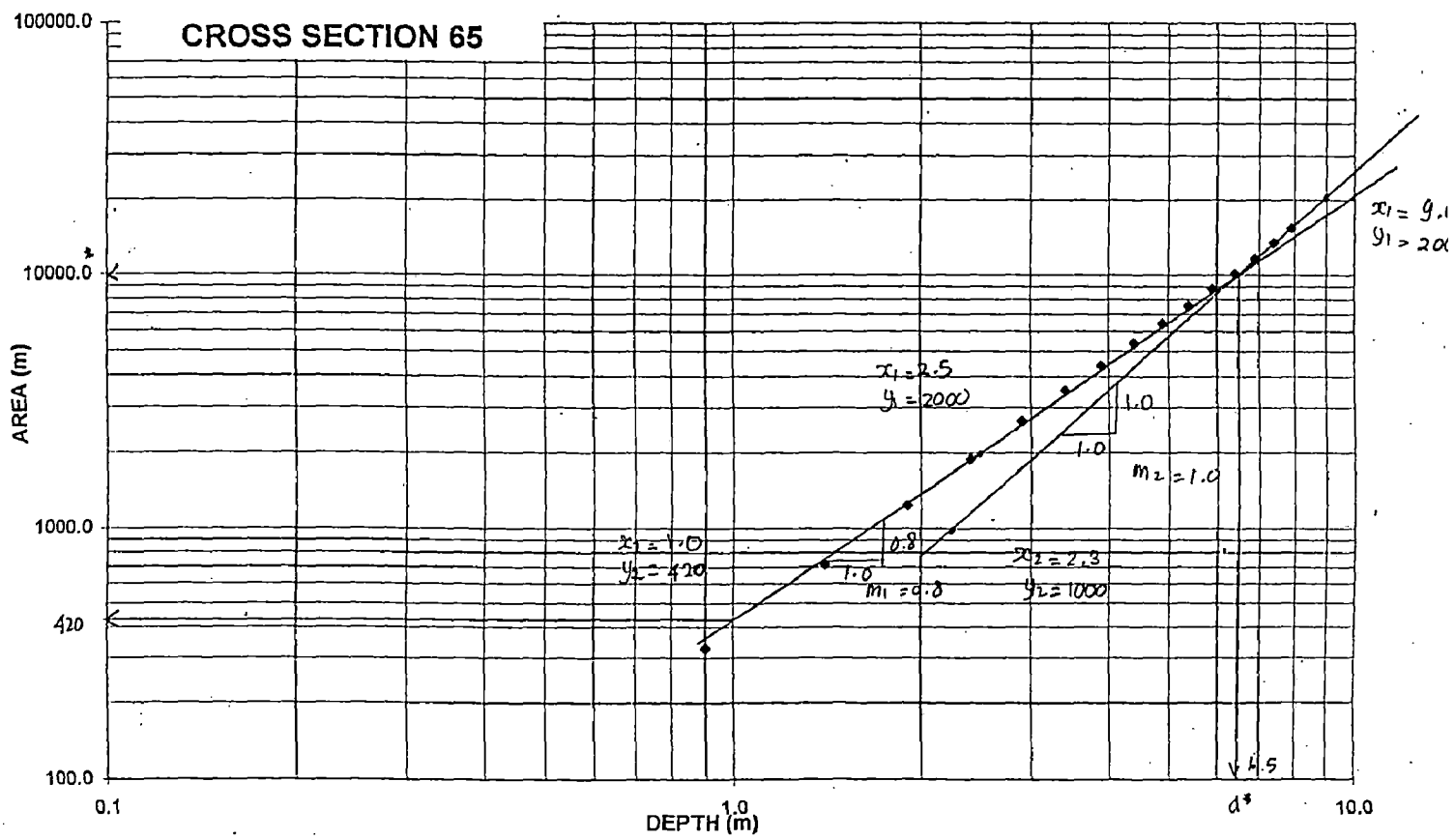
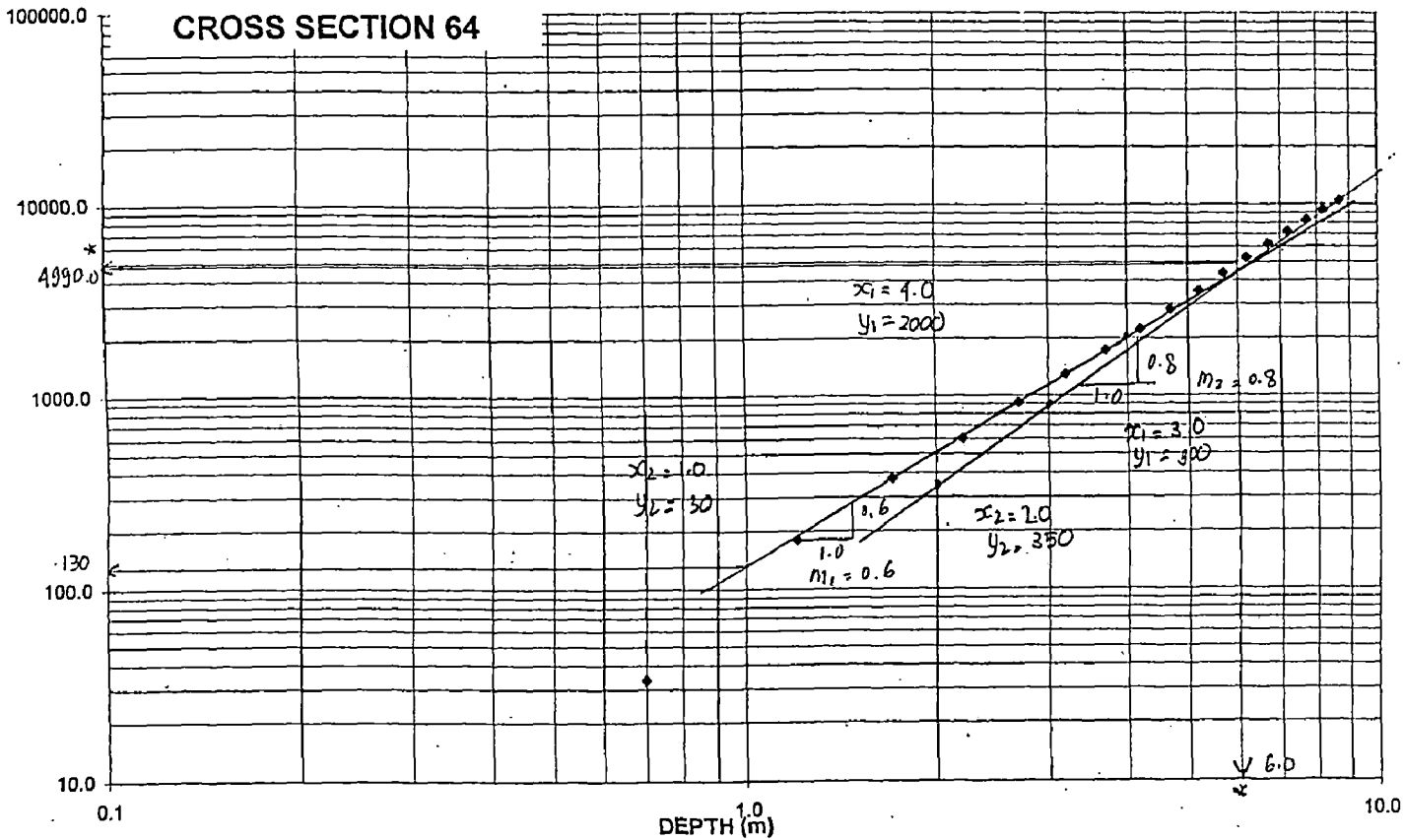












```

*****Program On River Hydrography*****
!      Computation of GEOMETRY OF A RIVER CROSS SECTION

!      Area =Area of Cross section
!      Perim=Wetted perimeter
!      R=hyd radius
!      d=depth of flow in meter
!      x= Abscissa co-ordinate along a C/S
!      y= y ordinate along a C/S
*****

      use portlib
      Dimension x(250),y(250),daa(250),dpp(250)
      character(9) TODAY
      call date (TODAY)
      open(unit=1,file='data.dat')
      open(unit=2,file='data.out')
      write(2,*) TODAY
      write(*,1)
1      format(1x,//30x,'** Welcome to the Program**')
      write(*,'(//)')
      pause '                                press enter to continue'
      write(*,'(//)')
      write(*,2)
2      format(t31,'GEOMETRY OF A RIVER CROSS SECTION')
      write(*,'(//)')
      pause '                                press enter to continue'
      write(*,'(//)')
      write(*,3)
3      format(' Name of the output file is "data.out"')
      write(*,'(//)')
      area=0.0
      perim=0.0
*****
!      Data Input
*****
Read(1,*)n,wl
      do 10 i=1,n
          read(1,*)x(i)
10      continue
do 11 i=1,n
      read(1,*)y(i)
11      continue

```



```

*****
!      Logic Formation
*****
      !do 20
      if(wl.le.ymin)exit
      wl=wl-0.5
      20          continue
      nml=n-1
do 30 i=1,nml
      if(y(i+1).ge.wl.and.y(i).ge.wl)          go      to 30
      if(y(i+1).lt.wl.and.y(i).gt.wl)then
          x(i)=x(i)+(x(i+1)-x(i))/(y(i+1)-y(i))*(wl-y(i))
          y(i)=wl
      endif
      if(y(i+1).gt.wl.and.y(i).lt.wl)then
          x(i+1)=x(i)+(x(i+1)-x(i))/(y(i+1)-y(i))*(wl-y(i))
          y(i+1)=wl
      endif
          da=abs(2.0*wl-y(i+1)-y(i))/2.0
          daa(i)=da*(x(i+1)-x(i))
          dpp(i)=sqrt((x(i+1)-x(i))**2+(y(i+1)-y(i))**2)
          Area=area+daa(i)
          Perim=perim+dpp(i)
30          continue
20          continue
          Radius=Area/perim
          write(2,50)
40          format(/8x,'OUTPUT'/8x,5('~*~')/)
write(2,50)
50          format(/1x,70('='))
          write(2,*)' Area of CS Wetted      Hyd Radius '
          write(2,*)' Cross Section Perimeter '
          write(2,*)'(m2) (meter) (meter)'
          write(2,50)
          Write(2,60) Area,Perim,Radius
60 format(4x,'Area=',f10.2,2x,'Perimeter=', f8.2,2x,'Hyd Radius=', f8.3)
          close(1)
          close(2)
          stop
          end
*****
!      End of Program
*****

```